

Development of binding and functional assays for the neuropeptide Y Y₂ and Y₄ receptors

Dissertation

zur Erlangung des Doktorgrades der Naturwissenschaften (Dr. rer. nat.)
der Naturwissenschaftlichen Fakultät IV – Chemie und Pharmazie –
der Universität Regensburg



vorgelegt von
Ralf Ziemek
aus Leverkusen
2006

Die vorliegende Arbeit entstand in der Zeit von April 2002 bis Mai 2006 unter der Leitung von Herrn Prof. Dr. A. Buschauer am Institut für Pharmazie der Naturwissenschaftlichen Fakultät IV – Chemie und Pharmazie – der Universität Regensburg.

Das Promotionsgesuch wurde eingereicht im April 2006

Tag der mündlichen Prüfung: 26. Mai 2006

Prüfungsausschuss:

Prof. Dr. J. Heilmann	(Vorsitzender)
Prof. Dr. A. Buschauer	(Erstgutachter)
Prof. Dr. S. Elz	(Zweitgutachter)
Prof. Dr. A. Göpferich	(Drittprüfer)

für meine Eltern

Auf jede Frage eine Antwort wissen nur Dummköpfe

John Steinbeck, amerikanischer Schriftsteller, 1902-1968

Danksagungen

An dieser Stelle möchte ich mich bedanken bei:

Herrn Prof. Dr. A. Buschauer für die Gelegenheit, an einem so interessanten Projekt arbeiten zu dürfen, für seine wissenschaftlichen Anregungen und seine konstruktive Kritik bei der Durchsicht der Arbeit,

Herrn Prof. Dr. G. Bernhardt für seine fachliche Anleitung und Vorschläge bei experimentellen Problemen, sowie für seine kritische Durchsicht der Arbeit,

Frau Prof. Dr. A. Beck-Sickinger (Universität Leipzig) für die Bereitstellung der Peptide sowie des hY₄-eYFP-QC_{kor} Vektors,

Frau Dr. C. Cabrele für die Bereitstellung weiterer Peptidliganden und ihre stete Hilfsbereitschaft,

Herrn Prof. Dr. B. Conklin (University of California) für die Bereitstellung des pcDNA1-qi5-HA Vektors,

Herrn Prof. Dr. S. Thayer (University of Minnesota) für die Bereitstellung des pMTAEQ Vektors,

Herrn Dr. W. Schneider und O. Merkel für die freundliche Unterstützung und Bereitstellung des pQCXIP und pCL-Eco Vektors sowie der HEK293T Zellen,

Herrn Dr. T. Dobner für die Bereitstellung des pcDNA3.1/Hygro und pcDNA3.1/Zeo Vektors,

Frau Dr. P. Rose (Bristol-Myers Squibb) für die Bereitstellung des pcDNA3-hY₂ Vektors,

Frau Prof. Dr. D. Männel für die Bereitstellung des pEGFP-N1 Vektors,

Herrn Dr. J. Langer (University of New Jersey) für die Bereitstellung des pcDEF3 Vektors,

Herrn Prof. Dr. S. Parker (University of Tennessee) für die Bereitstellung der CHO-rY₄ Zellen,

Herrn Dr. J. Daniels (Glaxo Wellcome) für die Bereitstellung des Liganden GW1229,

Frau E. Schreiber für die zuverlässige Durchführung der Fura-2 Assays sowie die Unterstützung in der Betreuung der Zellkulturen,

Herrn A. Brennauer für die Bereitstellung der Y₂ Antagonisten und die entspannte Gesellschaft während des Zusammenschreibens,

Herrn Dr. E. Schneider für die fachliche Unterstützung insbesondere im Umgang mit dem Durchflußzytometer und für die Montagswitze, die ich allerdings nicht immer verstanden habe,

Frau A. Kraus und Dr. P. Gohrai für die Bereitstellung der H₂ Agonisten,

Herrn M. Keller für seine Hilfe mit der HPLC Analytik und Herrn D. Gross für die Hilfe mit der konfokalen Mikroskopie,

Herrn Dr. J. Klar für die wertvollen Tipps zur Molekularbiologie,

Frau S. Bollwein für ihre Unterstützung auf dem Gebiet der Zellkultur,

Herrn P. Richthammer für seine Hilfsbereitschaft bei technischen Problemen und für seine gute Laune,

Frau S. Heinrich und Frau M. Luginger für Ihre Unterstützung bei organisatorischen Problemen,

meinen Kollegen Stephan Braun, Hendrik Preuss, Edith Hofinger, Manuela Menke, Christine Müller, Peter Jarzyna und Patrick Igel, die mir auch außerhalb der Universität eine schöne Zeit in Regensburg ermöglichten,

allen Mitgliedern des Lehrstuhls für ihre Kollegialität, Hilfsbereitschaft und das gute Arbeitsklima,

dem Graduiertenkolleg 760 der DFG für die finanzielle Unterstützung und wissenschaftliche Förderung,

meiner Freundin Kathrin für ihre Geduld und ihr Verständnis,

und vor allem meinen Eltern und meiner Schwester, auf deren Hilfe und Unterstützung ich mich immer verlassen konnte.

Poster Presentations

1st Summer School Medicinal Chemistry, Regensburg, September 2002:

R. Ziemek, G. Bernhardt, A. Beck-Sickinger, S. Parker, A. Buschauer

"A fluorescence labelled analogue of human pancreatic polypeptide, Cy5[Lys⁴]hPP, for the flow cytometric determination of NPY Y₄ receptor binding data"

Annual Meeting of the GDCh, Fachgruppe Medizinische Chemie, "Frontiers in Medicinal Chemistry", Fulda, September 2003:

Ziemek, R., Schneider, E., Mayer, M., Bernhardt, G., Beck-Sickinger, A., Parker, S., Buschauer, A.

"Determination of Activity and Affinity of Neuropeptide Y Receptor Ligands by Flow Cytometry"

7th International NPY Meeting, Coimbra/Portugal, February 2004:

R. Ziemek, G. Bernhardt, C. Cabrele, A. Beck-Sickinger, S. Parker, A. Buschauer

"A fluorescence labelled analogue of human pancreatic polypeptide, Cy5-[Lys⁴]hPP, for the flow cytometric determination of NPY Y₄ receptor binding data"

Annual Meeting of the GDCh, Fachgruppe Medizinische Chemie, "Frontiers in Medicinal Chemistry", Erlangen, March 2004:

R. Ziemek, G. Bernhardt, C. Cabrele, A. Beck-Sickinger, S. Parker, A. Buschauer

"Flow cytometric determination of binding constants of NPY Y₄ receptor ligands"

2nd Summer School Medicinal Chemistry, Regensburg, October 2004:

Ziemek, R., Brennauer, A., Bernhardt, G., Cabrele, C., Beck-Sickinger, A., Buschauer, A.

"Fluorescence-based determination of affinity and activity at the human neuropeptide Y Y₂ receptor using flow cytometry"

Annual Meeting of the German Pharmaceutical Society (DPhG), Regensburg, October 2004:

R. Ziemek, G. Bernhardt, C. Cabrele, A. Beck-Sickinger, A. Buschauer

"Fluorescent Cy5-[K⁴]hPP: A tool for the characterization of Neuropeptide Y Y₄ receptor ligands"

Meeting of the ChemBioNet, Frankfurt, December 2004:

Ziemek, R., Brennauer, A., Bernhardt, G., Cabrele, C., Beck-Sickinger, A., Buschauer, A.

"Determination of affinity and activity at the human neuropeptide Y Y₂ receptor by flow cytometry and aequorin luminescence"

Annual Meeting of the GDCh, Fachgruppe Medizinische Chemie, "Frontiers in Medicinal Chemistry", Leipzig, March 2005:

Ziemek, R., Brennauer, A., Bernhardt, G., Cabrele, C., Beck-Sickinger, A., Buschauer, A.

"Fluorescence- and luminescence-based methods for the pharmacological characterization of neuropeptide Y Y₂ receptor ligands"

CONTENTS

1	GENERAL INTRODUCTION	1
1.1	G-protein coupled receptors	2
1.2	Receptor models	4
1.3	Pancreatic polypeptides and their receptors	7
1.3.1	Distribution and physiological effects of PP-fold peptides	9
1.3.1.1	Pancreatic polypeptide	9
1.3.1.2	Peptide YY	10
1.3.1.3	Neuropeptide Y	11
1.3.2	NPY receptors	12
1.3.2.1	The NPY Y ₁ receptor	14
1.3.2.2	The NPY Y ₂ receptor	17
1.3.2.3	The NPY Y ₄ receptor	20
1.3.2.4	The NPY Y ₅ receptor	21
1.3.2.5	The NPY y ₆ receptor	24
1.3.2.6	The NPY Y ₇ receptor	24
2	SCOPE AND OBJECTIVES	27
3	DEVELOPMENT OF A FLOW CYTOMETRIC BINDING ASSAY FOR THE HUMAN NPY Y₂ RECEPTOR	29
3.1	Stable expression of the hY₂ receptor gene	30
3.1.1	Introduction	30
3.1.1.1	Heterologous expression systems	30
3.1.1.2	Transient versus stable transfection	31
3.1.1.3	Choice of the host cell	32
3.1.1.4	Choice of the expression vector	32
3.1.1.5	Transfection of mammalian cells	33
3.1.1.6	Selection and screening of cell clones	33
3.1.2	Materials and Methods	34
3.1.2.1	Preparation of media and agar plates	34
3.1.2.2	Preparation of competent <i>E. coli</i>	34
3.1.2.3	Transformation of <i>E. coli</i>	35
3.1.2.4	Preparation of plasmid DNA	35
3.1.2.4.1	<i>Mini-Prep</i>	35
3.1.2.4.2	<i>Maxi-Prep</i>	36
3.1.2.4.3	<i>Determination of DNA concentration</i>	36
3.1.2.5	Restriction enzyme digestion	36
3.1.2.6	Agarose gel electrophoresis	37
3.1.2.7	Recovery of DNA fragments from agarose gels	37
3.1.2.8	Subcloning of the pcDNA3-eGFP and pcDEF3-eGFP vector	38
3.1.2.9	Cell culture	40
3.1.2.10	Transient transfection of CHO-K1 cells with pcDNA3-eGFP and pcDEF3-eGFP using FuGENE and Metafectene	40
3.1.2.10.1	<i>Fluorescence microscopy</i>	40
3.1.2.10.2	<i>Flow cytometry</i>	40
3.1.2.10.3	<i>Chemosensitivity assay</i>	41
3.1.2.11	Restriction analysis of the pcDNA3-hY ₂ vector and stable transfection of CHO-K1 cells	42
3.1.2.12	Analysis of selected cell clones for the specific binding of Cy5-pNPY	43
3.1.3	Results and Discussion	44
3.1.3.1	Optimization of the transfection procedure	44
3.1.3.2	Stable transfection of CHO-K1 cells with the hY ₂ receptor gene	46

3.2	Flow cytometric binding assay	46
3.2.1	Introduction	46
3.2.2	Materials and Methods	48
3.2.2.1	Synthesis and purification of cy5-pNPY	48
3.2.2.1.1	<i>Estimation of the molar extinction coefficient of hydrolysed cy5 dye in mobile phase</i>	49
3.2.2.2	Y ₂ receptor antagonists	50
3.2.2.3	Flow cytometry	51
3.2.2.4	Confocal microscopy	52
3.2.3	Results	52
3.2.3.1	Flow cytometric binding assay	52
3.2.3.2	Confocal microscopy	54
3.3	Whole cell radioligand binding assay	56
3.3.1	Introduction	56
3.3.2	Materials and Methods	57
3.3.2.1	Radioligand binding assay	57
3.3.2.2	Acid extraction of cell-associated radioligand	58
3.3.2.3	HPLC analysis of adsorption of BIIE0246	58
3.3.3	Results	59
3.4	Conclusions	66
4	DEVELOPMENT OF FUNCTIONAL ASSAYS FOR THE HUMAN NPY Y₂ RECEPTOR	67
4.1	Flow cytometric calcium assay	68
4.1.1	Introduction	68
4.1.1.1	Functional assays for the NPY Y ₂ receptor	68
4.1.1.2	Coupling of NPY Y ₂ receptor activation to the phospholipase C pathway	69
4.1.1.3	Flow cytometric calcium assay	70
4.1.1.4	Spectrofluorimetric calcium assay	70
4.1.2	Materials and Methods	71
4.1.2.1	Standard media and cloning procedures	71
4.1.2.2	Subcloning of pcDNA3.1/hygro-qi5	71
4.1.2.3	Transfection of CHO-hY2-K9 cells	74
4.1.2.4	Flow cytometric calcium assay	74
4.1.2.5	Spectrofluorimetric calcium assay	77
4.1.3	Results and discussion	79
4.1.3.1	Characterization of the transfectants using peptidic agonists in the flow cytometric calcium assay	79
4.1.3.2	Comparision of wild type and transfected CHO cells	80
4.1.3.3	Binding properties of the transfected cell line	81
4.1.3.4	Effect of solvents on intracellular calcium mobilization	81
4.1.3.5	Effect of the speed of injection	82
4.1.3.6	Characterisation of antagonists in the flow cytometric calcium assay	83
4.1.3.7	Spectrofluorimetric calcium assay	84
4.2	Aequorin assay	86
4.2.1	Introduction	86
4.2.2	Materials and Methods	90
4.2.2.1	Subcloning of pcDNA3.1/zeo-mtAEQ	90
4.2.2.2	Aequorin assay	91
4.2.2.2.1	<i>Stable transfection of CHO-hY₂-K9-qi5-K9 cells</i>	91
4.2.2.2.2	<i>Screening of the cell clones</i>	91
4.2.2.2.3	<i>Comparison of CHO-hY2-K9-qi5-K9-mtAEQ cell clones with respect to luminescence response upon pNPY-stimulation</i>	92
4.2.2.2.4	<i>Optimisation of assay parameters</i>	93
4.2.2.2.5	<i>Measurements with 2 injectors</i>	94
4.2.2.3	Analysis of mRNA expression of the transfected constructs by RT-PCR	94
4.2.2.4	Analysis of the dissociation kinetics of 2 replacing cy5-pNPY	95
4.2.3	Results	96
4.2.3.1	Selection of transfected cell clones	96
4.2.3.2	Optimisation of assay parameters	97
4.2.3.3	Aequorin agonist assay	100
4.2.3.4	Aequorin antagonist assay	101

4.2.3.5	Aequorin assay with two injectors	104
4.2.3.6	Comparison of mRNA expression by transfected cells	106
4.2.3.7	Antagonism of BIIIE0246	107
4.3	Other techniques to measure a calcium response in CHO-hY₂-K9-qi5-K9-mtAEQ-A7 cells ..	110
4.3.1	Introduction	110
4.3.2	Materials and methods	110
4.3.2.1	Confocal microscopy	110
4.3.2.2	Luminescence detection with CCD camera	111
4.3.3	Results	111
4.3.3.1	Confocal microscopy	111
4.3.3.2	CCD camera	112
4.4	Conclusions	114
5	BINDING AND FUNCTIONAL ASSAYS FOR THE NPY Y₄ RECEPTOR	115
5.1	Development of a flow cytometric binding assay for the rat NPY Y₄ receptor	116
5.1.1	Introduction	116
5.1.2	Materials and Methods	116
5.1.2.1	Cell culture	116
5.1.2.2	Y ₄ receptor ligands	117
5.1.2.3	Synthesis and purification of cy5-[K ⁴]-hPP and S0586-[K ⁴]-hPP	117
5.1.2.3.1	<i>Synthesis and purification of cy5-[K⁴]-hPP (10)</i>	118
5.1.2.3.2	<i>Synthesis and purification of S0586-[K⁴]-hPP (11)</i>	118
5.1.2.4	Flow cytometry	119
5.1.3	Results	119
5.1.3.1	Flow cytometric binding assay for the rat Y ₄ receptor	119
5.1.3.2	Binding affinity of cy5-[K ⁴]-hPP (10) to other NPY receptor subtypes	120
5.1.3.3	Screening of cell lines for binding of cy5-[K ⁴]-hPP (10)	121
5.2	Development of a flow cytometric binding assay for the human NPY Y₄ receptor	124
5.2.1	Introduction	124
5.2.1.1	Retroviral transduction	124
5.2.2	Materials and Methods	127
5.2.2.1	Standard cloning techniques in molecular biology	127
5.2.2.2	Subcloning of the pcDNA3-hY ₄ vector	127
5.2.2.3	Site-directed mutagenesis of pcDNA3-hY ₄	128
5.2.2.4	Transfection of CHO-K1 cells	129
5.2.2.5	Flow cytometric screening of transfected cells	130
5.2.2.6	Subcloning of the pQCXIP-hY ₄ and the QCXIP-S99A-hY ₄ vector	130
5.2.2.7	Transduction of P388-D1 cells	131
5.2.2.8	Cell sorting	132
5.2.2.9	Isolation of cell clones	132
5.2.2.10	Flow cytometric binding assay	133
5.2.3	Results and discussion	133
5.2.3.1	Transfection of CHO-K1 cells	133
5.2.3.2	Retroviral transduction of P388-D1 cells	135
5.3	Development of functional assays for the hY₄ receptor	138
5.3.1	Introduction	138
5.3.2	Materials and Methods	139
5.3.2.1	Y ₄ receptor ligands	139
5.3.2.2	Introduction of a stop-codon and subcloning of the pcDNA3-hY ₄ receptor	139
5.3.2.3	Transfection of CHO-K1 cells with the pcDNA3-hY ₄ vector	141
5.3.2.4	Screening of transfected cell clones for binding of cy5-[K ⁴]-hPP	141
5.3.2.5	Transfection of CHO-hY ₄ -K13b cells with pcDNA3.1/hygro-qi5	141
5.3.2.6	Screening of transfected cell clones for calcium response upon stimulation with hPP	142
5.3.2.7	Transfection of CHO-hY ₄ -K13b-qi5-K8 cells with pcDNA3.1/zeo-mtAEQ	142
5.3.2.8	Screening of transfected CHO-hY ₄ -K13b-qi5-K8 cell clones for aequorin luminescence signal upon stimulation with hPP	142
5.3.2.9	Aequorin assay	143
5.3.2.9.1	<i>Agonist assay</i>	143
5.3.2.9.2	<i>Antagonist assay</i>	143

5.3.2.9.3	<i>Measurement with 2 injectors</i>	143
5.3.2.10	Flow cytometric binding assay	144
5.3.2.11	Spectrofluorimetric calcium assay.....	144
5.3.2.12	Luminescence detection with CCD camera	144
5.3.2.13	Confocal microscopy.....	144
5.3.3	Results and discussion	145
5.3.3.1	Establishment of a stable cell clone co-expressing the hY ₄ receptor, the chimeric G protein qi5 and mitochondrial targeted apoaequorin	145
5.3.3.2	Aequorin assay with two injectors	149
5.3.3.3	Spectrofluorimetric fura-2 calcium assay	151
5.3.3.4	Low throughput screening.....	152
5.3.3.5	Luminescence detection with the CCD camera	156
5.3.3.6	Confocal microscopy.....	157
5.3.3.7	Transfection of CHO-rY ₄ cells with the qi5 construct	158
5.4	Conclusions	160
6	SUMMARY	161
	References	164

Abbreviations

AA	amino acid
AC	adenylyl cyclase
Ahx	6-aminohexanoic acid
AM-ester	acetoxymethylester
β -ACC	β -aminocyclopropanecarboxylic acid
BRET	bioluminescence resonance energy transfer
BSA	bovine serum albumin
cAMP	cyclic adenosinemonophosphate
cDNA	copy-DNA
CCD camera	charge coupled device camera
CHO cells	chinese hamster ovary cells
CRET	chemiluminescence resonance energy transfer
CSF	cerebral ventricular fluid
CTC model	cubic ternary complex model
CNS	central nervous system
cytAEQ	cytoplasmically targeted aequorin
DAG	diacylglycerol
DAD	dioden array detector
DAPI	4',6-diamidino-2-phenylindole
DEPC	diethylpyrocarbonate
DMF	dimethylformamide
DMSO	dimethylsulfoxide
DPP IV	dipeptidyl peptidase IV
Dpr	2,3-diaminopropionic acid
DTT	dithiothreitol
EC ₅₀	agonist concentration which induces 50% of the maximum effect
ECL	extracellular loop
EDTA	ethylenediaminetetraacetic acid (Ca ²⁺ -chelator)
EGF	epidermal growth factor
eGFP	enhanced green fluorescent protein
EGTA	ethyleneglycol-O, O'-bis(2-aminoethyl)-N, N, N', N'-tetracetic acid (Ca ²⁺ -chelator)
ER	endoplasmic reticulum
ESI-MS	electrospray ionisation mass spectrometry
eYFP	enhanced yellow fluorescent protein
FACS	fluorescence activated cell sorter
FCS	fetal calf serum
FITC	fluoresceinisothiocyanate
FI-1, FI-2, FI-3, FI-4	fluorescence channels of the flow cytometer
FLIPR	fluorescence imaging plate reader
FRET	fluorescence resonance energy transfer
FSC	forward scatter
G418	geneticin
GDP	guanosinediphosphate
GFP	green fluorescent protein
GI	gastrointestinal tract
GPCR	G-protein coupled receptor
GRK	G-protein coupled receptor kinase
GTP	guanosinetriphosphate
h, p, r, m, gp, z	in context with a receptor name: human, porcine, rat, mouse, guinea pig, zebrafish
HA	hemagglutinin
HEC-1B cells	human endometrial carcinoma cells
HEK 293 cells	human embryonic kidney cells

HEL cells	human erythroleukemia cells
HEPES	N-(2-Hydroxyethyl)piperazine-N'-(2-ethanesulfonic acid)
HPLC	high performance (pressure) liquid chromatography
IC ₅₀	antagonist concentration which suppresses 50% of an agonist induced effect
ICL	intracellular loop
IP ₃	inositoltrisphosphate
K _D	dissociation constant (binding assay, saturation curve)
K _i	dissociation constant (competition binding assay)
LB	Luria bertani broth (for <i>E. coli</i> culture)
MeCN	acetonitrile
mRNA	messenger RNA
mtAEQ	mitochondrial targeted aequorin
NHS	N-hydroxysuccinimide
NPY	neuropeptide Y
NMR	nuclear magnetic resonance
PBS	phosphate buffered saline
PCR	polymerase chain reaction
P _i	inorganic phosphate
PAO	phenylarsine oxide
PIP ₂	phosphatidylinositolbisphosphate
PIPES	piperazine-1,4-bis(2-ethanesulfonic acid)
PKA, PKC	protein kinase A, protein kinase C
PLC	phospholipase C
PMT	photomultiplier tube
PP	pancreatic polypeptide
PY	fish pancreatic peptide
PYY	peptide YY
RFU	relative fluorescence unit
RIA	radio immuno assay
RLU	relative luminescence unit
RNA	ribonucleic acid
RP	reversed phase
Rpm	revolutions per minute
RT	reverse transcription
RT-PCR	combined reverse transcription and polymerase chain reaction
SDS	sodiumdodecylsulfate
SEM	standard error of the mean
SDM	site-directed mutagenesis
SOC	salt optimized + carbon broth (for transformation of <i>E. coli</i>)
SPA	scintillation proximity assay
SSC	sideward scatter
TBE	tris-borat-EDTA-buffer
TFA	trifluoroacetic acid
TM	transmembrane domain
Tris	tris(hydroxymethyl)aminomethan
Y ₁ , Y ₂ , Y ₃ , Y ₄ , Y ₅ , Y ₆ , Y ₇	neuropeptide Y receptor subtypes

Chapter 1

General introduction

1.1 G-protein coupled receptors

G-protein coupled receptors (GPCRs) represent the most important class of qualified drug targets for pharmaceutical research and biomedical application. Approximately 60 % of all commercially available drugs work by selective modulation of distinct members of this target family (Gurrath, 2001). The GPCRs constitute one of the largest gene superfamilies of the human genome (Civelli *et al.*, 2001) encoded by approximately 720 genes (Malmstrom *et al.*, 2001; Wise *et al.*, 2004). The significance of GPCRs as drug targets lies in their physiological roles as cell-surface receptors responsible for transducing exogenous signals into cellular responses (Fang *et al.*, 2003) enabling the communication between individual cells, tissues or organs. Activators of GPCRs are manifold including light, odorants, ions, small molecules, peptides and proteins (Bockaert and Pin, 1999). Although there is little conservation at the amino acid level among GPCR sequences and despite a broad variation in biological responses, the GPCRs are believed to share a characteristic common receptor protein topology. Based on the crystal structure of bovine rhodopsin (Palczewski *et al.*, 2000; Schertler *et al.*, 1993; Unger *et al.*, 1997) several homology models exist for different GPCRs. The structure paradigm is a seven helix bundle that spans the cell membrane in an almost perpendicular orientation, thereby establishing a functional link between the extracellular space and the cytoplasm of the cell (Gurrath, 2001). The seven α -helical transmembrane regions consist of 20-25 amino acids connected sequentially by intracellular and extracellular loops with an extracellular amino terminus (N-terminus) and an intracellular carboxy terminus (C-terminus).

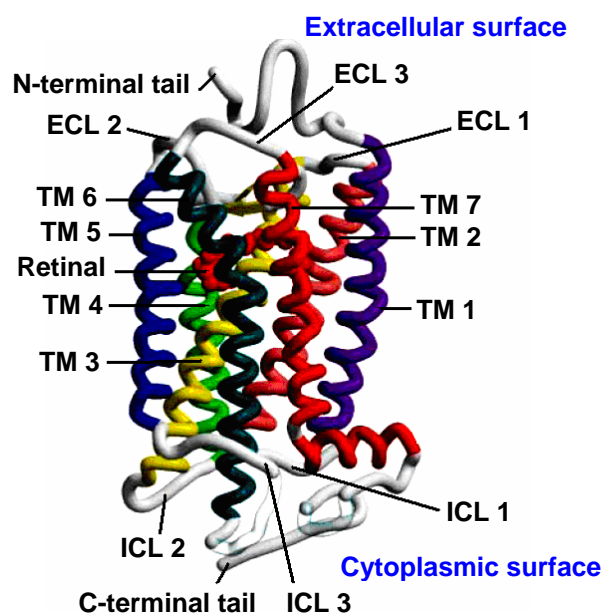


Fig. 1: Scheme of the structure of bovine rhodopsin, based on x-ray crystallographic analysis (adapted from (Ellis, 2004)). **ECL:** extracellular loop; **ICL:** intracellular loop; **TM:** transmembrane domain.

Upon extracellular binding of an agonist, the central core domain (7TM domain) is believed to undergo a conformational change depending on the GPCR type (Kristiansen, 2004) followed by an activation of the GDP-bound G-protein on the cytosolic side of the membrane. The G-protein is a heterotrimeric protein composed of a $G\alpha$ subunit and a $G\beta\gamma$ heterodimer. The agonist-promoted conformational change of the GPCR and subsequently of the G-protein itself leads to a release of GDP and binding of GTP at the α -subunit of the G-protein. GTP-binding causes the dissociation of the α -subunit from the $\beta\gamma$ -subunit and further activation of different effector proteins by the two complexes. The slow intrinsic GTPase activity of the α -subunit leads to a hydrolysis of GTP to GDP and P_i , thus terminating the $G\alpha$ -induced effector activation and allowing the re-association of the subunits to begin a new cycle.

At least 20 α -subunits, 6 β -subunits and 12 γ -subunits of G-proteins have been cloned and identified in mammals (Hamm, 1998; Kristiansen, 2004). According to structural and functional similarities of the α -subunits, G-proteins have been classified into four main families, namely the $G\alpha_s$, $G\alpha_{i/o}$, $G\alpha_{q/11}$ and $G\alpha_{12/13}$ (Cabrera-Vera *et al.*, 2003; Offermanns, 2003).

The $G\alpha_s$ subunit mainly activates adenylyl cyclase (AC) leading to an increased production of cAMP, whereas the $G\alpha_i$ -subunit decreases cAMP production by inhibition of the enzyme. The modulated concentration of the second messenger cAMP can affect various protein kinases or modify gene transcription, eventually activating the final physiological response of the cell to the original extracellular stimulus. Degradation of cAMP by phosphodiesterases may terminate the signal. All nine isoforms of the membrane bound AC can be activated to different extents (only very weak stimulation of AC9 (Premont *et al.*, 1996)) by forskolin, an agent commonly used in pharmacological studies to boost the cAMP production in the cell.

The $G\alpha_q$ -subunit mainly stimulates phospholipase C β (PLC β) catalyzing the cleavage of phosphatidyl-inositol-4,5-bisphosphate (PIP₂) to the second messengers diacylglycerol (DAG) and inositol-1,4,5-trisphosphate (IP₃). IP₃ binds to an IP₃ receptor, a ligand-gated calcium channel in the membrane of the endoplasmic reticulum, leading to a release of calcium ions into the cytoplasm. In addition, IP₃ is phosphorylated to inositol-1,3,4,5-tetrakisphosphate (IP₄) with multiple functions. IP₄ inhibits hydrolysis of IP₃ by inositol phosphate 5-phosphatase, enhances IP₃-induced store-operated Ca²⁺-entry and is supposed to act directly on unknown Ca²⁺ channels (Irvine, 2001).

However, in high concentrations IP_4 can act as an antagonist at the IP_3 receptor which may contribute to the termination of the calcium signal (Irvine, 2001). DAG activates protein kinase C, which in turn activates various intracellular proteins by phosphorylation. The signal is terminated by phosphorylation of DAG to phosphatidic acid, and dephosphorylation of IP_3 , which is then joined with phosphatidic acid to form PIP_2 again.

The proteins of the $G_{\alpha_{12/13}}$ family have recently been described to indirectly activate Rho GTPases via interaction with several guanine nucleotide exchange factors (Tanabe *et al.*, 2004). In addition to the activation of effectors by the G_{α} -subunits, it has been shown that the different $G_{\beta\gamma}$ heterodimers are also capable to interact with effector proteins, e.g. $PLC\beta$ (Katz *et al.*, 1992) or AC (Tang and Gilman, 1991).

Besides the described main signalling pathways of G-proteins, the mechanisms of signalling by G-proteins are much more complex and diverse (e.g. additional effectors or simultaneous functional coupling of GPCRs with distinct unrelated G-proteins), and the knowledge is still expanding, described in a variety of reviews (Cabrera-Vera *et al.*, 2003; Hermans, 2003; Kristiansen, 2004; Offermanns, 2003).

1.2 Receptor models

One of the earliest simple mechanistic models of receptor-ligand equilibria is the occupancy theory, established by Clark (Clark, 1933, 1937). Clark's model suggests that occupation of a receptor by a ligand (following the laws of mass action) can evoke an effect. In order to further differentiate drugs that simply occupied the receptor from those which, in addition, changed the receptor (to evoke a response), a proportionality factor (intrinsic activity) was added for the latter drugs (Ariens, 1954). Further extensions were made by the introduction of "efficacy" in order to make it more applicable to experimental pharmacology (Stephenson, 1956). With the discovery of the G-proteins (Sternweis *et al.*, 1981), the classical model has proven inadequate (Kenakin, 1989). Auxiliary membrane-associated proteins have been introduced in the mobile receptor hypothesis of Cuatrecasas (Cuatrecasas, 1974) and the ternary complex model (De Lean *et al.*, 1980). In the ternary complex model, the receptor (R) can interact with ligand (L) and G-Protein (G), leading to the four receptor species R, LR, RG and LRG existing in equilibrium. But this model, as the classical view, still considers agonist activation of the receptor as a prerequisite to G-protein activation, and can not account for effects as constitutive activity and inverse

agonism. Therefore, the two-state theory was introduced leading to the extended ternary complex model described below. The two-state model (Leff, 1995) describes an equilibrium between an active (R_a) and an inactive (R_i) conformation of a receptor. Because of the intrinsic property of the receptor, the receptor system can have basal constitutive activity in the absence of an agonist. If a ligand is added, the equilibrium of receptor states will be shifted towards the preferred conformation. The active state will be preferred by an agonist, whereas an inverse agonist will stabilize the inactive conformation. Neutral competitive antagonists will bind to both conformations and do not change the basal constitutive activity. Partial agonists will shift the equilibrium towards the active conformation to a minor extent compared to a full agonist.

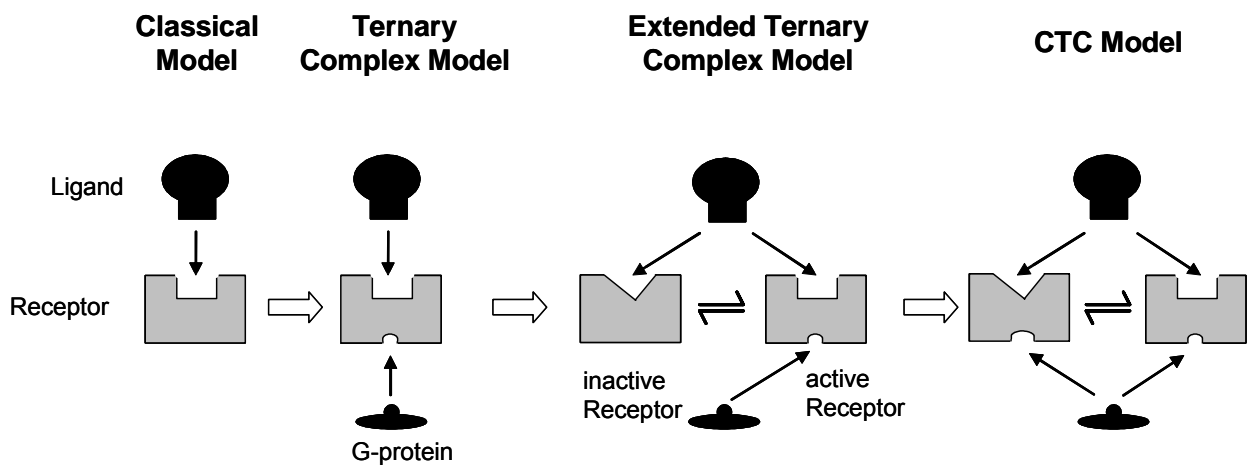


Fig. 2: Increasing complexity of different pharmacological models. Graph adapted from (Weiss *et al.*, 1996a).

In the extended ternary complex model (Samama *et al.*, 1993), the simple ternary complex model is extended by the two different receptor states, leading to the six possible receptor states R_i , R_a , LR_i , LR_a , R_aG and LR_aG . G-protein coupling and receptor activation are separate steps, and receptor activation is a necessary precondition for G-protein coupling (Weiss *et al.*, 1996a). In order to accomplish thermodynamic closure, the model was further extended to the cubic ternary complex model (CTC model) in which the inactive receptor state can also bind G-protein (Kenakin *et al.*, 2000; Weiss *et al.*, 1996a, b, c). As shown in Fig. 3, in the CTC model, eight receptor species exist in equilibrium.

Ligands can bind to four different receptor states. Agonists will favour the active states (R_a and R_aG) whereas inverse agonist will bind and stabilize the inactive receptor states (R_i and R_iG). Partial agonists exhibit affinity to both receptor states

with a preference for the active state, still causing receptor activation, whereas pure antagonists will not preferably bind to a distinct receptor state and will therefore not alter the basal constitutive activity of the system. In this model, the two receptor states R_aG and LR_aG are capable of signalling. However, it should be mentioned that because of the large numbers of terms describing the conversion of the receptor species (not shown for clarity reasons) and the lack of estimatability of the single constants, the CTC model has a descriptive role and is not amenable to the fitting of real data (Kenakin *et al.*, 2000).

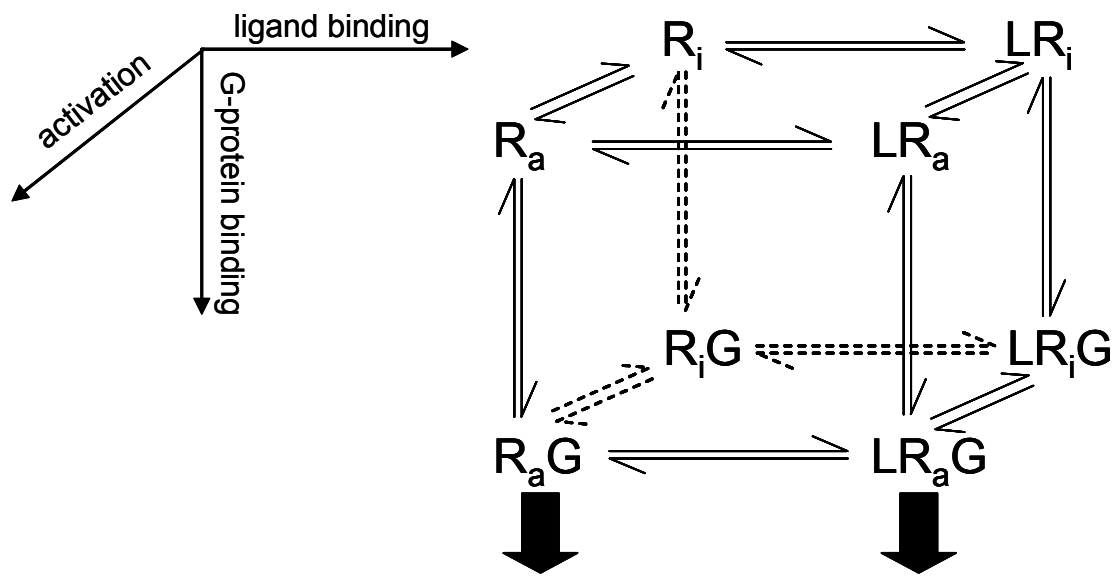


Fig. 3: Geometric representation of the CTC model, adapted from (Gurrath, 2001). R_i : inactive receptor; R_a : active receptor; L : ligand; G : G-protein; filled arrows mark complexes capable of signaling.

1.3 Pancreatic polypeptides and their receptors

The pancreatic polypeptide family consists of the three naturally occurring bioactive peptides neuropeptide Y (NPY), peptide YY (PYY) and pancreatic polypeptide (PP). PP was the first member isolated as a contaminant in chicken insulin (Kimmel *et al.*, 1968; Kimmel *et al.*, 1975) and later in extracts of bovine insulin (Lin and Chance, 1974). Because its function was unknown at that time, PP was named by its organ of origin. Seven years later, PYY was discovered while searching for C-terminally amidated peptides in the extracts of porcine intestine (Tatemoto, 1982b). Because of its flanking tyrosine residues it was named after the single letter abbreviation for tyrosine (Y). NPY was isolated in the same year from porcine brain using the same method as for PYY (Tatemoto, 1982a; Tatemoto *et al.*, 1982). An additional peptide related to the PP-family was found in the anglerfish (*Lophius* spp.) pancreas (Andrews *et al.*, 1985). The 37 amino acid non-amidated peptide was later shown to be the precursor form of the now named fish pancreatic peptide (PY), which actually consists of 36 amino acids exhibiting Y residues and C-terminal amidation (Balasubramaniam *et al.*, 1989). It seems that it has derived from a gene duplication of PYY only occurring in fish (Cerdeira-Reverter *et al.*, 1998; Cerdeira-Reverter and Larhammar, 2000; Larhammar, 1996).

The peptides NPY, PYY and PP are structurally closely related, consist of 36 amino acids each (with exception of chicken PYY consisting of 37 (Conlon and O'Harte, 1992) and Burmese python PP consisting of 35 amino acids (Larhammar *et al.*, 2004)) with an amidated carboxy-terminus and share a considerable amino acid homology (Table 1).

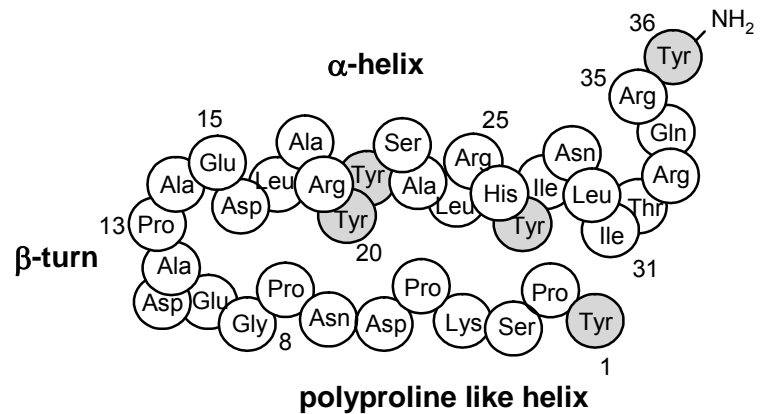
Table 1: Amino acid sequences of hNPY, hPYY and hPP. Amino acids which are homologous to the top sequence (hNPY) are shown in bold. The constant positions among all species (Larhammar, 1996) are underlined for each peptide.

hNPY	Y <u>P</u> <u>S</u> <u>K</u> <u>P</u> <u>D</u> <u>N</u> <u>P</u> <u>G</u> <u>E</u> <u>D</u> <u>A</u> <u>P</u> <u>A</u> <u>E</u> <u>D</u> <u>M</u> <u>A</u> <u>R</u> <u>Y</u> <u>Y</u> <u>S</u> <u>A</u> <u>L</u> <u>R</u> <u>H</u> <u>Y</u> <u>I</u> <u>N</u> <u>L</u> <u>I</u> <u>T</u> <u>R</u> <u>Q</u> <u>R</u> <u>Y</u> -NH ₂
hPYY	Y <u>P</u> <u>I</u> <u>K</u> <u>P</u> <u>E</u> <u>A</u> <u>P</u> <u>G</u> <u>E</u> <u>D</u> <u>A</u> <u>S</u> <u>P</u> E <u>E</u> <u>L</u> <u>N</u> <u>R</u> <u>Y</u> <u>Y</u> <u>A</u> <u>S</u> <u>L</u> <u>R</u> <u>H</u> <u>Y</u> <u>L</u> <u>N</u> <u>L</u> <u>V</u> <u>T</u> <u>R</u> <u>Q</u> <u>R</u> <u>Y</u> -NH ₂
hPP	A <u>P</u> <u>L</u> <u>E</u> <u>P</u> <u>V</u> <u>Y</u> <u>P</u> <u>G</u> <u>D</u> <u>N</u> <u>A</u> <u>T</u> <u>P</u> E <u>Q</u> <u>M</u> <u>A</u> <u>Q</u> <u>Y</u> <u>A</u> <u>A</u> <u>D</u> <u>L</u> <u>R</u> <u>R</u> <u>Y</u> <u>I</u> <u>N</u> <u>M</u> <u>L</u> <u>T</u> <u>R</u> <u>P</u> <u>R</u> <u>Y</u> -NH ₂

NPY is one of the most evolutionary conserved peptides known. Between mammals, only two of the 36 amino acids of NPY are variable, 22 positions are identical in all NPY sequences known (Larhammar, 1996). The second member of the pancreatic

polypeptide family is less conserved with eight variable amino acids between mammals, whereas PP is one of the least-conserved peptides known (Conlon, 2002). The tertiary structure of avian PP has been elucidated by X-ray crystallography (Blundell *et al.*, 1981), which could also be confirmed using NMR data for PYY (Keire *et al.*, 2000) and for the synthetic analogue [Leu³¹,Pro³⁴]-NPY (Khiat *et al.*, 1998). According to this PP-fold model, the amino acid residues 1-8 form a type II proline helix followed by a β -turn (residues 9-13). The α -helix formed by residues 14-31 runs roughly antiparallel to the polyproline helix forming a hydrophobic core by packing together nonpolar groups of these regions. The last four C-terminal amino acids form a flexible loop.

Fig. 4: Schematic structure of peptides of the PP-fold family (according to (Allen *et al.*, 1987)), shown for porcine NPY. Residues 1-8 form a polyproline helix followed by a β -turn and an α -helix comprised of the residues 15-30.



Because of the arrangement of the polyproline helix and the amphiphilic α -helix due to the hydrophobic interactions, the peptide forms a U-shaped conformation, the so-called PP-fold or hairpin structure. This folded structure results in a close association of the N- and the C-terminus of the molecule, an important feature for receptor recognition. Because of the high sequence homology, the PP-fold was also proposed for the structure of NPY (Allen *et al.*, 1987) and confirmed by 2D-NMR data (Darbon *et al.*, 1992). By contrast, a dimer of NPY in which the (bent) α -helices of the two NPY molecules form a handshake-type interaction with unordered N-terminal residues was described based on NMR studies (Cowley *et al.*, 1992; Monks *et al.*, 1996). However, covalently cross-linked antiparallel dimeric analogs of NPY did not facilitate the binding to the Y₂ receptor (Uegaki *et al.*, 1997) indicating that the dimeric state is not essential for the interaction with the receptor. A conformation equilibrium between hand-shake dimer and monomeric PP-fold has been described using CD spectroscopy data (Nordmann *et al.*, 1999) and it has been proposed that dimeric

NPY, which is abundant at high concentrations used for NMR studies may act in vivo at locally high concentrations as a slow-release form of active NPY monomers assuming the PP-fold. The dissociation of the NPY dimer at lower concentrations (in the low micromolar range) was also observed in FRET studies, but instead of the PP-fold, a less ordered structure was described for the monomer (Bettio *et al.*, 2002). The exact structure of NPY during the binding process still remains unclear, but it seems that interaction with the membrane before receptor binding plays an important role for the formation of the active conformation (Bader *et al.*, 2001).

1.3.1 Distribution and physiological effects of PP-fold peptides

1.3.1.1 Pancreatic polypeptide

The hormone PP is almost exclusively expressed in an endocrine cell type (PP cells) of the duodenal pancreas which is different from those that store insulin, glucagons or somatostatin (Schwartz, 1983; von Horsten *et al.*, 2004). PP cells are also found in the peripheral areas of the islet and within the exocrine portion and, more frequently, in the duodenal part of the pancreas (Ekblad and Sundler, 2002). In the gastrointestinal tract, PP cells are found in the gastric mucosa of opossum, cat and dog (Cox, 1998). In rat (El-Salhy *et al.*, 1983) and man (Tsutsumi, 1984) a few PP cells appear in the gastric mucosa for a short postnatal period only. The expression of PP in the adrenal gland is controversial. PP-immunoreactive cells in the rat adrenal medulla have been described (Malendowicz *et al.*, 1996; Vaillant and Taylor, 1981), but studies using well-defined antibodies in RIA failed to reveal any expression of PP in adrenal medullary cells of the rat (Miyazaki and Funakoshi, 1988). Contradictory results were also reported concerning the expression of PP in the central nervous system. In extracts from pig brain, PP has been found in several regions of the CNS by radioimmunoassays (Inui *et al.*, 1985) and PP mRNA has been detected in rat brain (Bhattacharya *et al.*, 1994; Whitcomb *et al.*, 1994). However, in other studies, no PP mRNA (Pieribone *et al.*, 1992) or peptide (Miyazaki and Funakoshi, 1988) could be detected in the rat brain. It has been suggested that the PP monitored in pig brain is rather of peripheral, mainly pancreatic origin (Fetissov *et al.*, 2004) as it was shown that radiolabelled PP can overcome the blood-brain barrier in mice (Banks *et al.*, 1995). Cross reactivity with other peptides of the NPY family might account for the discrepancies in the results (Ekblad and Sundler, 2002). Nevertheless, besides the controversial detection of PP peptide and its mRNA,

there are additional aspects discussed, suggesting that PP is expressed within some areas of the CNS (Whitcomb *et al.*, 1997). In contrast to plasma PP, the immunoreactive PP in the CSF did not increase in response to feeding, insulin hypoglycaemia or infusion of exogenous PP (Inui *et al.*, 1993) indicating a possible independent PP release from a central source.

The effects of pancreatic polypeptide are primarily found in the digestive tract. PP release by the pancreas in response to meals is primarily under vagal control (Schwartz *et al.*, 1976; Schwartz, 1983). Depending on dose, PP inhibits or stimulates gastric secretion, decreases gall bladder contraction, inhibits exocrine pancreatic secretion and suppresses gastric and upper intestinal motilities (for review see Hazelwood, 1993). In addition, PP has been found to inhibit ileum contractions (Feletou *et al.*, 1999) and stimulate colon contractions (Pheng *et al.*, 1999). Metabolic effects of PP include glycogenolysis, hyperglycerolemia, hypercholesterolemia, and a decrease in free fatty acid levels (Gehlert, 1998). As binding sites for PP have been found in several regions of the rat brain (Trinh *et al.*, 1996; Whitcomb *et al.*, 1997), central effects of PP are assumed. Centrally administered PP has been shown to stimulate feeding in rats (Campbell *et al.*, 2003; Clark *et al.*, 1984), mice (Asakawa *et al.*, 1999; Katsuura *et al.*, 2002) and dogs (Inui *et al.*, 1991), whereas peripherally administered PP induced negative energy balance in mice by decreasing food intake and gastric emptying while increasing energy expenditure (Asakawa *et al.*, 2003; Katsuura *et al.*, 2002; Moran, 2003). In another study, it has been reported that i.v. administered PP reduces appetite and food intake in humans (Batterham *et al.*, 2003).

1.3.1.2 Peptide YY

PYY is mainly expressed in endocrine cells throughout the mucosa of the terminal ileum, colon, and rectum (Cerdeira-Reverter and Larhammar, 2000; Ekblad and Sundler, 2002). Very few immunoreactive (to PYY) cells are found in the gastric, duodenal, or jejunal regions of the gut (Lundberg *et al.*, 1982). In contrast to all other gut peptides (except glicentin), the concentration of PYY along the gastrointestinal tract rises from stomach to rectum (Hazelwood, 1993). As PP, PYY is released in response to meals, unlike PP, vagal activity does not significantly contribute to its release. Beside intestinal endocrine cells, PYY has also been found in enteric neurons, islet cells of the pancreas and in the human adrenal glands (Ekblad and

Sundler, 2002). In the central nervous system, PYY-immunoreactive nerve cells have been found in several regions of the rat brain (Ekman *et al.*, 1986). Finally, PYY-immunoreactive material was detected by RIA in the lung of rat (Kraiczi *et al.*, 1997) and syrian golden hamster (Keith and Ekman, 1990).

The effects of PYY on the gastrointestinal tract are similar but more intense to those of PP. PYY causes a decrease in gastric acid secretion, gastric motility, exocrine pancreatic secretion, gall bladder activity, and intestinal motility (Hazelwood, 1993). In addition to these peripheral effects, PYY inhibits the secretion of fluid and electrolyte in the intestinal tract (Eto *et al.*, 1997). As PYY is a potent vasoconstrictor, it may be responsible for the re-distribution of blood flow during digestion (Gehlert, 1998). The expression of the polypeptide in the central nervous system indicates further neuronal functions. An anorectic effect of peripherally administered PYY₃₋₃₆, which is formed by cleavage of PYY by dipeptidylpeptidase IV (DPP IV) *in vivo*, was described for rat, mice and humans (Abbott *et al.*, 2005; Batterham *et al.*, 2002), but the published results are in question as most attempts to replicate and extend the reported effects of PYY₃₋₃₆ failed (Boggiano *et al.*, 2005; Tschop *et al.*, 2004).

1.3.1.3 Neuropeptide Y

NPY is one of the most abundant peptides within the CNS and sympathetic nervous system of mammals, although it has also been found in the parasympathic and the enteric nervous system (Sundler *et al.*, 1993). Within the central nervous system, the highest concentrations of NPY are found in the hypothalamus (Fetissov *et al.*, 2004; Hazelwood, 1993). NPY is co-stored and co-released with noradrenaline in brainstem as well as in peripheral postganglionic sympathetic fibres throughout the body (von Horsten *et al.*, 2004). Vast parts of the vasculature and various organ systems are innervated by NPY-containing fibres including pancreas, intestinal tract, heart, glands, thyroid, lung, kidney, and gonads (Gehlert, 1998; von Horsten *et al.*, 2004). Expression of NPY has been found in rat platelets (Myers *et al.*, 1988), whereas no NPY mRNA was detected in human and porcine bone marrow (Ericsson *et al.*, 1991). It has been proposed that the expression of the NPY gene in platelets of all species including humans is normally downregulated by unknown factors (von Horsten *et al.*, 2004).

NPY is one of the most potent orexigenic peptides known. After central administration, NPY induces an increase in food intake in several species (Berglund

et al., 2003a; Levens *et al.*, 2004; Pedrazzini *et al.*, 2003), whereas centrally administered antisense oligonucleotides against NPY reduce feeding in rats (Hulsey *et al.*, 1995). In obese Zucker rats (Dryden *et al.*, 1995) and during poor metabolic condition such as fasting (Sahu *et al.*, 1988), hypothalamic NPY and its mRNA are increased. Thus, NPY plays an important role in the regulation of appetite and obesity (Kalra and Kalra, 2004). Other effects of centrally administered NPY are decreased energy expenditure (Hwa *et al.*, 1999), thermogenesis (Lopez-Valpuesta *et al.*, 1996), anticonvulsant activity (Erickson *et al.*, 1996), inhibition of sedation (Naveilhan *et al.*, 2001), mood, and memory (Redrobe *et al.*, 2002b; Redrobe *et al.*, 2004; Thiele and Heilig, 2004). NPY has been suggested to play a role in neuronal development (Hansel *et al.*, 2001). It is involved in the regulation of reproduction by stimulation of luteinizing hormone-releasing hormone release (Kalra *et al.*, 1998) and it has been implicated in the circadian rhythm (Yannielli and Harrington, 2001). NPY acts as antinociceptive peptide in pain modulation (Broqua *et al.*, 1996; Wettstein *et al.*, 1995) and is proposed to be involved in the regulation of ethanol consumption (Silva *et al.*, 2002). NPY is a long-acting vasoconstrictor (Franco-Cereceda and Liska, 1998) and plays an important role in the central and peripheral regulation of cardiovascular function (Morris, 2004).

1.3.2 NPY receptors

Neuropeptide Y, peptide YY and pancreatic polypeptide exert their biological actions in mammals by interacting with at least five distinct G protein-coupled receptors designated Y₁, Y₂, Y₄, Y₅ and y₆ (Michel *et al.*, 1998). All these receptors have been cloned. Surprisingly, there is a very low sequence homology of 27-31 % between the different subtypes. In addition to the mammalian NPY receptor subtypes, there are several receptor subtypes reported in fishes, namely the Y_a, Y_b and Y_c receptors discovered in zebrafish (Starback *et al.*, 1999), and the Y₇ receptor found in zebrafish, frog and rainbow trout (Fredriksson *et al.*, 2004; Larsson *et al.*, 2005). Phylogenetic analyses show that the Y receptors can be separated into three subfamilies. Subfamily Y₁ consist of the Y₁, Y₄ and Y₆ receptors and the teleost fish Y_a, Y_b and Y_c receptors (Larhammar and Salaneck, 2004). Subfamily Y₂ includes the Y₇ receptor, while no additional members of the Y₅ family exist.

All NPY receptor subtypes belong to the class A, i.e. the rhodopsin-like GPCRs.

Table 2: Binding properties and signal transduction of NPY receptors

Receptor	Binding Profile	Selective Ligands	Signal transduction
Y ₁	NPY ≈ PYY ≈ [Leu ³¹ , Pro ³⁴]NPY > NPY ₂₋₃₆ > NPY ₃₋₃₆ ≥ PP > NPY ₁₃₋₃₆	[Phe ⁷ , Pro ³⁴]NPY ^a , BIBP3226 ^b , BIBO3304 ^b , SR120819A ^b , LY357897 ^b , J-115814 ^b , H 394/84 ^b	G _{i/o} inhibition of adenylyl cyclase; increase in intracellular [Ca ²⁺]
Y ₂	NPY ≥ NPY ₂₋₃₆ ≈ NPY ₃₋₃₆ ≈ NPY ₁₃₋₃₆ >> [Leu ³¹ , Pro ³⁴]NPY	NPY ₁₃₋₃₆ ^a , Ac-[Lys ²⁸ , Glu ³²]- (25-36)-NPY ^a , TASP-V ^a , T4-[NPY(33-36)] ₄ ^b , BIIE0246 ^b , JNJ-5207787 ^b	G _{i/o} inhibition of adenylyl cyclase; increase in intracellular [Ca ²⁺]
Y ₄	PP > PYY ≥ NPY > NPY ₂₋₃₆	PP ^a	G _i inhibition of adenylyl cyclase; increase in intracellular [Ca ²⁺]
Y ₅	NPY ≈ PYY ≈ NPY ₂₋₃₆ > hPP > [D-Trp ³²]NPY > NPY ₁₃₋₃₆ > rPP	[Ala ³¹ , Aib ³²]NPY ^a , CGP 71683A ^b , FR 233118 ^b , L-152,804 ^b	G _i inhibition of adenylyl cyclase; increase in intracellular [Ca ²⁺]
Y ₆	(^c) NPY ≈ PYY ≈ [Leu ³¹ , Pro ³⁴]NPY >> PP (^d) PP > [Leu ³¹ , Pro ³⁴]NPY > NPY ≈ PYY	-	inhibition of adenylyl cyclase
Y ₇	PYY > NPY > NPY ₂₋₃₆ > NPY ₁₃₋₃₆ >> [Leu ³¹ , Pro ³⁴]NPY, NPY ₁₈₋₃₆	-	inhibition of adenylyl cyclase

^a agonist; ^b antagonist; ^c according to (Weinberg *et al.*, 1996); ^d according to (Gregor *et al.*, 1996a)

The main signal transduction pathway of the NPY receptors is the coupling to pertussis toxin sensitive G proteins of the G_{i/o} family, leading to an inhibition of forskolin stimulated cAMP accumulation (Holliday *et al.*, 2004; Michel *et al.*, 1998). However, besides the predominant inhibition of adenylyl cyclase, elevation of the intracellular calcium concentration after Y receptor stimulation has been shown in cells natively expressing (Michel, 1998) as well as in cells heterologously expressing Y receptors (Bard *et al.*, 1995; Gerald *et al.*, 1995; Grouzmann *et al.*, 2001; Selbie *et al.*, 1995). But in contrast to the ubiquitous occurrence of cAMP signals, the Ca²⁺ response upon NPY receptor activation is very much dependent on the cell type (Holliday *et al.*, 2004). In addition, inhibition of cAMP formation and elevation of the intracellular calcium concentration can influence PKA and PKC, leading to an altered gating of ion channels, which can contribute to the constriction of vascular smooth muscle (Tanaka *et al.*, 1995) or anti-secretory actions in epithelial cells (Bouritius *et al.*, 1998). In neurons, direct interactions of Gβγ or Gα_{i/o} subunits with K⁺ and Ca²⁺ channels are discussed (Dascal, 2001).

1.3.2.1 The NPY Y₁ receptor

The Y₁ receptor was the first PP-fold peptide binding receptor to be cloned. It was found as a rat orphan receptor in 1990 (Eva *et al.*, 1990) and was later shown to be a Y₁ receptor based on its anatomical distribution (Krause *et al.*, 1992). The cloning of the human Y₁ receptor was first published in 1992 (Herzog *et al.*, 1992; Larhammar *et al.*, 1992). In contrast to the other PP-fold receptors, the coding region of the Y₁ gene harbors an 100 bp intron after TM5 (Herzog *et al.*, 1993a). This intron has been shown to enhance the expression of Y₁ and Y₅ receptors in vitro (Marklund *et al.*, 2002). In humans the Y₁ receptor is a 384-amino acid protein. Across all species, the Y₁ receptor displays greater than 95 % amino acid sequence identity in the transmembrane regions (Larhammar *et al.*, 2001).

The pharmacological profile of the Y₁ receptor is characterized by high affinity for NPY and PYY and a low affinity for PP (Cabrele and Beck-Sickinger, 2000). Truncation of the N-terminal part of NPY leading to NPY₂₋₃₆ or NPY₃₋₃₆ or NPY₁₃₋₃₆ results in a distinct decrease in affinity to the Y₁, but not to the Y₂ receptor. By contrast, Pro³⁴-substituted analogs of NPY and PYY (e.g. [Pro³⁴]NPY or [Leu³¹,Pro³⁴]NPY) retain their high affinity for the Y₁ but not for the Y₂ receptor (Krause *et al.*, 1992; Rose *et al.*, 1995). However, the NPY analogs [Pro³⁴]NPY and [Leu³¹,Pro³⁴]NPY have still high affinity to the Y₅ receptor (Gerald *et al.*, 1996). Therefore, many more analogues of NPY were developed to further increase the Y₁ receptor selectivity including the exchange of some residues with D-amino acids and the synthesis of shortened and cyclized NPY derivatives (Mullins *et al.*, 2001). The most significant preference for the Y₁ receptor was obtained with [Phe⁷,Pro³⁴]NPY (Soll *et al.*, 2001). In addition, N-terminally shortened cyclic peptides (Takebayashi *et al.*, 2000) and linear peptides containing β-ACC (β-aminocyclopropanecarboxylic acid) building blocks in position 32 and 34 (Koglin *et al.*, 2003) have been reported to show high Y₁ receptor affinity and selectivity despite the lack of the NPY N-terminus.

Although short N-terminally truncated analogs of NPY are poor ligands at the Y₁ receptor, some C-terminally modified nonapeptides of NPY have been found to antagonize the NPY-induced increase in the intracellular calcium concentration in HEL cells with IC₅₀ values in the low nanomolar range. Their sequences are INPIXRLRY, where X can be F, (4-Ph)-F, or (2,6-dichloro-benzyl)-Y, or INPXRYRLRY, where X is Aib (aminoisobutyric acid), or INXIYRLRY, where X is (3,4-dehydro)-P (Cabrele and Beck-Sickinger, 2000). The homodimeric peptide GW1229, also called

GR231118 or 1229U91, is another N-terminally truncated analogue of NPY with high affinity to the Y_1 receptor. It consists of the two nonapeptides IEPXYRLRY, where X is 2,3-diaminopropionic acid (Dpr) and which are connected by two E-Dpr lactam bridges. The peptide is an antagonist at the Y_1 receptor but also an agonist with high affinity at the Y_4 receptor (Daniels *et al.*, 1995; Parker *et al.*, 1998).

The first nonpeptidic Y_1 receptor antagonist described in the literature was the H_2 receptor agonist BU-E-76 (HE 90481) with a pA_2 value of 4.43 in a Ca^{2+} assay using HEL cells (Michel and Motulsky, 1990). Later, more potent antagonists have been synthesized, e.g. the (R)-argininamides BIBP3226 (Rudolf *et al.*, 1994) and BIBO3304 (Wieland *et al.*, 1998). The first orally active Y_1 antagonist, SR120819A (Serradeil-Le Gal *et al.*, 1995) has been described in 1995. Furthermore, trisubstituted indoles as LY357897 (Hipskind *et al.*, 1997) and 1,3-disubstituted benzodiazepines (Murakami *et al.*, 1999) have been characterized as potent, selective Y_1 antagonists. The morpholinopyridine J-115814 (Kanatani *et al.*, 2001) and the dihydropyridine derivative H 394/84 (Malmstrom *et al.*, 2001) were also able to block the Y_1 receptor. Recently, a new class of tetrahydrocarbazole derivatives with modest antagonistic activity at the Y_1 receptor was published (Di Fabio *et al.*, 2006).

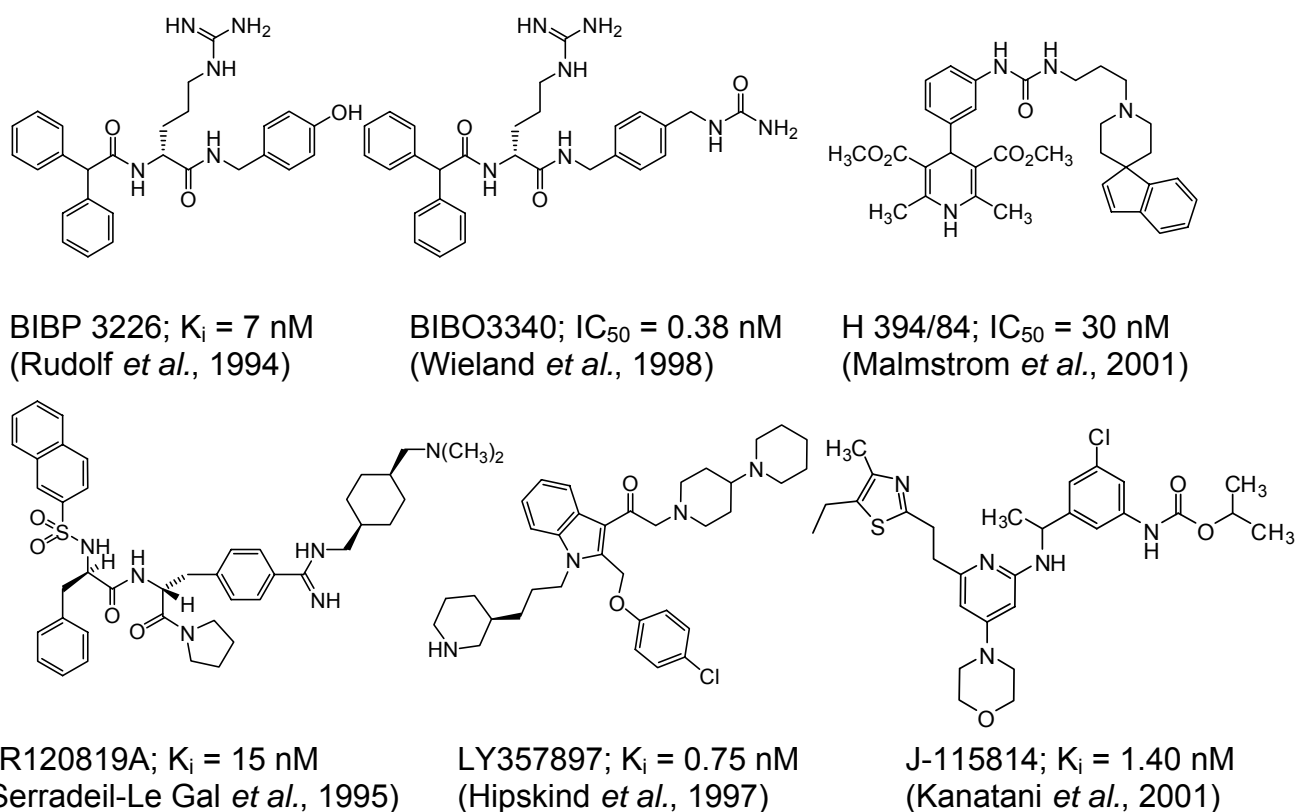


Fig. 5: Various NPY Y_1 receptor antagonists.

A detailed review on Y_1 antagonists was given by Brennauer and co-workers (Brennauer *et al.*, 2004). The Y_1 mRNA distribution has been determined in man, rat, mouse and has been investigated in brain, heart, kidney and the gastrointestinal tract (Larsen *et al.*, 1993; Nakamura *et al.*, 1995; Wharton *et al.*, 1993). In rat brain, Y_1 protein and mRNA have been reported in the cerebral cortex, hippocampus, thalamus, as well as in the hypothalamus (Fetissov *et al.*, 2004; Kopp *et al.*, 2002). NPY Y_1 receptors are also located in blood vessels (Franco-Cereceda and Liska, 1998), the amygdala (Silva *et al.*, 2002) and human adipocytes (Serradeil-Le Gal *et al.*, 2000). Among the NPY functions, the Y_1 receptor is responsible for the most vascular effects (Capurro and Huidobro-Toro, 1999; Franco-Cereceda and Liska, 1998; Wiest *et al.*, 2006) and antinociceptive effects (Zhang *et al.*, 2000), as well as decreased anxiety (Wahlestedt *et al.*, 1993) and depression (Redrobe *et al.*, 2002a). The Y_1 receptor seems also to be implicated in the regulation of feeding (Kanatani *et al.*, 2001; Mullins *et al.*, 2001), ethanol intake (Schroeder *et al.*, 2003) and arousal (Naveilhan *et al.*, 2001).

Y_1 receptors are constitutively expressed in human erythroleukemia (HEL) (Motulsky and Michel, 1988) and in neuroblastoma SK-N-MC (Aakerlund *et al.*, 1990) cells. Y_1 receptor activation leads to the inhibition of adenylyl cyclase and to an increase in the intracellular Ca^{2+} concentration. It has been proposed that the calcium response in HEL cells is preferentially mediated by the $G_{\alpha_{i3}}$ protein (Michel, 1998) as the calcium response as well as the $G_{\alpha_{i3}}$ expression is reduced after treatment of HEL cells with DMSO. The involvement of a $PLC\beta$ independent pathway (Motulsky and Michel, 1988) as well as the activation of $PLC\beta$ (Daniels *et al.*, 1992) have been described for HEL cells. In rabbit mesenteric small arteries, Y_1 receptor activation (blocked by BIBP 3226) inhibits forskolin stimulated cAMP formation, increases intracellular calcium concentration and potentiates the actions of co-released noradrenaline (Prieto *et al.*, 2000). In a recent review, the basal $G_{q/11}$ tone has been proposed to be decisive for the coupling of activated Y_1 receptors to $PLC\beta$ (Holliday *et al.*, 2004).

Y_1 receptor desensitization has been observed in isolated arterioles (Van Riper and Bevan, 1991) and in cells expressing endogenous or transfected Y_1 receptors (Gicquiaux *et al.*, 2002; Michel, 1994). For the desensitization of Ca^{2+} responses in HEL cells, a role for PKC is proposed (Daniels *et al.*, 1992), whereas in cells and tissues, where the predominant Y receptor response is an inhibition of adenylyl cyclase, a recruitment of GPCR kinases (GRKs) through $G\beta\gamma$ subunits followed by

phosphorylation of activated receptors and subsequent binding of a member of the β -arrestin family is discussed (Holliday *et al.*, 2004).

The Y_1 receptor shows a considerable agonist-driven internalization, which has been determined by radioligand binding (Parker *et al.*, 2001b), confocal microscopy with fluorescent ligands (Fabry *et al.*, 2000) or with GFP tagged Y_1 receptor (Gicquiaux *et al.*, 2002).

1.3.2.2 The NPY Y_2 receptor

Originally, the Y_2 receptor was postulated based on pharmacological studies with amino terminally truncated fragments of NPY and PYY, such as NPY₃₋₃₆ and NPY₁₃₋₃₆, using vascular preparations (Wahlestedt *et al.*, 1986). In contrast to the Y_1 receptor, the truncated peptides were full agonists with similar potency as the native peptides at the postulated Y_2 receptor. Further peptidic agonists are the cyclic NPY analogues Ac-[Lys²⁸,Glu³²](25-36)-NPY (cyclized by lactamization of the substituted residues) (Rist *et al.*, 1996) and Cyclo S-S [Cys²⁰,Cys²⁴]-pNPY (Soll *et al.*, 2001) or TASP-V (Malis *et al.*, 1999), a molecule composed of a cyclic template connecting two C-terminal fragments NPY₂₁₋₃₆.

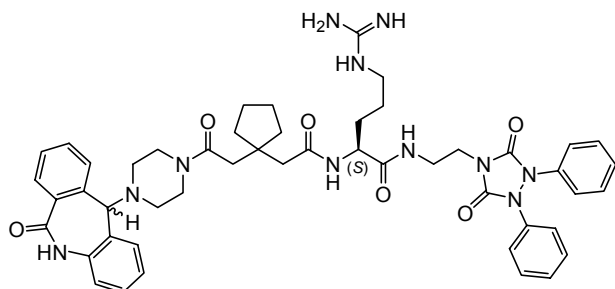
On the other hand, when positions 31 and 34 of NPY or PYY are replaced with the corresponding amino acids of PP (L and P), the resulting peptides show much lower affinity to the Y_2 receptor, indicating that the C-terminal part is more important for binding at this receptor (Fuhlendorff *et al.*, 1990). Even the single replacement at position 34 of NPY or PYY abolished the high affinity to the Y_2 receptor (Potter *et al.*, 1991).

The Y_2 receptor cDNA was first cloned in 1995 from human SMS-KAN cells (Rose *et al.*, 1995) and subsequently from human brain cDNA libraries (Gehlert *et al.*, 1996a; Gerald *et al.*, 1995) and the human neuroblastoma cell line KAN-TX (Rimland *et al.*, 1996). A peripheral PYY-preferring receptor mediating an inhibition of small intestinal secretion has been shown to be a Y_2 receptor (Goumain *et al.*, 2001). In man the Y_1 receptor is a 381-amino acid protein, which is, like the Y_1 receptor, highly conserved between species with more than 90 % identity between different orders of mammals (Berglund *et al.*, 2003a). However, compared to the Y_1 and Y_4 receptors, the Y_2 receptor shows only 30 % homology.

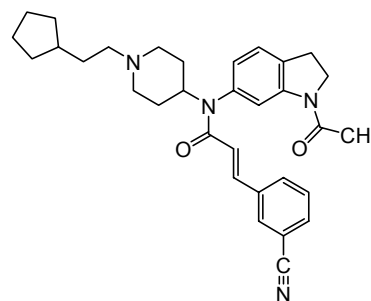
The Y_2 receptor is naturally expressed in SMS-KAN (Shigeri and Fujimoto, 1994), LN319 (Beck-Sickinger *et al.*, 1992), CHP234 (Lynch *et al.*, 1994) and SH-SY5Y (Connor *et al.*, 1997) cells. In addition, Y_2 -like responses have been found in rat

neurons (Bleakman *et al.*, 1991; Wiley *et al.*, 1993). The major signal transduction pathway is an inhibition of adenylyl cyclase (Michel *et al.*, 1998), but also other pathways, e.g. inhibition of Ca^{2+} release from intracellular stores (Shigeri and Fujimoto, 1994) or Ca^{2+} influx (Lynch *et al.*, 1994) as well as Ca^{2+} release from intracellular stores (Perney and Miller, 1989) are described. The increase in the intracellular calcium concentration after activation of cells heterologously expressing the Y_2 receptor is discussed controversially (see 4.1.1.2), but seems to be largely dependent on the cell type used.

The TASP molecule $T_4\text{-[NPY(33-36)]}_4$, consisting of four truncated NPY fragments attached to a cyclic carrier molecule, has been shown to be a selective antagonist at the Y_2 receptor (Grouzmann *et al.*, 1997). In 1999, the first nonpeptide ligands, the L-arginine derivative BIEE 0246 and related compounds were reported to be potent and selective Y_2 receptor antagonists (Brennauer *et al.*, 2004; Doods *et al.*, 1999; Dumont *et al.*, 2000). Recently, JNJ-5207787, a new selective Y_2 receptor antagonist with nanomolar affinity was synthesized (Bonaventure *et al.*, 2004; Jablonowski *et al.*, 2004).



BIEE0246; $IC_{50} = 3.3$ nM
(Doods *et al.*, 1999)



JNJ-5207787; $IC_{50} = 100$ nM
(Bonaventure *et al.*, 2004)

Fig. 6: Nonpeptidic Y_2 receptor antagonists.

The Y_2 receptor is predominantly located presynaptically, acting as an autoreceptor by inhibiting further release of NPY and other neurotransmitter (King *et al.*, 2000; Smith-White *et al.*, 2001; Wahlestedt *et al.*, 1986). It is mainly expressed in the brain (Kaga *et al.*, 2001), preferentially the hippocampus, but low expression has also been found in the gastrointestinal tract, in blood vessels and other peripheral tissue (Goumain *et al.*, 1998; Goumain *et al.*, 2001; Pheng *et al.*, 1997; Zhang *et al.*, 1997). As the Y_2 receptor acts mainly as an autoreceptor, it modulates predominantly the

effects caused by the Y_1 receptor. Hence, Y_2 receptor activation by centrally released NPY increases anxiety (Nakajima *et al.*, 1998) and arousal as well as blood pressure, which is decreased after activation of central Y_1 receptors (Morton *et al.*, 1999). In addition, the Y_2 receptor can directly mediate vascular effects of NPY (Malmstrom, 2001; Smith-White *et al.*, 2002). The Y_2 receptor plays a role in NPY-induced angiogenesis (Zukowska-Grojec *et al.*, 1998) and NPY-mediated effects on circadian rhythms (Golombek *et al.*, 1996; Huhman *et al.*, 1996). In the central nervous system, Y_2 receptor agonists delay gastric emptying (Fujimiya *et al.*, 2000; Ishiguchi *et al.*, 2001). Experiments with Y_2 receptor knockout mice have shown that this receptor is also involved in the regulation of bone formation (Baldock *et al.*, 2002), heart rate and food intake (Lin *et al.*, 2004). The potential anorectic effect of the Y_2 receptor agonist PYY₃₋₃₆ is discussed in section 1.3.1.2. The Y_2 receptor seems also be implicated in the modulation of ethanol consumption (Cowen *et al.*, 2004; Thiele *et al.*, 2004). Desensitization of the Y_2 receptor after stimulation with NPY was observed in LN319 cells (Grouzmann *et al.*, 2001), but unlike the Y_1 receptor, the Y_2 receptor is not internalized after prolonged agonist stimulation (Gicquiaux *et al.*, 2002; Parker *et al.*, 2001b) or is internalized very slowly.

Based on pharmacological studies on mammalian tissues, the existence of another receptor subtype, designated as Y_3 , with the preferred peptide potency of NPY>NPY₁₃₋₃₆>PYY has been proposed (Lee and Miller, 1998; Michel *et al.*, 1998). Y_3 receptor-like binding sites were found in human adrenal medulla where it mediates the NPY-induced secretion of catecholamines, in the rat nucleus tractus solitarius, in rat cardiac membranes, and in bovine chromaffin cells (Silva *et al.*, 2002). The peptide NPY₁₈₋₃₆ has been described to appear as an antagonist for the Y_3 receptor mediated inhibition of isoproterenol-stimulated adenylyl cyclase activity of rat cardiac ventricular membranes (Balasubramaniam and Sheriff, 1990; Balasubramaniam *et al.*, 1990). However, cloning of the receptor failed (Herzog *et al.*, 1993b; Jazin *et al.*, 1993), and with the sequencing of the human genome it seems unlikely that such a protein exists. The observed results may be due to the involvement of homo- or heterodimerization of the known NPY receptors, which was described for the hY₁, hY₂ and hY₅ (Dinger *et al.*, 2003) as well as for the rhY₄ (Berglund *et al.*, 2003b) receptor or explained by ligand preferences induced by interactions with intracellular proteins such as G proteins.

1.3.2.3 The NPY Y₄ receptor

The third cloned human receptor of the PP-fold family was identified in 1995 and first called “PP1” receptor (Bard *et al.*, 1995; Lundell *et al.*, 1995) because of its high affinity for PP. Later, the Y₄ receptor homologs of other species, e.g. rat (Lundell *et al.*, 1996; Walker *et al.*, 1997; Yan *et al.*, 1996) or mouse (Gregor *et al.*, 1996b), were cloned. The highest homology within the PP-fold family of receptors was found with the Y₁ receptor (42 % identity), but the most interesting feature of the Y₄ receptor is its low degree of sequence identity between species. The human and rat Y₄ sequences share only 75 % identity (Lundell *et al.*, 1996). Apparently, the Y₄ receptor and its favoured ligand PP co-evolved very rapidly to the present state in mammals (Larhammar and Salaneck, 2004). This is also reflected by the fact that PPs from other species have often much lower affinity to the Y₄ receptor, e.g. aPP has a > 40-fold lower affinity for the hY₄ receptor compared to hPP (Gehlert *et al.*, 1996b). NPY and PYY bind poorly to the rat Y₄, better to the human Y₄, and with high affinity to the native rabbit PP receptor (Parker *et al.*, 2001a) or to the cloned chicken Y₄ receptor (Lundell *et al.*, 2002). In addition, the affinity for the rat receptor increases when position 34 of NPY or PYY is replaced by proline, whereas the human receptor is unaffected by this exchange (Berglund *et al.*, 2003a). A unique feature of the hY₄ receptor is its very high affinity for hPP (Lundell *et al.*, 1995) and a lower affinity for NPY, whereas the data vary widely with K_i values for NPY ranging from 2 nM (Bard *et al.*, 1995) to > 1 μM (Voisin *et al.*, 2000). The large variations may be explained by the use of different radioligands, as it has been shown that the frequently used ¹²⁵I-PYY appears to recognize only a fraction of the receptor population recognized by ¹²⁵I-PP (Berglund *et al.*, 2001).

The Y₁ receptor antagonist GW1229 has been shown to be an agonist at the human Y₄ receptor (Parker *et al.*, 1998; Schober *et al.*, 1998). Nonapeptide analogues related to GW1229 have been shown to have reasonable affinities for the hY₄ receptor without inhibiting cAMP formation, indicating an antagonism. However, none of those peptides exhibited significant antagonistic activity in a cAMP assay with Y₄ receptor expressing cells at a concentration of 100 nM (Balasubramaniam *et al.*, 2001). Recently, the peptide VD-11 (differing from GW1229 only by C-terminal oxymethylation) has been proposed for a Y₄ receptor antagonist, as it did not promote the internalization of ¹²⁵I-labeled hPP, which was observed for other Y₄ receptor agonists (Parker *et al.*, 2005). In addition, VD-11 did not (or only to a small

degree) inhibit forskolin-stimulated cAMP formation nor stimulate [³⁵S]GTP- γ -S binding (Parker *et al.*, 2005). However, in a cAMP assay of a former study, the peptide (100 nM) was not able to shift the concentration-response curve of PP rightwards (Balasubramaniam *et al.*, 2001). Several PP/NPY chimera with high affinity to the hY₄ receptor have been synthesized, but these peptides are non-selective, since they also bind to the Y₅ receptor (Cabrele *et al.*, 2001). Up to now, no nonpeptidic ligand for the Y₄ receptor is known.

The hY₄ receptor is mainly expressed in the prostate, the colon and the small intestine (Lundell *et al.*, 1995), where it is believed to mediate many of the PP-produced gastrointestinal effects (Pheng *et al.*, 1999). Y₄ receptor binding sites and low mRNA levels are found in various human CNS regions (Fetissoff *et al.*, 2004; Lundell *et al.*, 1995). As intracerebroventricular injection of GW1229 induced a release of luteinizing hormone (Raposinho *et al.*, 2000), the Y₄ receptor has been proposed to be involved in the regulation of reproduction, but later it was shown that this effect is also observed in Y₄ receptor deficient mice (Raposinho *et al.*, 2004a). As PP reduces appetite in humans (Batterham *et al.*, 2003) and food intake in mice (Asakawa *et al.*, 1999; Asakawa *et al.*, 2003; Katsuura *et al.*, 2002), the Y₄ receptor, which is also expressed in orexin neurons of the hypothalamus (Campbell *et al.*, 2003), might be involved in appetite regulation (Moran, 2003).

In terms of agonist-promoted desensitization and internalization, the published results are contradictory. No desensitization and internalization was observed in hY₄ receptor expressing CHO cells (Voisin *et al.*, 2000), whereas considerable internalization was observed by Parker and co-workers (Parker *et al.*, 2005; Parker *et al.*, 2001b).

Activation of the Y₄ receptor leads to an inhibition of adenylyl cyclase, which is sensitive to pertussis toxin (Voisin *et al.*, 2000). An increase in intracellular calcium concentrations was observed in LMTK⁻ cells stably expressing the hY₄ receptor. Functional assays for the Y₄ receptor are discussed in detail in section 5.3.1.

1.3.2.4 The NPY Y₅ receptor

The existence of a Y₅ receptor was first proposed based on the observation that NPY and NPY₂₋₃₆ produced a large increase in feeding after intracerebroventricular administration (Stanley *et al.*, 1992), whereas the NPY analogue [D-Trp³²]NPY selectively inhibited NPY-induced feeding (Balasubramaniam *et al.*, 1994) despite its

low affinity for the Y₁ and Y₂ receptors (Balasubramaniam *et al.*, 1996). Expression cloning of the Y₅ receptor from rat hypothalamus was published in 1996 (Gerald *et al.*, 1996; Hu *et al.*, 1996). The receptor is the largest protein of the PP-fold family of receptors, consisting of 445 amino acids in humans. It contains an extended third cytoplasmatic loop with about 100 amino acids more compared to the other NPY-receptors. The genes for the Y₁ and Y₅ receptors are located on the same human chromosome, overlapping each other, which suggest an at least partially coordinated regulation of gene expression (Herzog *et al.*, 1997). The Y₅ receptor is well conserved with 88-90 % overall amino acid identity (Borowsky *et al.*, 1998; Lundell *et al.*, 2001) but shares low homology (approximately 30 %) with the Y₁ or Y₂ receptors (Larhammar and Salaneck, 2004).

The Y₅ receptor binds all three endogenous ligands, their long C-terminal fragments and Pro³⁴-substituted ligands. Interestingly, rat PP has very low affinity to the rat and human Y₅ receptor, whereas human and bovine PP had affinities similar to those of NPY and PYY (Borowsky *et al.*, 1998; Gerald *et al.*, 1996). The first Y₅ selective agonist [Ala³¹,Aib³²]NPY (Aib = aminoisobutyric acid), synthesized in 2000 (Cabrele *et al.*, 2000) was active in a cAMP assay and was also able to induce feeding in rats. In addition, two selective, peptidic radioligands, [¹²⁵I][hPP¹⁻¹⁷,Ala³¹,Aib³²]NPY (Dumont *et al.*, 2003) and [¹²⁵I][cPP¹⁻⁷,NPY¹⁹⁻²³,Ala³¹,Aib³²,Gln³⁴]hPP (Dumont *et al.*, 2004) were characterized. The first selective Y₅ receptor antagonist was disclosed in 1997 (Criscione *et al.*, 1997). CGP 71683A showed a >1000-fold affinity to the Y₅ receptor compared to the Y₁, Y₂ and Y₄ subtypes (Criscione *et al.*, 1998). Various studies using this compound for the blockade of the Y₅ receptor in vivo have been performed in order to determine the involvement of the Y₅ receptor in feeding (Criscione *et al.*, 1998; Duhault *et al.*, 2000; Kask *et al.*, 2001; Polidori *et al.*, 2000), but due to its unfavourable properties (poor solubility, toxic side effects) and considerable affinity to other neurotransmitter receptors (e.g. muscarinic receptors and serotonin transporters) the compound was found to be an imprecise tool for the investigation of the role of the Y₅ receptor in the regulation of food consumption (Della Zuana *et al.*, 2001). A variety of analogues of CGP 71683A and other heterocyclic Y₅ receptor antagonists have been synthesized (for a recent review see Brennauer *et al.*, 2004). The expression of the Y₅ receptor is mainly confined to the brain, primarily the hypothalamus, hippocampus and amygdala (Durkin *et al.*, 2000; Fetissov *et al.*, 2004; Parker and Herzog, 1998, 1999). The highest level of receptor

expression in the periphery was found in spleen, testis and pancreas (Gerald *et al.*, 1996; Goumain *et al.*, 1998; Statnick *et al.*, 1998). Studies with Y₅ receptor agonists (Cabrele *et al.*, 2000; Mashiko *et al.*, 2003; Parker *et al.*, 2000), knock-out animals (Kanatani *et al.*, 2000b) and antisense knock-down (Schaffhauser *et al.*, 1997) revealed that the Y₅ receptor contributes to the regulation of feeding behaviour but is not the only receptor involved.

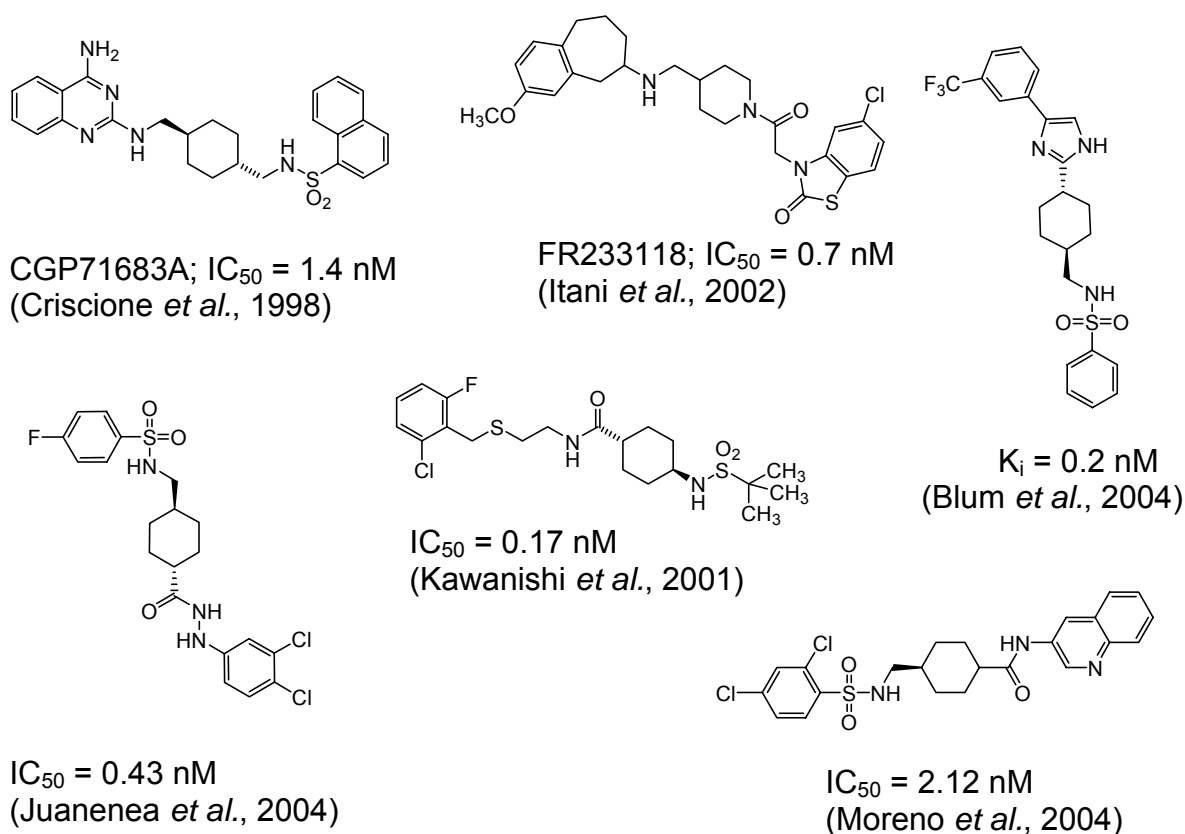


Fig. 7: Various Y₅ receptor antagonists.

In fact, Y₅ receptor deficient mice show no hypophagic phenotype but even develop mild obesity (Marsh *et al.*, 1998). In addition, some Y₅ selective antagonists failed to inhibit food intake (Turnbull *et al.*, 2002). Because of the contradictory results, the importance of the Y₅ receptor in feeding behaviour is controversially discussed (Levens *et al.*, 2004; Raposinho *et al.*, 2004b). Other effects of Y₅ receptor activation are inhibition of luteinizing hormone release (Raposinho *et al.*, 2001), decrease of energy expenditure (Mashiko *et al.*, 2003), and regulation of circadian rhythms (Yannielli *et al.*, 2004), seizures (Woldbye and Kokaia, 2004) and brain excitability (Guo *et al.*, 2002).

The Y₅ receptor heterologously expressed in HEC-1-B cells couples to an inhibition of adenylyl cyclase (Bischoff *et al.*, 2001; Moser *et al.*, 2000) but can also couple to

an increase in intracellular calcium concentration when expressed in LMTK cells (Criscione *et al.*, 1998; Kanatani *et al.*, 2000a). Therefore, the signal transduction pathway seems to depend on the used cell line. Recently, endogenous expression of the Y_1 , Y_2 , and Y_5 receptor has been described in SK-N-MC cells (Li and Ritter, 2005).

1.3.2.5 The NPY y_6 receptor

The y_6 receptor was cloned in 1996 from a mouse genomic library and first designated as “Y5” or “PP2” (Gregor *et al.*, 1996a; Weinberg *et al.*, 1996). Homologous receptors were cloned from human, rabbit and monkey libraries (Matsumoto *et al.*, 1996) and different designations were used before the subtype was renamed the y_6 receptor (Michel *et al.*, 1998). The receptor is functional expressed in rabbit and mouse, while no y_6 gene was detected in rat (Burkhoff *et al.*, 1998). In humans and other primates, the receptor is non-functional because of a frameshift mutation (single base deletion) in the third intracellular loop causing an in-frame stop codon after the 6th transmembrane region, leading to a truncated receptor protein, unable to bind any peptides of the PP-fold family (Rose *et al.*, 1997). The y_6 receptor is presumably a transcribed pseudogene in primates, although it cannot be excluded that this receptor may oligomerize with other NPY receptors to form a functional protein or it may undergo post-transcriptional modification resulting in a functional receptor (Rose *et al.*, 1997). Human y_6 mRNA was detected in heart and skeletal muscle and at low levels in the hypothalamus (Matsumoto *et al.*, 1996). The pharmacological profile of the expressed mouse y_6 receptor is discussed controversially (Michel *et al.*, 1998), but recent studies propose a Y_1 -like phenotype (Mullins *et al.*, 2000).

1.3.2.6 The NPY Y_7 receptor

In 2004, the Y_7 receptor was discovered in the teleosts zebrafish and rainbow trout and the amphibians marsh frog and western clawed frog (Fredriksson *et al.*, 2004; Larsson *et al.*, 2005). The zebrafish Y_7 receptor was functionally expressed in HEK 293 EBNA cells and characterized by peptide binding studies. In contrast to the mammalian Y_2 receptor, the zebrafish Y_7 (as well as the zY_2 receptor (Fredriksson *et al.*, 2006)) receptor does not (or much weaker) bind N-terminally truncated fragments

of NPY. In addition, no binding was observed with the Y_2 receptor antagonist BIIE0246 or the Y_1 receptor ligands p[Leu³¹,Pro³⁴]NPY or BIBP3226. Activation of the Y_7 receptor expressed in HEK 293 EBNA cells leads to an inhibition of forskolin-stimulated cAMP formation. The zY_7 receptor is widely expressed in the gastrointestinal tract and eye, but also in the brain (Fredriksson *et al.*, 2004). The function of the Y_7 receptor remains to be explored.

Chapter 2

Scope and Objectives

Scope and objectives of the work

G-protein coupled receptors represent the most important class of drug targets in the field of drug discovery. GPCRs are associated with almost every major therapeutic category or disease class. The encoding of the human genome has further expanded the number of possible targets and there is a great need for the establishment of simple, fast and robust assays for the screening and characterization of large numbers of new compounds which have become available by the use of combinatorial chemistry.

This thesis aims at the development of binding and functional assays for the NPY hY₂, hY₄ and rY₄ receptor. Flow cytometry was chosen for the establishment of binding assays, as this technique allows the determination of binding constants in equilibrium without the need to separate bound from unbound ligand. Therefore, peptide ligands of the GPCRs are to be fluorescence labelled and used in binding assays as well as for the visualization of the binding using confocal microscopy. The respective receptors have to be recombinantly expressed by mammalian cells using non-viral and retroviral expression systems. For comparison of the determined binding constants, the establishment of a radioligand binding assay is planned and studies on receptor internalization and sequestration will be performed.

For the development of functional assays, the signal transduction pathway ought to be redirected to the PLC β pathway by stable co-transfection of the receptor gene and the gene encoding for the chimeric G-protein G_{qi5}. Receptor activation should then result in an increase of intracellular calcium concentration, which can be quantified by spectrofluorimetric and flow cytometric methods using fluorescent calcium indicator dyes.

Additional stable co-transfection with the gene encoding for the apoaequorin protein targeted to the mitochondrion should convert the calcium signal into a luminescence signal, which can be detected by a luminescence plate reader, making the assay amenable to the 96-well format. The assays must be validated with known receptor ligands, and small compound libraries are to be screened for new potential receptor ligands. The calcium signal is planned to be visualized using confocal microscopy and a CCD camera to estimate a possible application in a HTS-instrument equipped with a CCD camera.

Chapter 3

Development of a flow
cytometric binding assay for the
human NPY Y₂ receptor

3.1 Stable expression of the hY₂ receptor gene

3.1.1 Introduction

Several approaches to the development of binding assays for the Y₂ receptor have been reported in the literature. Some authors use tissue preparation, e.g. rat forebrain tissue (Parker *et al.*, 2002b), rabbit kidney membranes (Beck-Sickinger *et al.*, 1992), rat jejunal crypt cells (Goumain *et al.*, 2001) or human frontal cortex membrane homogenate (Dumont *et al.*, 2000). Disadvantages of these preparations are the time consuming preparation procedure and the presence of other receptors especially NPY receptor subtypes, interfering with ligand binding to the Y₂ receptor. To circumvent this problem, Y₂ selective labeled ligands are used, and the pharmacological binding profile is determined with known NPY receptor ligands. Nevertheless, it cannot be excluded that binding is partly mediated by other receptor subtypes than the Y₂ receptor. The frequently used Y₂ receptor ligand hPYY binds with the same affinity to hY₁ and hY₂ receptors and even the Y₂ preferring ligand hPYY₃₋₃₆ shows considerable affinity to the Y₁ receptor ($K_i = 0.24$ nM for the hY₂ receptor vs. $K_i = 13.3$ nM for the hY₁ receptor) as has been reported by Gehlert and co-workers (Gehlert *et al.*, 1996a).

Another receptor source for binding assays are cells constitutively expressing the Y₂ receptor, namely the astrocytoma cell line LN319 (Beck-Sickinger *et al.*, 1992) and the two neuroblastoma cell lines SMS-KAN (Shigeri and Fujimoto, 1994) and CHP234 (Lynch *et al.*, 1994). The receptor expression is sufficient for radioligand binding assays (especially when membrane preparations are used) but the aforementioned cell lines are not suited when higher expression levels of the Y₂ receptor are required, e.g. in cellular assays.

3.1.1.1 Heterologous expression systems

Heterologous expression has become an invaluable tool for the establishment of receptor binding assays. Recombinant GPCRs have been expressed in bacteria (Marullo *et al.*, 1988), yeast (Weiss *et al.*, 1995), insect cells (Figler *et al.*, 1996), frog oocytes (Lee and Durieux, 1998) and mammals cells (Neve and Neve, 1998). Although all of these expression systems produce receptors, there are substantial differences in expression levels and post-translational modification of the resulting

receptor proteins. For example, bacteria lack the machinery for protein glycosylation, which is a requirement for the correct folding and transport of some receptors to the cell surface (Tiff *et al.*, 1992). Nevertheless, N-glycosylation is not always essential, and several GPCRs have been expressed in *E. coli* (for an overview, see Grisshammer, 1998). In insect cells proteins are post-translationally glycosylated, but these cells lack the galactose and sialic acid transferase and are therefore unable to convert N-linked oligosaccharides to complex sugars (Miller, 1988), resulting in GPCRs glycosylated to a lesser degree than their mammalian counterparts (Kobilka, 1995). Concerning post-translational modifications, mammalian cells are best suited for the study of GPCRs in binding and functional assays.

3.1.1.2 Transient versus stable transfection

Heterologous expression of a GPCR in mammalian cells can be achieved by stable or transient transfection. In a transient expression system high levels of the gene product are expressed over a limited period of time shortly after transfection (usually 2-4 days). Compared to stable transfection, in most cases this method yields higher expression levels which can be attained much more rapidly since the time consuming procedure to generate, isolate and characterize transfected cells is not required. Therefore, transient expression is often used for the purification of receptors, for the development of antibodies or as a receptor source for binding or functional assays. One drawback of transient expression is the fact that the transfection efficiency can vary considerably depending on the purity of the DNA preparations and the state of the cells to be transfected. Furthermore, the ratio of recombinant receptors to other cellular components can not be maintained at a constant level. This variable stoichiometry can interfere especially with functional assays. Stably transfected cells have incorporated the receptor cDNA into the genome and propagate it with each mitotic event. Therefore, a defined, constant quantity of the recombinant receptor is expressed for many generations. Another advantage of stable vs. transient transfection is that once a cell line, stably expressing the receptor, is generated, the laborious transfection procedure is not required anymore.

3.1.1.3 Choice of the host cell

The host cell line into which the GPCR is to be transfected should not endogenously express other receptor subtypes which could interfere with the binding of the ligand. This allows the determination of binding and functional data on a null background. Other features of a host cell line to be considered are transfection efficiency, growth rate and routine maintenance. Concerning clonal selection, the cells should be able to grow at a very low density. Suspension cells are easier to culture and more convenient for the use in many applications, but in most cases they are more difficult to transfect. Most of the available cell lines are adherently growing cells, and in most cases standard cell lines as e.g. HEK 293, CHO-K1 or COS-7 are used.

3.1.1.4 Choice of the expression vector

There are many commercially available vectors that will enable expression of receptor cDNA in mammalian cells. Most of them contain a ColE1 or pUC derived origin of replication for propagation and the ampicillin resistance gene, encoding β -lactamase for selection in *Escherichia coli*. The three key features promoter, transcription termination and RNA processing signals, and a selectable marker should be considered when selecting an appropriate expression vector. Viral enhancer-promoter sequences from the human cytomegalovirus (CMV) immediate early gene, the simian virus (SV-40) early gene, and the Rous sarcoma virus long terminal repeat (RSV LTR) are commonly used to achieve high levels of constitutive expression of the receptor. The cDNA is incorporated into the vector in the sense direction downstream of viral promoter elements and upstream of a polyadenylation signal. Although these promoters work well in a wide variety of cell lines, the suitability of a promoter depends on the host cell line used for transfection and should be tested if necessary. This also holds for RNA processing signals which are necessary for the stability of the transgenic mRNA. Polyadenylation signal and transcription termination signal sequences are commonly taken from SV-40 or the bovine growth hormone (BGH) gene. Dominant selectable markers which confer resistance to certain antibiotics are used to isolate stable transfectants. In most of the modern expression vectors the drug-resistance cassette is included in the same vector containing the cDNA of interest. However, it is also possible to co-transfect an expression vector with another vector containing the drug-resistance cassette.

Commonly used selection markers are resistance to neomycin (G418), zeocin, blastocidin, hygromycin, puromycin and bleomycin.

Usually, only the protein-coding region of the cDNA is inserted into the expression vector. Non-coding sequences upstream the translational start site may contain regulatory regions compromising gene expression. Also the 3' untranslated region may impair gene expression, but this region is usually less problematic. The insertion of a Kozak's consensus sequence (Kozak, 2002) at the translational start site can often enhance the expression of a foreign gene.

3.1.1.5 Transfection of mammalian cells

Many different techniques are known by which exogenous DNA can be incorporated and expressed by mammalian cells. These include direct methods like microinjection of RNA and DNA, transfection by calcium phosphate precipitation or lipofection, electroporation and particle-bombardment-mediated gene transfer. The cheapest method is the standard CaPO₄ precipitation (Chen and Okayama, 1987), but in most cases higher transfection efficiencies can be achieved by electroporation or lipid-mediated gene transfer reagents. Usually, each transfection protocol has to be optimized for each cell line. An alternative method is the use of viral vectors. Compared to mechanical and chemical transfection strategies, the use of recombinant viruses is very effective as viruses have evolved successful mechanisms for entering cells, transferring genetic material, and optimizing expression of the exogenous (viral) proteins. On the other hand, the virus-based systems are more challenging in terms of vector construction and the optimization of transfection efficiency.

3.1.1.6 Selection and screening of cell clones

Usually selection of transfected cells is carried out 2-3 days after transfection allowing the transfected cells to express the drug-resistance cassette. As drug sensitivity markedly varies among cell lines, the concentration of the antibiotic sufficient to kill the non-transfected wild type cells should be determined prior to the transfection or non-transfected cells should be incubated with the antibiotic as a control in parallel. Resistant cell clones are selected and propagated, but because

the expression of the recombinant receptor can vary, the cell clones should be screened in binding or functional assays.

Human Y₂ receptors have been expressed in HEK293 (Berglund *et al.*, 2002; Dautzenberg *et al.*, 2005; Dumont *et al.*, 2000), COS-7 and CHO (Gerald *et al.*, 1995; Goumain *et al.*, 2001; Rose *et al.*, 1995) cells. In each case the authors used membrane preparations for the binding assays except for Rose and co-workers, who used whole cells.

3.1.2 Materials and Methods

3.1.2.1 Preparation of media and agar plates

LB medium containing 1 % bacto tryptone (Difco, Detroit, USA), 0.5 % yeast extract (Roth, Karlsruhe, Germany) and 0.5 % NaCl (Merck, Darmstadt, Germany) was prepared by adding all ingredients to 1000 ml of millipore water (pH 7.0). For sterilization the medium was autoclaved for 20 min and then stored at 4 °C.

Selective amp-LB resp. kan-LB medium was prepared by adding 100 mg/ml ampicillin (Sigma, Deisenhofen, Germany) or 30 µg/ml kanamycin (Sigma) to the sterile LB medium.

For the preparation of selective agar plates, 1.5 % agar (Roth) was added to 1000 ml of LB medium and autoclaved. After sterilization, the medium was cooled to 60-65 °C, ampicillin (100 µg/ml) or kanamycin (30 µg/ml) was added and plates were prepared. Selective plates were stored at 4 °C for 3 to 4 weeks.

SOC medium was prepared by addition of 0.25 ml of KCl (Merck) (1 M), 1 ml MgCl₂ (Merck) (1M) and 1 ml MgSO₄ (Merck) (1 M) solution to 97 ml LB medium. After autoclaving, 1 ml of sterile 1 M glucose (Merck) solution was added.

3.1.2.2 Preparation of competent *E. coli*

Competent cells were prepared using the *E. coli* K12- XL-blue strain. 5 ml of an overnight culture were grown in LB medium. Then, 200 ml of sterile LB medium were inoculated with 2 ml of the overnight culture. Cells were grown with vigorous shaking (190 rpm) at 37 °C to an OD₆₀₀ of 0.2. The bacterial suspension was aliquoted into 8 prechilled, sterile polypropylene tubes and left on ice for 10 min. Cells were collected by centrifugation at 1500 g for 7 min at 4 °C, the supernatant was poured off, and

each cell pellet was resuspended in 5 ml of ice-cold CaCl₂ solution containing 60 mM CaCl₂, 10 mM PIPES and 15 % glycerol at pH 7. Cells were centrifuged for 5 min at 1000 g, resuspended in 5 ml of ice-cold CaCl₂ solution and incubated on ice for 30 min. After another centrifugation step at 1000 g for 5 min the supernatant was discarded and each pellet was resuspended in 1 ml of ice-cold CaCl₂ solution. 200 µl aliquots of cell suspension were pipetted into 1.5 ml microfuge tubes and left on ice for 2 h. Finally, competent cells were frozen in liquid nitrogen and stored at -80 °C.

3.1.2.3 Transformation of *E. coli*

For chemical transformation, 200 µl of competent cell suspension were thawed on ice and the plasmid DNA or the ligation product was added prior to incubation on ice for 30 min. Cells were heat-shocked by transferring the tubes into a 42 °C water bath for 90 s. For the recovery and expression of the antibiotic resistance gene needed for the positive selection of the transformants, 1 ml of SOC medium pre-warmed to 37 °C was added, and the bacteria were incubated for 45 min at 37 °C with gentle shaking (200 rpm).

20 - 50 µl of the transformant suspension were plated onto selective agar and the plates were incubated overnight at 37 °C. Colonies were picked and used for overnight cultures in selective medium.

3.1.2.4 Preparation of plasmid DNA

3.1.2.4.1 Mini-Prep

Small scale alkaline lysis procedures for the preparations of DNA were performed according to the protocol described by Birnboim and Doly (Birnboim and Doly, 1979).

Buffers were prepared as follows:

Buffer P1: 50 mM tris-HCl (Serva, Heidelberg, Germany), 10 mM titriplex III (Merck) and 100 µg/ml Rnase A (MBI Fermentas, St. Leon-Rot, Germany) in millipore water, pH 8.0.

Buffer P2: 0.2 M NaOH (Merck) and 1 % SDS (Sigma) in millipore water

Buffer P3: 3 M KAc (Merck) in millipore water, pH 5.5

5 ml of selective LB medium were inoculated with bacteria from an isolated colony and incubated overnight at 37 °C with vigorous shaking (200 rpm). 1.5 ml of this

culture was centrifuged for 30 s at 13000 rpm (Biofuge 13, Sartorius, Göttingen, Germany). The supernatant was discarded and the cell pellet was resuspended in 100 µl of P1. For the degradation of bacterial RNA the cell suspension was incubated for 5 min at room temperature. Lysis of the cells was performed by addition of 200 µl of P2, gentle mixing and incubation on ice for 5 min. Addition of 150 µl ice-cold P3 and further incubation for 10 min led to neutralization of the lysate and precipitation of SDS, denaturation of proteins and chromosomal DNA. After centrifugation for 15 min at 13000 rpm the supernatant was transferred into a new reaction vessel and mixed with 400 µl of phenol-chloroform-isoamylalcohol (25:24:1) (Roth, Karlsruhe, Germany) by vigorous vortexing. Phase separation was achieved by centrifugation for 3 min at 13000 rpm. The purified supernatant was transferred into a new tube and plasmid DNA was precipitated by addition of 1 ml of ice-cold ethanol (Mallinckrodt Baker, Griesheim, Germany). After centrifugation for 20 min at 13000 rpm, the pellet was washed with 1 ml of 70 % ethanol, air dried, and dissolved in 10 µl of millipore water. The DNA solutions were stored at -20 °C.

3.1.2.4.2 Maxi-Prep

Large scale preparations of plasmid DNA were performed using the Qiagen Plasmid Purification Kit (Qiagen, Hilden, Germany) according to the manufacturer's instructions.

3.1.2.4.3 Determination of DNA concentration

Usually, a 1:50 dilution of a Maxi-Prep DNA was prepared, and the DNA concentration was determined photometrically according to the following equation:

$$c \text{ (}\mu\text{g/ml)} = 70 A_{260} - 40 A_{280}$$

3.1.2.5 **Restriction enzyme digestion**

For the subcloning of DNA fragments and the restriction analysis of plasmid DNA the enzymes *Hind*III (Roche Diagnostics, Mannheim, Germany), *Not*I (MBI Fermentas, St. Leon-Rot, Germany), *Eco*RI (MBI Fermentas) and the corresponding reaction buffers provided by the manufacturers were used. When performing a double digestion, a buffer was chosen in which both enzymes showed no star activity and at least 50 % activity according to the manufacturer's specifications. In general, enzyme restriction digestion was performed in 20 µl of millipore water containing 2 µl of the appropriate

10x reaction buffer, 1 µl (10-15 U) of enzyme stock solution (resp. 2 µl for double digestion) and 500 - 1000 ng of DNA. The reaction was carried out for 90 min at 37 °C in an Eppendorf reaction vessel, and enzymes were heat-inactivated for 15 min at 70 °C.

For agarose gel electrophoresis 5 µl of 6x gel loading buffer (Peqlab, Erlangen, Germany) were added to each sample.

3.1.2.6 Agarose gel electrophoresis

Agarose gels were prepared by dissolving 0.5 g of agarose (pegGOLD Universal-Agarose; Peqlab) in 50 ml of TBE buffer containing 44.5 mM tris-base (USB, Cleveland, USA), 44.5 mM boric acid (Merck) and 1.0 mM EDTA (Titriplex III; Merck). To visualize DNA, 2 µl of ethidium bromide solution (10 mg/ml in H₂O; Janssen Chimica, Beerse, Belgium) were added. The warm agarose solution was poured into the gel chamber and let gel for 30 min.

Prior to electrophoresis, TBE buffer was filled into the gadget and 25 µl of each sample were pipetted per pocket. As reference, the peqGOLD DNA (Peqlab) ladder mix was prepared according to the manufacturer's instructions.

Electrophoresis was performed for 60 - 90 min at 90 V until the tracking dye moved at least 2/3 of the gel length. Then, the gel tray was removed from the electrophoresis chamber and DNA bands were visualized by illumination with UV light at 254 nm (Gel Doc 2000; Bio-Rad Laboratories, München, Germany). Quantity One software (Bio-Rad) was used for data analysis.

3.1.2.7 Recovery of DNA fragments from agarose gels

DNA bands were excised from the gel under UV light (254 nm) with a clean, sharp scalpel and DNA was extracted using the QIAEX II (Qiagen, Hilden, Germany) purification kit according to the manufacturer's protocol. Finally, DNA was eluted with 20 µl of millipore water.

3.1.2.8 Subcloning of the pcDNA3-eGFP and pcDEF3-eGFP vector

The pEGFP-N1 vector (BD biosciences, Heidelberg, Germany) was kindly provided by Prof. Männel, Institute of Pathology, University of Regensburg, Germany. The pcDNA3.1/His/lacZ vector was purchased from Invitrogen (Karlsruhe, Germany).

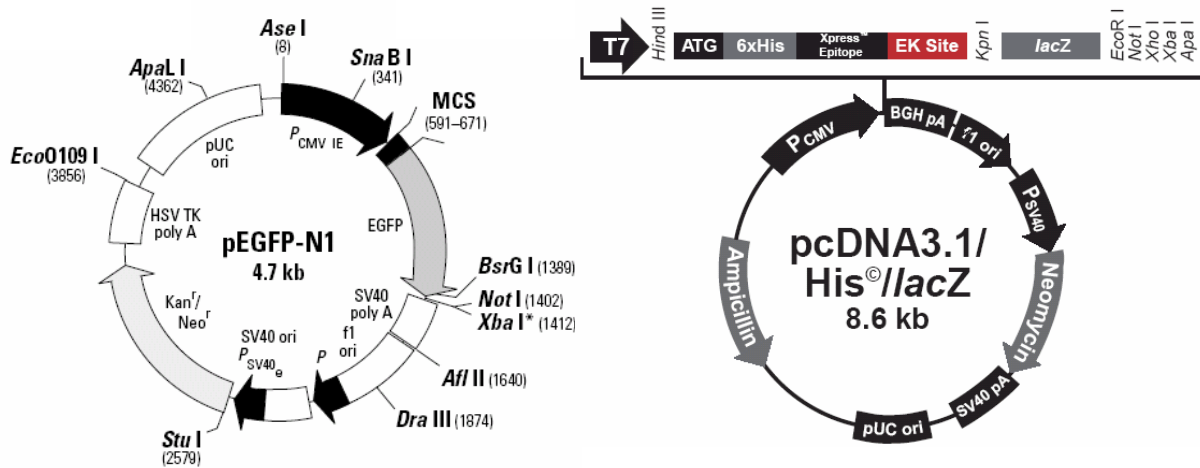


Fig. 8: Vector maps of pEGFP-N1 and pcDNA3.1/His/lacZ

The pcDEF3 vector was a gift from Dr. J. Langer, University of New Jersey, USA. This vector is a modified pcDNA3 vector with a EF-1 alpha promoter of pEF-BOS which replaces the CMV promoter of pcDNA3 (Goldman *et al.*, 1996).

The pcDNA3.1/His/lacZ vector was digested with *Hind*III and *Not*I using buffer B (Roche Diagnostics, Mannheim, Germany). DNA fragments were separated via gel electrophoresis revealing two expected bands of 5363 bp and 3214 bp (released His/lacZ-insert). The 5363 bp fragment was excised from the gel and purified using the QIAEX II purification kit.

The pcDEF3 vector was digested with *Eco*RI and *Not*I using buffer H (Roche Diagnostics). The 6067 bp fragment was separated from the 27 bp fragment via gel electrophoresis and purified using the QIAEX II purification kit.

The pEGFP-N1 vector was digested either with *Hind*III and *Not*I using buffer B or with *Eco*RI and *Not*I using buffer H. DNA fragments were separated over an agarose gel, and the eGFP inserts were purified using the QIAEX II purification kit.

Ligation reactions were performed using the following cohesive-end ligation protocol: 2 µl of linearized vector were incubated for 1 h at room temperature with 1 µl T4 ligase (1 Weiss U/µl; MBI Fermentas, St. Leon-Rot, Germany), 2 µl 10x ligase buffer (MBI Fermentas) and increasing amounts (1 - 4 µl) of properly digested insert in 20 µl of millipore water. T4 DNA ligase was heat-inactivated by incubation at 65 °C for 10 min. The samples were stored at -20 °C or directly used for transformation.

5 ml of Amp-LB medium was inoculated with resistant bacteria and DNA was purified by Mini-Prep. Composition of plasmid DNA was confirmed by restriction enzyme digestion. The pcDNA3-eGFP plasmid was linearized with *Hind*III (6142 bp, lane A) and treated with *Hind*III and *Not*I resulting in the two expected bands (lane B) with 5363 bp and 779 bp (very weak).

Digestion of pcDEF3-eGFP with *Eco*RI resulted in the linearized vector with 6847 bp (lane D); treatment of pcDEF3-eGFP with *Hind*III and *Not*I led to the formation of two fragments with a length of 4746 and 2101 bp which was expected as the properly subcloned vector contains one *Hind*III restriction site at bp 265 and one *Not*I restriction site at 2366 bp.

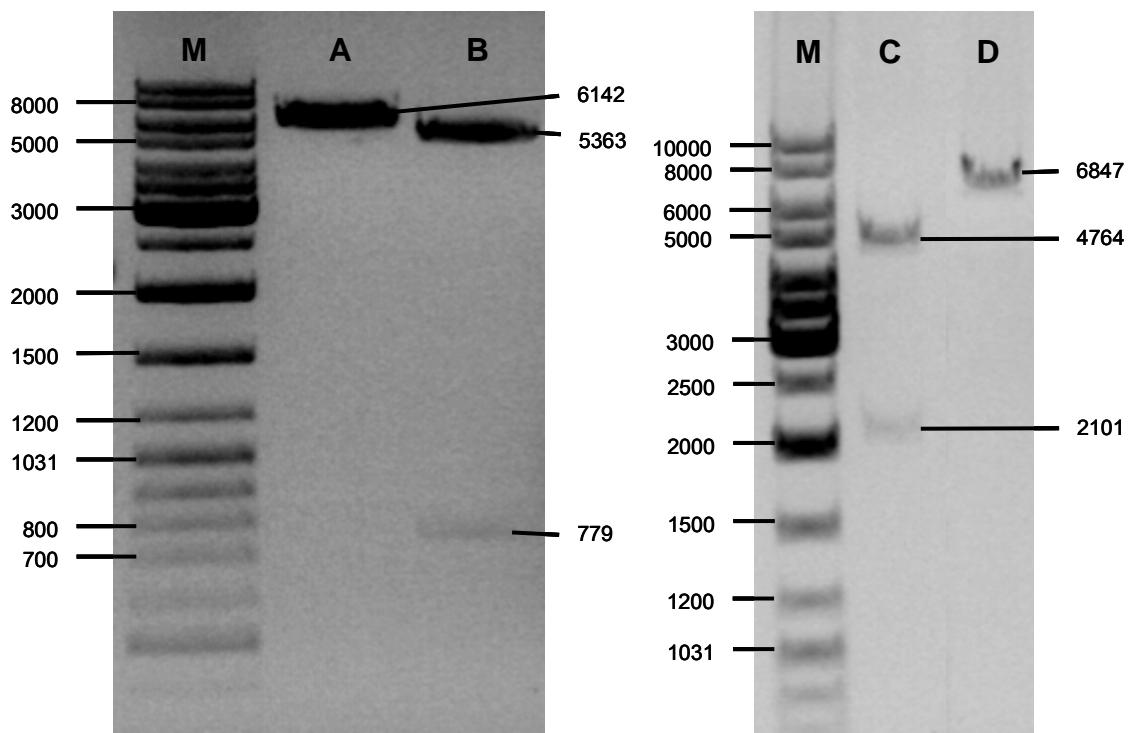


Fig. 9: Restriction analysis of pcDNA3-eGFP (A: linearized vector, B: *Hind*III and *Not*I digestion) and pcDEF3-eGFP (C: *Hind*III and *Not*I digestion, D: linearized vector)

For transient transfection, Maxi-Preps of pcDNA3-eGFP and pcDEF3-eGFP were prepared.

3.1.2.9 Cell culture

CHO-K1 cells were maintained in Ham's F12 medium supplemented with 10 % FCS in 75 cm² flasks. Cells were grown in 5 % CO₂, water saturated atmosphere at 37 °C. Subculturing was performed twice a week by 1:10 dilution after trypsinization.

Cells were routinely monitored for mycoplasma contamination by PCR using the VenorGEM™ mycoplasma detection kit (Minerva Biolab, Berlin, Germany).

3.1.2.10 Transient transfection of CHO-K1 cells with pcDNA3-eGFP and pcDEF3-eGFP using FuGENE and Metafectene

FuGENE™ 6 transfection reagent was purchased from Roche Diagnostics, Mannheim, Germany and Metafectene™ was obtained from Biontix, München, Germany.

One day before transfection, CHO-K1 cells were seeded in 500 µl of Ham's F12 medium plus 10 % FCS into 24-well plates. The cell density was adjusted that 60-70 % confluence was reached at the day of transfection.

DNA concentration was 300 and 600 ng/well and DNA (µg) per transfection reagent volume (µl) ratios were 1:4, 1:6 and 1:8. Concentrations of DNA stock solutions were 650 µg/ml (pcDNA3-eGFP) and 437 µg/ml (pcDEF3-eGFP), respectively. Transfections were performed according to the manufacturers' instructions. Briefly, DNA and transfection reagent were preincubated in serum-free Ham's F12 medium for 15 min at RT. This mixture was added dropwise to the cells, and after 5 h of incubation in the incubator the medium was replaced with fresh culture medium. 24 and 48 h after transfection the cells were analyzed by fluorescence microscopy and flow cytometry.

3.1.2.10.1 Fluorescence microscopy

Living cells were analyzed under a LEICA DM IRB inverse microscope equipped with a PL FLUOTAR 10x/0.30 Ph1 objective and a FITC fluorescence filter. Images were made with a Nikon Coolpix 4500 digital camera.

3.1.2.10.2 Flow cytometry

For flow cytometric determination of transient eGFP expression the medium was removed by suction and the cells were trypsinized by adding 300 µl of trypsin/EDTA solution for 5 min at RT. Trypsin was inactivated by addition of 700 µl of Ham's F12

medium containing 10 % FCS, and the cells were detached by gentle pipetting before they were transferred into microcentrifuge tubes. CHO cells were centrifuged for 5 min at 300 g in a microcentrifuge, and the cell pellets were resuspended in 500 µl of PBS containing 0.2 g of KCl, 0.2 g of KH₂PO₄, 1.15 g of Na₂HPO₄ and 8 g of NaCl in millipore water, pH 7.4. Cells were stored on ice until measurement. Samples were measured with a Becton Dickinson FACSCalibur™ flow cytometer; instrument settings were: FSC: E-1, SSC: 310, FL1: 450, Flow: HI (65µl/min), Time: 2 min.

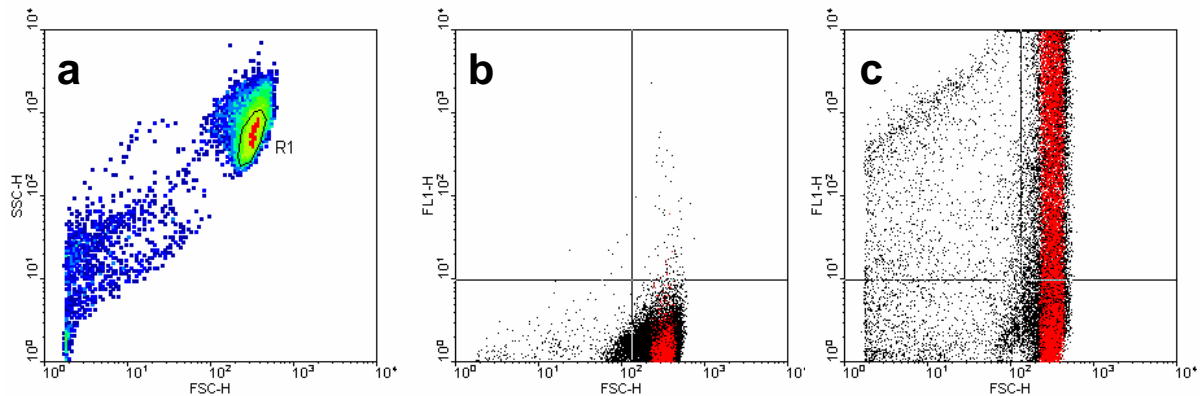


Fig. 10: Flow cytometric analysis of transient eGFP expression: Cells were gated in a density plot (a) and analysed in a FL1 vs. FSC dot plot. A quadrant was set to distinguish autofluorescence of wild type cells (b) from eGFP fluorescence of transfected cells (c)

The homogeneous CHO cell population was gated as shown in the density plot diagram in Fig. 10a. A quadrant was set in a FL-1 vs. FSC dot plot in order to distinguish cellular autofluorescence from eGFP fluorescence and increase in fluorescence of the gated population (shown in red) could be determined using the statistical analysis program of the WinMDI software.

3.1.2.10.3 Chemosensitivity assay

The sensitivity of CHO-K1 cells to neomycin (G418) was determined by the crystal violet assay (Bernhardt *et al.*, 1992). Cells were seeded in 100 µl medium at a density of ~ 5 cells per microscope field (320x, Diavert microscope, Leitz, Wetzlar, Germany) in 96 well flat-bottomed microtitration plates (Nunc, Wiesbaden, Germany) and incubated overnight. Then, additional 100 µl of medium containing increasing concentrations of neomycin were added. Medium of the control cells contained no neomycin. 16 wells were used for each concentration. After various incubation times the culture medium was shaken off and cells were fixed with 100 µl 1 % glutardialdehyde in PBS for 20 min. The fixative was replaced by 180 µl of PBS and plates were stored at 4 °C. For the staining of the cells, PBS was discarded and cells

were incubated with 100 μ l of 0.02 % crystal violet solution (N-hexamethyl-pararosaniilin · HCl in water) for 20 min. Wells were washed 3 times with demineralized water followed by an incubation step with water for 20 min at room temperature. Water was discarded and plates were dried. Cell bound dye was extracted by addition of 200 μ l 70 % ethanol and incubation for 3 h at RT with permanent shaking on a Köttermann 4010 shaker. Absorbance was measured at 578 nm using a BioTek EL 309 Autoreader (Bad Friedrichshall, Germany) and the average and standard deviation values were calculated. Absorbance outside of the confidence interval (95%) was not considered for the calculations.

3.1.2.11 Restriction analysis of the pcDNA3-hY2 vector and stable transfection of CHO-K1 cells

The pcDNA3-hY₂ expression vector was a gift from Dr. Patricia M. Rose (Department of Microbial Molecular Biology, Bristol-Myers Squibb, Princeton, New Jersey, USA). The hY₂ insert (Rose *et al.*, 1995, Genbank No. U32500) is subcloned into the *Bam*HI and *Xba*I cassette of the multiple cloning site of the pcDNA3.

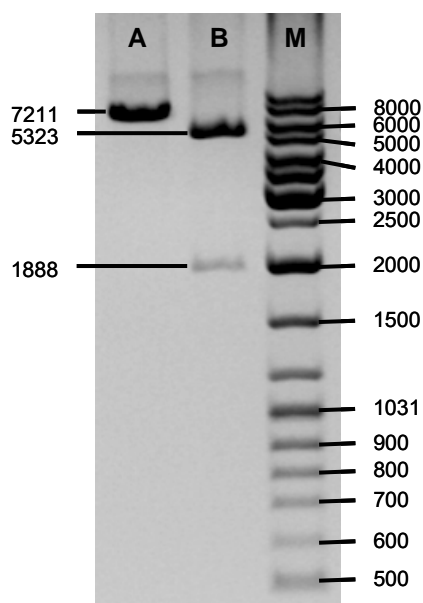


Fig. 11: Restriction analysis of the vector pcDNA3-hY₂. **A:** after linearization; **B:** after *Bam*HI and *Xba*I digestion

Digestion with *Bam*HI led to the linearized vector with 7211 bp (Fig. 11, lane A). A small band of uncut vector was visible. Double digestion with *Bam*HI and *Xba*I (Fig. 11, lane B) using Buffer B released the hY₂ insert with a length of 1888 bp. The second band at 5323 bp corresponded to the pcDNA3 vector fragment.

One day before transfection, CHO-K1 cells were seeded in 500 μ l of Ham's F12 + 10% FCS on a 24 well plate. Cell density was adjusted that the next day 70% optical confluence was reached. 300 ng of plasmid DNA and 2.4 μ l FuGENE transfection reagent were incubated with serum-free Ham's F12 medium in a final volume of 20 μ l for 15 min at RT.

Then, the transfection mixture was added dropwise to the cells following incubation at 37 °C, 5% CO₂, water saturated atmosphere. After 5 h the medium was replaced and incubation of the cells was continued. 48 h post

transfection the cells were trypsinized and transferred into 6 well plates in presence of selective medium containing 400 µg/ml geneticin. Resistant cells were passaged (splitting 1:10) every 3-4 days for 4 weeks.

3.1.2.12 Analysis of selected cell clones for the specific binding of Cy5-pNPY

After 4 weeks of propagation in selective medium transfected cells were seeded at very low density (< 10 cells/ml) in 150 mm tissue culture dishes (Becton Dickinson, Franklin Lakes, NJ., USA). Cells were grown to isolated colonies of 50-100 cells within 1 - 2 weeks. The medium was removed by suction, and 7 ml of trypsin/EDTA were added for 3-5 min at room temperature. Using an inverse microscope (Leitz, Wetzlar, Germany) with a 32x objective, cell colonies were picked with a sterile pipette and transferred to a 24-well-plate containing selective medium. Single clones were expanded and tested for specific binding at the flow cytometer as described in 3.2.2.3.

3.1.3 Results and Discussion

3.1.3.1 Optimization of the transfection procedure

In stable transfection the critical steps are the efficiency of cellular uptake of the exogenous DNA and the frequency of stable integration into the chromosomal DNA of the recipient cells. Because it is difficult to influence the latter process, stable transfection was optimized by exploring the conditions leading to maximum transient transfection efficiency. CHO-K1 cells were chosen for transfection as these cells grow rapidly and are known for transfection efficiency. For the optimization of the transient transfection protocol, CHO-K1 cells were transfected with the pcDNA3-eGFP and the pcDEF3-eGFP vector. Transfection efficiency was determined by flow cytometry 24 h after transfection. Effects of the expression vector, the transfection reagent and the amount DNA were quantified via the expression of eGFP (Chalfie *et al.*, 1994).

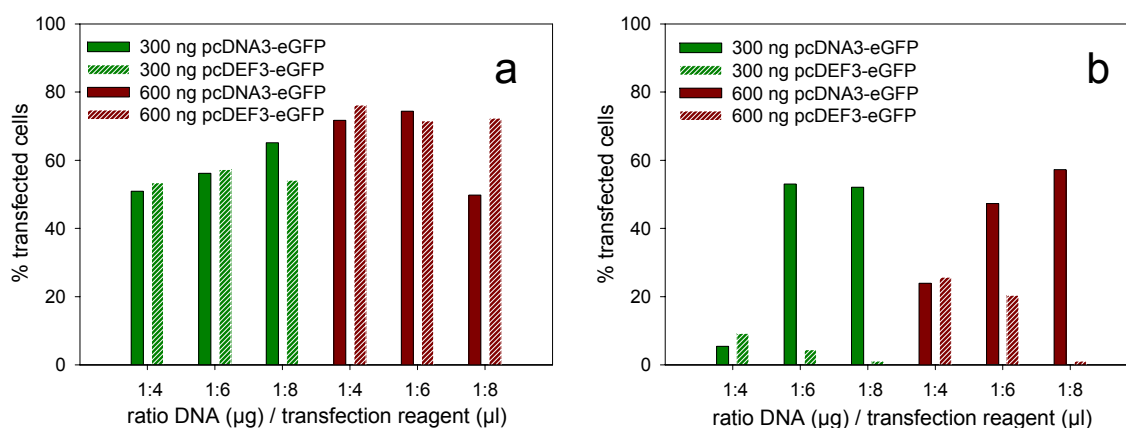


Fig. 12: Transient transfection of CHO-K1 cells with pcDNA3-eGFP and pcDEF3-eGFP using FuGENE (panel a) and metafectene (panel b) transfection reagent with varying amounts of DNA and ratios of DNA / transfection reagent.

As shown in Fig. 12, with respect to transfection efficiency FuGENE was superior to metafectene in case of both vectors and almost all DNA-reagent ratios tested. Additionally, metafectene appeared to be much more cytotoxic against CHO cells as the total cell number (counted for 2 min) was less than 50 % compared to that of the FuGENE transfected cells.

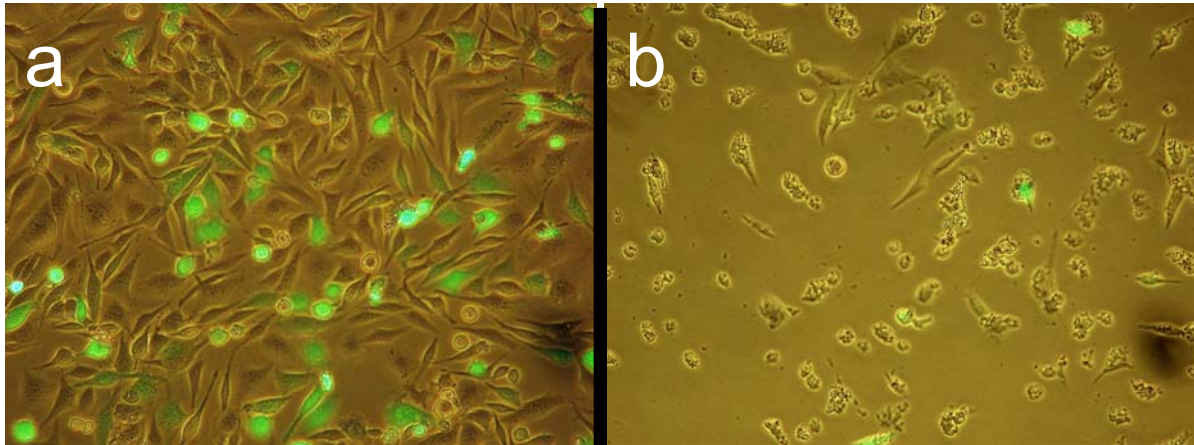


Fig. 13: Microscopic image of CHO-K1 cells transfected with pcDNA3-eGFP; overlay of phase contrast and fluorescence (green) images. **a:** FuGENE, 300 ng DNA, ratio 1:4; **b:** metafectene, 600 ng DNA; ratio 1:8.

This was confirmed by fluorescence microscopy as exemplarily shown in Fig. 13. Using FuGENE, transfection efficiency was higher than 45 % in all samples. The highest eGFP expression (76 %) was reached with 600 ng of pcDEF3-eGFP vector and a DNA/reagent ratio of 1:4. To save costs, for further transfections a DNA amount of 300 ng/well and a DNA/reagent ratio of 1:6 were chosen for both vectors as the transfection efficiency under these conditions was by far sufficient (higher than 50 %).

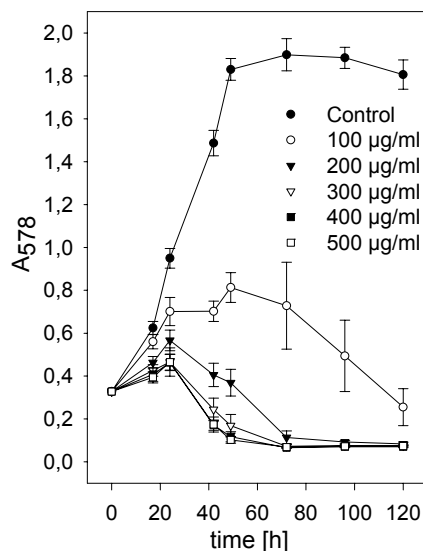


Fig. 14: Effect of G418 on the proliferation of CHO-K1 cells. Crystal violet assay (mean values \pm SD (n=16)).

In the literature the concentrations of neomycin (Geneticin[®], G418) used for the selection of transfected CHO-K1 cells range from 100 µg/ml (Parker *et al.*, 2001a) to 1000 µg/ml (Gehlert *et al.*, 1997). The sensitivity of CHO-K1 cells to neomycin was determined in a crystal violet assay. As shown in Fig. 14, the antibiotic was cytotoxic at all concentration tested. Cell growth was inhibited with increasing concentrations of geneticin.

No difference was measured between 400 µg/ml and 500 µg/ml. For the selection of transfected cells, a concentration of 400 µg/ml of the antibiotic was chosen as wild type cells die in selective medium after an incubation period of three days.

3.1.3.2 Stable transfection of CHO-K1 cells with the hY_2 receptor gene

CHO-K1 cells were transfected and selected under optimized conditions and cell clones were analysed for the specific binding of cy5-pNPY (see 3.2.2.1). Clone 9 was found to exhibit high specific binding as shown in Fig. 15. The geometric mean of total cell bound fluorescence after incubation with 10 nM cy5-pNPY was 401 relative fluorescence units (RFU). It was reduced when the cells were incubated in the presence of 1 μ M unlabeled pNPY (unspecific binding; geometric mean: 92), corresponding to an unspecific binding of 23 %.

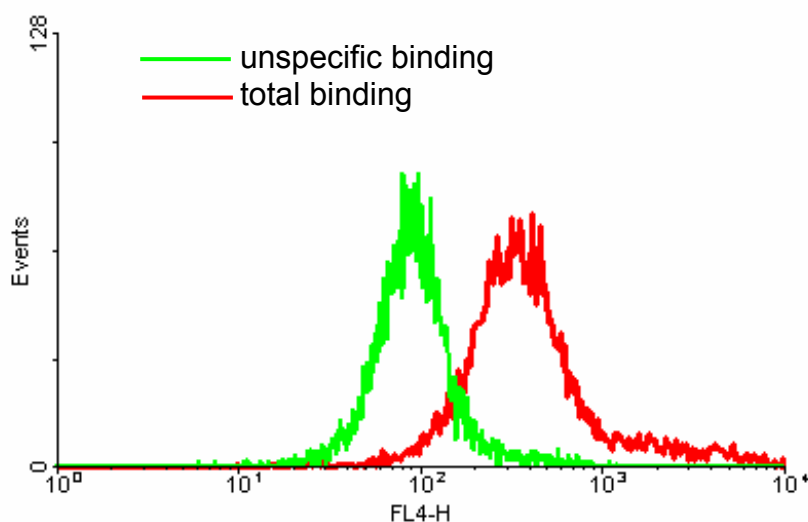


Fig. 15: Total and unspecific (in presence of 1 μ M pNPY) binding of 10 nM cy5-pNPY to CHO- hY_2 -K9 cells (clone 9).

3.2 Flow cytometric binding assay

3.2.1 Introduction

Flow cytometry provides a sensitive and quantitative method for the measurement of fluorescence or light scattering of cells. During the measurement the cells are hydrodynamically focused in a laminar flow of sheath fluid. Therefore, in the flow cell the single cells pass through the laser beams sequentially. The light is scattered and detected by a photomultiplier tube and a photodiode, respectively. Scattered light intensity in a narrow angle of 0.5 to 2.0° (forward scatter light, detected in the FSC channel, photodiode) depends on the size of the particles, whereas the light intensity scattered at an angle of 90° (sideward scatter light, detected in the SSC channel) depends on the inner structure of the cells (granularity). Fluorescence light emitted

by fluorescent dyes associated with the cell is spectrally separated from the sideward scatter light by mirrors and filters and detected by different photomultipliers. The FACSCalibur™ flow cytometer is equipped with an argon laser ($\lambda = 488 \text{ nm}$) and an additional red diode laser ($\lambda = 635 \text{ nm}$).

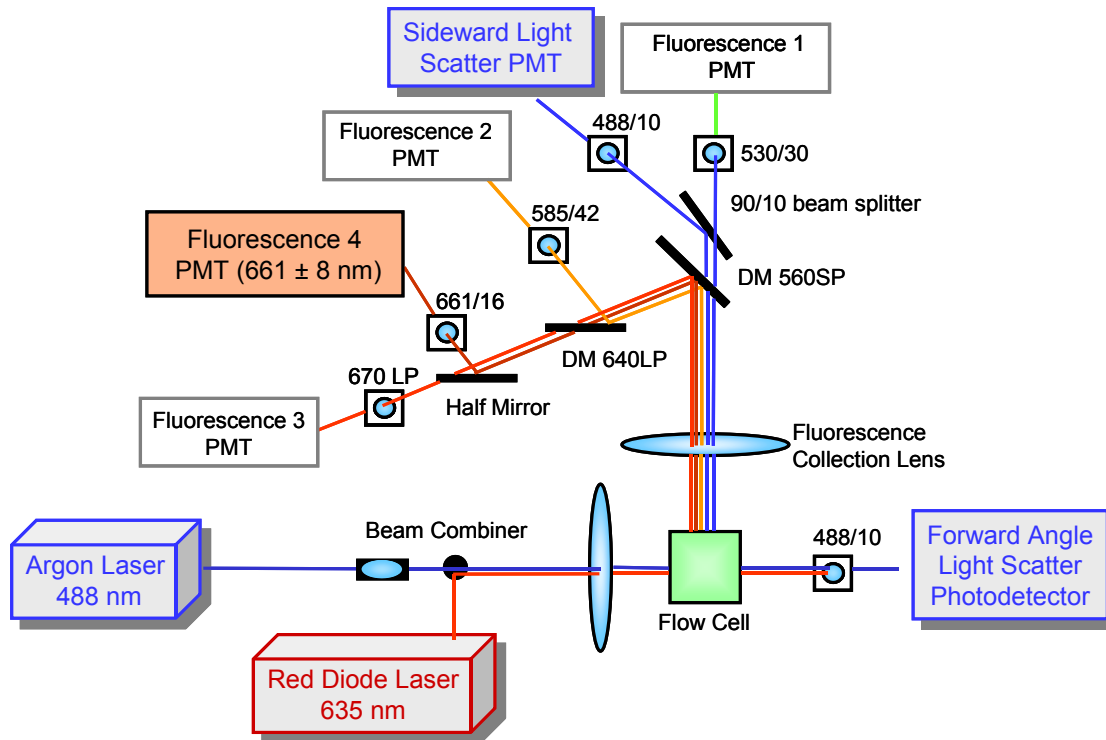


Fig. 16: Optical setup of the FACSCalibur™ flow cytometer. The cells are illuminated in the flow cell by an argon and a red diode laser. Scattered light and fluorescence are spectrally separated by filters and dichroic mirrors and detected by different photomultiplier tubes (adapted from Mayer, 2002).

The scattered light from the argon laser is detected in the FSC and the SSC channels. Fluorescence resulting from excitation at 488 nm is detected by the photomultipliers FL-1, FL-2 and FL-3. The photomultiplier FL-4 detects only the red fluorescence emitted after excitation with the diode laser. The optical setup of the FACSCalibur™ is shown in Fig. 16.

Flow cytometry is widely used for the analysis of blood cells, which can be separated due to the unique light-scattering properties of individual cell populations in combination with immunophenotyping by fluorescence labeled antibodies. In addition, this technique has been used for the investigation of DNA content (Simon *et al.*, 1992), oxidant production (Robinson *et al.*, 1994), cell cycle (Dressler and Seamer, 1994), activation of reporter genes (Ropp *et al.*, 1995), apoptosis (Darzynkiewicz *et al.*, 1997), calcium elevation (June and Rabinovitch, 1994), membrane potential (Shapiro, 1994) and pH changes (Boyer and Hedley, 1994).

The application of flow cytometric binding assays has been described e.g. for the chemokine receptor CXCR4 (Hatse *et al.*, 2004), the EGF receptor (Stein *et al.*, 2001) or the α -factor receptor in yeast (Bajaj *et al.*, 2004).

The main advantage of a flow cytometric binding assay compared to a classic radioligand binding assays is the fact that the separation of bound and free ligand is not required. The probe volume, defined by the intersection of the laser beam with the sample stream is very small (several picoliters (Nolan and Sklar, 1998)). Therefore, the background signal caused by free dye is very low compared to the signal from the cell and becomes negligibly small, if the concentration of free dye is not too high. Thus, binding of fluorescent ligands to GPCRs can be determined at equilibrium.

3.2.2 Materials and Methods

3.2.2.1 Synthesis and purification of cy5-pNPY

Porcine NPY (peptide content: 70 %) was synthesized and provided by Prof. Dr. A. Beck-Sickinger, Institute of Biochemistry, University of Leipzig. The cyanine dye Cy5 was purchased from Amersham Biosciences, Little Chalfont, Buckinghamshire, UK. For the labelling reaction, 0.5 mg of pNPY were dissolved in 20 μ l of DMSO (Merck, Darmstadt, Germany) and 250 μ l of 0.1 M sodium carbonate/bicarbonate buffer, pH 9.5, containing 33 % acetonitrile (Mallinckrodt Baker, Deventer, Netherlands) were added. One portion of Cy5 (ca. 0.2 mg) was dissolved in 20 μ l of anhydrous DMSO and added to the peptide solution. Under these conditions, the dye is coupled to the ϵ -amino group of K⁴ of pNPY. After 3 h of incubation at room temperature the labelled pNPY was purified by HPLC using the following instrumentation: a Hitachi F1000 fluorescence detector was adjusted for the detection of the tyrosine fluorescence ($\lambda_{\text{ex}} = 275 \text{ nm}$; $\lambda_{\text{em}} = 305 \text{ nm}$) of the peptide and an HPLC 430 UV/VIS detector (Kontron, Neufahrn, Germany) was used to detect absorbance of the dye at 649 nm. Pump, gradient mixer and autosampler were from Kontron, Neufahrn, Germany. The Nucleosil 300 5-C18 column (Macherey-Nagel, Düren, Germany) was thermostatted at 35 °C with a Shimadzu CTO-2A column oven. The gradient was formed by a mixture of solvent A (acetonitrile / 0.1 % trifluoroacetic acid in millipore water: 60/40) and solvent B (0.1 % trifluoroacetic acid in millipore water). After 15 min of equilibration with 50 % solvent A at a flow rate of 1 ml/min the sample was injected

and the fraction of solvent A was raised to 80 % over 40 min in a linear manner. After each HPLC run a washing step of 10 min with 100 % A was performed.

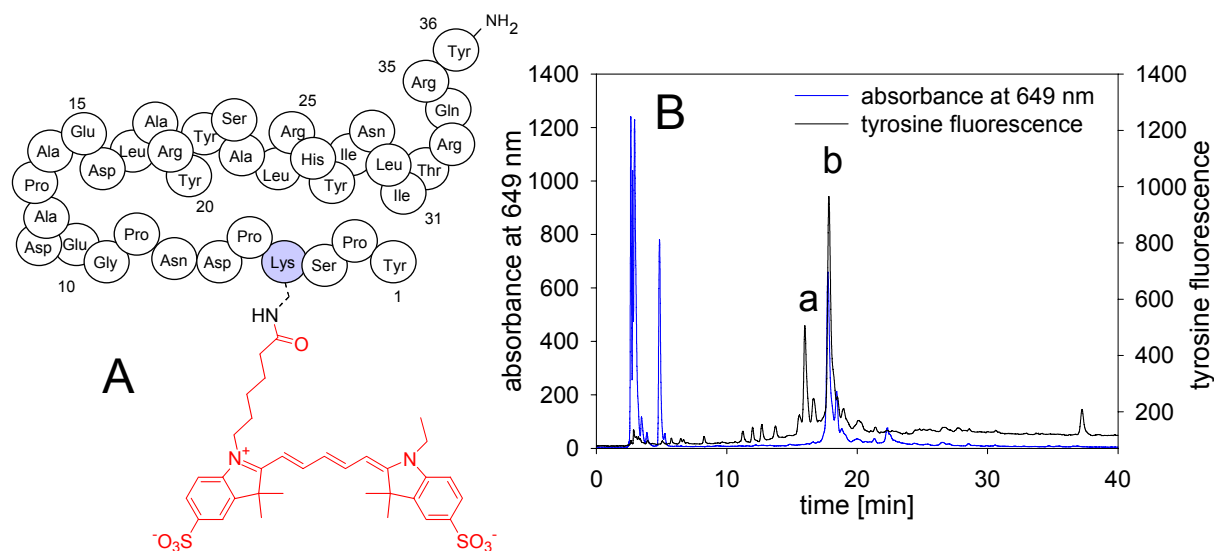


Fig. 17: **A:** Structure of cy5-pNPY(1). **B:** HPLC purification of 1. **a:** unlabeled pNPY; **b:** cy5-pNPY.

For the purification of cy5-pNPY, 40-50 μ l of the reaction mixture were injected. The retention time of unlabeled pNPY was 15.8 min, whereas cy5-labeled pNPY was eluted after 18 min indicated by the concomitant increase in absorption and tyrosine fluorescence. Peaks were collected by hand and absorbance at $\lambda = 649$ nm was determined.

3.2.2.1.1 Estimation of the molar extinction coefficient of hydrolysed cy5 dye in mobile phase

Due to the very low amounts of cy5 and cy5-pNPY, the determination of the extinction coefficients by photometric measurement of samples of defined weights is impossible. Therefore, the manufacturer's specification ($\epsilon = 250000 \text{ M}^{-1} \text{ cm}^{-1}$ at $\lambda = 649$ nm in millipore water) was used. As cy5-pNPY is not completely soluble in millipore water the effect of the solvent on the extinction coefficient was measured. For this purpose equal amounts of hydrolyzed dye obtained from HPLC were dissolved in the same volume of various solvents with increasing amounts of acetonitrile and absorbance at $\lambda = 649$ nm was determined.

Table 3: Influence of solvent composition on the extinction coefficient of cy5.

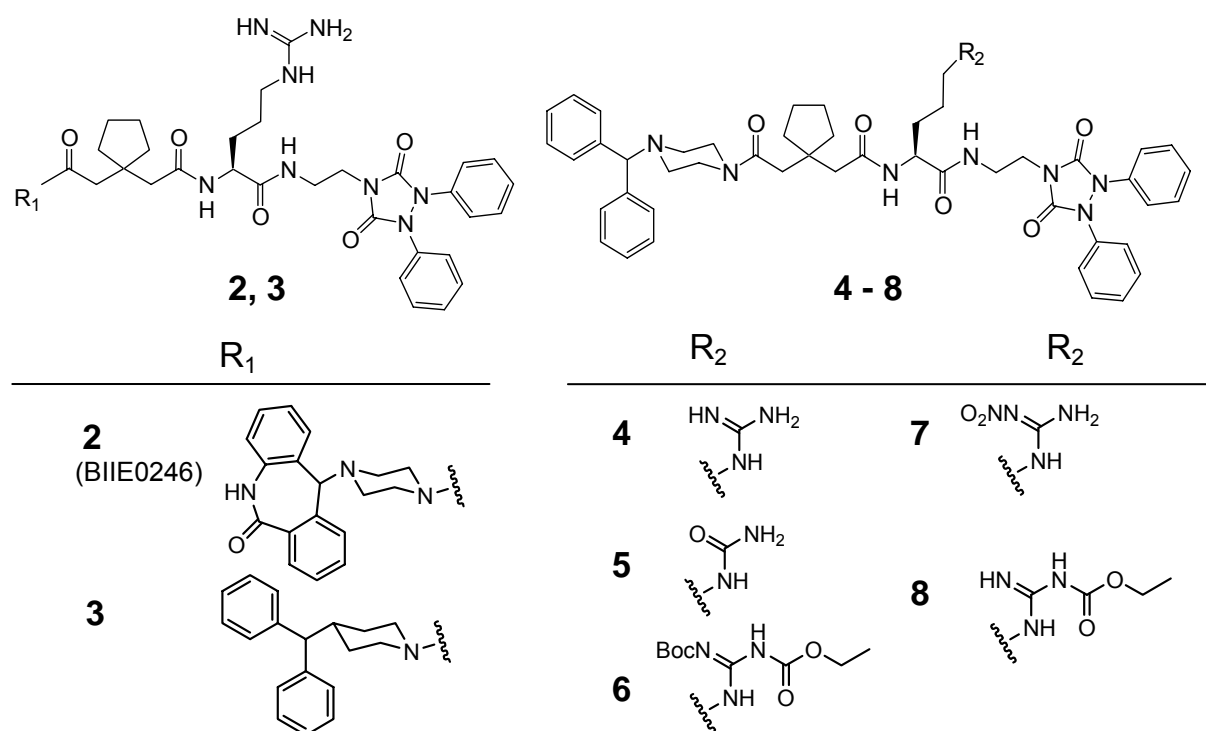
solvent	absorbance	ϵ [$M^{-1} cm^{-1}$] related to ϵ (millipore water)
millipore water	0.4271	250000
PBS buffer, pH 7.1	0.4467	261472
TFA (0.1%)	0.3853	225533
TFA (0.1%) / MeCN 80/20	0.5357	313568
TFA (0.1%) / MeCN 60/40	0.5215	305256
TFA (0.1%) / MeCN 40/60	0.5296	309998
TFA (0.1%) / MeCN 20/80	0.5279	309003
MeCN	not soluble	---

The addition of acetonitrile led to an increase in absorbance resulting in calculated extinction coefficients of 305256 to 313568 [$M^{-1} cm^{-1}$]. The mobile phase at 18 min (i.e. retention time of cy5-pNPY) contained 38.1 % acetonitrile. For the determination of cy5-pNPY concentration in mobile phase, a molar extinction coefficient of 310000 $M^{-1} cm^{-1}$ was assumed.

The labelled peptide was aliquoted (1 nmol) into 1.5 ml microtubes (NeoLab, Heidelberg, Germany), and the solvent was evaporated in the vacuum concentrator at room temperature. Aliquots were stored at $-80\text{ }^{\circ}C$.

3.2.2.2 Y_2 receptor antagonists

The Y_2 receptor antagonists BIIE0246 (**2**) and the structural analogs **3-8** (Fig. 18) were synthesized by Albert Brennauer.

**Fig. 18:** Y_2 receptor antagonists used in the assays.

3.2.2.3 Flow cytometry

In general, cells were grown to 80-90 % confluence, trypsinized and resuspended in Ham's F12 medium, containing 10 % FCS for the inactivation of trypsin. Cells were counted, centrifuged for 5 min at 1200 rpm (Minifuge RF, Heraeus, Hanau, Germany) and resuspended at a density of 10⁶ cells/ml in binding buffer (Sheikh and Williams, 1990), containing 25 mM Hepes, 2.5 mM CaCl₂ and 1 mM MgCl₂ in millipore water, pH 7.4, supplemented with 1 % BSA and 0.1 mg/ml bacitracin (Sigma, Deisenhofen). Cells were incubated at room temperature in 1.5 ml polypropylene tubes which were siliconized using Sigmacote™ (Sigma, Deisenhofen, Germany) to prevent protein adsorption. The incubation was accomplished with gentle shaking (120 rpm) in the dark to circumvent cell aggregation and photobleaching of the dye.

Samples were measured without further processing with a Becton Dickinson FACSCalibur™ flow cytometer; instrument settings were: FSC: E-1, SSC: 280 V FL4: 800 V, Flow: HI; measurement stopped when 20000 gated events were counted. The cells were gated and the geometric means of fluorescence were calculated using the WinMDI software. For the screening of cell clones, 490 µl of cell suspension were incubated with 10 µl of cy5-pNPY (250 nM in 10 mM HCl plus 0.1 % BSA) for 60-90 minutes. Cell clones with high specific cell-bound fluorescence were expanded and analyzed in saturation experiments.

Association kinetics was determined by incubation of CHO-hY₂-K9 cells with 5 nM cy5-pNPY. Samples were taken at different time periods and measured.

For saturation experiments, 485 µl of cell suspension were added to 10 µl of cy5-pNPY and 5 µl of solvent resp. unlabelled pNPY (for the determination of total resp. unspecific binding). Cells were incubated for 120 min at room temperature.

Competition experiments were performed using 485 µl of cell suspension, 10 µl of cy5-pNPY (final concentration 5 nM) and 5 µl of test compound. Incubation time was 120 min at room temperature. The constant K_i for the inhibition of cy5-pNPY binding by unlabeled competitors was calculated from the concentration of unlabeled competitor, producing 50 % inhibition (IC₅₀) of the specific cy5-pNPY binding using the following relation $K_i = IC_{50} \cdot [K_d / (K_d + L)]$ where K_d is the dissociation constant and L the concentration of cy5-pNPY (Cheng and Prusoff, 1973).

3.2.2.4 Confocal microscopy

CHO-hY₂-K9-qi5-K9-mtAEQ-A7 cells (see 4.2.3.1) were seeded in 200 µl Ham's F12 medium containing 10 % FCS on a Lab-Tek[®] II, 8 chamber coverglass system (Nalge Nunc, Naperville, IL, USA) two days prior to the experiment and were grown to 50-70 % confluence. The medium was replaced with 200 µl of L-15 Leibowitz medium (Sigma) containing 10 nM cy5-pNPY and incubated at room temperature for 30 min. For the visualization of unspecific binding, 1 µM of unlabeled pNPY was added to the incubation medium. Cells were washed with PBS (3.1.2.10.2) and fixed with paraformaldehyde (4 % in PBS) for 30 min. Nuclei were stained with 500 nM Sytox[®] Green (Invitrogen, Karlsruhe, Germany) in PBS for additional 30 min at room temperature, followed by a washing step with PBS. Confocal microscopy was performed with a Zeiss Axiovert 200 M microscope, equipped with the LSM 510 laser scanner, using a Plan-Apochromat 63x/1.4 objective with oil immersion. For the excitation of the cyanine dye, the 633 nm laser line was used with a laser power of 51 %. Fluorescence was detected using the 650 nm longpass filter. The nuclear dye Sytox[®] Green was excited at 488 nm with a laser power of 3 %. Emitted fluorescence was detected using a 505 nm longpass filter. The scanning mode was multi track. Control scans were performed without Sytox[®] Green to exclude that cy5-pNPY fluorescence is detected in the channel of the nuclear dye.

3.2.3 Results

3.2.3.1 Flow cytometric binding assay

Before competition binding experiments were performed, the incubation time, allowing the system to approach equilibrium, was determined (Fig. 19).

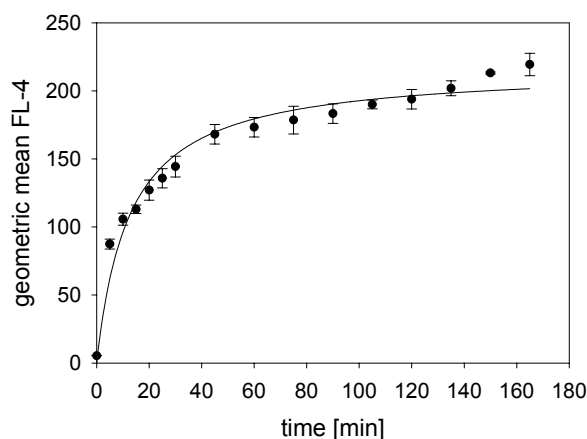


Fig. 19: Equilibrium binding experiment. CHO-hY₂-K9 cells were incubated with 5 nM Cy5-pNPY at room temperature. 95 % of maximum binding was reached after 112.4 min (mean values \pm SEM, n=3).

As after 112.4 min ($t_{1/2} = 12.5$ min) 95 % of maximum binding was reached, an incubation period of 2 h was considered appropriate.

Accordingly, a K_d of 5.2 ± 2.1 nM was determined in a flow cytometric saturation experiment with a fit to a one site hyperbolic curve (Fig. 20a). As the fraction of unspecific binding was below 30 % (21.5 %) at 5 nM cy5-pNPY, this concentration of the labeled ligand was chosen for competition assays as shown in Fig. 20b. the investigated Y₂ antagonists (Fig. 18) displaced the fluorescent ligand cy5-pNPY (Fig. 20b).

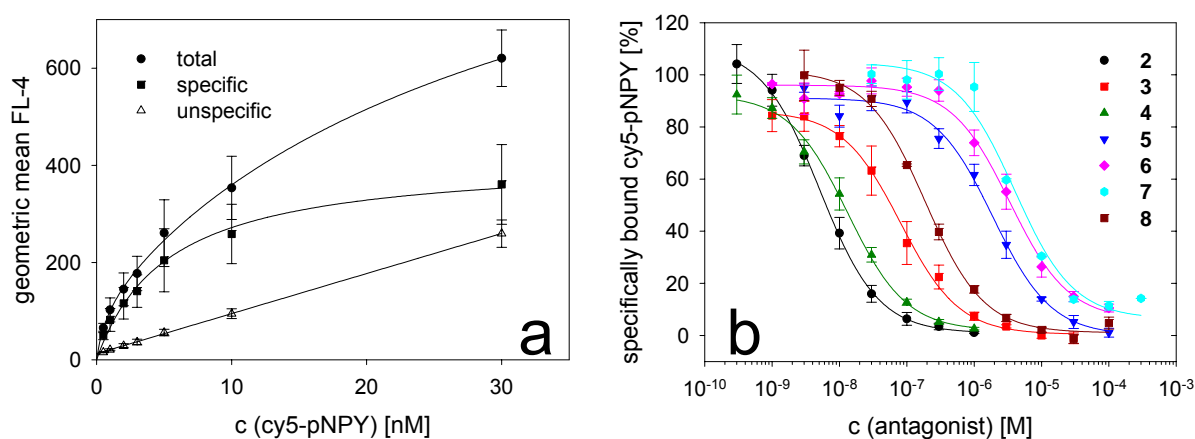


Fig. 20: Flow cytometric experiments with CHO-hY₂-K9 cells. **a:** saturation assay with cy5-pNPY; unspecific binding was determined in the presence of 1 μ M unlabeled pNPY. **b:** Competition assay with 5 nM cy5-pNPY in presence of various concentrations of antagonists; unspecific binding was determined in the presence of 1 μ M pNPY (mean values \pm SEM, $n=3$).

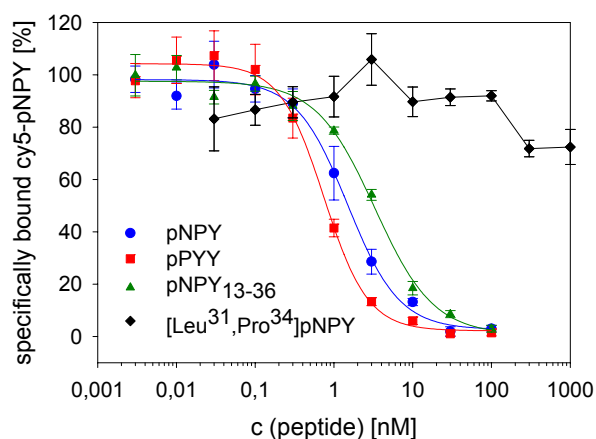
The known Y₂-selective antagonist BIIE0246 (**2**) (Doods *et al.*, 1999) bound with high affinity ($K_i = 2.6 \pm 1.2$ nM) to the hY₂ receptor. This is in good agreement with the literature as the authors (Doods *et al.*, 1999) reported on an IC₅₀ value of 3.3 nM, determined with hY₂ receptor expressing SMS-KAN cells and [¹²⁵I]neuropeptide Y as radioligand. Goumain and co-workers published K_i values for the rat Y₂ receptor ranging from 6.5 nM (rat jejunal crypt cells) to 9.0 nM (CHO-rY₂ cells) determined with [¹²⁵I]PYY as radioligand (Goumain *et al.*, 2001) and Dumont and co-workers determined an IC₅₀ of 15 nM using HEK 293 cells transfected with the rat Y₂ receptor cDNA and [¹²⁵I]PYY₃₋₃₆ as radioligand (Dumont *et al.*, 2000).

Compound **4** containing the α -diphenylmethyl residue also showed high affinity with a K_i value of 6.8 ± 2.3 nM. Exchange of the piperazine by a piperidine ring reduced the

affinity as shown for substance **3** ($K_i = 41.6 \pm 12.9$ nM). Further alterations of the argininamide structure led to decreased affinities of compounds **5** ($K_i = 976.2 \pm 250.8$ nM), **6** ($K_i = 1753 \pm 492$ nM), **7** ($K_i = 2065 \pm 652$ nM) and **8** ($K_i = 96.7 \pm 23.6$ nM).

Binding affinities of peptide ligands were determined using CHO-hY₂-K9-qi5-mtAEQ-A7 cells described in chapter 4.2 .

Fig. 21: Competition of various peptide ligands with 5 nM cy5-pNPY for the binding to CHO-hY₂-K9-qi5-mtAEQ-A7 cells (mean values \pm SEM, n=3).



The results (Fig. 21) confirmed the typical pharmacological profile of the Y₂ receptor. pNPY and pPYY bound with high affinity (K_i values 0.8 ± 0.2 nM resp. 0.4 ± 0.1 nM). For comparison, Gerald et al. used [¹²⁵I]-PYY and membranes of transiently transfected COS-7 cells in a radioligand binding assay and determined comparable K_i values (K_i (pNPY) = 0.85 nM and K_i (pPYY) = 0.35 nM) (Gerald *et al.*, 1995). The Y₂ preferring ligand pNPY₁₃₋₃₆ bound with high affinity ($K_i = 1.7 \pm 0.4$ nM) which has been also reported by Gerald et al. ($K_i = 2.82$ nM), whereas the Y₁ preferring ligand [L³¹, P³⁴]-pNPY was not able to displace cy5-pNPY up to a concentration of 1000 nM.

3.2.3.2 Confocal microscopy

Binding of cy5-pNPY (**1**) to CHO-hY₂-K9-qi5-K9-mtAEQ-A7 cells (see section 4.2) was visualized by means of confocal microscopy. As shown in Fig. 22, the fluorescence-labeled ligand enriched at the cell membrane. This binding was abolished in the presence of 1 μ M pNPY. The counterstaining of the nuclei with Sytox[®] Green was used to ensure that the scanning plane was within the cells.

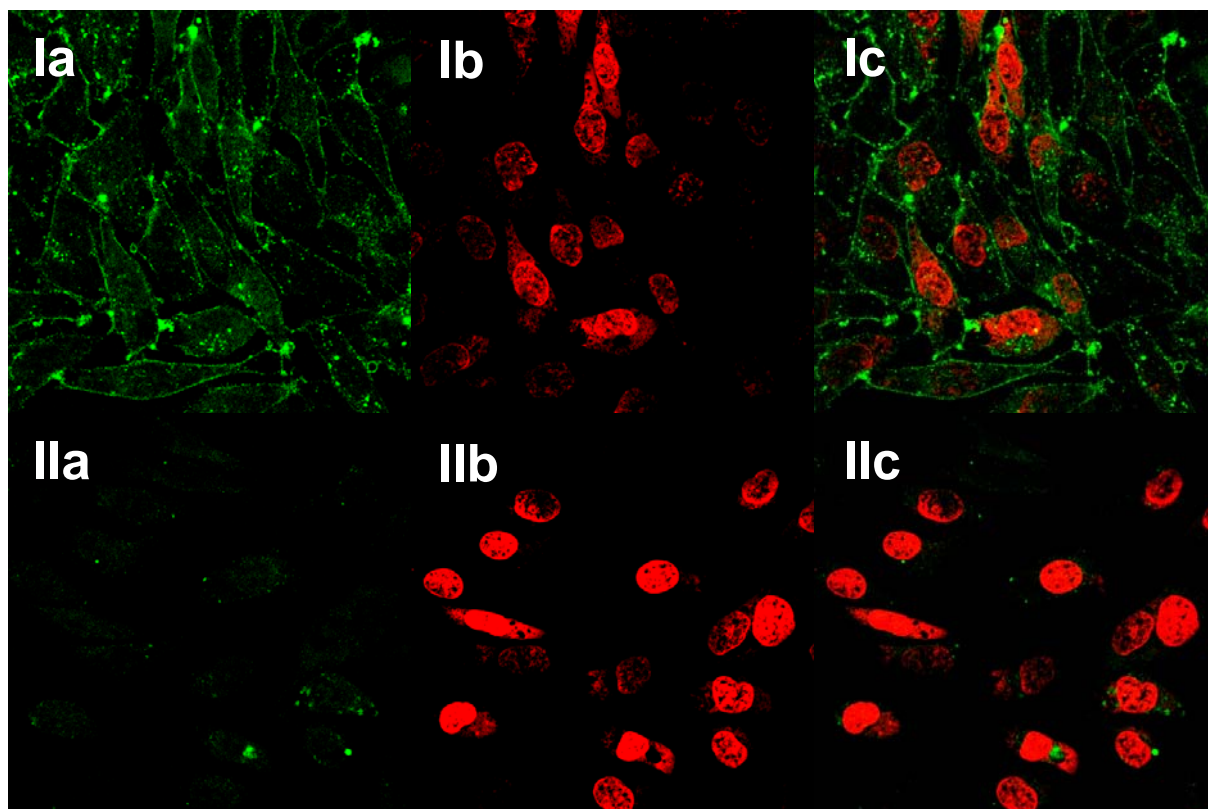


Fig. 22: Confocal microscopy of CHO-hY₂-K9-qi5-K9-mtAEQ-A7 cells incubated with 10 nM cy5-pNPY. Total binding (**Ia-c**) and unspecific binding (**IIa-c**) in the presence of 1 μ M unlabeled pNPY. Fluorescence of cy5-pNPY is shown in green (**a**); nuclei were stained with 500 nM Sytox® Green, shown in red (**b**). Merged images shown in panels **c**. For instruments settings see section 3.2.2.4.

The formation of clusters of fluorescent ligand within the cells might indicate receptor-mediated internalization as the formation of such clusters is also reported for Y₁-expressing SK-N-MC cells binding carboxyfluorescein-NPY (Fabry *et al.*, 2000), although the Y₂ receptor is characterized by a lower rate of internalization compared to the Y₁ receptor when expressed in CHO cells (Parker *et al.*, 2001b). However, it cannot be excluded that these clusters are artefacts due to fixation. Nevertheless, internalized agonist [³H]-pNPY was also found in radioligand binding studies (see 3.3.3). Further experiments should include three-dimensional laser scanning microscopy of living cells with an appropriate counterstaining in order to localize internalized cy5-pNPY more precisely.

3.3 Whole cell radioligand binding assay

3.3.1 Introduction

To compare the flow cytometric binding data determined with the stably transfected CHO-hY₂-K9 cells not only with data from the literature but also with a standard binding assay, a radioligand binding assay with whole cells was established. For this purpose CHO-hY₂-K9-qi5-K9-mtAEQ-A7 cells were used as the affinity of the agonist cy5-pNPY to the hY₂ receptor was not altered after transfection of CHO-hY₂-K9 cells with the G_{qi5} construct (see section 4.1.3.3). Additional transfection of the cells with the mtAEQ construct should not affect the binding properties of the hY₂ receptor.

The most common preparations used for binding assays are isolated membranes. The use of intact cells for binding assays provides some advantages but some disadvantages as well. The most obvious advantage using whole cells is that the receptor can be studied in its natural environment in the cell membrane. Any gradients of pH or other ions that normally exist across the membrane remain intact, and also the intracellular parts of the receptor remain in their natural cytosolic environment containing G-proteins, nucleotides, ions, enzymes and other proteins. Binding of receptor ligands can only occur from the extracellular side of the membrane as it is expected under physiological conditions unless the ligand is able to cross the membrane by diffusion or other mechanisms. Binding properties are determined using the same preparations as the ones used for the measurement of functional parameters (although some functional assays are already performed with membranes) making the data more comparable. The preparation of the samples is faster and more convenient compared to the preparation of membranes. This is very advantageous when many cell clones are screened for expression of the recombinant receptor. Changes in receptor expression due to agonist-induced desensitization, internalization, and down-regulation can be determined as well as changes in subcellular distribution and modification (e.g. phosphorylation). Adherently growing cells are convenient for whole cell radioligand binding assays in multiwell plates as separation of free radioligand from bound radioligand is accomplished simply by suction of the incubation medium followed by washing steps. Using flow cytometry, only the intact, whole cells are gated and the amount of cell-bound fluorescent ligand can be determined at equilibrium.

The disadvantages using intact cells for binding assays originate mainly from the dynamics of living cells. Receptors are constantly being synthesized, degraded, internalized and recycled, making it difficult to find equilibrium conditions where constant numbers of cell surface receptors are present. Exposure to agonists will often alter these processes, leading to a loss of cell surface receptors. Agonist-induced internalization of labeled agonist can greatly increase the apparent non-specific binding or regulatory changes in receptor properties as phosphorylation or uncoupling may occur and seriously alter the binding properties of receptors measured on whole cells. Furthermore, it is very difficult to vary or control the assay conditions inside the cell, e.g. pH value or the concentration of other ions or GTP. Because the only radiolabeled ligands for the Y₂ receptors known so far are agonists, the rate of receptor internalization should be considered when using such radioligands.

3.3.2 Materials and Methods

3.3.2.1 Radioligand binding assay

[³H]-pNPY (specific activity: 1.91-3.96 TBq/mmol) was purchased from Amersham Biosciences. The CHO-hY₂-K9-qi5-K9-mtAEQ-A7 cells were seeded at a density of 25000 cells/well in 500 µl Ham's F12 medium plus 10 % FCS on 24-well plates (Falcon Plastics 3226) two days before the experiment. The medium was removed by suction, and 200 µl of binding buffer (see section 3.2.2.3) were added. 25 µl of test compound (10-fold the final concentration in binding buffer) were added prior the addition of 25 µl of the 10-fold concentrated radioligand in binding buffer. Cells were incubated at room temperature under slight shaking for 2 h. Then, the supernatant was sucked off and the adherent cells were washed twice with ice-cold buffer. Lysis of the cells was accomplished by the addition of 200 µl of lysis buffer, containing 8 M urea (Merck), 3 M acetic acid (Merck) and 1 % Triton-X-100 (Sigma) in millipore water, followed by 30 min incubation at room temperature under slight shaking. The lysates were transferred into scintillation vials and each well was washed with another 200 µl of lysis buffer. After addition of 2 ml of Rotiscint-eco (Roth, Karlsruhe, Germany) and vigorous shaking radioactivity was measured in a LS 1801 β-counter (Beckmann Instruments, München, Germany). Unspecific binding was determined in the presence of 1 µM of unlabeled pNPY. Assays were performed in triplicate.

3.3.2.2 Acid extraction of cell-associated radioligand

Cells were prepared and incubated with the radioligand as described in section 3.3.2.1. Acid extraction procedure was performed as described (Haigler *et al.*, 1980; Parker *et al.*, 2001b; Sullivan and Schonbrunn, 1986). After the incubation with the radioligand the cells were washed twice with 500 μl of ice-cold binding buffer to remove non-specifically adsorbed radioligand and then treated with 200 μl ice-cold 0.2 M acetic acid, 0.5 M NaCl at pH 2.5 (acid wash solution) for 15 min. The cell monolayer was washed with another 200 μl of ice-cold acid wash solution and the collected acid extract was counted with the β -counter. The cells were lysed and the lysate was measured as described in 3.3.2.1.

3.3.2.3 HPLC analysis of adsorption of BIIE0246

A solution of compound **2** in binding buffer II (5 μM) was prepared in a glass vessel aliquoted into different types of assay vessels and incubated at room temperature for 2 h. Prior to injection acetonitrile was added to the samples to a final concentration of 15 % yielding the composition of the initial mobile phase. Samples were filtrated using Millex[®]-HN (0.45 μm) syringe driven filter units (Millipore Corp., Billerica, MA, USA) and subsequently analyzed by HPLC. Separation and quantification of the samples was performed using an HPLC system by Thermo Separation Products (Egelsbach, Germany) equipped with a SN 4000 controller, a P4000 pump, an AS3000 autosampler and a Spectra FOCUS UV-VIS detector. A Nucleodur 100-5 C18 column (Macherey-Nagel, Düren, Germany) was thermostatted at 30 °C. Solvents were acetonitrile and 0.05 % aqueous trifluoroacetic acid.

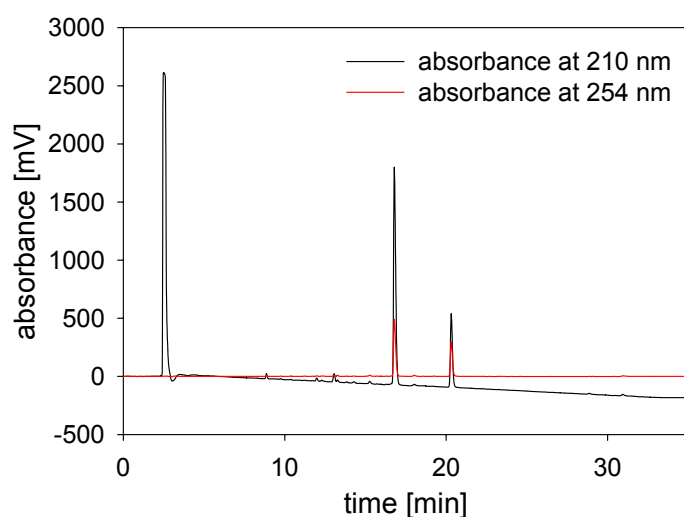


Fig. 23: HPLC analysis of BIIE0246 (**2**) Injection of 50 μl of a 100 μM solution. The compound was eluted at 16.8 min. The peak at 20.3 min results from a by-product generated during synthesis.

After 10 min of equilibration with 15 % acetonitrile, 95 μ l of the sample were injected and the fraction of acetonitrile was raised to 85 % over 30 min as a linear gradient at a flow rate of 0.8 ml/min. Absorbance was detected at 210 and 254 nm.

The purity of the compound was analyzed with HPLC revealing two peaks at 16.8 and 20.3 min. The fractions were collected and analyzed with ESI-MS. The first peak (16.8 min) is the product peak consistent with the calculated exact mass of 895 g/mol. The second fraction contained a compound with a mass of 897 g/mol. Presumably, this impurity was formed during the synthesis by hydrogenolysis of the triazolidine ring. The same ratio of product to by-product was found in a six months old solution of **2** in DMSO and in a freshly prepared solution. Therefore, it can be excluded that the by-product was formed during storage in solution.

3.3.3 Results

The internalization of hY₂ receptors stably expressed in CHO-hY₂-K9-qi5-K9-mtAEQ-A7 cells after exposure to the agonist [³H]-pNPY was determined. The acid extraction of cell associated ligand was used to discriminate between externally bound ligand from internalized ligand. The ligand stripped from washed cells by ice-cold CH₃COOH/0.5 M NaCl was considered as dissociated from cell-surface receptors, whereas the residual radioactivity determined after cell lysis was considered as internalized ligand (Parker *et al.*, 2001b). All experiments were done at room temperature (22 °C) by analogy with the radioligand binding assays.

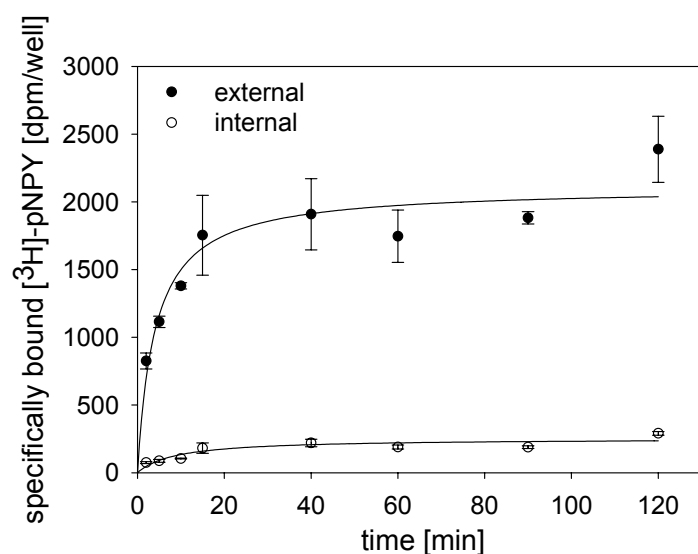


Fig. 24: Kinetics of labeling of cell surface and internalized receptors with 0.48 nM [³H]-pNPY. Data were fitted to a single rectangular hyperbolic curve (2 parameter). The half-time to maximum binding was 4.1 ± 1.2 min for surface receptors and 8.8 ± 4.1 min for internalized receptors. The fraction of internalized receptors was 10.7 % in equilibrium. Unspecific binding was determined in presence of 1 μ M pNPY (mean values \pm SEM, $n=3$).

As shown in Fig. 24, $t_{1/2}$ of maximum binding to surface receptors was 4.1 ± 1.2 min. 95 % of maximum binding (2107 dpm) was reached after 77.4 min. Therefore, an incubation time of 2 h was considered sufficient to reach equilibrium in competition assays using comparable concentrations of radioligand. For internalized receptors, binding kinetics was slightly delayed with a $t_{1/2}$ of 8.8 ± 4.1 min. 10.7 % of specifically bound radioligand was internalized at equilibrium.

To compare whether the transfection with the G_{q15} construct has an effect on receptor internalization an analogous experiment was performed with CHO-hY₂-K9 cells.

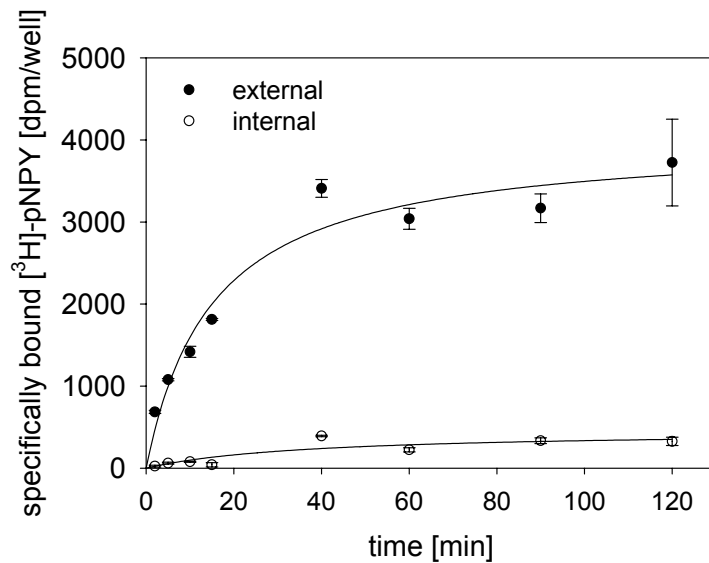


Fig. 25: Kinetics of the labeling of cell surface receptors and receptor internalization with 0.51 nM [³H]-pNPY. Data were fitted to a single rectangular hyperbolic curve (2 parameter). $t_{1/2}$ of maximum binding was 15.2 ± 3.8 min for surface receptors and 36.7 ± 31.7 min for internalized receptors. The fraction of internalized receptors was 10.2 % at equilibrium. Unspecific binding was determined in the presence of 1 μ M pNPY (mean values \pm SEM, $n=3$).

In Fig. 25, the kinetics of radioligand binding (0.51 nM) to surface receptors and receptor internalization is shown. With respect to maximum binding to surface receptors $t_{1/2}$ (15.2 min) was delayed compared to the G_{q15^-} and mtAEQ-transfected cells but the fraction of internalized receptors was almost the same (10.2 %). These data suggest that the transfection with the G_{q15} and the mtAEQ constructs have no significant effect on receptor internalization following exposure to [³H]-pNPY.

Hypertonic sucrose has been shown to prevent receptor-mediated endocytosis of GPCRs (Grady *et al.*, 1995). Therefore, the effect of high concentrations of sucrose on the internalization of the hY₂ receptor was determined. The result is shown in Fig. 26. For internalized receptors, the maximum observed binding relative to control was 62.2 % at 0.25 M and 41.3 % at 0.5 M sucrose. $t_{1/2}$ estimates of maximum binding were 15.0 min and 3.5 min for 0.25 M and 0.5 M sucrose, respectively, compared to 6.8 min in the control. In parallel, the rate of ligand binding to cell-surface receptors was lowered. Maximum binding to surface receptors was reduced relative to control

(33.2 % and 30.3 % at 0.25 M and 0.5 M sucrose, respectively). Therefore, the percentage of internalized receptors was increased in the presence of sucrose while the absolute amount of internalized receptor decreased. The data suggest that the diminished receptor internalization is due to the decreased binding of the ligand to cell-surface receptors and not a result of the inhibition of receptor-mediated endocytosis caused by the hypertonic sucrose solution.

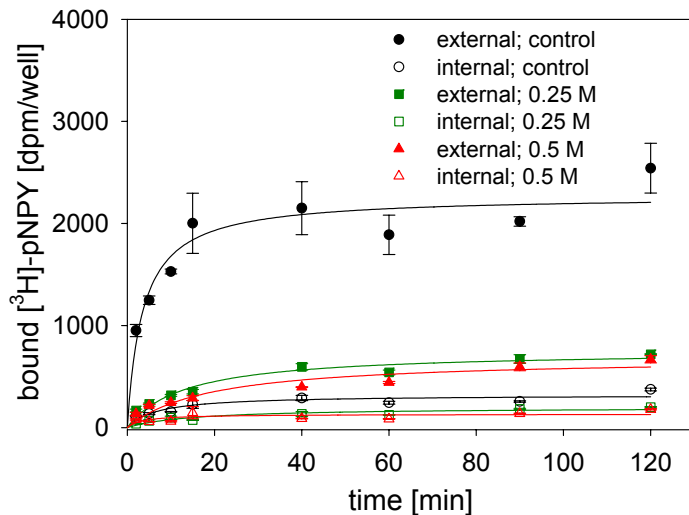


Fig. 26: Effect of sucrose on the labeling of surface-attached and internalized receptors. The concentration of [³H]-pNPY was 0.48 nM (mean values \pm SEM, n=3).

Many receptors of the rhodopsin family were described as partly cryptic, hidden, masked, or compartmentalized, for example the thrombin receptor (Kawabata and Kuroda, 2000), the α_2 adrenergic receptor (Adler *et al.*, 1987) and the 5-HT_{1B} receptor (Adham *et al.*, 1993). Also the cloned guinea-pig Y₂ receptor expressed in CHO cells as well as the rat Y₂ receptor, natively expressed in the rat forebrain, have been shown to consist of two fractions (Parker *et al.*, 2002b). One fraction is readily accessible to radiolabeled agonists and comprises less than 30 % of Y₂ receptors detected in the membrane preparation of the cell homogenate. The larger fraction of Y₂ receptors is sequestered and not accessible for agonists in intact cells. This masking of the Y₂ receptor could be abolished by the addition of phenylarsine oxide (PAO), resulting in an increased binding of agonist to intact cells by fourfold to fivefold.

The existence of a hY₂ receptor reserve, which could be unmasked by PAO, was investigated (Fig. 28). At a concentration of 30 μ M the membrane-permeable, vicinal cysteine-bridging phenylarsine oxide caused a strong increase in [³H]-pNPY binding to CHO-hY₂-K9-qi5-K9-mtAEQ-A7 cell monolayers (external).

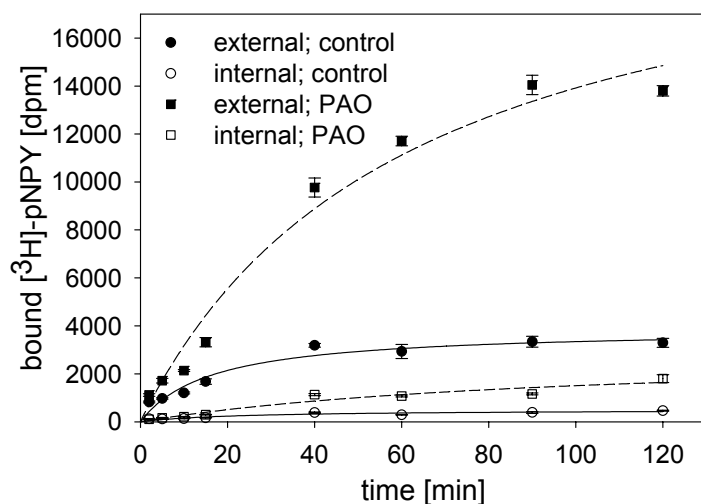


Fig. 27: Unmasking of a hY_2 receptor reserve by PAO. The number of external and internal binding sites labeled by [3 H]-pNPY is increased in presence of 30 μ M of PAO compared to the control. The concentration of [3 H]-pNPY was 0.50 nM (mean values \pm SEM, $n=3$).

Because this activation of additional surface sites was not saturated over the observed interval, no reliable kinetic estimates could be made. After 120 min of incubation, the increase was 4.2-fold compared to the control. This is consistent with the results of Parker *et al.* who determined a fourfold to fivefold increase in [125 I]-hPYY₁₃₋₃₆ binding to CHO cell monolayers expressing the guinea-pig Y_2 receptor in the presence of 30 μ M PAO (Parker *et al.*, 2002b). The fraction of internalized receptor after 120 min was almost unchanged with 11.5 % in the presence and 12.4 % in the absence of PAO.

Unmasking of sequestered surface receptors by PAO was also described for macroglobulin, transferrin and mannose-tipped glycoprotein receptors (Kaplan *et al.*, 1985). The mechanism of the activation of masked surface receptor by PAO remains unclear. As PAO is well membrane-permeable, target proteins can be supposed in the membrane as well as at intracellular sites. Parker and co-workers referred to many possible explanations such as alteration of the communication between the extracellular matrix and the actin cytoskeleton, de-anchoring of the receptor due to a change of membrane protein arrangement, increase in cell permeability, alteration of the state of receptor aggregation, or modification of proteasome subunits. Even G-protein β - and γ -subunits that contain vicinal cysteins might be modified by PAO (Parker *et al.*, 2002b). Further experiments, e.g. using confocal microscopy to visualize subcellular distribution of Y_2 receptors in the presence of PAO, should be done to discover the mechanism of PAO activation of masked surface receptor sites.

The determination of the K_d value of the radioligand is inevitable for the calculation of K_i values according to the Cheng-Prusoff equation (Cheng and Prusoff, 1973). Therefore, a saturation experiment was performed to determine the K_d value of [³H]-pNPY. The result is shown in Fig. 29. The radioligand bound with high affinity and a K_d value of 0.7 ± 0.2 nM. This value is almost identical with the K_i value of pNPY determined in the flow cytometric binding assay ($K_i = 0.8 \pm 0.2$ nM, see section 3.2.3.1).

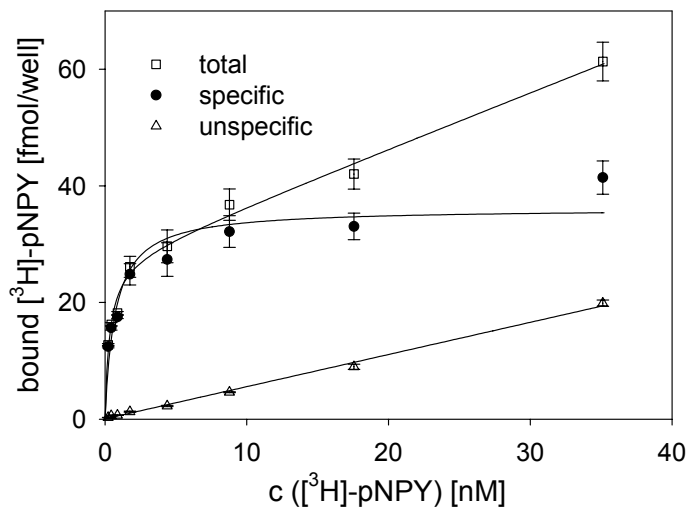


Fig. 29: Saturation experiment with CHO-hY₂-K9-qi5-K9-mtAEQ-A7 cells. The determined K_d value of [³H]-pNPY is 0.8 ± 0.2 nM (mean values \pm SEM, $n=3$).

Other peptide ligands were tested in various radioligand competition assays. The assays were performed with different concentrations of [³H]-pNPY and K_i values were calculated according to the Cheng-Prusoff equation. Competition curves are summarized in Fig. 30.

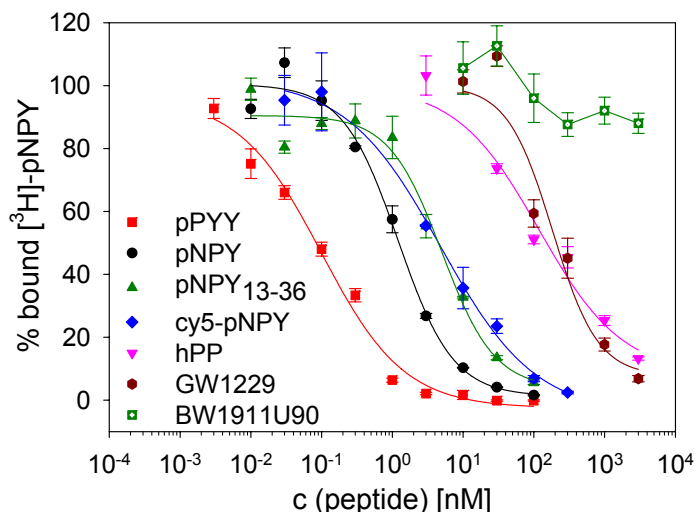


Fig. 30: Inhibition of [³H]-pNPY binding to CHO-hY₂-K9-qi5-K9-mtAEQ-A7 cells. The concentration of the radioligand was 0.49 nM for pPYY, 1.43 nM for pNPY and pNPY₁₃₋₃₆, 0.43 nM for cy5-pNPY and 0.54 nM for hPP, GW1229 as well as BW1911U90. Calculated K_i values are described in the text (mean values \pm SEM, $n=3$).

[³H]-pNPY was displaced from the CHO-hY₂-K9-qi5-K9-mtAEQ-A7 cells by the peptides with a pharmacological profile consistent for the Y₂ receptor. As expected, pPYY showed the highest affinity ($K_i = 0.06 \pm 0.01$ nM), followed by pNPY and pNPY₁₃₋₃₆ ($K_i = 0.4 \pm 0.1$ nM and 1.7 ± 0.4 nM). The K_i value of cy5-pNPY was 3.0 ± 1.3 nM in the radioligand binding assay. This value is slightly lower compared to the K_d values determined in the flow cytometric saturation assays (5.3 nM and 5.3 nM determined with CHO-hY₂-K9 cells and CHO-hY₂-K9-qi5-K9-mtAEQ-A7 cells, respectively) but still in the same range. The peptides hPP and GW1229 bound with low affinity ($K_i = 67.9 \pm 26.9$ nM and 105.1 ± 29.9 nM) compared to pPYY and pNPY. The Y₂ selective antagonist BIIE0246 (**2**) was tested in the radioligand binding assay. 1.0 nM [³H]-pNPY was displaced by **2** with an IC₅₀ value of 66.3 nM (Fig. 31).

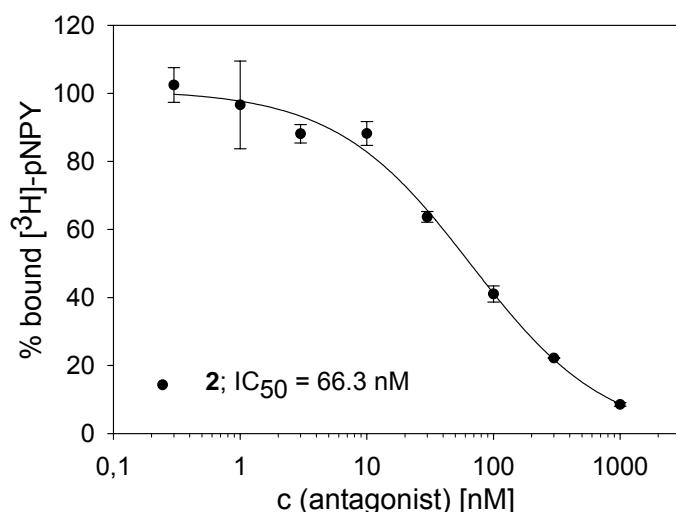


Fig. 31: Competition binding of 1.01 nM [³H]-pNPY in the presence of **2** (mean values \pm SEM, $n=3$).

The calculated $K_i = 27.6 \pm 10.9$ nM is more than tenfold higher compared to the K_i value determined with the flow cytometric binding assay ($K_i = 2.6$ nM, see Fig. 20b). Therefore, the adsorption of the compound to the material of the used 24-well plates (Falcon[®]) was investigated and compared to the adsorption to other microplates and different cups.

Compound **2** was incubated for 2-3 h at room temperature at a concentration of 5 μ M in binding buffer. The amount of “non-adsorbed” compound was determined using HPLC and compared to the reference prior to incubation. As shown in Fig. 32, after incubation of the compound in the 24-well plate used for the radioligand binding assay, only 39 % of the compound was recovered. Bearing in mind that adsorption was determined at a very high concentration of 5 μ M (due to the detection limit of the HPLC), one can assume that the percentage of adsorbed compound will be even higher when used at concentrations in the nanomolar range.

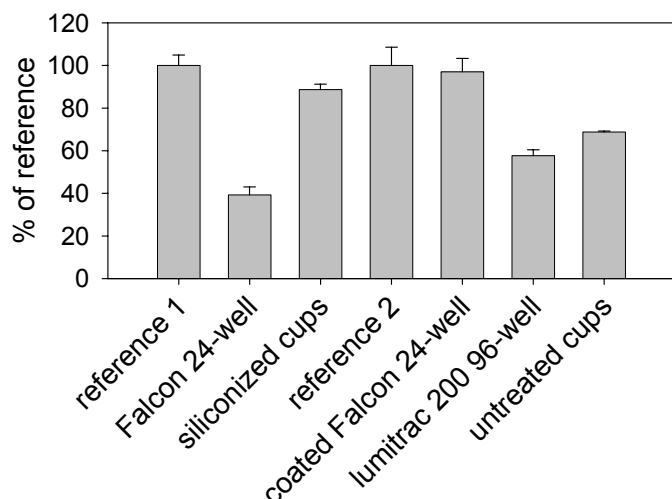


Fig. 32: Adsorption of compound **2**, used as 5 μ M solution in binding buffer, to various materials (mean values \pm SEM, $n=3$).

Adsorption occurred also during incubation of the compound with the other tested materials. 89 % of the compound was recovered following incubation in siliconized reaction vessels used for the flow cytometric binding assay. Incubation in the lumitrac[®] 200 96-well plate used for the aequorin assay led to adsorption of 42 % of the compound and 31 % of the compound were adsorbed to surface material after incubation in untreated (not siliconized) reaction vessels. Adsorption to the 24-well plate used for the radioligand binding assay could be reduced to 3 % by coating the well-plate with fetal calf serum overnight, but the K_i value of **2** determined using the coated plate (Fig. 33) was still 10-fold higher compared to the flow cytometric binding assay. A K_i value of 36.1 nM determined in a SPA assay using SMS-KAN membranes and [¹²⁵I]-PYY was published by Dautzenberg. As this assay was performed in a 96-well-plate (Dautzenberg, 2005) adsorption can not be excluded.

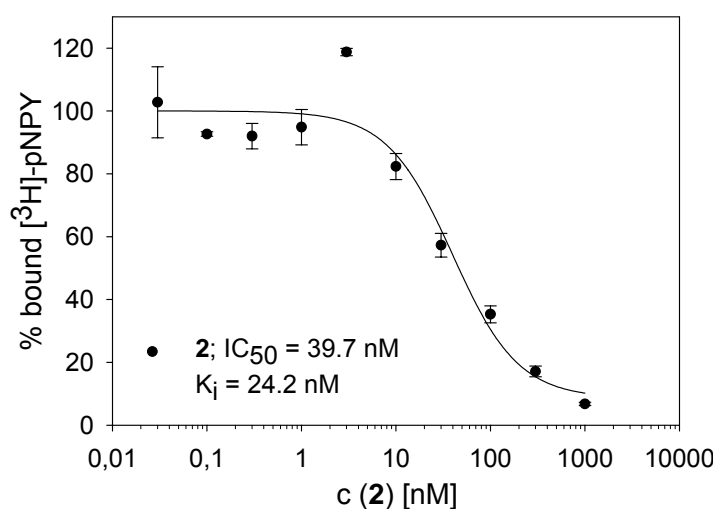


Fig. 33: Inhibition of 0.46 nM [³H]-pNPY binding to CHO-hY₂-K9-qi5-K9-mtAEQ-A7 cells in presence of BIIE0246 (**2**). The assay was performed in a 24-well plate coated with fetal calf serum (mean values \pm SEM, $n=3$).

Because of the structural similarities of the compounds the adsorption of compounds **3-8** to the solid phase used for binding assays is supposed to be similar to **2**. Nevertheless, it can not be excluded that different compound-specific adsorption effects interfere with the determination of the K_i values, especially when measured at low concentrations.

3.4 Conclusions

The flow cytometric binding assay using CHO cells, stably transfected with the hY₂ receptor gene, and cy5-labelled pNPY is a reliable and robust method for the determination of binding data at equilibrium. As summarized in Table 4 for the tested peptide ligands, the calculated K_i values are comparable with the data obtained from a radioligand binding assay.

Table 4: Comparison of K_i values calculated from flow cytometric and radioligand binding assay. (a: saturation experiment; ND: not determined)

ligand	K_i [nM] flow cytometric assay	K_i [nM] radioligand binding assay
pPYY	0.38 ± 0.10	0.059 ± 0.012
pNPY	0.76 ± 0.20	0.40 ± 0.08
pNPY ₁₃₋₃₆	1.69 ± 0.42	1.67 ± 0.41
cy5-pNPY	5.23 ± 2.15^a	3.01 ± 1.25
[L ³¹ ,P ³⁴]-pNPY	> 100	ND
[³ H]-pNPY	ND	0.72 ± 0.15

Lipophilic compounds such as **2** and related structures tend to adsorb to the materials used in the assay. The K_i value determined in the flow cytometric binding assay is in the same range as that described in the literature. But because of its lipophilic properties, the compound tends to adsorb to the “plastics” material resulting in decreased free concentrations as described in case of the radioligand binding assay in 3.3.3. These effects must be kept in mind when affinity data of argininamide **2** and related compounds are determined.

Chapter 4

Development of functional
assays for the human NPY Y₂
receptor

4.1 Flow cytometric calcium assay

4.1.1 Introduction

4.1.1.1 Functional assays for the NPY Y₂ receptor

For the determination of the activity of Y₂ receptor ligands, potent and robust functional assays are required. In contrast to classical binding assays, which can only detect molecules occupying the same binding pocket as the labelled ligand, allosterism can be detected in functional assays too (Kenakin, 2004). The most commonly used assay is based on the inhibition of forskolin-induced cAMP formation (Beck-Sickinger *et al.*, 1992; Goumain *et al.*, 2001) as the Y₂ receptor is known to couple to the G_{i/o} pathway (Michel *et al.*, 1998). The human neuroblastoma cell line SMS-KAN endogenously expressing the hY₂ receptor was found to couple to three intracellular signal transduction pathways (Shigeri and Fujimoto, 1994). Activation of the Y₂ receptor led to a decrease in angiotensin II- or bradykinin-induced Ca²⁺ release from intracellular stores and resulted in an inhibition of forskolin-stimulated cAMP accumulation as well as in high ω-conotoxin-sensitive K⁺-induced calcium influx. These pathways are indirect mechanisms as they are based on the inhibition of stimuli and they are not well suited for the establishment of functional assays. For example, in cAMP assays the forskolin-mediated prestimulation can vary even in substrains of the same cell line (Dautzenberg, 2005), and the agonist-mediated inhibition of cAMP formation rarely exceeds 60 % of the forskolin signal (Coward *et al.*, 1999) resulting in a limited dynamic range and a low signal-to-noise ratio of the assay. In addition, assays aiming at the quantification of adenylylcyclase inhibition are variable, time consuming and inappropriate for high throughput applications. The GTPγ³⁵S scintillation proximity assay (Ferrer *et al.*, 2003) has been successfully applied to the hY₂ receptor (Dautzenberg *et al.*, 2005), although the determined EC₅₀ values of Y₂ receptor agonists were 3- to 10-fold higher, compared to the cAMP assay. Furthermore, this intricate and expensive technique requires the purification of membrane components and the handling of radioisotopes, and lacks the intrinsic signal amplification, occurring in living cells under physiological conditions.

The most convenient signal transduction pathway for the establishment of functional assays is an increase in intracellular calcium concentration following receptor activation. Changes in [Ca²⁺]_i can be easily measured using fluorescent indicator

dyes (for an overview see Tepikin, 2001) or genetically encoded calcium indicators such as aequorin (see section 4.2) or cameleons (Miyawaki *et al.*, 1999; Miyawaki *et al.*, 2001).

4.1.1.2 Coupling of NPY Y₂ receptor activation to the phospholipase C pathway

Reports in the literature on Y₂ receptor coupling to mobilization of intracellular calcium are controversial. An increase in the intracellular calcium concentration in hY₂ transfected HEK293 cells was described by Gerald (Gerald *et al.*, 1995) but was not observed by Dautzenberg (Dautzenberg *et al.*, 2005). For CHP-234 cells (Lynch *et al.*, 1994) and CHO cells transfected with the hY₂ gene (Rose *et al.*, 1995) calcium responses were also reported. By contrast, only a very slight increase in intracellular calcium was measured in our laboratory in the spectrofluorimetric fura-2 assay using transfected CHO cells stably expressing the human Y₂ receptor.

An increase in intracellular calcium as a result of GPCR activation via the phospholipase C pathway is usually mediated by α -subunits of heterotrimeric G proteins of the G_q family (Offermanns, 2003). However, IP₃ generation mediated by $\beta\gamma$ -subunits of G_i upon receptor activation is discussed too (Offermanns and Simon, 1995). The G_q family comprises the G_q, G₁₁, G₁₄ and G_{15/16} proteins. G_q and G₁₁ are almost ubiquitously expressed in mammalian cells, whereas expression of G₁₄ is restricted to kidney, lung and spleen. The more distantly related G₁₅ and G₁₆ proteins were found to be only expressed in a subset of hematopoietic cells (Amatruda *et al.*, 1991; Wilkie *et al.*, 1991). Because G₁₅ and G₁₆ are (unlike the other members of the G_q family) capable to link the activation of many G_s-, G_i- and G_q-coupled receptors to the phospholipase C pathway with subsequent intracellular Ca²⁺ increase, co-expression of G₁₆ and GPCRs has been successfully performed (Knight *et al.*, 2003; Milligan *et al.*, 1996; Offermanns and Simon, 1995; Stables *et al.*, 1997; Zhu and Birnbaumer, 1996) aiming at the development of functional assays with a simple and robust readout (e.g. FLIPR assay). However, the coupling of G₁₆ is less effective to G_i- compared to G_s-coupled receptors (Knight and Grigliatti, 2004; Kostenis, 2001). In order to improve the coupling of G_i-coupled receptors to the PLC/IP₃ pathway, several chimeric G proteins derived from G_q were constructed (Conklin *et al.*, 1996; Conklin *et al.*, 1993; Coward *et al.*, 1999). Replacement of the five C-terminal amino

acids of G_q with the corresponding G_i residues considerably enhanced the coupling efficiency to G_i -coupled receptors. Other modifications of G_q proteins are discussed by Kostenis (Kostenis, 2001) and Milligan and Rees (Milligan and Rees, 1999). Chimeric G proteins have already been used for the mobilization of calcium from intracellular stores in response to agonist stimulation by the generation of appropriate cells (Coward *et al.*, 1999; Dautzenberg, 2005; Dautzenberg *et al.*, 2005; Knight and Grigliatti, 2004).

4.1.1.3 Flow cytometric calcium assay

Flow cytometric kinetic measurements of calcium mobilization require a technique which allows continuous registration during the addition of an agonist without interrupting the sample flow. Several sophisticated techniques have been developed using a stopped-flow mixing approach in order to reduce (Nolan *et al.*, 1995) or using microfluidic mixing approaches to completely abolish (Edwards *et al.*, 2004; Jackson *et al.*, 2002a; Jackson *et al.*, 2002b; Nolan and Sklar, 1998; Scampavia *et al.*, 1995) the dead-time needed for mixing the cell suspension with the sample before the measurement. A simple technique was established by Schneider (Schneider, 2005) using a purpose-build glass sample tube closed by a silicon septum. Variable volumes of ligand solutions can be added by injection with a hamilton syringe to a stirred cell suspension during continuous measurement. As the FACSCalibur flow cytometer is equipped with an argon and a red diode laser providing only the two fixed wavelengths at 488 and 635 nm for excitation of fluorescent Ca^{2+} indicator dyes, Schneider chose the non-ratiometric Ca^{2+} indicator dye fluo-4 (excitation maximum = 494 nm) for the measurement of calcium responses with flow cytometry (Schneider, 2005). The increase in fluorescence emission due to binding of intracellular calcium could be detected in channel 1 (FL-1, see Fig. 16) of the flow cytometer. Schneider constructed concentration-response curves for the thrombin receptor agonist thrombin on HEL cells using a spectrofluorimetric (fura-2) and a flow cytometric (fluo-4) calcium assay and concluded that both assays are comparable.

4.1.1.4 Spectrofluorimetric calcium assay

The use of the ratiometric Ca^{2+} indicator fura-2 is a standard method for the measurement of intracellular calcium mobilization (Daniels *et al.*, 1992; Petr and

Wurster, 1997). Binding of Ca²⁺ results in a shift of the excitation maximum so that intracellular calcium concentration can be calculated using the ratio (R) of fluorescence intensity after alternating excitation at two different wavelengths (see 4.1.2.5). Therefore, the signal (R) is independent of intracellular dye concentration, which can vary due to differences in the loading of the cells or because of dye leakage. This is the main advantage of ratiometric calcium indicator dyes compared to non-ratiometric ones. The use of fura-2 has been successfully applied to HEL cells for the determination of functional data of hY₁ receptor ligands (Geselle, 1998).

4.1.2 Materials and Methods

4.1.2.1 Standard media and cloning procedures

Agar plates, LB and amp-LB media were prepared as described in 3.1.2. Competent *E. coli* cells were prepared using the TOP10 *E. coli* strain (Invitrogen, Karlsruhe, Germany) by analogy with the procedure described in chapter 3.1.2.2. For transformation with the pcDNA1 vector, containing the *supF* gene for selection, one Shot[®] TOP10/P3 competent cells were purchased from Invitrogen. Transformation, preparation of the plasmid DNA, restriction enzyme digestion and agarose gel electrophoresis were performed as described in chapter 3.1.2.

4.1.2.2 Subcloning of pcDNA3.1/hygro-qi5

The pcDNA1-qi5-HA vector was a generous gift of Dr. Bruce R. Conklin, Gladstone Institute of Cardiovascular Disease, University of California, San Francisco, USA. The construct G_{qi5} originates from q4WT, which encodes for Gq alpha with an HA epitope engineered into an internal site that does not seem to affect receptor coupling in multiple studies (Wedegaertner *et al.*, 1993). The last 5 C-terminal amino acids of the encoded construct are exchanged from G_q alpha to G_i alpha residues (EYNLV to DCGLF). As the carboxyl-terminus of the G alpha protein is a key determinant of receptor specificity (Conklin *et al.*, 1996; Conklin *et al.*, 1993), this construct allows many G_i-coupled receptors to stimulate phospholipase C (PLC). The construct G_{qi5} was subcloned into the Bam HI/NsiI cassette of the pcDNA1 vector. The pcDNA3.1/Hygro vector was a gift of Dr. Thomas Dobner, Institute of Microbiology and Hygiene, University of Regensburg, Germany.

The restriction sites *Nsi*I and *Xba*I downstream of the construct couldn't be used for subcloning because of the absence of a *Nsi*I restriction site in the multiple cloning site of the target vector and the presence of an *Xba*I site within the construct at bp 834. Therefore, a new *EcoRV* site was introduced at the 3'-end of the construct by PCR. Primers were synthesized by MWG (Ebersberg, Germany). The sense primer matches to the T7 promoter/priming site of the pcDNA1 and the antisense primer contains the mutated *EcoRV* restriction site (in bold):

sense: 5'-TAA TAC GAC TCA CTA TAG GG-3' (20 b, Tm: 53.2 °C)

antisense: 5'-CGC **GAT ATC** ATG CAT TCA GAA GAG GCC AC-3'
(29 b, Tm: 68.1 °C)

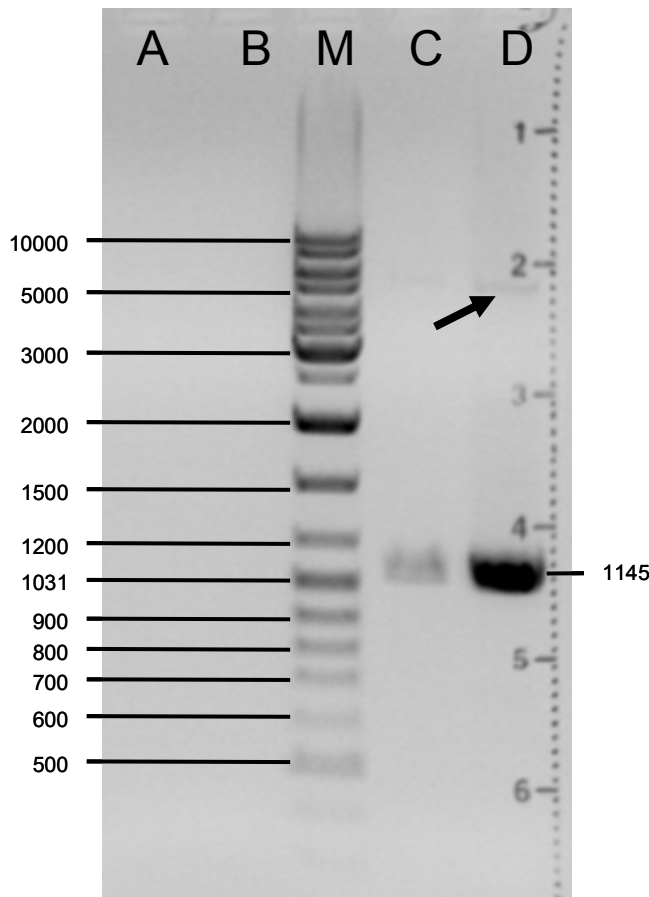


Fig. 34: Formation of *qi5* construct with introduced *EcoRV* restriction site at increasing annealing temperatures (A – D: 50 °C – 60 °C). Concomitant formation of a by-product (black arrow) in D.

PCR reactions were prepared in a final volume of 50 µl containing 5 µl 10x PCR buffer (peqLab, Erlangen, Germany), 20 ng of dsDNA template, 15 pmol of each primer, 5 µl of dNTP mix (2 mM, MBI Fermentas), 1 U of Pwo-DNA-polymerase (peqLab, Erlangen, Germany) and millipore water. PCR was performed in a Mastercycle gradient Thermocycler (Eppendorf, Hamburg, Germany) using a linear temperature gradient during the annealing step.

Cycling parameters were:

- 1) initial denaturation: 95 °C, 60 s
- 2) denaturation: 95 °C, 30 s
- 3) annealing: 50 – 60 °C, 1 min
- 4) extension: 72 °C, 2 min
- 5) final extension: 72 °C, 5 min
- 6) hold: 4 °C

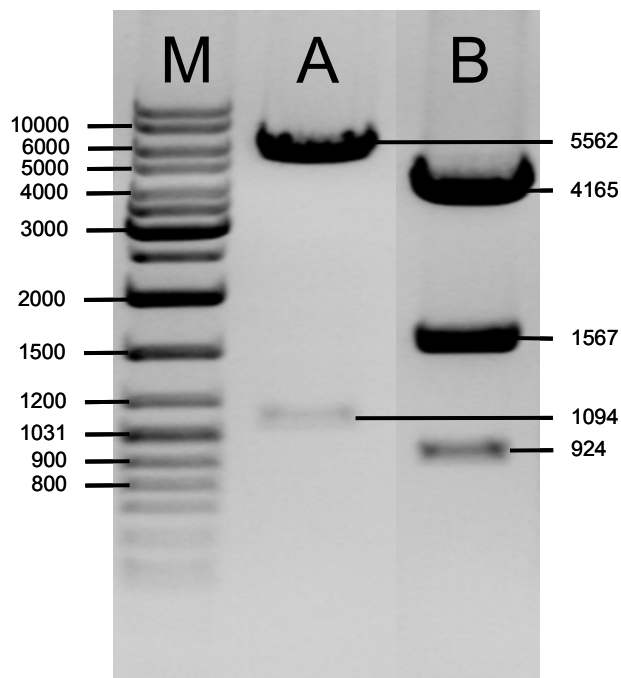
Steps 2) – 4) were repeated 30 times.

Formation of the PRC product with the expected size (1145 bp) was best with annealing temperature of 60 °C (Fig. 34). A by-product of 5000 bp (Fig. 34, black arrow) was also detected. The PCR product (1145 bp) was excised from the gel and purified with the QIAEX II purification kit (Quiagen, Hilden, Germany). DNA was eluted with 20 µl of millipore water.

The purified insert and 2 µg of the pcDNA3.1/Hygro vector were both digested with *Bam*HI (MBI Fermentas) and *Eco*RV (MBI Fermentas) using SuRE/Cut buffer B (Roche Diagnostics) for 3 h at 37 °C. DNA fragments were purified with the Qiagen PCR purification kit (Qiagen) and eluted with 20 µl of millipore water.

For the ligation reactions, 2 µl of linearized vector were incubated with 2, 4, 6, or 8 µl of insert in the presence of 1 Weiss unit of T4 DNA ligase (MBI Fermentas), 2 µl of 10x ligation buffer (MBI Fermentas) and water in a final volume of 20 µl. The samples were incubated for 60 min at room temperature and directly used for transformation without inactivation of the T4 ligase.

Fig. 35: Restriction analysis of the pcDNA3.1/Hygro-qi5 vector.
A: *Bam*HI / *Eco*RV digestion;
B: *Bam*HI / *Eco*RI digestion



Transformation of *E. coli* was carried out with 10 µl of each ligation product. Ampicillin resistant bacterial colonies were propagated in overnight cultures using amp-LB medium and the plasmid DNA was isolated by MiniPrep as described in chapter 3.1.2. Correct insertion of the G_{qi5} construct was verified by restriction analysis (Fig. 35). The new pcDNA3.1/Hygro-qi5 vector has a length of 6656 bp with a *Bam*HI site at 929 bp, an *Eco*RV site at 2023 bp and two *Eco*RI sites at 1853 and 3420 bp. Restriction enzyme digestion with *Bam*HI and *Eco*RV releases the G_{qi5} construct (1094 bp) from the vector (5562 bp) as shown in Fig. 35, **A**. Double

digestion of the plasmid with *Bam*HI and *Eco*RI leads to three DNA fragments with lengths of 924, 1567 and 4165 bp (Fig. 35, **B**). Plasmid DNA was purified using the Qiagen Plasmid Purification Kit (Qiagen, Hilden, Germany), the construct was sequenced (Entelechon, Regensburg, Germany) and the sequence was compared with that obtained from Dr. Conklin. Five conservative mutations were found: G144A, A157T, G158C, C159G, and G288A (counted from the ATG start codon of the construct).

4.1.2.3 Transfection of CHO-hY₂-K9 cells

CHO-hY₂-K9 cells were seeded in 500 µl of Ham's F12 supplemented with 10 % FCS on a 24-well plate. On the day of transfection, 60-70 % confluence was reached. The pcDNA3.1/Hygro-q15 vector was linearized with *Eam*11051 for 1 h at 37 °C and subsequently purified with the Qiagen PCR purification kit (Qiagen). The DNA was assumed to be 90 % of the amount of the applied DNA as the manufacturer specifies 90-95 % recovery of the DNA after purification. For transfection, 300 ng of linearized plasmid and 1.8 µl of FuGENE™ were used per well. Transfections were performed according to the manufacturer's instructions. Medium was replaced 24 h after transfection. Two days post-transfection, the cells were trypsinized and transferred into 25-cm² tissue culture flasks (Becton Dickinson, Franklin Lakes, N.J., USA) with Ham's F12 containing 10 % FCS, 400 µg/ml of geneticin and 400 µg/ml of hygromycin, respectively. Untransfected CHO-hY₂-K9 cells were maintained in the same selective medium as a negative control. Cells were passaged by 1:10 splitting every 3 days. After 3 weeks control cells were dead and single clones of the transfected cells were selected as described in 3.1.2.12 and expanded for analysis in a flow cytometric calcium assay.

4.1.2.4 Flow cytometric calcium assay

Cells were grown for 2 days to 70-90 % confluence, trypsinized and detached with Ham's F12 supplemented with 10 % FCS to inactivate trypsin. Cells were counted in a hemocytometer, centrifuged for 5 min at 300 g at room temperature and resuspended at a density of $2.66 \cdot 10^6$ cells / ml in loading buffer (Gessele, 1998) containing 120 mM NaCl, 5 mM KCl, 2 mM MgCl₂, 1.5 mM CaCl₂, 25 mM HEPES and 10 mM glucose at pH 7.4. For the preparation of the loading suspension, 3 µl of

fluo-4-AM (Molecular Probes; 1 mM stock solution in anhydrous DMSO) were added to 5 μ l of pluronic™ F-127 (Molecular Probes; 20 % stock solution in DMSO) and mixed carefully before addition of 1 ml of loading buffer containing 2 % BSA. 330 μ l of loading suspension were added to 1 ml of cell suspension resulting in a cell number of $2 \cdot 10^6$ cells / ml and a dye concentration of 0.7 μ M.

The cells were incubated in the dark for 30 min at room temperature and recentrifuged at 300 g for 5 min. After resuspension in loading buffer at a density of $0.5 - 1 \cdot 10^6$ cells/ml, the cells were incubated again for 30 min at room temperature in the dark; during this postincubation step, the AM-ester is intracellularly cleaved and thus the calcium indicator is trapped in the cell.

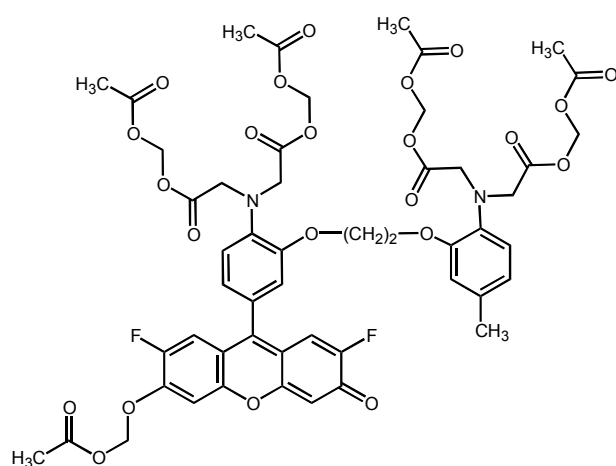
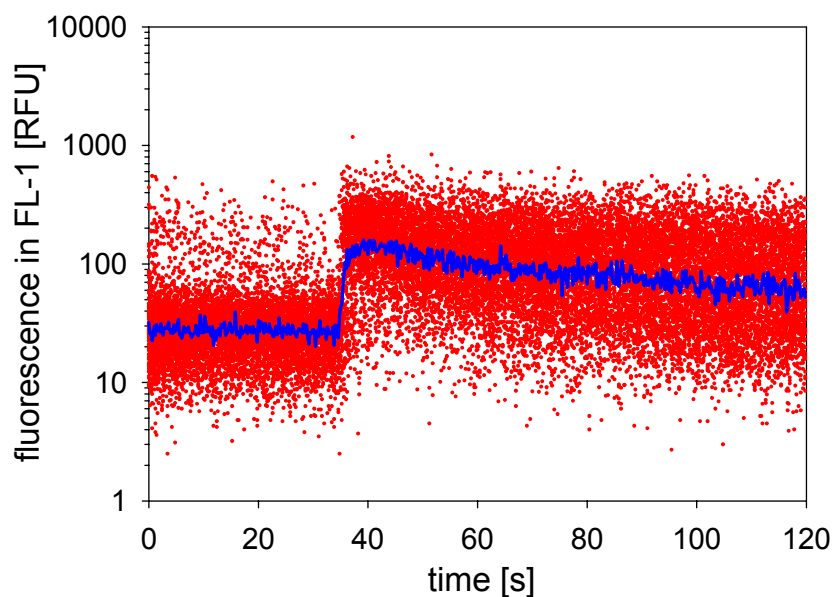


Fig. 36: Structure of the fluo-4 AM ester.

Measurements were performed in a purpose-built glass tube closed by a silicon septum as described (Schneider, 2005). This instrumentation allows injections into the samples during continuous flow cytometric measurements. A tube containing 1 ml of the cell suspension was connected with the flow cytometer under permanent stirring and the recording was started. Instrument settings were: FSC: E-1; SSC: 280; FL-1: 350; flow: high.

After 30 s of measurement of the basal fluorescence 10 μ l of peptide agonist solution were injected with a hamilton syringe and data were recorded for another 90 s. The needle of the flow cytometer was washed with millipore water after each measurement. Raw data were first averaged with the WinMDI software and then exported to Sigma Plot™ 8.0.

Fig. 37: Flow cytometric calcium assay. Fluorescence of fluo-4-loaded cells was recorded in channel 1 (FL-1) over 2 min. After 30 s, injection of 100 nM pNPY causes an increase in fluorescence of gated qi5-transfected CHO-hY₂-K9 cells. Values were averaged with WinMDI software (blue line).



Data were further smoothed (running average) with SigmaPlot™. The level of increase in fluorescence was calculated from the difference between the baseline (mean fluorescence of the first 25 s) and the highest value of the averaged curve. These amplitudes of the averaged signals were used to construct concentration-response curves. For the determination of EC₅₀ values of agonists, every third measurement was a 100 % reference signal elicited with 1 μM pNPY.

Dilutions of Y₂ receptor antagonists (Fig. 18) were made in DMSO, and 10 μl of antagonist was preincubated with 990 μl of cell suspension for 1 min before the measurement. Calcium response was triggered with 10 μl of 70 μM pNPY in 10 mM HCl containing 0.1 % BSA. The 100 % reference signal was induced in every third measurement, too. In this case, cells were preincubated in the presence of the solvent without antagonist. EC₅₀ and IC₅₀ values were calculated with Sigma Plot™ (Version 8.0, SPSS Inc.) using the equation of the four parameter logistics function.

4.1.2.5 Spectrofluorimetric calcium assay

The spectrofluorimetric calcium assay with the ratiometric Ca²⁺ indicator fura-2 was performed as described for HEL cells by Gessele (Gessele, 1998). Cells were grown to 70-80 % confluence, trypsinized and resuspended in FCS containing medium for trypsin inactivation. Cells were counted, centrifuged at 300 g for 5 min and resuspended at $1.3 \cdot 10^6$ cells/ml in loading buffer. 0.75 ml cell suspension were added to 0.25 ml of loading suspension containing 20 mg of BSA, 5 μ l of pluronic F-127 (20 % in DMSO) and 4 μ l of fura-2/AM (Molecular Probes; 1 mM in anhydrous DMSO) in 1 ml of loading buffer. The addition of pluronic F-127 facilitates the solubilization of the lipophilic calcium indicator dye and the following dye loading as described for fluo-3 in (M. E. Granados, 1997) and (Kao *et al.*, 1989). Final concentrations were: $1 \cdot 10^6$ cell/ml, 1 μ M fura-2/AM, 0.2 % DMSO and 0.025 % pluronic F-127. The cells were incubated for 30 min at room temperature in the dark, centrifuged and resuspended in the same volume of loading buffer. In order to achieve complete intracellular cleavage of the AM-ester, the cells were incubated for additional 30 min in the dark, washed twice with loading buffer and resuspended at a density of $1 \cdot 10^6$ cells/ml.

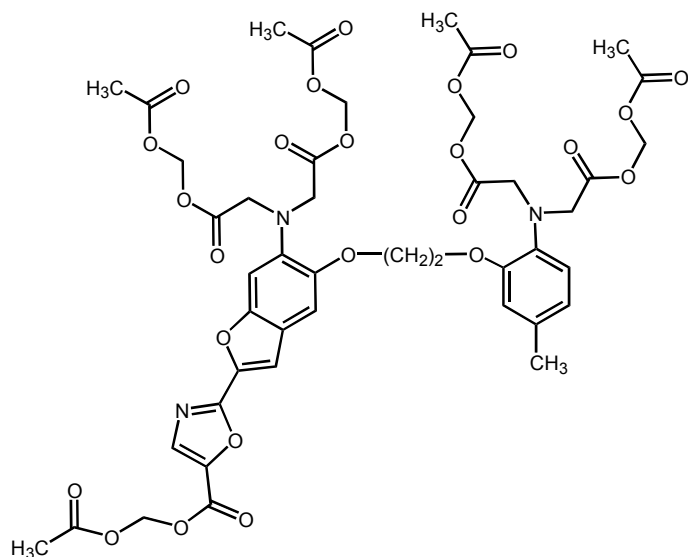


Fig. 38: Structure of the fura-2 AM ester.

For the measurement, 1 ml of the cell suspension was transferred into a cuvette containing 1 ml of loading buffer under stirring. The baseline was recorded for 30 s before the agonist was added. Antagonists were added to the cell suspension 1 min before the calcium signal was triggered by the addition of a fixed concentration of

agonist. Every third measurement was a reference signal. For the determination of agonist activity, the reference signal was triggered by 1 μM pNPY; for the determination of IC_{50} values of antagonists, the reference signal was elicited in the absence of antagonist. Instruments settings were $\lambda_{\text{ex}} = 340$ and 380 nm (alternating) with slit = 10 nm and $\lambda_{\text{em}} = 510$ nm with slit = 10 nm. Stirring was low and temperature was 25 °C.

The ratio R of fluorescence intensity at 510 nm after excitation at 340 and 380 nm was used for the calculation of the calcium concentration according to the Grynkiewicz equation (Grynkiewicz *et al.*, 1985):

$$[\text{Ca}^{2+}] = K_D \cdot \frac{(R - R_{\min})}{(R_{\max} - R)} \cdot \text{SFB}$$

The K_D value is the dissociation constant of the fura-2- Ca^{2+} complex. R_{\max} is the fluorescence ratio in presence of a saturating Ca^{2+} concentration, determined after the addition of 10 μl of digitonin solution (2% in water, Sigma), which caused lysis of the cells and saturation of the dye with the calcium ions of the loading buffer. R_{\min} is the ratio in absence of free Ca^{2+} , determined after the addition of 50 μl of EGTA solution (600 mM in 1 M tris buffer, pH 8.7) to the lysed cells. The correction factor SFB is the ratio of fluorescence intensity at 510 nm after excitation at 380 nm of the Ca^{2+} free and Ca^{2+} saturated dye.

4.1.3 Results and discussion

4.1.3.1 Characterization of the transfectants using peptidic agonists in the flow cytometric calcium assay

Four weeks after transfection of CHO-hY₂-K9 cells with the linearized G_{q15} construct and culturing in selective medium, 24 cell clones were selected, expanded and analysed in the flow cytometric calcium assay. Following injection of 20 nM pNPY, clone 9 showed a robust increase in fluorescence. As shown in Fig. 39A, this increase was concentration dependent and reached its maximum at 1 μM pNPY with a 5.3-fold increase in fluorescence (from 26.7 to 140.6 RFU). This maximum increase is dependent on the condition of the cells, especially on the degree of confluence, and varies between different cell preparations. The strongest calcium responses were obtained using cells which had grown to ca. 80 % confluence in two days. In order to account for this variation and for alterations of the fluorescence signal due to dye leakage during the test series 100 % reference samples were included by injection of 1 μM pNPY (every third measurement). This allowed the construction of concentration-response curves (Fig. 39B). The EC₅₀ value of pNPY at the hY₂ receptor was 18.1 ± 2.9 nM. The Y₂ preferring agonist pNPY₁₃₋₃₆ caused a comparable effect with an EC₅₀ value of 13.3 ± 6.2 nM and the ligand pPYY was even more potent with an EC₅₀ value of 7.9 ± 5.5 nM. This pharmacological profile is characteristic of the human Y₂ receptor. Dautzenberg reported on EC₅₀ values in the same range determined in a FLIPR assay using G_{q19}-transfected SMS-KAN (Dautzenberg, 2005) or HEK293 cells co-transfected with hY₂ and G_{q19} (Dautzenberg *et al.*, 2005).

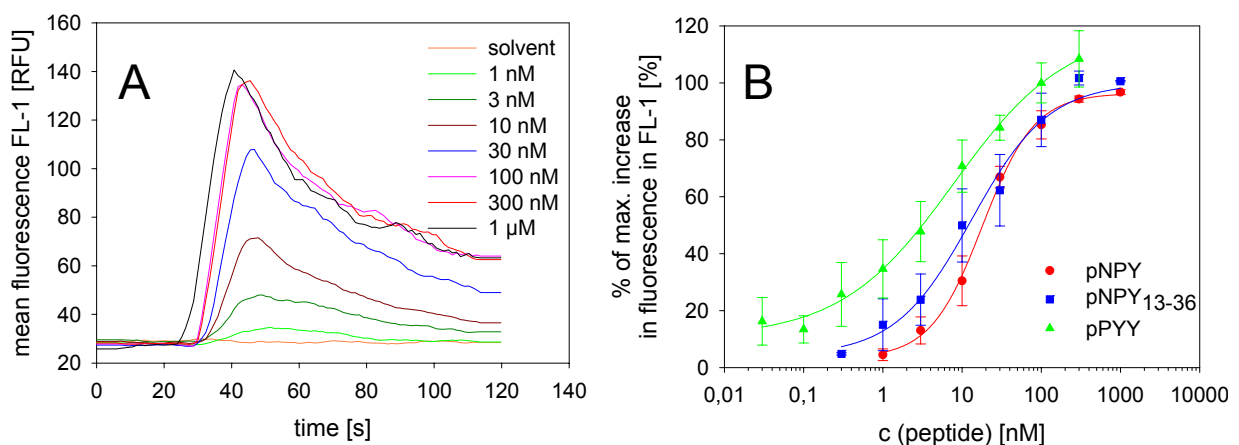


Fig. 39: Flow cytometric Ca²⁺ assay with CHO-hY₂-K9-q15-K9 cells loaded with fluo-4. **A:** concentration dependent increase in fluorescence after injection of pNPY. **B:** concentration-response curves of Y₂ agonists. Maximal reference signal was elicited with 1 μM pNPY (mean values ± SEM, n=3).

4.1.3.2 Comparisation of wild type and transfected CHO cells

In order to evaluate the effect of the stable co-transfection with the G_{qi5} construct, CHO, CHO-h Y_2 -K9 and CHO-h Y_2 -K9-qi5-K9 cells were loaded with fura-2 and analysed with respect to their response upon stimulation with pNPY.

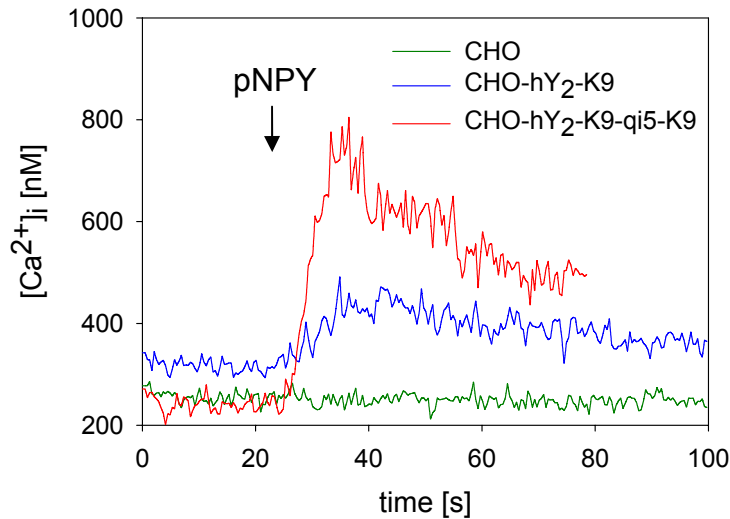


Fig. 40: Increase in the intracellular calcium concentration in CHO cells loaded with fura-2. The calcium response was elicited with 50 nM pNPY.

As expected, wild-type CHO cells did not respond to the addition of 50 nM pNPY. A slight increase in the intracellular calcium concentration was observed with CHO cells stably transfected with the h Y_2 receptor gene. But this increase rarely exceeded 20 % of the basal calcium concentration and is not sufficient for the development of a robust functional calcium assay. After the transfection with the construct encoding for the chimeric G protein, stimulation of the cells with the Y_2 agonist pNPY led to a strong calcium signal, providing a sufficient signal-to-noise ratio for the establishment of robust functional assays.

4.1.3.3 Binding properties of the transfected cell line

In order to evaluate whether the transfection with the G_{qi5} construct influences precoupling of the receptor and G protein and therefore alters the affinity of ligands, the K_d value of cy5-pNPY was determined in a saturation experiment using CHO-hY₂-K9-qi5-K9 cells.

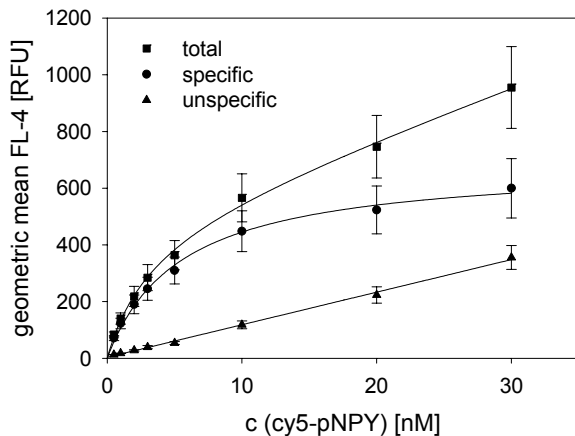


Fig. 41: Saturation experiment with CHO-hY₂-K9-qi5-K9 cells. Cy5-pNPY binds with a K_d value of 5.5 ± 1.7 nM. Unspecific binding was determined in the presence of 1 μ M unlabeled pNPY (mean values \pm SEM, n=6).

As shown in Fig. 41, the K_d value of cy5-pNPY determined with G_{qi5}-transfected cells is 5.5 ± 1.7 nM. Compared to the K_d value of 5.2 ± 2.2 nM determined with CHO-hY₂-K9 cells (see Fig. 20a), the affinity of cy5-pNPY remains almost unchanged after transfection with the G_{qi5} construct.

4.1.3.4 Effect of solvents on intracellular calcium mobilization

As test compounds selected for functional and binding assays are usually dissolved in DMSO, the effect of this solvent was determined in the fluo-4 assay. The calcium signal was elicited with 70 nM pNPY and the cell suspension was preincubated for 1 min with increasing concentrations of DMSO. As shown in Fig. 42, up to 1 % DMSO the calcium signal was only slightly reduced (by 4-8 %) compared to the reference.

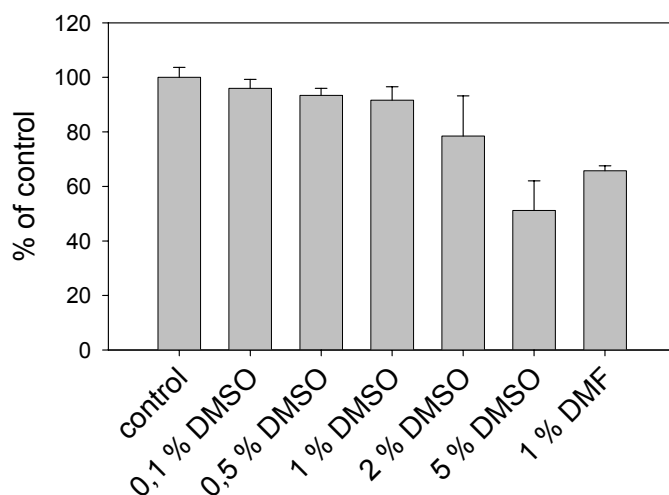


Fig. 42: Effect of DMSO on the calcium response. CHO-hY₂-K9-qi5-K9 cells were preincubated with the indicated concentrations of DMSO or DMF for 1 min. Then the calcium response was elicited with 70 nM pNPY (mean values \pm SEM, n=3).

With increasing concentrations of DMSO the signal dropped down to 79 % of the reference at 2 % DMSO and to 51 % at 5 % DMSO, respectively. Preincubation of the cells with 1 % DMF resulted in a decrease of the calcium signal to 65.8 %. Therefore, the determination of antagonistic activity was performed at a final DMSO concentration of 1 %.

4.1.3.5 Effect of the speed of injection

Another important parameter of the flow cytometric calcium assay is the velocity of agonist injection. Upon bolus injection the calcium response is fast and intense, whereas after slow injection of the agonist the calcium signal is reduced and delayed which is typical for receptor desensitization. Relatively low concentrations of the agonist cause receptor phosphorylation by both second messenger-dependent protein kinases and G protein-coupled receptor kinases (GRKs) during the injection period.

Usually, phosphorylation is followed by binding of arresting proteins (e.g. β -arrestins) which enables receptor internalization via clathrin-coated vesicles and subsequent receptor sequestration or resensitization (Ferguson *et al.*, 1998). The interaction of NPY receptors and β -arrestin 2 is described by Berglund and co-workers (Berglund *et al.*, 2003c). As shown in Fig. 43, injection of the agonist over a period of 2 s reduced the calcium signal by 59 % compared to a bolus injection.

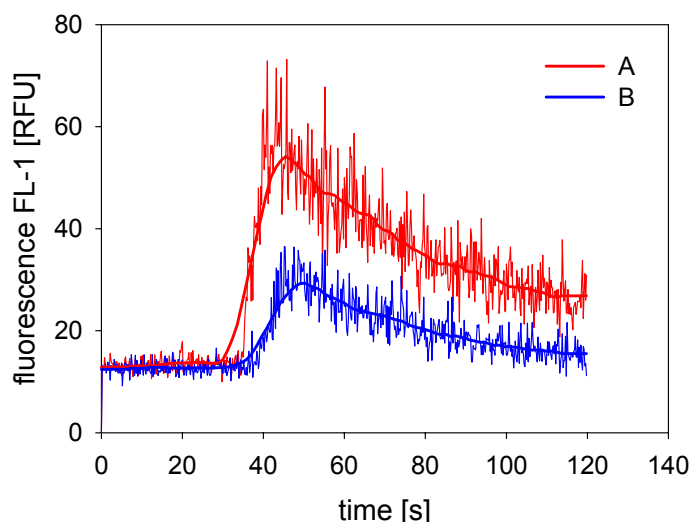


Fig. 43: Effect of injection speed on calcium response. 70 nM pNPY were used as agonist. **A:** bolus injection. **B:** injection over a period of 2 s.

These data point out that injection of the agonist should be as fast as possible. Slow injection reduces the calcium response and impairs the quality of determined data.

4.1.3.6 Characterisation of antagonists in the flow cytometric calcium assay

NPY Y₂ receptor antagonists (**3-8**, Fig. 18) derived from BIIE0246 (**2**) were analysed with respect to their antagonistic activity in the flow cytometric calcium assay. The assay was performed with CHO-hY₂-K9-qi5-K9 cells and 70 nM pNPY to trigger intracellular calcium mobilisation. The cell suspension was preincubated with the antagonists for 1 min at a final DMSO concentration of 1 %.

The Y₂ selective antagonist BIIE0246 (**2**) inhibited the pNPY-induced intracellular calcium increase with an IC₅₀ value of 20.4 ± 2.9 nM. Dautzenberg et al. reported on an IC₅₀ of ~ 100 nM determined in a FLIPR assay with hY₂- and G_{qi9}-cotransfected HEK293 cells using 10 nM PYY (Dautzenberg *et al.*, 2005). It is important to notice

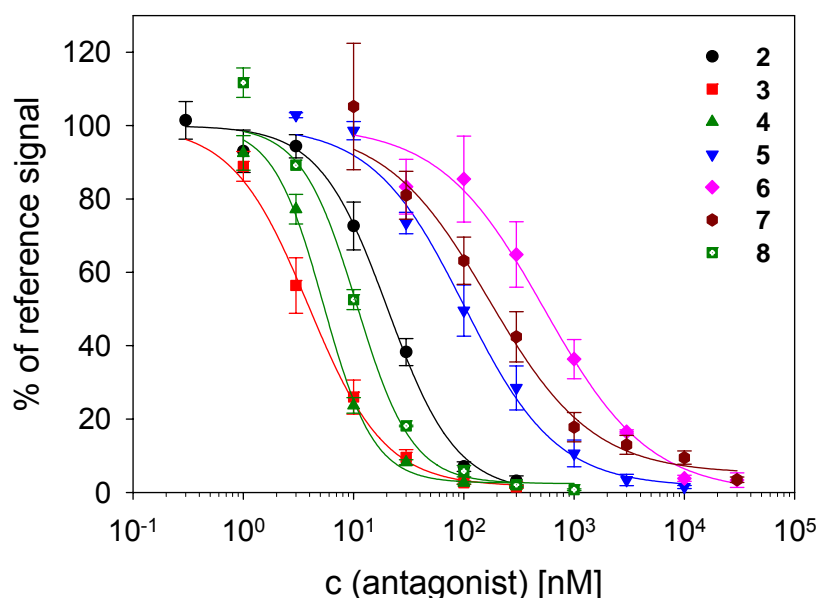


Fig. 44: Flow cytometric fluo-4 Ca²⁺ assay for Y₂R antagonists. Inhibition of pNPY (70 nM)-induced calcium response in CHO-hY₂-K9-qi5-K9 cells (mean values ± SEM, n=3-7).

that in the FLIPR assay, agonist and antagonist are added simultaneously, whereas in the flow cytometric calcium assay, the cells were preincubated with the antagonist for 1 min. Furthermore, the more potent agonist PYY was used. Nevertheless, the IC₅₀ values determined in the different assays are in the same order of magnitude. Surprisingly, compounds **3**, **4** and **8** were more active compared to **2** with IC₅₀ values of 3.9 ± 1.2 nM, 5.3 ± 0.5 nM and 10.7 ± 1.1 nM, respectively. This result was unexpected as the compounds showed lower affinities compared to **2** in the flow cytometric binding assay. In the fluo-4 assay, compounds **5**, **6** and **7** were less active than **2** with IC₅₀ values of 101.1 ± 18.0 nM, 536.5 ± 179.5 nM and 168.7 ± 62.3 nM, respectively. This was also the case in the binding assay although compound **6** had a higher affinity compared to **7**.

4.1.3.7 Spectrofluorimetric calcium assay

The CHO-hY₂-K9-qi5-K9-mtAEQ-A7 cells were also used to assess Y₂ receptor agonists and antagonists in the spectrofluorimetric fura-2 assay. As shown in Fig. 45, the concentration-response curves correspond to those obtained in the flow cytometric fluo-4 assay (Fig. 39) and the aequorin assay (Fig. 59). The EC₅₀ values

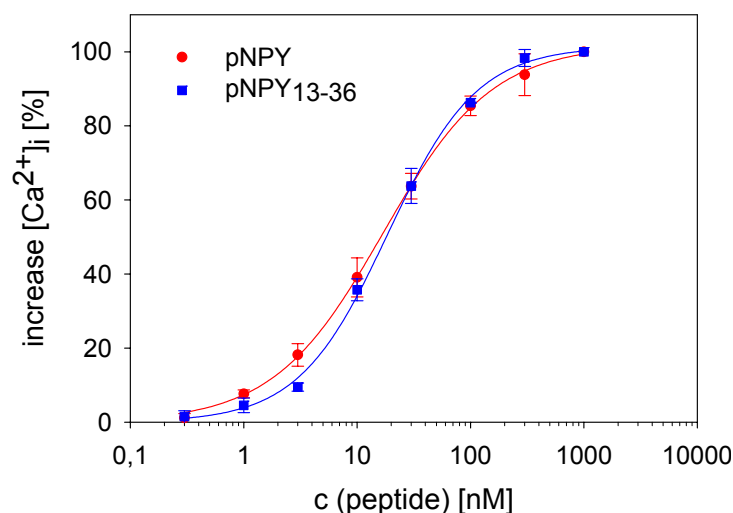


Fig. 45: Spectrofluorimetric Ca²⁺ assay with CHO-hY₂-K9-qi5-K9-mtAEQ-A7 cells and fura-2 as calcium indicator. Every third measurement was a 100 % reference signal elicited with 1 μM pNPY. The EC₅₀ value of pNPY and pNPY₁₃₋₃₆ is 16.9 ± 2.5 nM and 18.6 ± 1.5 nM, respectively (mean values ± SEM, n=2-3).

of pNPY and the Y₂ preferring ligand pNPY₁₃₋₃₆ are 16.9 nM and 18.6 nM respectively. Y₂ antagonists were tested in the fura-2 assay with a fixed agonist concentration of 70 nM pNPY as shown in Fig. 46. The IC₅₀ value of **2** was 28.9 ± 2.0 nM and thus in the same range as the IC₅₀ values obtained in the fluo-4 (20.2 nM) and aequorin

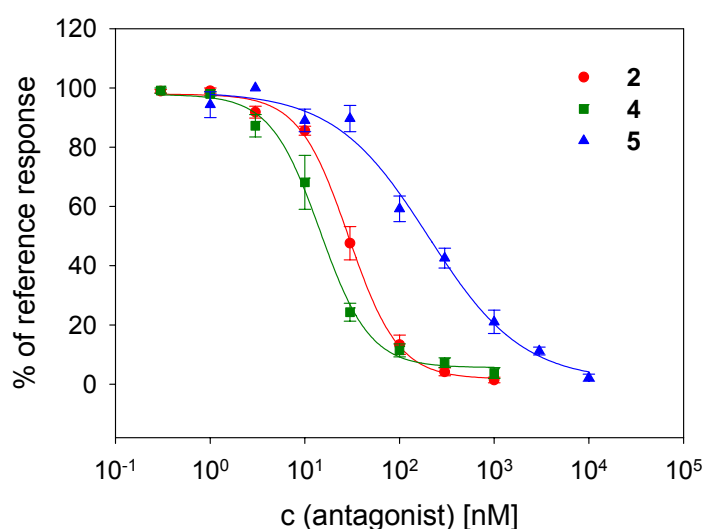


Fig. 46: Inhibition curves of Y₂ receptor antagonists obtained in a spectrofluorimetric Ca²⁺ assay using fura-2. Cells were preincubated with the antagonists **2**, **4** and **5** 1 min before the signal was elicited with 70 nM pNPY (mean values ± SEM, n=3).

assay (29.1 nM, Fig. 60). Compound **4** was more active (IC₅₀ = 14.5 ± 1.5 nM) compared to **2** in the fura-2 assay, as this is the case in the fluo-4 assay, too. In the

aequorin assay compound **4** was less active (see Fig. 60) compared to **2** and also in the flow cytometric binding assay compound **4** showed lower affinity compared to **2**.

The IC₅₀ value of **5** is with 201.4 ± 37.3 nM between the IC₅₀ value determined in the fluo-4 assay (101.1 nM) and in the aequorin assay (313.0 nM, Fig. 60).

The main difference between the fura-2 and the fluo-4 assay on one hand and the flow cytometric binding and the aequorin assay on the other hand is the incubation time. In the former ones the cells and the antagonist were incubated for one minute before the agonist is added, whereas in the binding and the aequorin assay incubation times were 2 h resp. 1 h.

4.2 Aequorin assay

4.2.1 Introduction

Since its isolation from the jellyfish *Aequoria victoria* (Shimomura *et al.*, 1962) natural aequorin has been widely used to visualize changes of intracellular calcium (Blinks, 1978; Cobbold, 1980; Gilkey *et al.*, 1978; Ridgway and Ashley, 1967; Ridgway *et al.*, 1977). The active holoprotein is formed *in vitro* in the presence of molecular oxygen and 2-mercaptoethanol from the 21-kDa protein apoaequorin and its cofactor, coelenterazine (Shimomura and Johnson, 1975). The chromophore coelenterazine is attached to the protein by a peroxide linkage and therefore carries its own oxidizing agent (Jones *et al.*, 1999; Shimomura and Johnson, 1978).

The binding of Ca^{2+} to the three Ca^{2+} -binding sites causes a conformational change, converting the protein into an oxygenase (luciferase). Light emission ($\lambda_{\text{max}} = 470 \text{ nm}$) occurs as a result of an intramolecular reaction in which coelenterazine is oxidized to coelenteramide and CO_2 , catalyzed by luciferase.

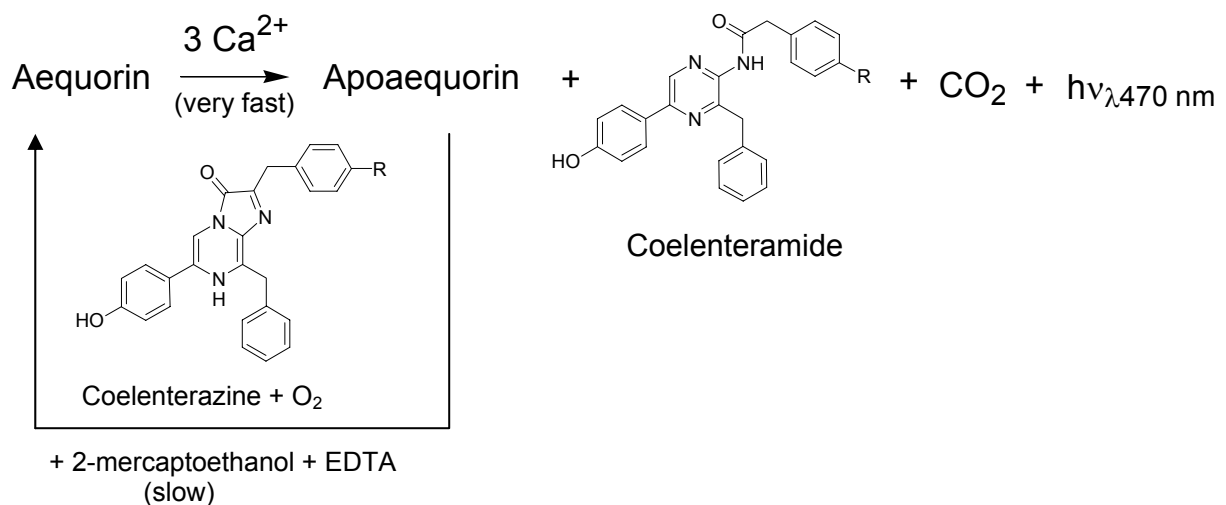


Fig. 47: Bioluminescence reaction and regeneration of aequorin *in vitro*. Native coelenterazine *n* ($R = \text{OH}$) or coelenterazine *h* ($R = \text{H}$) is oxidized to the respective coelenteramide accompanied by the emission of light.

Aequorin luminescence increases linearly with the calcium concentration between about 500 nM and 10 μM , where its sensitivity is highest (Gurney, 1990). The photoprotein responds very quickly to changes in $[\text{Ca}^{2+}]$. Luminescence increases with a time constant of $\sim 10 \text{ ms}$, sufficient for the measurement of calcium responses. Aequorin is highly specific for Ca^{2+} . Beside Sr^{2+} and Ba^{2+} , which are about 100-fold less potent than Ca^{2+} , Ln^{3+} is able to trigger luminescence. Mg^{2+} competes with Ca^{2+}

for binding but is not able to release luminescence and at the levels of Mg²⁺ found in cells, the competing effect of Mg²⁺ should be small (Gurney, 1990). Because aequorin can not penetrate across the plasma membrane, the purified photoprotein had to be microinjected, limiting its use as a calcium indicator in cells. Cloning of the apoaequorin cDNA sequence (Inouye *et al.*, 1985; Prasher *et al.*, 1985) allowed the recombinant expression of apoaequorin, which greatly simplified and extended aequorin-based Ca²⁺ measurements. Reconstitution of recombinantly expressed active aequorin, can be obtained in living cells by simple addition of coelenterazine to the medium. The highly hydrophobic cofactor has been shown to permeate across the cell membranes of various cell types, ranging from the slime mold *Dictyostelium discoideum* to mammalian and plant cells (Pozzan *et al.*, 1994). Alterations of the C-terminus of the protein abolish or dramatically impair Ca²⁺-dependent luminescence (Nomura *et al.*, 1991), whereas manipulations at the N terminal of aequorin are well tolerated. Therefore, chimeric aequorin cDNAs have been prepared targeting the photoprotein to specific intracellular localizations as cytoplasm, mitochondria, nucleus, Golgi apparatus, endo- or sarcoplasmic reticulum or subplasmalemma region (Brini *et al.*, 1999; De Giorgi *et al.*, 1996; Magalhaes *et al.*, 2001; Robert *et al.*, 2000; Sala-Newby *et al.*, 2000). Transfection of cells with these chimeras allowed the selective measurement of calcium concentrations in defined subcellular regions of the cell, which has not been achieved with fluorescent indicator dyes. There are further advantages of aequorin compared to commonly used fluorescent dyes. Because there are usually no luminescent proteins present in mammalian cells, the background signal is extremely low, resulting in an excellent signal-to-noise ratio. Aequorin luminescence does not need excitation light, which simplifies instrumentation and avoids phototoxicity. Because of its wide dynamic range, aequorin allows the determination of increases in [Ca²⁺]_i concentrations ranging from approximately 0.3 μM to > 10 μM. Furthermore, in contrast to fluorescence indicator dyes used at high concentrations (usually 20-200 μM) aequorin (usually recombinantly expressed < 1 μM) does not significantly affect endogenous Ca²⁺ buffer capacity (Brini *et al.*, 1995). In addition, fluorescence dyes applied as AM-esters release hydrolysis products into the cell which may alter the physiological response. By contrast, no toxic products are formed during the aequorin reaction. The main disadvantage of aequorin with respect to the fluorescent indicator dyes is the low amount of light generated by the photoprotein. Less than one photon is

emitted by one aequorin molecule compared to $> 10^4$ photons in the case of fluorescent dyes. Furthermore, aequorin is consumed during the measurement, while this phenomenon is negligible in case of fluorescent dyes. For these reasons, aequorin is poorly suited for single-cell measurements. A promising approach is the fusion of GFP and aequorin allowing an efficient intramolecular chemiluminescence resonance energy transfer (CRET) increasing the quantum yield of the luminescence reaction (Baubet *et al.*, 2000).

The use of cytoplasmically expressed apoaequorin for functional GPCR assays was first described by Button and Brownstein (Button and Brownstein, 1993) and was further modified and extended (Knight and Grigliatti, 2004; Knight *et al.*, 2003; Ungrin *et al.*, 1999). The comparison of cytoplasmically expressed (cytAEQ) and mitochondrially targeted (mtAEQ) apoaequorin used as a reporter for GPCR signalling (Stables *et al.*, 1997; Stables *et al.*, 2000) showed that both constructs yielded the same functional data. However, the luminescence signal obtained with the mtAEQ construct was 10-fold higher compared to cytAEQ. These results were confirmed for different transfected cell lines (Dupriez *et al.*, 2002).

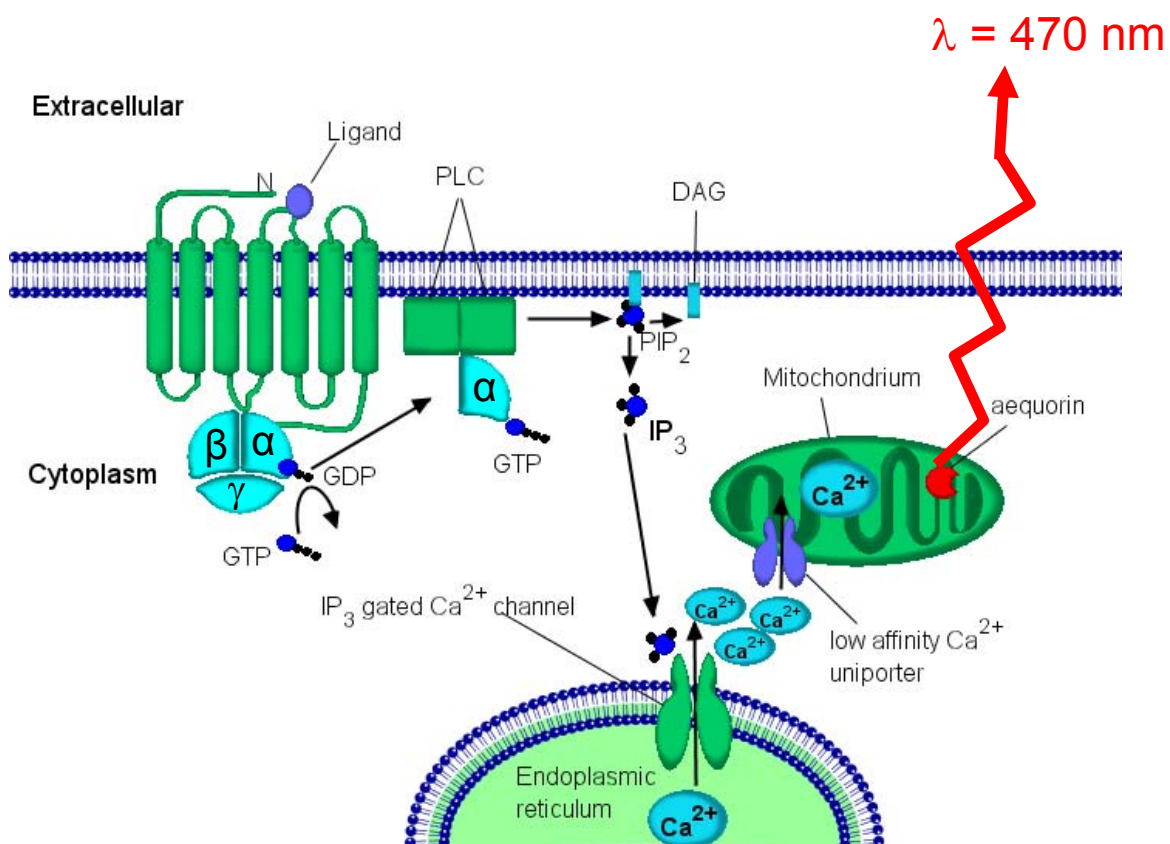


Fig. 48: Signal transduction pathway of GPCRs coupled to G_q . Receptor activation leads to IP_3 generation and subsequently to the release of Ca^{2+} from the endoplasmic reticulum. Local high Ca^{2+} concentrations in close vicinity to the mitochondrion activate the low affinity Ca^{2+} uniporter. Further explanations in the text.

The increase in the mitochondrial calcium concentration results indirectly from the activation of G_q-coupled receptors.

The proposed signal transduction pathway is shown in Fig. 48. After activation of the GPCR and exchange of GDT by GTP, the α -subunit of the G protein activates phospholipase C β , resulting in the generation of DAG and IP₃. Activation of IP₃ gated Ca²⁺ channels in the membrane of the endoplasmic reticulum causes a release of calcium ions into the cytoplasm. As the affinity of the Ca²⁺ uniporter in the inner membrane of the mitochondria is very low (under physiological Mg²⁺ concentrations, the K_d is > 10 μ M) the IP₃-triggered increase in bulk cytosolic [Ca²⁺] (which hardly exceeds 1-2 μ M) is insufficient to activate mitochondrial calcium transporters.

The reason for the parallel and rapid increase in cytoplasmic and mitochondrial calcium concentrations is the close vicinity of endoplasmic reticulum and mitochondrion (Rizzuto *et al.*, 1992; Rizzuto *et al.*, 1993; Rizzuto *et al.*, 1998; Rizzuto *et al.*, 2000). Local high [Ca²⁺] microdomains induced by the release from the ER are sufficient to activate the low affinity mitochondrial Ca²⁺ uniporter (Pinton *et al.*, 1998; Szabadkai *et al.*, 2003) triggering the increase of mitochondrial [Ca²⁺] and therefore the aequorin luminescence signal. The termination of the large mitochondrial Ca²⁺ uptake (up to 10 μ M) is caused by diffusion of Ca²⁺ from the microdomains into the residual cytosol. The role of mitochondrial calcium has been reviewed (Duchen, 2000; Pozzan *et al.*, 2000; Pozzan and Rizzuto, 2000).

Mitochondrially targeted aequorin has been used for the establishment of functional assays for GPCRs in insect and mammalian cells (Dupriez *et al.*, 2002; Le Poul *et al.*, 2002; Stables *et al.*, 1997; Torfs *et al.*, 2002). The multiple transfection of mammalian cells with GPCR, chimeric G protein and mitochondrially targeted aequorin has shown to be a successful approach for the establishment of functional assays.

4.2.2 Materials and Methods

4.2.2.1 Subcloning of pcDNA3.1/zeo-mtAEQ

The pMTAEQ vector was a generous gift from Prof. Dr. Stan Thayer, Department of Pharmacology, University of Minnesota, USA.

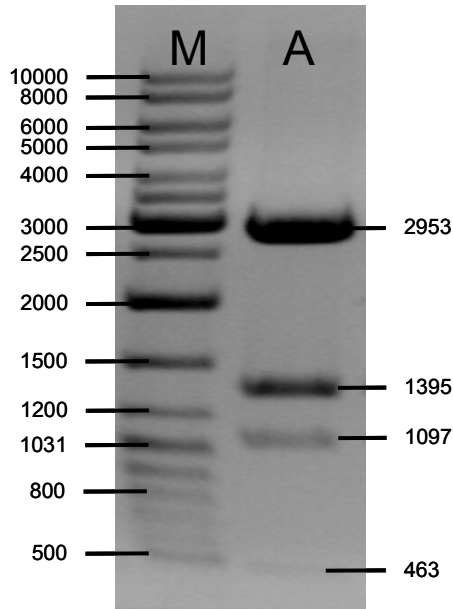


Fig. 49: Restriction analysis of the pMTAEQ vector with *Bam*HI.

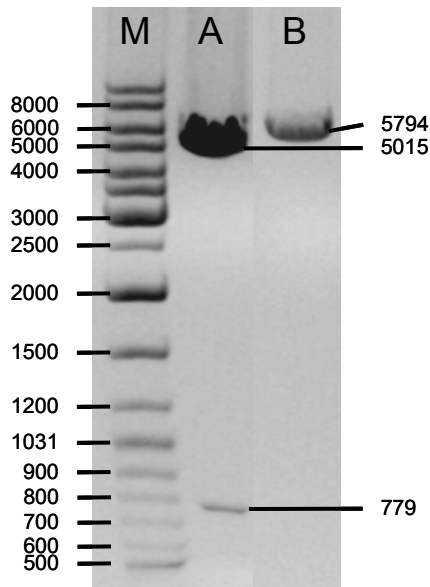


Fig. 50: Restriction analysis of the pcDNA3.1/Zeo-mtAEQ plasmid. A: *Eam*11051 digestion. B: *Eco*RI digestion

The plasmid contains the apoaequorin-encoding cDNA fused to a sequence encoding a mitochondrial-targeting peptide from subunit VIII of human cytochrome c oxidase. The construct was subcloned into the *Eco*RI site of the host vector. The total vector has a length of 5908 bp with *Bam*HI sites at 345, 1740, 2837 and 3300 bp. Approximately 1 μ g of pMTAEQ plasmid DNA was provided on a filter paper. The DNA was eluted with 20 μ l of millipore water at room temperature and directly used for transformation. Resistant colonies were propagated in overnight cultures, and the plasmid DNA was isolated with MiniPrep. Restriction enzyme digestion with *Bam*HI led to the formation of the four expected bands at 463 bp (very weak), 1097 bp, 1395 bp and 2953 as shown in Fig. 49. Plasmid DNA was prepared with the Qiagen Plasmid Purification Kit (Qiagen, Hilden, Germany).

2 μ g of the pMTAEQ vector were digested with *Eco*RI, and the released insert (779 bp) was isolated from the gel using the QIAEX II (Qiagen, Hilden, Germany) purification kit.

The pcDNA3.1/Zeo vector was a gift of Dr. Thomas Dobner, Institute of Microbiology and Hygiene, University of Regensburg, Germany. The vector was linearized with *Eco*RI and purified with the Quiagen PCR purification kit (Quiagen). To avoid self-ligation, the linearized vector was treated with

0.003 U of phosphatase from calf intestine (Roche Diagnostics) for 1 h at room temperature and subsequently purified with the Quiagen PCR purification kit.

For the ligation reactions, 2 µl of linearized vector was incubated with 2, 4, 6, or 8 µl of insert in presence of 1 Weiss unit T4 DNA ligase (MBI Fermentas), 2 µl of 10x ligation buffer (MBI Fermentas) and water at a final volume of 20 µl. The samples were incubated for 60 min at room temperature and directly used for transformation without inactivation of the T4 ligase.

Transformation was performed as described in chapter 3.1.2.3. Resistant colonies were used for overnight cultures and the plasmid DNA was isolated by MiniPrep. Treatment with *EcoRI* released the mtAEQ insert (779 bp) and the empty linearized pcDNA3.1/zeo vector (5015) as shown in Fig. 50A. Restriction enzyme digestion with *Eam11051* linearized the vector generating a DNA fragment with 5794 bp (Fig. 50B). Plasmid DNA was purified on large scale with the Quiagen Plasmid Purification Kit (Quiagen).

4.2.2.2 Aequorin assay

4.2.2.2.1 Stable transfection of CHO-hY₂-K9-qi5-K9 cells

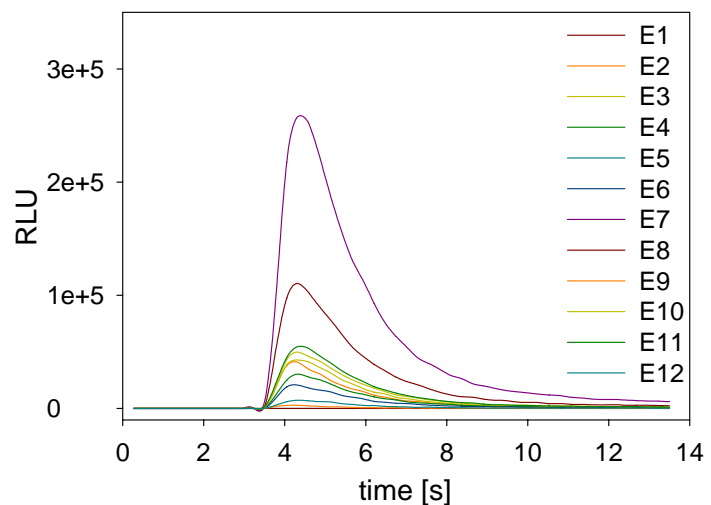
Plasmid linearization and transfection with the pcDNA3.1/Zeo-mtAEQ vector was performed by analogy with the procedure described in section 4.1.2.3. The selective medium contained 400 µg/ml of G418, 400 µg/ml of hygromycin and 250 µg/ml of zeocin (InvivoGen, San Diego, USA). Transfected cells were maintained in selective medium for 3 weeks; untransfected control cells died due to this treatment. Selected stable transformants were maintained in selective medium and passaged 1:10 twice a week.

4.2.2.2.2 Screening of the cell clones

3 weeks after transfection cells were seeded at very low densities in selective medium (see 4.2.2.2.1) into 150 mm tissue culture dishes (Becton Dickinson, Franklin Lakes, NJ., USA) and grown to isolated colonies for 1-2 weeks. Isolated colonies were picked with a sterile pipette as described in section 3.1.2.12 and transferred into a 96-well plate (Nunc). All cell clones were grown to maximum confluence. Then the medium was sucked off, cells were trypsinized and transferred into a white 96-well luminescence plate with transparent bottom (Nunc) by 1:20

dilution. On the day of the experiment most of the cell clones were confluent. The medium was removed and 50 μ l of Ham's F12 medium containing 10 % FCS and 2 μ M coelenterazine h were added per well. The plate was incubated at room temperature for 2 h in the dark. The medium was sucked off and 50 μ l of loading buffer (see section 4.1.2.4) were added. The plate was inserted into the GENios Pro™ (Tecan, Salzburg, Austria) plate reader and 50 μ l of 0.2 % triton-X-100 in loading buffer were injected per well. Luminescence was recorded for 13.5 s in 200 ms integration steps as shown exemplarily for row E in Fig. 51. Instrument settings were: no attenuation.

Fig. 51: Analysis of CHO-hY₂-K9-qj5-K9-mtAEQ cell clones loaded with 2 μ M coelenterazine h in response to 0.1 % triton-X-100. Measurements were made in a TECAN Genios Pro plate reader.



Cell clones with the strongest luminescence signal indicating a high aequorin expression were selected and maintained in selective medium for further investigations.

4.2.2.2.3 Comparison of CHO-hY₂-K9-qj5-K9-mtAEQ cell clones with respect to luminescence response upon pNPY-stimulation

Selected cell clones were seeded in Ham's F12 medium containing 10 % FCS on 175-cm² culture flasks. On the day of the experiment, the confluence had reached 80-90 %. Cells were trypsinized, detached with Ham's F12 medium containing 10 % FCS and counted. After centrifugation at 300 g for 5 min, cells were resuspended in DMEM without phenol red supplemented with 1 % FCS at a density of 10⁷ cells/ml. Coelenterazine h (1 mM stock solution in methanol) was added to the cell suspension to a final concentration of 2 μ M, and reconstitution of the holoenzyme was accomplished by incubation for 2h at room temperature under gentle stirring in

the dark. Cell suspensions were diluted with loading buffer (see 4.1.2.4) to $5 \cdot 10^5$ cells/ml and incubated in the dark at room temperature for 30 min.

pNPY dilutions were prepared as 100-fold concentrated feed solutions in 10 mM HCl containing 0.1 % BSA and were then diluted 1:25 with loading buffer containing 0.1 % BSA. 50 μ l of each dilution were pipetted into a 96-well luminescence plate.

150 μ l of the stirred cell suspension were injected to each well and luminescence was recorded over 40 s as a series of 200 ms integrations.

Luminescence [RLU] was plotted against time [s] and the area under the peak was calculated with SigmaPlot™ Software and used to construct concentration-response curves.

4.2.2.2.4 Optimisation of assay parameters

CHO-hY₂-K9-qi5-K9-mtAEQ-A7 cells were seeded, cultured, harvested and incubated with coelenterazine h for 2 h as described in section 4.2.2.2.3. Cells were diluted with loading buffer to $5 \cdot 10^5$ cells/ml and incubated for the indicated periods of time. 10-fold dilution series of peptide agonist were prepared in loading buffer with a blank sample containing solvent and a 100 %-sample containing 0.1 % triton-X-100 (final assay concentration) instead of pNPY solution was included per row. The assay was performed according to section 4.2.2.2.3 except that 180 μ l of cell suspension were injected to 20 μ l of sample dilution. For the construction of concentration-response curves, the blank value was subtracted from each value and the percentage of maximum luminescence was calculated using the value of the 100 %-sample for each time point.

For the calculation of pIC₅₀ values of **2** after various incubation times the logit-transformation was used. The maximum signal was induced by 300 nM pNPY and antagonist concentrations reducing the pNPY-induced luminescence signal to 20 % - 80 % were used. The percentage inhibition (P) relative to control (no antagonist) was determined and the logit (P) was calculated using following equation:

$$\log \frac{P(\%)}{100\% - P(\%)} = \text{logit}(P)$$

The logit (P) is plotted versus log (antagonist) and the pIC₅₀ values (logit (P) = 0) are calculated by linear regression.

4.2.2.2.5 Measurements with 2 injectors

CHO cells were prepared as described in 4.2.2.2.3 and incubated for the indicated periods of time. A 10-fold concentrated pNPY dilution series (containing 1 % BSA) was pipetted into the 96-well plate and 162 μl of the cell suspension were autoinjected per well to 18 μl of the peptide solution. Luminescence was recorded for 43 s (peak 1) before the injection of the 1 % triton-X-100 solution (20 μl). Emitted luminescence was recorded for another 22 s (peak 2) and the area under the two peaks was calculated with SigmaPlot™ 8.0. Fractional luminescence was calculated by dividing the area of the agonist peak by the sum of the areas of peak 1 and 2. In each row, a blank sample containing solvent only and a triton-X sample containing 0.1 % triton-X-100 (final assay concentration) were included. For the construction of concentration-response curves, the blank value was subtracted from each value.

4.2.2.3 **Analysis of mRNA expression of the transfected constructs by RT-PCR**

The four cell lines CHO-K1, CHO-hY₂-K9, CHO-hY₂-K9-qi5-K9 and CHO-hY₂-K9-qi5-K9-mtAEQ-A7 were seeded on 75-cm² culture flasks in Ham's F12 medium containing 10 % FCS and were grown to 70-90 % confluence. All materials used for the RNA isolation and reverse transcription were RNase-free or treated with DEPC water (0.1 % DEPC (Fluka, Steinheim, Germany) in millipore water). The cells were trypsinized and the mRNA of each cell type was isolated with the RNeasy Mini Kit (Qiagen) according to the manufacturer's instructions. The concentration of the mRNA was determined photometrically at $\lambda = 260 \text{ nm}$ using the following relation: $A_{260} = 40 \mu\text{g/ml}$.

cDNA was prepared by reverse transcription according to the following protocol:

1 μg of RNA and 1 μl of oligo (dT₁₂₋₁₈) primer solution (Invitrogen) were added in 10 μl of autoclaved DEPC water. The solution was heated for 5 min to 70 °C in the thermocycler and then cooled on ice. A master mix was prepared by addition of 16 μl of 5x first strand buffer (Invitrogen), 16 μl of dNTP mix (MBI Fermentas), 2 μl of DTT (Roche, Basel, Switzerland) and 4 μl of M-MLV reverse transcriptase (200 u/ μl , Invitrogen). 10 μl of the master mix were added to each 10 μl RNA solution and then incubated for 1 h at 37 °C. Finally, the enzyme was heat-inactivated for 2 min at 95 °C. The cDNA samples were stored at -20 °C.

For the amplification of specific cDNA fragments a primer mix containing 1 pmol/ μl of each primer in millipore water was prepared. The PCR sample contained 2 μl of

cDNA solution, 2 µl of primer mix, 2 µl of 10x PCR buffer (Qiagen), 2 µl of dNTP mix, 11 µl of millipore water and 1 µl of Taq DNA polymerase (5 u/µl; Qiagen).

Cycling parameters were:

- 1) initial denaturation: 95 °C, 30 s
- 2) denaturation: 95 °C, 30 s
- 3) annealing: 60 °C, 30 s
- 4) extension: 72 °C, 90 s
- 5) final extension: 72 °C, 2 min
- 6) hold: 4 °C

Steps 2) – 4) were repeated 34 times. 4 µl of 6x gel loading buffer were added to the PCR reaction and agarose gel electrophoresis was performed as described in 3.1.2.6. The PeqGOLD 100bp DNA ladder (Peqlab) was used as reference. Primers were synthesized by MWG. The sequences are shown in Table 5.

Table 5: Sequences of the used primers.

gene	sense primer	antisense primer	amplified product length
β-actin	5'- CGG GAT CCC CGC CCT AGG CAC CAG GGT G - 3'	5'- GGA ATT CGG CTG GGG TGT TGA AGG TCT CAA A -3'	286 bp
hY ₂	5'- AAT AGG TGC AGA GGC TGA TGA GAA CC -3'	5'- TAA TCA GGA AGC TGA TTC GCT TGG AGA -3'	497 bp
G _{qi5}	5'- CAC CTT CAT CAA GCA GAT GAG GAT CAT CCA -3'	5'- AAG AGG CCA CAG TCC TTA AGG TTC A -3'	918 bp
mtAEQ	5'- TAC TCC GTG CCA TCA TGT CCG TCC T -3'	5'- TAG GGT GCA TCA CCA CCG TAG AGC TTC TTA -3'	707 bp

The antisense primer for the G_{qi5} construct hybridizes with the part of the sequence where the nucleotides encoding for the G_q protein are exchanged by the nucleotides of G_i to avoid amplification of untransfected G_q cDNA.

4.2.2.4 Analysis of the dissociation kinetics of 2 replacing cy5-pNPY

Preparation of CHO-hY₂-K9-qi5-K9-mtAEQ-A7 cells and flow cytometric measurements were performed as described in 3.2.3.1. Dissociation of bound cy5-pNPY was initiated by injection of 100 nM of **2** to the stirred cell suspension and the cell-bound fluorescence was recorded in channel 4 (FL-4). The averaged raw data were fitted to the equations $f = y_0 + a \cdot e^{(-bx)}$ (one dissociation rate constant) and $f = y_0 + a \cdot e^{(-bx)} + c \cdot e^{(-dx)}$ (two dissociation rate constants) without constraints.

4.2.3 Results

4.2.3.1 Selection of transfected cell clones

The CHO-hY₂-K9-qi5-K9 cells were transfected with the *Eam11051*-linearized pcDNA3.1/Zeo-mtAEQ vector. 96 cell clones were loaded with 2 μ M coelenterazine h and screened on the basis of their luminescence signal after cell lysis caused by 0.1% triton-X-100 (see Fig. 51). Provided that the cell density per well is similar, a strong luminescence signal should indicate high expression of functional apoaequorin. Three cell clones were selected, expanded and tested for their functional response upon agonist challenge.

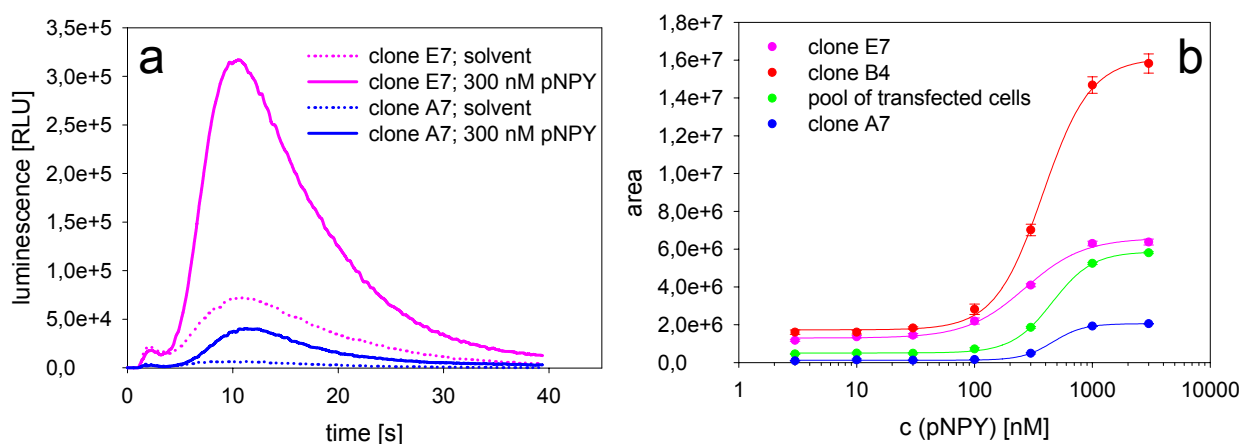


Fig. 52: Luminescence responses of isolated CHO-hY₂-K9-qi5-K9-mtAEQ cell clones after stimulation with increasing concentrations of pNPY ($n=3$; mean values \pm SEM).

As shown in Fig. 52, the particular cell clones responded differently. Each clone showed a saturable, concentration-dependent increase in luminescence upon stimulation with pNPY. The strongest signals were obtained with clones B4 and E7 (Fig. 52b) but even injection of the cells to solvent without agonist led to an increase in luminescence as shown exemplarily for clone E7 in Fig. 52a. This results in a high basal signal and therefore impairs the signal to noise ratio. The injection of cell suspension of clone A7 to solvent led only to a minimal increase in basal luminescence (Fig. 52a), resulting in a higher signal-to-noise ratio. The maximum increase in the luminescence signal upon saturating concentrations (3 μ M) of pNPY was 16-fold with clone A7 compared to 9.3- and 5-fold with the clones B4 and E7 respectively. Injection of the pool of transfected cells to solvent led to a basal signals ranging from the ones of clone A7 to those of E7. With this mixture of cell clones a maximum signal to noise ratio of 11.6 was obtained. Cell clones B4 and E7 were

frozen and the cell line CHO-hY₂-K9-qi5-K9-mtAEQ-A7 was used for the investigations on assay parameters.

4.2.3.2 Optimisation of assay parameters

In order to obtain reproducible results cells have to be prepared in a way that their response is constant during the measurement. As a single luminescence signal with these cells takes at least 40 s (see Fig. 52a), the measurement of a complete 96-well plate takes 64 min. The stability of the signal during this period is a prerequisite for the application of the assay in the 96-well format. The signal intensity depends on the concentration of reconstituted aequorin within the cells and the stimulus caused by a defined agonist concentration. As the latter remains unchanged during the measurement, parameters have to be found to provide constant concentrations of reconstituted aequorin. Due to the basal Ca²⁺ concentration within the mitochondria, aequorin is constantly discharged, but on the other hand, sufficient coelenterazine is available to reconstitute active aequorin because coelenterazine is kept continually in the cell suspension. Incubation conditions have to be found which allow a constant steady-state level of active aequorin depending on the equilibrium between entry of coelenterazine in the cell by passive diffusion, reconstitution of aequorin from apoaequorin and its consumption in the basal nonstimulated cell's conditions. In the literature there are different coelenterazine loading conditions described. For example Stables and colleagues report on the reconstitution of the holoenzyme by incubation of adherent growing transiently transfected CHO cells with 5 μM coelenterazine for 3 h at 37 °C in culture medium (Stables *et al.*, 1997). This

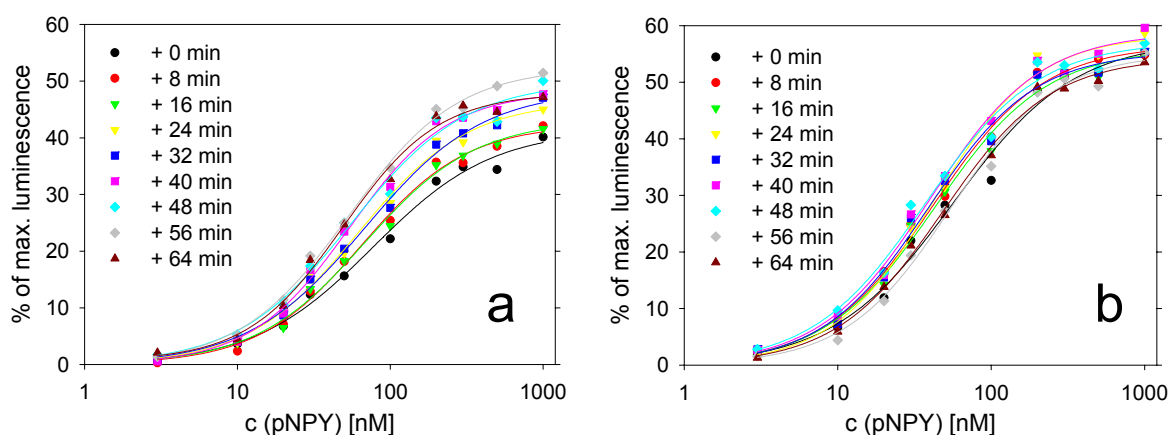


Fig. 53: Effect of postincubation time on the concentration-response curves of pNPY. CHO-hY₂-K9-qi5-K9-mtAEQ-A7 cells were incubated for 2 h with 2 μM coelenterazine h and post-incubated for 90 min (panel a) or 3 h (panel b). Total aequorin (100 %) was discharged after cell lysis by 0.1 % triton-X-100. Measurement time of each curve was 8 min (40 s per concentration).

procedure requires large amounts of the cofactor as only a small number of cells is loaded in a large volume. Incubation at 37 °C seems not to be very economic as more aequorin is consumed under basal conditions at higher temperatures (Blinks, 1978; Dupriez *et al.*, 2002). Loading of the cells in suspension at a high cell density and subsequent dilution appeared to be an effective and economic method (Dupriez *et al.*, 2002). After dilution with loading buffer, cells were “postincubated” at room temperature for different periods and concentration-response curves of pNPY were recorded. As shown in Fig. 53a, postincubation of 90 min is insufficient as luminescence signals increase during the measurement. Reproducible concentration-response curves were obtained after 3 h of postincubation (Fig. 53b). The data points of all curves were in the same range with acceptable deviations. This allows a temporal assay window of at least 64 min, sufficient for the measurement of a whole 96-well plate.

Another aspect of the aequorin assay is the use of different coelenterazine derivatives and their employed concentrations. As the synthetic commercially available derivatives

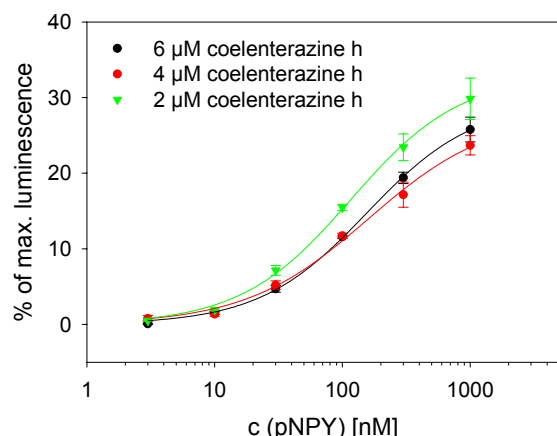


Fig. 54: Effect of various concentrations of coelenterazine h during the loading procedure. Cells were loaded for 2 h, diluted and postincubated for 3 h at room temperature (mean values \pm SEM, $n=3$).

are very expensive, the coelenterazine h derivate was chosen based on published results (Dupriez *et al.*, 2002). Using CHO-K1 cells stably coexpressing apoaequorin and the human 5-HT_{2B} receptor in a functional aequorin assay, coelenterazine h proved to be superior to the native and to the other synthetic derivatives coelenterazine n, f, hcp, cp and the benzyl derivative in terms of sensitivity and signal-to-noise ratio. To determine the optimal concentration of the cofactor, the cells were incubated in the presence of increasing concentrations of coelenterazine h. Cells were diluted and postincubated for 3 h. The results are shown in Fig. 54. There is no distinct tendency, but the strongest signals and the lowest EC₅₀ values were obtained after loading of the cells with cofactor at a concentration of 2 μM.

As test compounds are often dissolved in DMSO, the sensibility of the assay depending on the DMSO content was investigated. Cells were loaded with 2 μM coelenterazine h and postincubated with increasing DMSO concentrations for 3 h. Concentration-response curves of the agonist pNPY are shown in Fig. 55. Increasing concentrations of DMSO led to an elevated basal signal. This effect is presumably due to the impairment of the cells by the solvent. At 1 % of DMSO there is still a distinct concentration-dependent increase in emitted light after stimulation with pNPY (Fig. 55a). The EC₅₀ value is in the same range (147.9 nM) as that of control cells, which were postincubated in absence of solvent (EC₅₀ = 165.7 nM). Calculation of the percentage of maximal luminescence using the signal of cells lysed by 0.1 % triton-X-100 (100 % value) results in concentration-response curves almost identical for control cells and those incubated with 1 % DMSO (Fig. 55b). A reason for this is

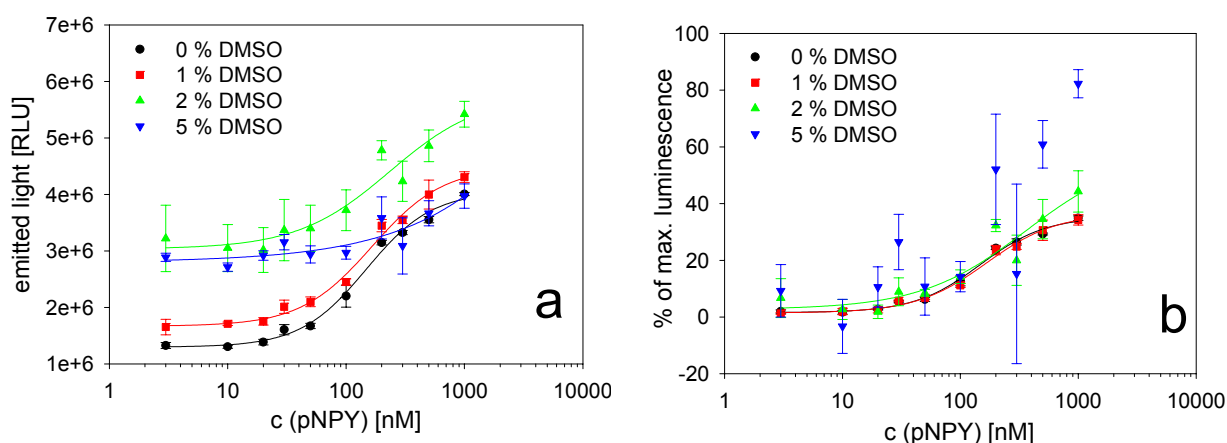


Fig. 55: Effect of DMSO. CHO-hY₂-K9-qi5-K9-mtAEQ-A7 cells were loaded with 2 μM coelenterazine h for 2 h, diluted and postincubated for 3 h with indicated DMSO contents. In panel a total emitted light is calculated from peak integrations of each signal. In panel b the percentage of maximal luminescence is calculated with the 100 % triton-X-100 signal as standard (mean values \pm SEM, n=3).

the higher basal consumption of aequorin in unstimulated cells in the presence of DMSO, which diminishes the 100 % value (triton-X-100) and increases the 0 % value. Incubation with 2 % and 5 % solvent caused considerably higher basal signals and greater deviations.

The maximally emitted light (100% value, not shown) of cells incubated with 5 % DMSO is only 45 % of the maximal signal obtained with the control cells, whereas the blank signal was 2.3-fold as high as the blank signal of the control cells.

As a final concentration of 1 % DMSO only marginally affected the concentration-response curves, this concentration can be used in the screening of antagonists

dissolved in DMSO. Additionally, in the assay, the antagonists dissolved in DMSO are preincubated with the cells for 1 h (see section 4.2.3.4) instead of 3 h, which diminishes the effect of the solvent.

4.2.3.3 Aequorin agonist assay

Peptidic neuropeptide Y receptor ligands were investigated in the aequorin assay under the optimized conditions, described in 4.2.3.2. Luminescence responses are exemplarily shown for pNPY in Fig. 56a. The first, minor peak is caused by the injection procedure due to cell damage; the main peak results from receptor activation by the agonist. In accordance with the literature, pPYY proved to be a potent agonist at the hY₂ receptor with an EC₅₀ value of 41.2 ± 4.2 nM. pNPY, [A¹⁹]-pNPY and the Y₂ preferring ligand pNPY₁₃₋₃₆ showed similar agonistic activity with EC₅₀ values of 121.8 ± 19.8 nM, 146.5 ± 36.6 nM and 156.3 ± 14.1 nM respectively. [L³¹,P³⁴]-pNPY, a selective agonist for Y₁ relative to Y₂, showed no agonistic activity up to a concentration of 3 μM. These data correspond to the typical Y₂ receptor pharmacology, although the EC₅₀ values are much higher compared to functional data determined in the fura-2 and fluo-4 assay.

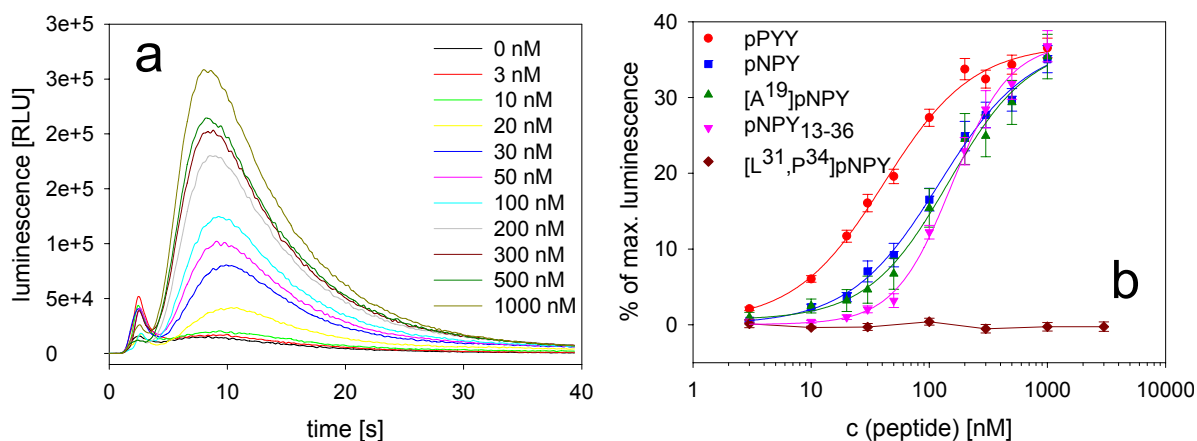


Fig. 56: Aequorin assay with CHO-hY₂-K9-qi5-K9-mtAEQ-A7 cells. 180 μl of cell suspension were injected to 20 μl of peptide solution. **a:** luminescence responses to increasing concentrations of pNPY. **b:** concentration-response curves of peptide ligands. Reference signal was elicited with 0.1 % triton-X-100 (mean values ± SEM, n=3-4).

4.2.3.4 Aequorin antagonist assay

Because the Tecan Genios Pro plate reader was initially equipped with only one injector, it is impossible to add the antagonist to the cell suspension (or vice versa) and trigger the luminescence signal by the addition of an agonist after one minute by analogy with the fura-2 and fluo-4 assays. Injection of the cell suspension into a mixture of agonist and antagonist results in IC₅₀ values much higher compared to the fluorescence based assays because of the lack of preincubation of the cells in the presence of the antagonist (data not shown, see also 4.2.3.7). When the antagonist receptor interaction has reached equilibrium the signal should be independent from the time of the addition of the agonist, provided that the cells are still excitable and a

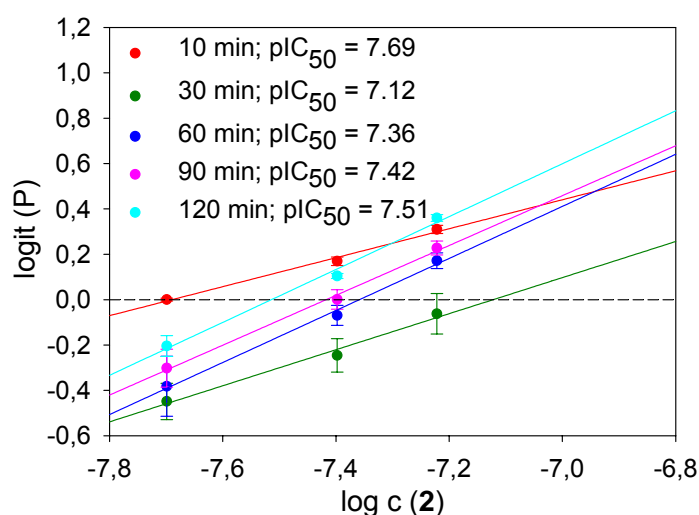


Fig. 57: Determination of pIC₅₀ values after various preincubation times using the logit-transformation (mean values \pm SEM, n=3).

constant concentration of active aequorin is available (see Fig. 53). The effect of the preincubation time of the cells in the presence of antagonist is shown in Fig. 57.

Cells were preincubated with 20, 40 and 60 nM of **2** and the signal was elicited with 300 nM pNPY. IC₅₀ values were calculated using the logit-transformation. Constant pIC₅₀ values (7.4 - 7.5) were obtained after preincubation of the cells in the presence of the antagonist for 60-90 min. Therefore, a preincubation time of 60 min should be sufficient and determined IC₅₀ values should be constant during the measurement of a whole plate (64 min). Y₂ receptor antagonists were investigated in the aequorin assay using 200 nM pNPY to elicit the luminescence signal (Fig. 58).

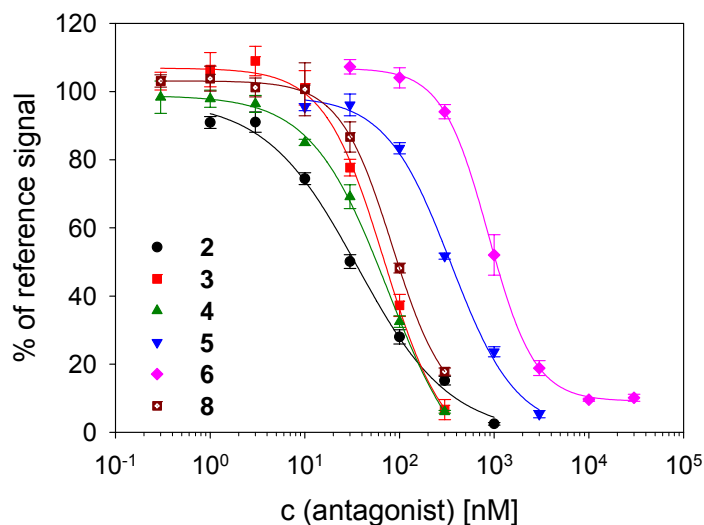


Fig. 58: Aequorin assay with CHO-hY₂-K9-qi5-K9-mtAEQ-A7 cells. The reference signal was triggered with 200 nM pNPY. IC₅₀ values are: 36.1 ± 4.3 nM (2), 68.9 ± 13.0 nM (3), 75.4 ± 17.3 nM (4), 349.1 ± 34.5 nM (5), 869.4 ± 61.1 nM (6) and 84.0 ± 15.7 nM (8) (mean values ± SEM, n=3-6).

Compared to the flow cytometric fluo-4 assay the IC₅₀ values obtained with the aequorin assay are higher and also the order of the inhibitory activities differs in the case of compounds 3, 4, and 8. An explanation for this deviating behaviour of the compounds in the two functional assays may be the different preincubation times of the cells in the presence of the antagonist and unequal adsorption of the test compounds to the different materials (glass and polystyrole).

These adsorption effects are not only restricted to nonpeptidic antagonists but can also occur with peptidic agonists. In the assay, agonist solutions were pipetted into the 96-well-plate prior to the injection of the cell suspension. The addition of 1 % BSA to the peptide solution reduced adsorption effects resulting in lower EC₅₀ values as shown in Fig. 59. pPYY, pNPY and pNPY₁₃₋₃₆ showed lower EC₅₀ values with 8.8 ± 2.4 nM, 30.9 ± 2.2 nM and 58.3 ± 9.9 nM. These EC₅₀ values are in the same range as those determined in the fluo-4 and fura-2 calcium assay.

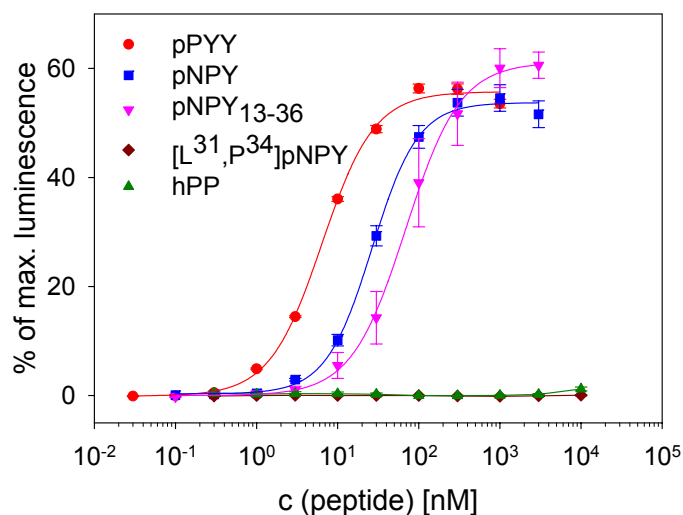


Fig. 59: Aequorin assay with CHO-hY₂-K9-qi5-K9-mtAEQ-A7 cells. Peptide solutions were prepared in the presence of 1 % BSA to reduce adsorption to the surface of the well-plate (mean values ± SEM n=3-9).

As expected, [L³¹,P³⁴]-pNPY and hPP had no agonistic activity up to a concentration of 3 μM. No signal was obtained after addition of the peptides rPP, [K⁴]-hPP, [hPP¹⁹⁻²³, P³⁴]-pNPY, GW1229 and BW1911U90 up to a concentration of 3 μM, too (data not shown).

As the high EC₅₀ value of pNPY obtained in absence of BSA (see Fig. 58) was due to adsorption effects, inhibition curves of Y₂ antagonist were measured again using a lower concentration of the agonist (70 nM).

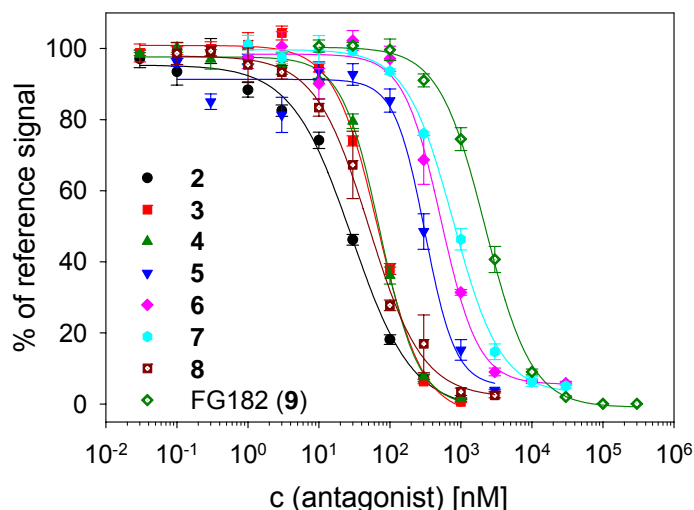


Fig. 60: Inhibition curves of Y₂ receptor antagonists. Reference signal was triggered with 70 nM pNPY. IC₅₀ values are: 29.1 ± 3.0 nM (2), 69.1 ± 4.7 nM (3), 72.6 ± 3.9 nM (4), 313.0 ± 74.5 nM (5), 521.4 ± 54.3 nM (6), 781.5 ± 53.2 nM (7), 50.6 ± 7.7 nM (8) and 2203.4 ± 123.1 nM (9) (mean values ± SEM, n=3-6).

The differences of the obtained IC₅₀ values compared to those determined with an agonist concentration of 200 nM were small, never exceeding 40 %. Compound **9** was selected after the screening of various substances synthesized by F. Graichen and C. Hutzler at a single concentration of 1 μM (data not shown). The structure of **9** is shown in Fig. 61.

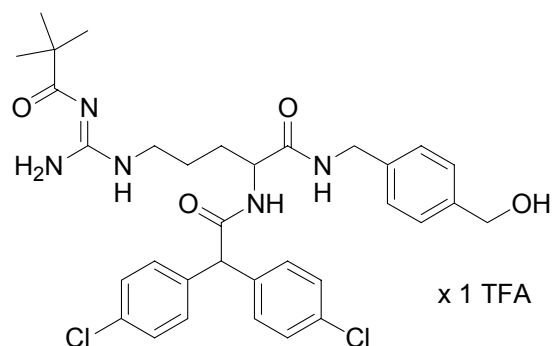


Fig. 61: Structure of **9**.

Compound **9**, a potent hY₁ antagonist (IC₅₀ = 34.5 nM, determined in a spectro-fluorimetric fura-2 calcium assay with HEL cells and 10 nM NPY (Graichen, 2002)) is derived from the known Y₁ antagonist BIBP 3226.

4.2.3.5 Aequorin assay with two injectors

As the Tecan Genios Pro™ plate reader was upgraded with a second injector, it became possible to inject a triton-X-100 solution to the cell suspension immediately after the aequorin luminescence signal. The subsequent addition of the detergent causes cell lysis and leads to the consumption of the residual active aequorin which has not been discharged during the transient luminescence signal caused by the activation of the Y_2 receptor. Therefore, the total luminescence can be calculated for each sample instead of using an external triton-X-100 reference as a 100 % standard. This approach makes the signals independent from variations in cell number which may occur due to sedimentation in the course of the measurement.

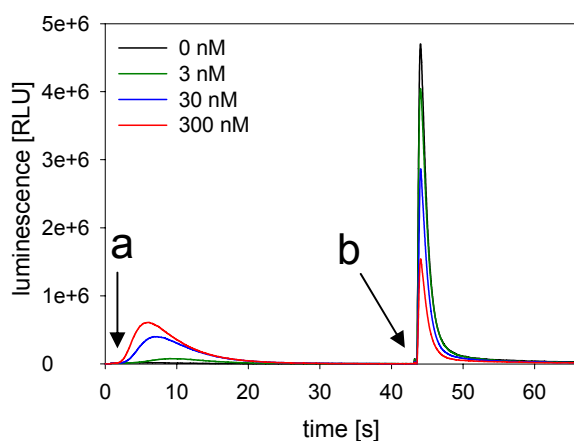


Fig. 62: Aequorin assay with CHO-h Y_2 -K9-qi5-K9-mtAEQ-A7 cells using two injectors. The cells were “postincubated” for 3 h and then injected into the agonist (pNPY) solution at time point ‘a’. Injection of 0.1 % triton-X-100 at time point ‘b’ leads to cell lysis and causes the consumption of the residual active aequorin.

The course of the measurement is shown in Fig. 62. The aequorin signal (peak 1, from ‘a’ to ‘b’) rose with increasing concentrations of the agonist pNPY, whereas the light produced by the residual fraction of charged aequorin (peak 2, from ‘b’ to end) decreased. The fraction of integrated luminescence was determined for each ligand concentration by dividing the area under peak 1 by the sum of the areas under peak 1 and 2.

In order to determine, whether the postincubation step after loading of the cells with the cofactor coelenterazine could be omitted when the fractional luminescence for each well was measured, the cells were injected to the pNPY solution after various periods of postincubation.

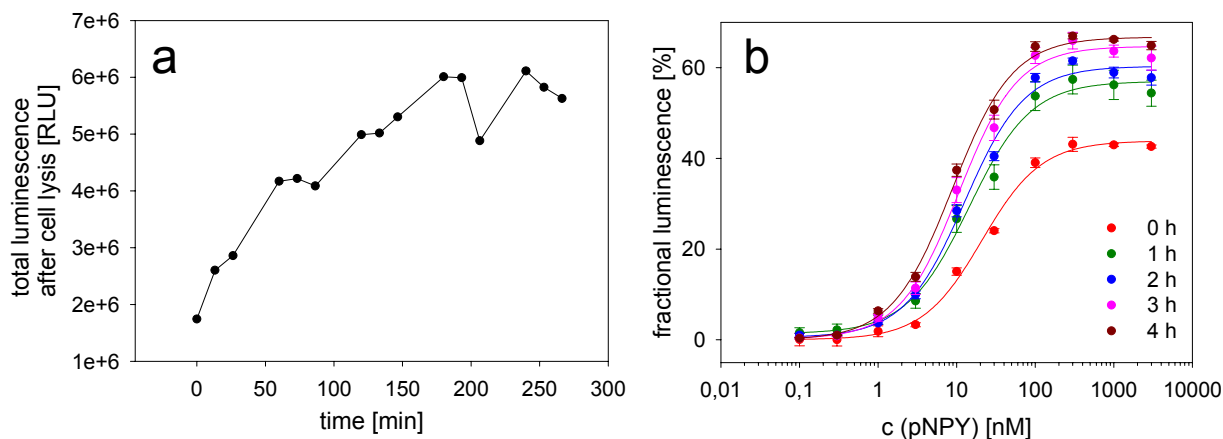


Fig. 63: Influence of the period of postincubation on the luminescence signals of CHO-hY₂-K9-qi5-K9-mtAEQ-A7 cells. Cells were incubated for 2 h with 2 μ M coelenterazine h and subsequently incubated for various periods of time. **a:** total luminescence emitted after cell lysis caused by 0.1 % triton-X-100. **b:** concentration-response curves of pNPY, determined after various postincubation times (mean values \pm SEM, n=3).

As shown in Fig. 63a, due to the slow formation of active aequorin from the apoprotein and the cofactor, the total luminescence emitted after cell lysis increased with longer periods of postincubation reaching a constant maximum after 3 h. This effect could not be corrected by the calculation of the fractional luminescence as shown in Fig. 63b. Although the determined EC₅₀ values were in the same range (EC₅₀ = 21.0, 14.3, 12.6, 10.6 and 8.8 nM for 0, 1, 2, 3 and 4 h of postincubation), the maximal fractional luminescence increased with longer postincubation times by analogy with the experiments performed with CHO-hY₄-K13b-qi5-K8-mtAEQ-E11-K11 cells (see section 5.3.3.2). Therefore, a postincubation period of 3 h is necessary, especially for the distinction between full agonists and partial agonists.

4.2.3.6 Comparison of mRNA expression by transfected cells

In order to confirm the stable transfection of the cells with the hY_2 , G_{qi5} and $mtAEQ$ genes the mRNA expression was analyzed. RNA was isolated and a RT-PCR was performed.

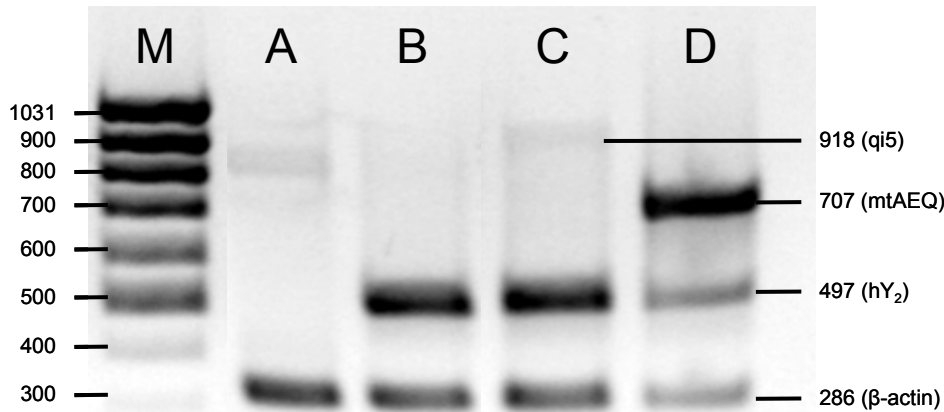


Fig. 64: mRNA transcription by transfected cells. **A:** CHO-K1 cells **B:** CHO- hY_2 -K9 cells **C:** CHO- hY_2 -K9- $qi5$ -K9 cells **D:** CHO- hY_2 -K9- $qi5$ -K9- $mtAEQ$ -A7 cells **M:** marker.

No mRNA of any transfected construct but a weak band of unspecific PCR product with a length of 800 – 900 bp was detected in CHO-K1 wild type cells (Fig. 64A). As expected, hY_2 receptor mRNA (497 bp) was identified in all transfected cell lines (B-D) and mRNA of the $mtAEQ$ construct (707 bp) was found only in the $mtAEQ$ -transfected cells. The PCR product for the G_{qi5} mRNA was found only in CHO- hY_2 -K9- $qi5$ -K9 cells (lane C) as a very weak band and was not detectable in CHO- hY_2 -K9- $qi5$ -K9- $mtAEQ$ -A7 cells. As the PCR was performed simultaneously with 8 primers, self-annealing of the primers or formation of secondary structures could not be excluded. Therefore, the PCR was repeated only with the primers for the G_{qi5} construct and the β -actin control (Fig. 65). The PCR product with the expected size (918 bp) was now easily detectable and was found only in the cells stably transfected with the G_{qi5} construct (lane C, D).

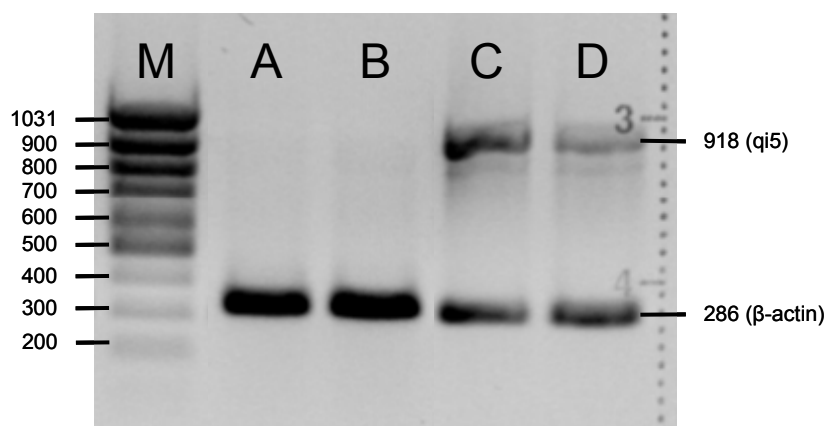


Fig. 65: mRNA expression of transfected cells. PCR was performed only in presence of primer pairs of G_{qi5} and β -actin. **A:** CHO-K1 cells **B:** CHO-hY₂-K9 cells **C:** CHO-hY₂-K9-qi5-K9 cells **D:** CHO-hY₂-K9-qi5-K9-mtAEQ-A7 cells **M:** marker.

4.2.3.7 Antagonism of BIIE0246

Concentration-response curves of pNPY were determined in the presence of the Y₂-selective antagonist BIIE0246. The cells were preincubated with increasing concentrations of the antagonist for 1 h before injection of increasing concentrations of the agonist.

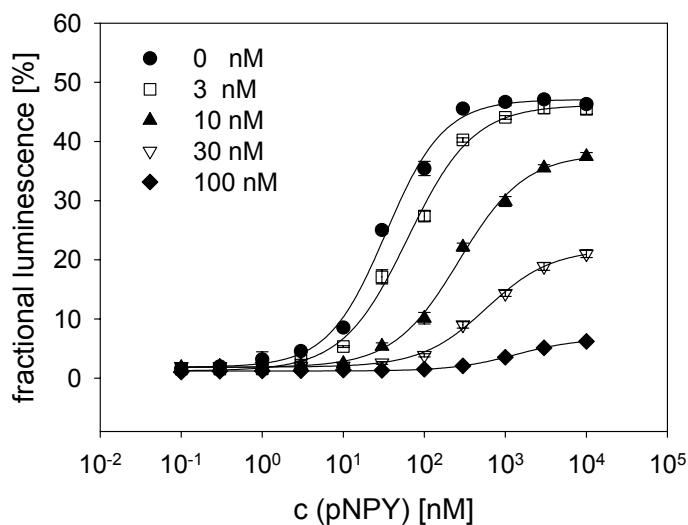


Fig. 66: Concentration-response curves of pNPY in the presence of BIIE0246 (**2**). CHO-hY₂-K9-qi5-K9-mtAEQ-A7 cells were preincubated with **2** for 1 h. Increasing concentrations of the antagonist led to a rightward shift and to a depression of the maximum of the luminescence signal. (mean values \pm SEM, $n=3$).

The concentration-response curves were shifted to the right with a concomitant depression of the maximum indicating mixed competitive-noncompetitive antagonism. This is in contrast to the competitive antagonism proposed for BIIE0246 (Dumont *et al.*, 2000; Weiser *et al.*, 2000). On the other hand, El Bahh and co-workers (El Bahh *et al.*, 2002) described an apparently insurmountable antagonism in hippocampal slices. Moreover, an insurmountable antagonism was found in the rat colon bioassay (Dumont *et al.*, 2000). El Bahh and co-workers suggested that BIIE0246 is a competitive antagonist, but because of its lipophilicity, the compound is enriched in

the membrane providing a much higher local concentration near the receptors compared to the concentration in the organ bath, simulating an insurmountable antagonism.

Surprisingly, there was no depression of the concentration-response curves in the aequorin assay observed without preincubation of the cells with the antagonist. (Fig. 67). After injection of the cell suspension to a mixture of agonist and antagonist higher concentrations of antagonist were needed to shift the concentration-response curves rightward. Schild regressions revealed a pA_2 value of 6.37 which is in dramatic contrast to the K_i value determined in the flow cytometric binding assay. However, comparing these data one has to consider that the binding assay was performed at equilibrium. Additionally, the strong adsorption of **2** to the 96-well plate (see Fig. 32) has to be regarded and usually much more data points are required for reliable calculations when performing a Schild plot. Nevertheless, these data indicate that the apparent mixed antagonism can be separated into two mechanisms with different kinetics.

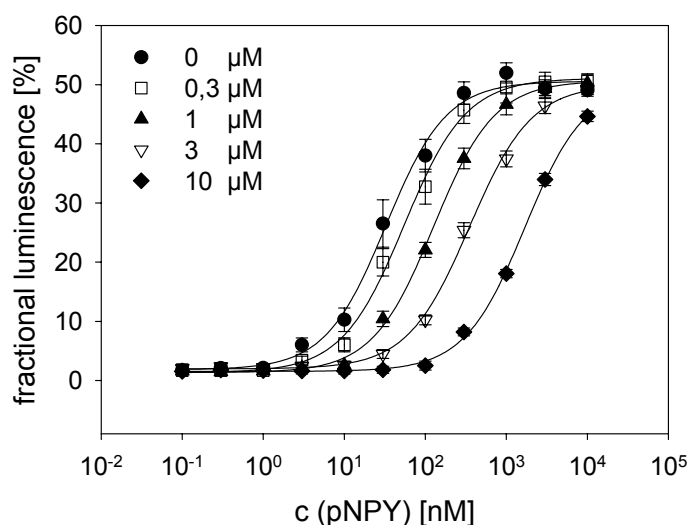


Fig. 67: Concentration-response curves of pNPY in the presence of the indicated concentrations of **2**. CHO-hY₂-K9-qj5-K9-mtAEQ-A7 cells were injected into a mixture of agonist and antagonist (mean values \pm SEM, n=3)

Therefore, the dissociation kinetics of BIIE0246 was measured. The cells were incubated with 5 nM cy5-pNPY for 2 h until equilibrium was reached (see Fig. 19). The bound fluorescence was recorded in channel 4 with the flow cytometer, and after 2 min 100 nM of **2** was injected to the cell suspension. The displacement of bound cy5-pNPY by **2** was followed recording the cell-bound fluorescence as shown in Fig. 68.

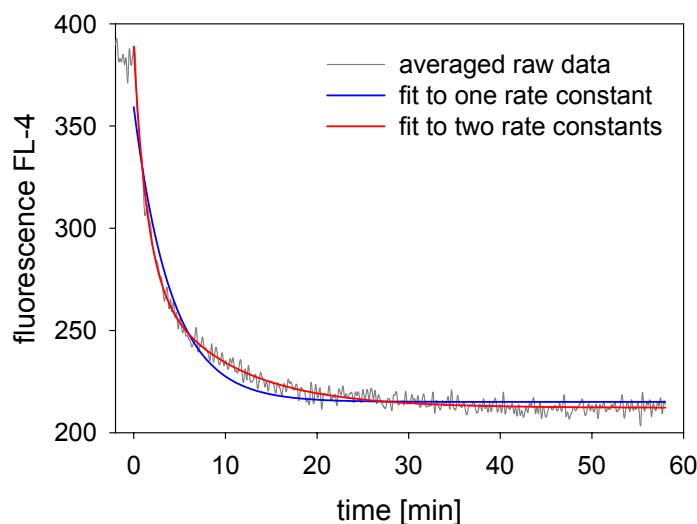


Fig. 68: Dissociation kinetics of **2** replacing cy5-pNPY at the hY₂ receptor recorded by flow cytometry. Data are best fitted with a model using two rate constants (red) compared to a model with one rate constant (blue).

The kinetics of displacement of cy5-pNPY by **2** can be described more precisely with a two-exponential fit ($R=0.994$) compared to a function which assumes only one dissociation rate constant ($R=0.979$). As cy5-pNPY is an agonist, this ligand distinguishes between precoupled and uncoupled receptors, and might bind as well as dissociate from the two different receptor states with different kinetics. Another explanation is the presence of two different binding sites for the antagonist **2**. The antagonist binds faster to the binding site of the labeled ligand as a competitive antagonism occurs when agonist and antagonist are added at the same time (Fig. 66). Binding to another allosteric binding site is slower indicated by a second dissociation rate constant and the presence of a mixed competitive-noncompetitive antagonism after preincubation of **2** with the cells.

In addition, the antagonist (100 nM) displaces only 44 % of the specific binding (unspecific binding was 44 [RFU], determined in presence of 1 μ M pNPY). This is in contrast to the binding data determined with CHO-hY₂-K9 cells (in competition with 5 nM cy5-pNPY, see section 3.2.3.1) where the same concentration of **2** displaced more than 90 % of the specifically bound cy5-pNPY (Fig. 20b). The data suggest that cy5-pNPY binds partially in an irreversible binding mode to the hY₂ receptor.

Recently, similar results were described by Dautzenberg and Neysari analyzing the binding kinetics of [¹²⁵I]-NPY and [¹²⁵I]-PYY to membranes of hY₂-expressing SMS-KAN and HEK293 cells (Dautzenberg and Neysari, 2005). After preincubation with the radioligand (120 min), not more than 20 % of bound [¹²⁵I]-NPY or [¹²⁵I]-PYY could be displaced from the receptor by addition of 10 μ M NPY, PYY or BIIE0246. This irreversible binding mechanism was not observed for the hY₁ or mY₅ receptor. In addition, in a FLIPR assay using HEK293 cells stably expressing the hY₂ receptor

and the chimeric Gq_{i9} protein, simultaneous addition of the agonist PYY and the antagonist **2** revealed a competitive antagonism whereas an insurmountable antagonism (with a minimal rightward shift of the EC₅₀ values) was observed after 30 min preincubation in presence of the antagonist. Dautzenberg suggested that the observed insurmountable effect of **2** is due to a lack of dissociation from its receptor sites (Dautzenberg and Neysari, 2005). Hence, the dissociation kinetics of the hY₂ receptor has to be considered in binding and functional assays. When available, measurements of binding kinetics should be performed with a labeled antagonist instead of labeled agonist in order to exclude different binding kinetics to different receptor states as well as dynamic processes as desensitization and internalization during the binding process.

4.3 Other techniques to measure a calcium response in CHO-hY₂-K9-qi5-K9-mtAEQ-A7 cells

4.3.1 Introduction

Confocal microscopy has often been used for the measurement of intracellular calcium concentrations in single cells (Lipp *et al.*, 2001). However, the highly sophisticated instrumentation makes this technique not very well suited for the application in a functional assay for routine compound screening. In addition, single cell measurements can vary to a high degree depending on the sample preparation which is unfavorable for quantitative determinations. Nevertheless, confocal microscopy is a useful tool for the visualization of changes in intracellular calcium.

The use of plate readers equipped with a CCD camera for the detection of flash luminescence has already been described (Dupriez *et al.*, 2002). Therefore, it was investigated whether the light generated by the transfected CHO cells upon agonist binding was sufficient for the detection with a CCD camera.

4.3.2 Materials and methods

4.3.2.1 Confocal microscopy

CHO-hY₂-K9-qi5-K9-mtAEQ-A7 cells were seeded in 200 µl Ham's F12 + 10 % FCS on a Lab-Tek[®] II, 8 chamber coverglass system (Nalge Nunc, Naperville, IL, USA) two days prior to the experiment and were grown to 50-70 % confluence. 330 µl of

loading suspension were prepared as described in section 4.1.2.4 and added to 1 ml of L-15 Leibovitz medium (Sigma). The medium of the cells was displaced with 300 μ l of this solution and the cells were incubated for 30 min at room temperature. Then, cells were washed once with loading buffer (see section 4.1.2.4) and incubated for 30 min with 270 μ l of Leibowitz medium at room temperature. The chamber was installed into a Zeiss Axiovert 200 M microscope, equipped with the LSM 510 laser scanner using a Plan-Apochromat 63x/1.4 objective with oil immersion. The laser power was set to 3 %, using the wavelength of 488 nm and the 505 longpass filter. A region of interest was defined for a single cell and a time series was adjusted with a scan speed which allows scanning one frame within 4 s. The measurement was started and 30 μ l of pNPY solution (1 μ M in loading buffer) were added to the cell chamber.

4.3.2.2 Luminescence detection with CCD camera

CHO-hY₂-K9-qi5-K9-mtAEQ-A7 cells were prepared as described in section 4.2.2.2. A 4-fold concentrated dilution series of pNPY was prepared in loading buffer and 50 μ l of each concentration were pipetted into a black, flat bottomed Cellstar 96-well plate (Greiner bio-one, Solingen, Germany). 150 μ l of the cell suspension were added per well at once per row with a multichannel pipette and the plate was immediately transferred into a darkbox. Recording was started with a Hamamatsu 1394 ORCA-II BTA 512 cooled CCD camera; settings were: gain: 2, exposure: 60 s, binning: 4 (16 bit). Total light dose was calculated with SimplePCI[®] software.

4.3.3 Results

4.3.3.1 Confocal microscopy

The calcium response could be visualized on the single cell level with confocal microscopy. Cells were loaded with fluo-4 and the signal was induced by the addition of 100 nM pNPY. Prior to the experiment, a single cell was scanned permanently for 2 min with the same laser power in order to estimate the effect of photobleaching. During this scanning process no distinct decrease in fluorescence was observed (data not shown).

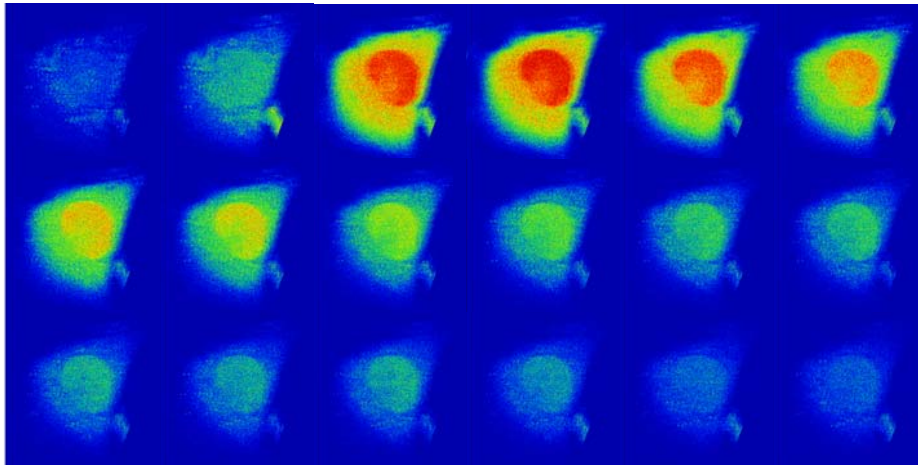


Fig. 69: Time series of CHO-hY₂-K9-qi5-K9-mtAEQ-A7 cells loaded with fluo-4 in response to 100 nM pNPY measured with confocal microscopy. Scanning time was 4 s per image. Images are shown in false colors (the warmer the color, the higher the fluorescence intensity).

As shown in Fig. 69 addition of 100 nM pNPY to the adherent growing cell results in a steep increase in fluorescence, reaching its maximum after 8 s followed by a slow decrease in fluorescence intensity over one minute. The kinetics differs slightly from the one obtained with the flow cytometer as shown in Fig. 37 due to relevant differences between the two methods. Dye-loading, postincubation, injection of agonist (no stirring) and, most important, long measuring time (4 s per image) of a single cell and therefore low temporal resolution result in an imprecise description of the kinetic course using the confocal microscope. In addition, as shown in Fig. 37, there is a high variation in fluorescence between different individual cells, which can not be displayed by confocal microscopy. High consumable costs, the inconvenient handling especially during the addition of the agonist and the very sophisticated quantification of calcium responses account for the inferiority of confocal microscopy compared to flow cytometry.

4.3.3.2 CCD camera

As many instruments used for high throughput screening are equipped with a CCD camera, it was investigated if the light intensity generated in the aequorin assay is sufficient for quantitative measurements with a CCD camera.

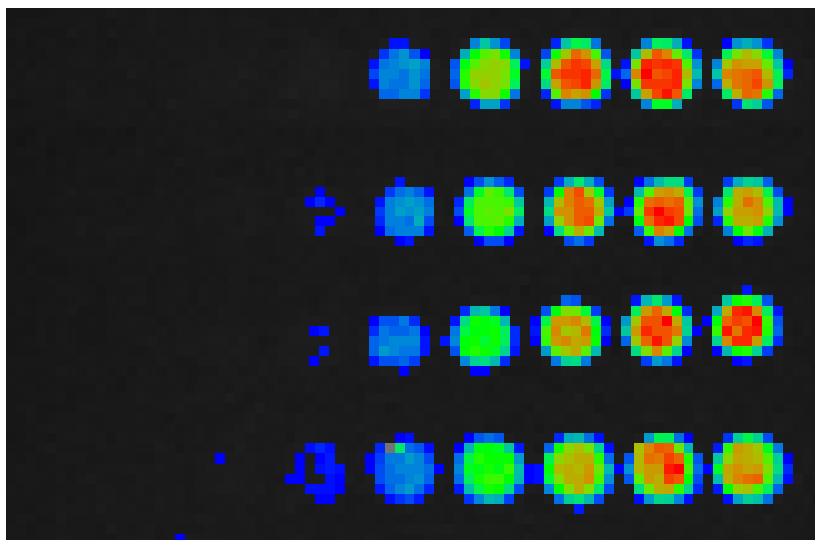


Fig. 70: Overlay picture of false color presentation of light intensities generated by CHO-hY₂-K9-qj5-K9-mtAEQ-A7 cells detected with a CCD camera. Luminescence signals were triggered by addition of increasing concentrations of pNPY.

As shown in Fig. 70, the luminescence light recorded for 60 s rises with increasing concentrations of the agonist. In spite of the difficult handling as described in section 4.3.2.2 the results were reproducible, and a quantitative analysis became possible. In order to compare the results obtained from the CCD camera, the same cell preparation was used in an aequorin assay performed with the TECAN Genios Pro plate reader. The calculated EC₅₀ values are in the same range as shown in Fig. 71. The highest concentration of 3 μM pNPY was not used for the determination of the EC₅₀ value with the CCD camera because the increase in luminescence starts immediately during transferring the plate into the darkbox and is therefore not completely detected by the CCD camera. This is also the reason for the higher deviations at high agonist concentrations. Nevertheless, these results show that the aequorin assay can be used for high-throughput applications using instruments equipped with a CCD camera.

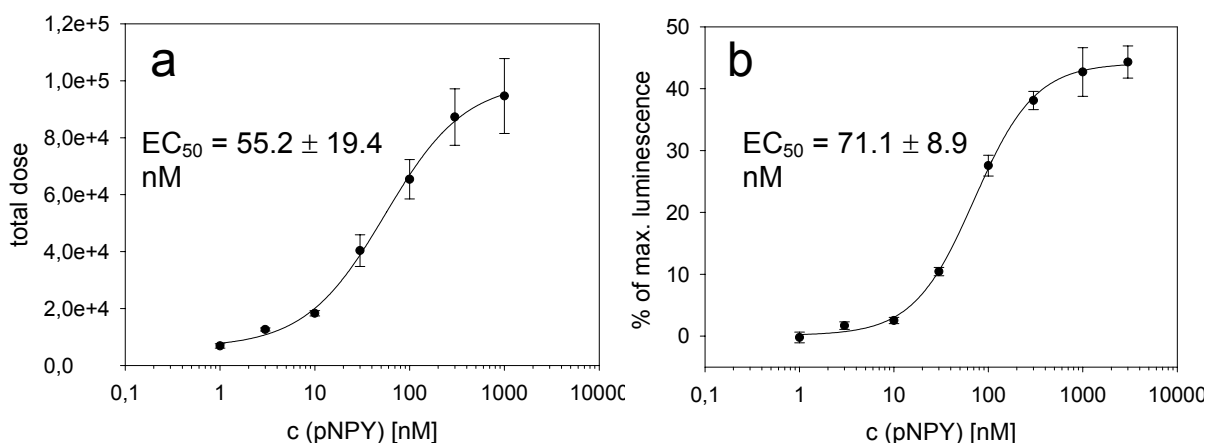


Fig. 71: Comparison of concentration-response curves generated with a Hamamatsu 1394 ORCA-II BTA 512 CCD camera (panel a) and with a TECAN Genios Pro plate reader (panel b) (mean values \pm SEM, $n=3$).

4.4 Conclusions

The stable co-transfection with the hY_2 receptor and the *Gqi5* gene led to a robust calcium signal after receptor activation. The cells showed unaltered binding properties compared to the hY_2 -transfected cells and proved to be suitable to establish fluorescence-based functional assays. Additional stable transfection of the cells with the apoaequorin gene targeted to the mitochondrial matrix converted the calcium signal into a luminescence signal which could be quantitated by a luminescence plate reader. The pharmacological constants of receptor agonists as well as antagonists determined in the three different functional assays are in good agreement as summarized in Table 6. Slight deviations may result from different incubation periods in presence of the antagonists and different adsorption to the synthetic material of microplates, cups and other small parts used in the assays.

Table 6: Functional data of selected compounds determined in different calcium assays on hY_2 receptor expressing cells.

Y_2 receptor ligand	Flow cytometry (fluo-4)	Spectrofluorimetry (fura-2)	Aequorin
pNPY	$18.1 \pm 2.9^{a,c}$	$16.9 \pm 2.5^{a,d}$	$30.9 \pm 2.2^{a,d}$
pNPY ₁₃₋₃₆	$13.3 \pm 6.2^{a,c}$	$18.6 \pm 1.5^{a,d}$	$58.3 \pm 9.9^{a,d}$
pPYY	$7.9 \pm 5.5^{a,c}$	ND	$8.8 \pm 2.4^{a,d}$
2	$20.4 \pm 2.9^{b,c}$	$28.9 \pm 2.0^{b,d}$	$50.9 \pm 12.9^{b,d}$
3	$3.9 \pm 1.2^{b,c}$	ND	$69.1 \pm 4.7^{b,d}$
4	$5.3 \pm 0.5^{b,c}$	$14.5 \pm 1.5^{b,d}$	$73.4 \pm 6.1^{b,d}$
5	$101.1 \pm 18.0^{b,c}$	$201.4 \pm 37.3^{b,d}$	$359.4 \pm 23.8^{b,d}$
6	$536.5 \pm 179.5^{b,c}$	ND	$521.4 \pm 54.3^{b,d}$
7	$168.7 \pm 62.3^{b,c}$	ND	$781.5 \pm 53.2^{b,d}$
8	$10.7 \pm 1.1^{b,c}$	ND	$50.6 \pm 7.7^{b,d}$
^a EC ₅₀ [nM] of agonists; ^b IC ₅₀ [nM] of antagonists, calcium mobilization induced with 70 nM pNPY ^c determined with CHO- hY_2 -K9-qi5-K9 cells; ^d determined with CHO- hY_2 -K9-qi5-K9-mtAEQ-A7 cells			

The calcium signal could be visualized by confocal microscopy as well as by a CCD camera indicating the suitability of the aequorin assay for the application in HTS-instruments equipped with a CCD camera.

Chapter 5

Binding and functional assays
for the NPY Y₄ receptor

5.1 Development of a flow cytometric binding assay for the rat NPY Y₄ receptor

5.1.1 Introduction

The rat Y₄ receptor gene was first cloned in 1996 from rat genomic DNA (Lundell *et al.*, 1996) (GenBank: Z68180) and from a rat whole brain cDNA library (Yan *et al.*, 1996) (GenBank: U42388). One year later, the receptor was cloned from a rat spleen genomic library (Walker *et al.*, 1997) and the sequence was submitted to the GenBank (Accession No.: U84245). The sequence published by Yan *et al.* differed in one amino acid, containing a serine instead of a proline in position 23. Various reports on binding assays for the rat Y₄ receptor have been published using transfected cells and [¹²⁵I]-rPP (Walker *et al.*, 1997; Yan *et al.*, 1996), [¹²⁵I]-hPP (Berglund *et al.*, 2001; Eriksson *et al.*, 1998; Parker *et al.*, 2002a; Parker *et al.*, 2005), [¹²⁵I]-GR231118 (Dumont and Quirion, 2000) or [¹²⁵I]-Leu³¹, Pro³⁴-PYY (Gehlert *et al.*, 1997). All described assays require an iodinated radioligand and comprise the general drawback that a filtration step is needed in order to separate bound from unbound radioligand. Therefore, a flow cytometric binding assay by analogy with the assay described for the human Y₂ receptor (see section 3.2) would be convenient.

5.1.2 Materials and Methods

5.1.2.1 Cell culture

All cell lines were maintained at 37 °C and 5 % CO₂ in water saturated atmosphere. CHO-rY₄ cells (Berglund *et al.*, 2001) were obtained from Prof. Dr. S. Parker, College of Medicine, University of Tennessee, Memphis, USA. Cells were maintained in Ham's F12 medium supplemented with 10 % FCS and 100 µg/ml G418. Subculturing was performed twice a week.

HEL cells were cultured in RPMI 1640 plus 5 % FCS and diluted weekly 1:10 with fresh medium. CHO-hY₂-K9-qi5-K9-mtAEQ-A7 cells were maintained as described in 4.2.2.2.1. HEC-1-B-hY₅ cells and HEC-1-B-hY₄ cells (clone 1 and 3) (Moser, 1999) were cultured in EMEM containing non-essential amino acids, 2.2 g/l NaHCO₃, 110 mg/l sodium pyruvate, 10 % FCS and 400 µg/ml G418. Subculturing by 1:10 dilution was performed every week.

The screened cell lines and their culture conditions are listed in Table 7.

Table 7: Culture conditions and origin of tested cell lines

Cell Line	Origin (Reference)	Culture Medium	Passaging
CAPAN-1	human pancreas adenocarcinoma (Fogh <i>et al.</i> , 1977b)	RPMI + 20 % FCS	1:2 – 1:4 every week
COLO-320	human colon adenocarcinoma (Quinn <i>et al.</i> , 1979)	RPMI + 10 % FCS	1:5 twice a week
DU-145	human prostate carcinoma (Stone <i>et al.</i> , 1978)	RPMI + 10 % FCS	1:3 – 1:5 twice a week
LNCAP	human prostate carcinoma (Gibas <i>et al.</i> , 1984)	RPMI + 10 % FCS	1:4 every week
HT-29	human colon carcinoma (Fogh <i>et al.</i> , 1977a)	McCoy's + 10 % FCS	1:5 every week
PANC-1	human pancreas carcinoma (Lieber <i>et al.</i> , 1975)	DMEM + 10 % FCS	1:10 every week
PC-3	human prostate carcinoma (Kaighn <i>et al.</i> , 1979)	45 % Ham's F12 + 45 % RPMI + 10 % FCS	1:10 every week
PC-12	rat adrenal pheochromocytoma (Greene and Tischler, 1976)	RPMI + 10 % FCS	1:10 every week
SW-403	human colon adenocarcinoma (Leibovitz <i>et al.</i> , 1976)	DMEM + 10 % FCS	1:10 every week

5.1.2.2 Y₄ receptor ligands

The peptides hPP and rPP were synthesized by Dr. C. Cabrele, Institute of Pharmacy, University of Regensburg. The Y₁ antagonist / Y₄ agonist GW1229 (also described as GR231118 or 1229U91) was a gift from Dr. J. Daniels, Glaxo Wellcome Inc.

5.1.2.3 Synthesis and purification of cy5-[K⁴]-hPP and S0586-[K⁴]-hPP

The peptide [K⁴]-hPP (peptide content: 70 %) was synthesized and provided by Prof. Dr. A. Beck-Sickinger, Institute of Biochemistry, University of Leipzig. The fluorescent cyanine dye S0586 was purchased from FEW chemicals (Wolfen, Germany). Labeling of the peptide was performed by analogy with the labeling procedure of pNPY described in 3.2.2.1. For the purification of the labeled peptide by HPLC, the same instrumentation and eluents as described in 3.2.2.1 were used with a modified gradient. After 15 min of equilibration with 50 % of solvent A at a flow rate of 1 ml/min the sample was injected and the fraction of solvent A was raised in a linear manner to 56.8 % over 30 min and subsequently to 71,2 % over 10 min. Afterwards, the column was washed with 100 % of solvent A and then re-equilibrated with 50 % of solvent A for 15 min.

5.1.2.3.1 Synthesis and purification of cy5-[K⁴]-hPP (10)

0.5 mg of [K⁴]-hPP were dissolved in 20 μ l of DMSO, and 250 μ l of labeling buffer (see 3.2.2.1) were added. One portion of cy5 was dissolved in 20 μ l of anhydrous DMSO and added to the peptide solution. The UV/VIS detector was set to 649 nm. The product was eluted after 35 min. The structure of the labeled peptide (exact mass: 4818.2 g/mol) was confirmed by ESI-MS revealing the following peaks: $m/z = 964.5$ for [M+5H]⁵⁺; $m/z = 1205.6$ for [M+4H]⁴⁺; $m/z = 1607.2$ for [M+3H]³⁺; and $m/z = 2410.1$ for [M+2H]²⁺. Sequencing of the N terminus verified the coupling of the dye at the K⁴ position of the peptide.

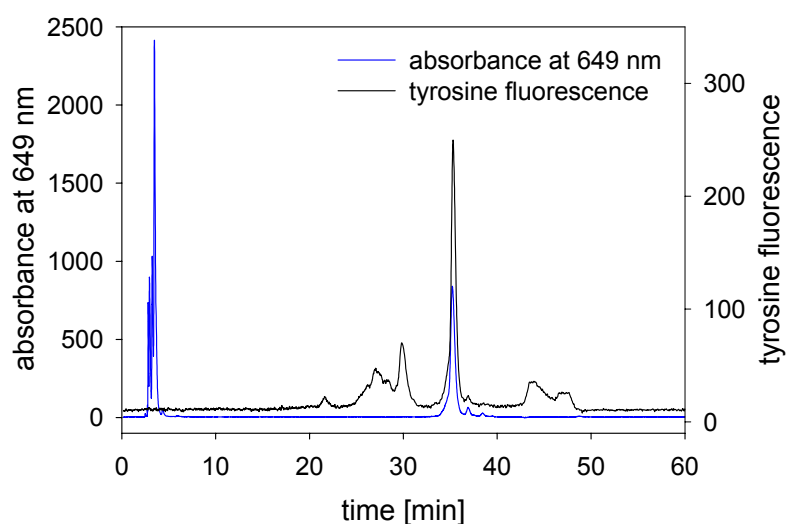


Fig. 72: HPLC-purification of cy5-[K⁴]-hPP

5.1.2.3.2 Synthesis and purification of S0586-[K⁴]-hPP (11)

0.5 mg of [K⁴]-hPP were dissolved in 400 μ l of labeling buffer. 0.28 mg of S0586 (348 nmol) were dissolved in 20 μ l of anhydrous DMSO and added to the peptide

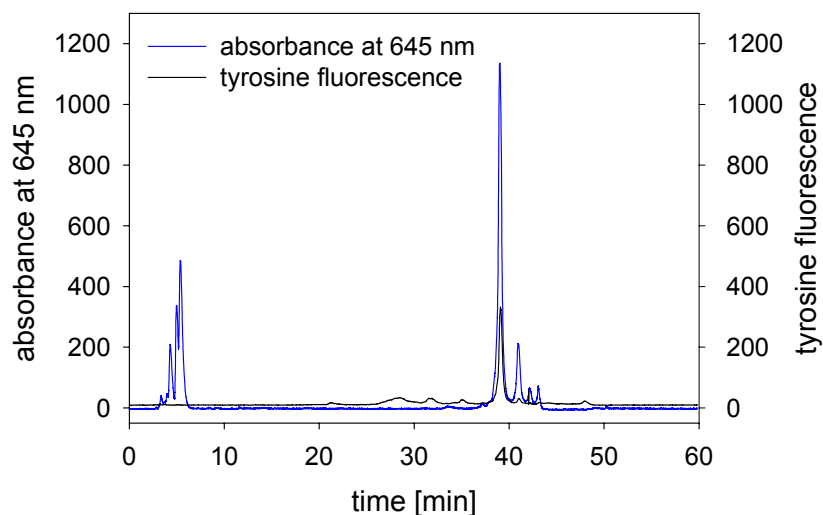


Fig. 73: Purification of S0586-[K⁴]-hPP

solution. The UV/VIS detector was set to 645 nm. The product was eluted after 37.5 min. The structure of the labeled peptide (exact mass: 4848 g/mol) was confirmed by ESI-MS revealing the following peaks: $m/z = 809.0$ for $[M+6H]^{6+}$; $m/z = 970.6$ for $[M+5H]^{5+}$; $m/z = 1213.4$ for $[M+4H]^{4+}$; and $m/z = 1617.5$ for $[M+3H]^{3+}$.

5.1.2.4 Flow cytometry

Cell samples were prepared and the flow cytometric measurements were performed with the same instrument settings as described in 3.2.2.3. The cells were preincubated for 90 – 120 min at room temperature in a final volume of 0.5 ml and analyzed without further processing. Unspecific binding at the rY₄ receptor was determined in the presence of 1 $\mu\text{mol/L}$ of unlabeled hPP or GW1229, respectively. Competition binding experiments were performed using cy5-[K⁴]-hPP (2 nM). For the screening of cell lines, the cells were incubated with 10 and 20 nM of **10**. Unspecific binding was determined in the presence of 1 μM hPP.

5.1.3 Results

5.1.3.1 Flow cytometric binding assay for the rat Y₄ receptor

The fluorescent ligand cy5-[K⁴]-hPP (**10**) showed high specific binding to CHO-rY₄ cells. As becomes obvious from Fig. 74a, the bound fluorescence of the gated cell population increased with higher concentrations of **10**. Binding of the ligand could be reduced in the presence of 1 μM hPP. The calculation of the geometric means allowed a saturation analysis, and a K_d value of 1.4 ± 0.3 nM was determined.

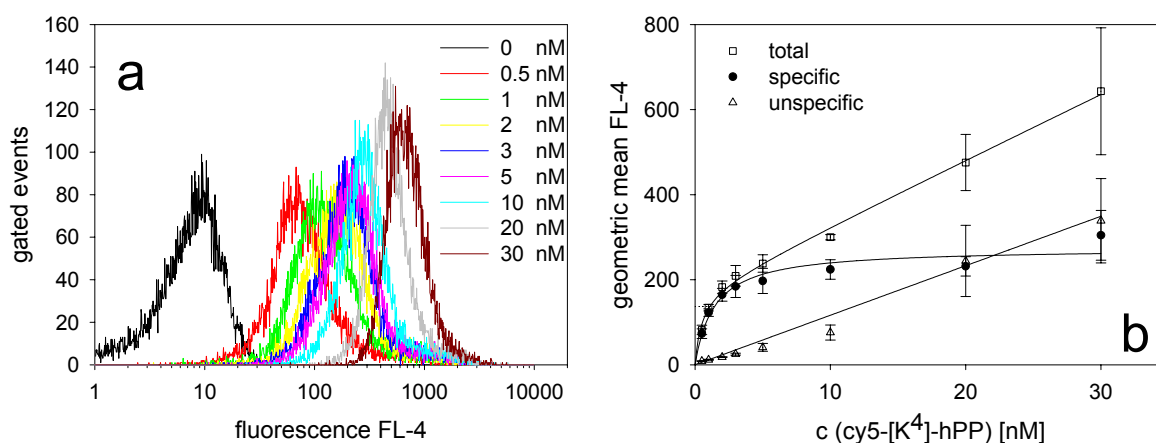


Fig. 74: Flow cytometric binding assay with CHO-rY₄ cells using cy5-[K⁴]-hPP. **a:** Fluorescence intensities of the gated cell population in channel 4 with increasing concentrations of cy5-[K⁴]-hPP. **b:** Saturation analysis with cy5-[K⁴]-hPP. Unspecific binding was determined in presence of 1 μM hPP (mean values \pm SEM, $n=3$).

5.1.3.2 Binding affinity of cy5-[K⁴]-hPP (10) to other NPY receptor subtypes

In order to determine the selectivity of the labeled ligand comparative binding experiments to rY₄, hY₁ and hY₂ receptors, were performed with HEL (hY₁) and CHO-hY₂-K9-qi5-K9-mtAEQ-A7 cells (see 4.2.3.1). No specific binding of **10** to HEL cells was observed up to a concentration of 30 nM (Fig. 75a). Binding of **10** and **11** to hY₂-expressing CHO cells (Fig. 75b) up to a concentration of 100 nM could not be abolished by 1 μM of the Y₂ selective antagonist **2** indicating that there is no specific binding to the hY₂ receptor.

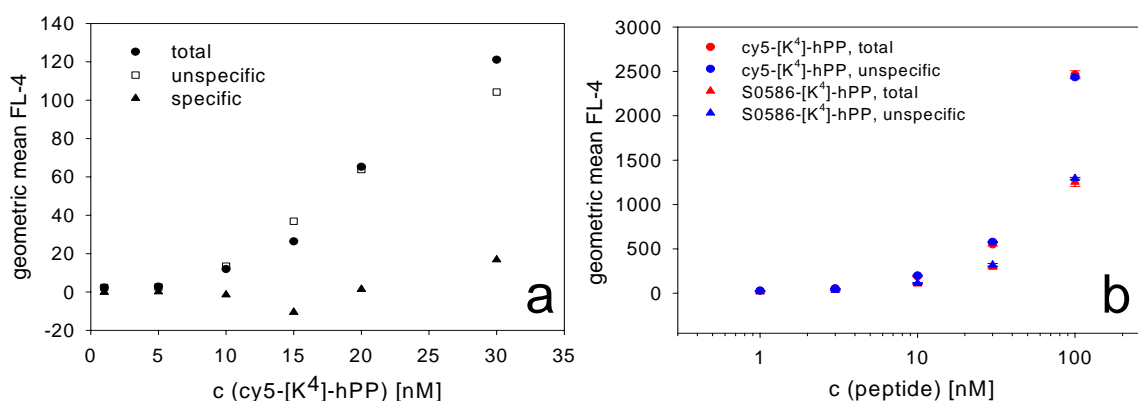


Fig. 75: Flow cytometric binding experiment with hY₁- and hY₂-expressing cells. **a:** Binding of **10** to hY₁-expressing HEL cells. Unspecific binding was determined in presence of 1 μM pNPY (*n*=1). **b:** Binding of **10** and **11** to CHO-hY₂-K9-qi5-K9-mtAEQ-A7 cells. Unspecific binding was determined in presence of 1 μM of **2**.

Binding of **10** to the hY₅ receptor was determined using stably transfected HEC-1-B-hY₅ cells described by Moser (Moser, 1999). Binding was not saturated over the concentration range tested but it was similar compared to the binding of **2**. In order to save labeled peptides, the exact determination of K_d values was abandoned.

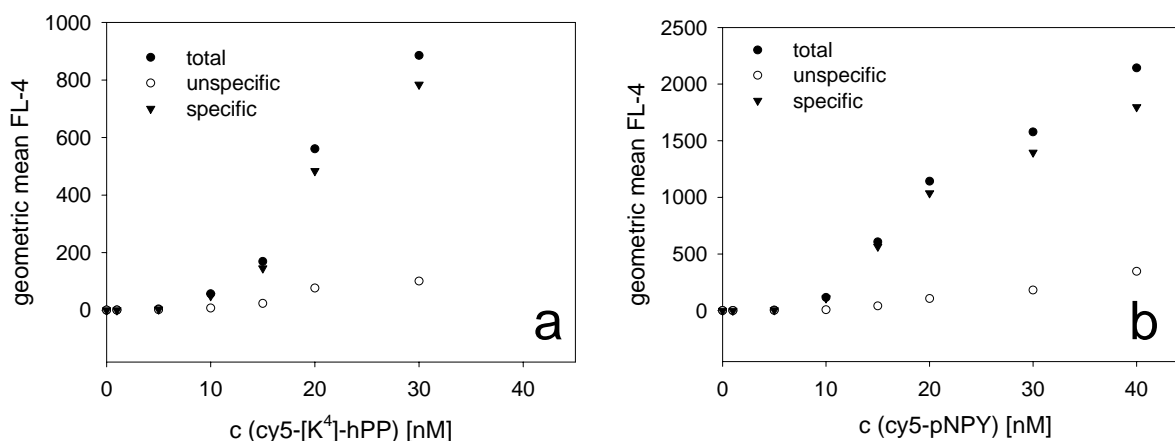


Fig. 76: Flow cytometric binding experiment with HEC-1-B-hY₅ cells. **a:** specific binding of **10**. **b:** specific binding of **2**. Unspecific binding was determined in presence of 2 μM pNPY (*n*=1).

The labeled peptide cy5-[K⁴]-hPP appeared to be selective for rY₄ towards hY₁ and hY₂ and showed a considerably lower affinity to the hY₅ receptor. Therefore, it was used for competition binding assays with known peptide ligands of the rY₄ receptor.

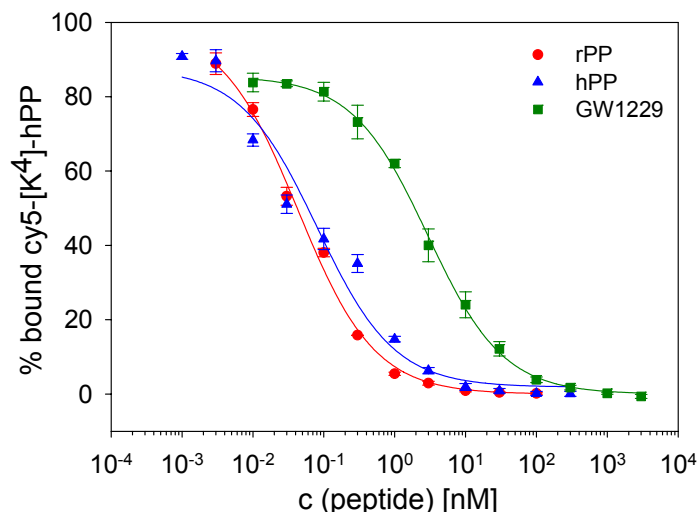


Fig. 77: Flow cytometric binding assay with CHO-rY₄ cells. Competition of binding of 2 nM cy5-[K⁴]-hPP in the presence of rPP, hPP and GW1229 (mean values \pm SEM, $n=3$).

The peptides rPP ($K_i = 18.0 \pm 3.3$ pM) and hPP ($K_i = 33.8 \pm 8.6$ pM) bound with high affinity to the rat Y₄ receptor which is in good agreement with radioligand binding assays described in the literature. Gehlert reported on a $K_i = 18$ pM for rPP and a $K_i = 14$ pM for hPP (Gehlert *et al.*, 1997) whereas Parker determined K_i values of 13.5 pM and 21 pM for rPP and hPP, respectively (Parker *et al.*, 2002a). The K_i value determined for GW1229 (1.23 ± 0.20 nM) is approximately 6-fold higher compared to the data published by Parker using [¹²⁵I]-pPYY in a radioligand binding assay (Parker *et al.*, 1998). Nevertheless, despite this deviation in case of GW1229, binding of the peptide ligands reflects the typical Y₄ receptor pharmacology indicating that the labeled peptide **10** is a useful tool for flow cytometric binding assays with CHO-rY₄ cells.

5.1.3.3 Screening of cell lines for binding of cy5-[K⁴]-hPP (10)

Northern hybridization experiments revealed that human Y₄ mRNA is mainly expressed in the colon, small intestine, and prostate. Low levels of expression were found in various CNS regions (Lundell *et al.*, 1995). Rat Y₄ mRNA was found mainly in testis and lung, and to a smaller extent in colon (Lundell *et al.*, 1996). Furthermore, PP-preferring receptors were described based on binding studies using dog intestinal mucosa (Gilbert *et al.*, 1988), rat PC12 pheochromocytoma cells (Schwartz *et al.*, 1987), rat brain area postrema (Whitcomb *et al.*, 1990), rat adrenal cortex and medulla (Whitcomb *et al.*, 1992). Functional assays using the rat vas deferens

(Jorgensen *et al.*, 1990) or human Col-24 colon adenocarcinoma cells (Cox *et al.*, 2001) describe also Y_4 receptor pharmacology. Therefore, various human colon, prostate, pancreas carcinoma cell lines and rat PC-12 cells were screened for specific binding of **10**. The cells were incubated with 10 and 20 nM of cy5-[K⁴]-hPP and bound fluorescence (total) of the gated cell populations was determined with flow cytometry. Unspecific binding was determined in the presence of 1 μ M unlabeled hPP and subtracted from total binding for the calculation of specific binding.

Neither CAPAN-1, COLO-320, DU-145, LNCAP, HT-29, PANC-1, PC-3 and SW-403 cells nor the HEC-1-B- Y_4 (clone 1 and 3) showed any distinct specific binding of the fluorescent ligand. As shown exemplarily for HT-29 cells in Fig. 78, the cell bound fluorescence could not be displaced by high concentrations of hPP.

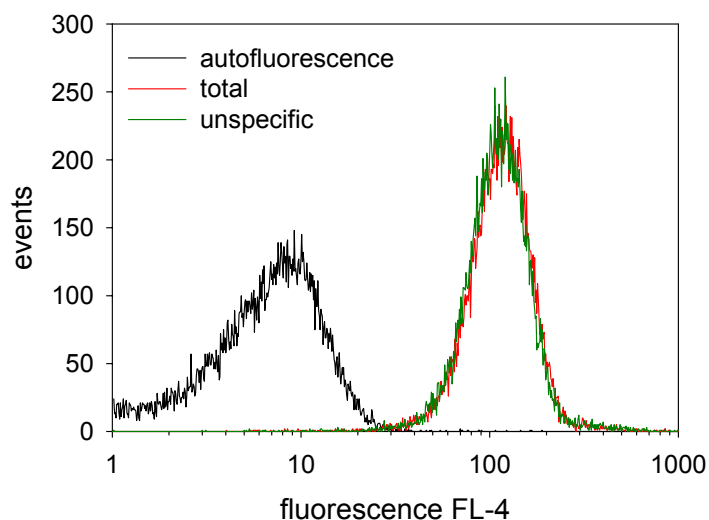


Fig. 78: Binding of 20 nM of **10** to HT-29 cells. Bound fluorescent ligand was not displaced in the presence of 1 μ M hPP (green). Geometric means calculated with WinMDI were 6 (autofluorescence), 112 (total) and 110 (unspecific).

PC-12 cells were very heterogeneous as shown in the density plot of Fig. 79a. The cell population in gate 4 consists of at least two subpopulations binding the fluorescent ligand to different extents indicated by the two maxima in the histogram (Fig. 79b). In presence of 1 μ M hPP the bound fluorescence was reduced by 22 % indicating low specific binding of **10**. But because of the large fraction of unspecifically bound ligand the cell line is not suited for a flow cytometric binding assay. It might be possible to select certain subpopulations which show high specific binding by cell sorting of PC-12 cells incubated with cy5-[K⁴]-hPP as described in section 5.2.3.2 for transduced P388 cells.

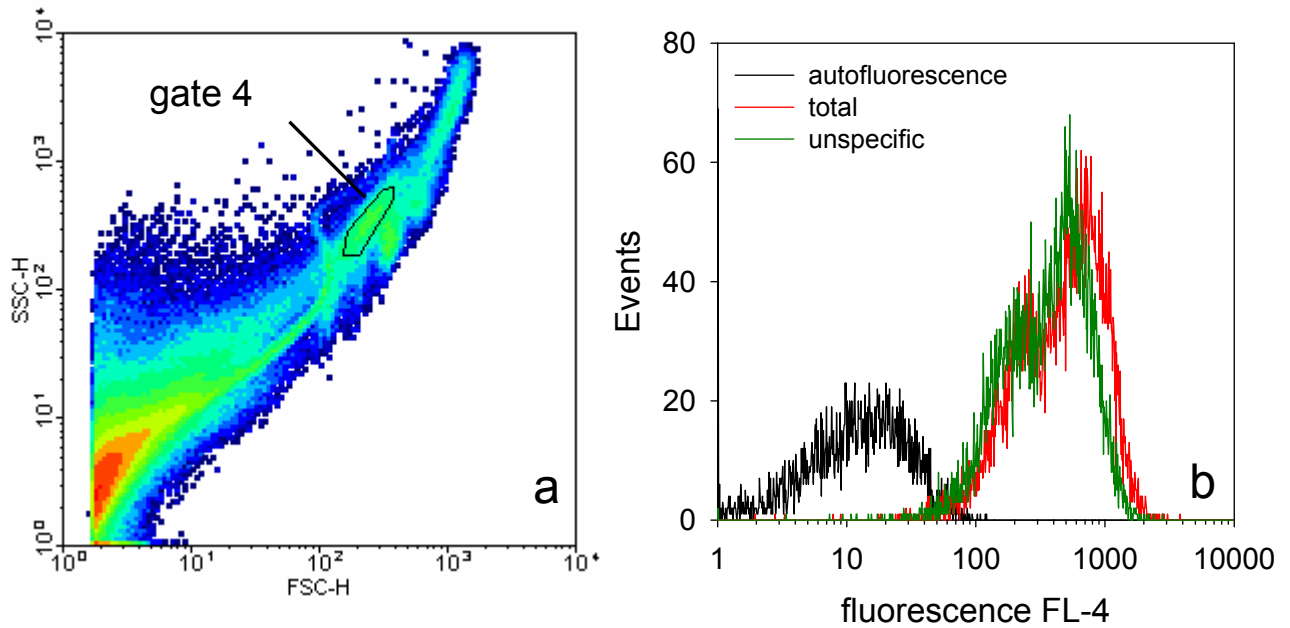


Fig. 79: **a:** Scattergram (density plot) of HT-29 cells. **b:** Bound fluorescence of gated (gate 4) cell population in absence (black) or presence (red, green) of 20 nM of **10**. Unspecific binding (green) was determined in presence of 1 μ M hPP. Geometric means calculated with WinMDI were 12 (autofluorescence), 436 (total) and 340 (unspecific).

5.2 Development of a flow cytometric binding assay for the human NPY Y₄ receptor

5.2.1 Introduction

The human Y₄ receptor gene was first cloned from a human placenta genomic library by Bard and co-workers (Bard *et al.*, 1995) and in the same year by Lundell and co-workers from a human lymphocytes genomic library (Lundell *et al.*, 1995). The cDNA sequences (Genbank Accession Number U35232 and Z66526) differed in 5 conservative mutations and encoded for a receptor protein consisting of 375 amino acids. One year later, Yan and co-workers published a hY₄ sequence (Genbank Accession Number U42387) cloned from a human fetal brain cDNA library (Yan *et al.*, 1996). The coding sequence was identical with the one published by Lundell *et al.* except one base resulting in one differing amino acid (serine instead of alanine in position 99). The fourth entry for the hY₄ gene in the Genbank by Kopatz (unpublished data, submitted 2003) is identical to the coding sequence published by Lundell *et al.*

5.2.1.1 Retroviral transduction

The use of retroviruses for gene transfer and expression has become a powerful tool for the stable introduction of genetic material into the genome of any dividing cell type (Miller, 1993). Retroviral vectors have several advantages compared to other non-viral transfection techniques because of their ability to transduce a variety of cell types, to integrate efficiently into the genome of the host cells and to express the transduced gene at high levels. The genome of a retrovirus is organized in four genes: *gag*, *pro*, *pol* and *env*. The *gag* gene encodes for the structural proteins forming matrix, capsid and nucleocapsid, while the envelope glycoprotein subunits are encoded by the *env* gene. The *pro* sequence encodes for a protease and the *pol* gene encodes the enzymes reverse transcriptase and integrase. In addition, the retroviral genome contains the regulatory sequences designated as long terminal repeats (LTRs) required to drive gene expression, reverse transcription and integration. The psi (Ψ) sequence (also called packaging signal) mediates the specific packaging of the RNA into the newly formed virions. Infection of a host cell is initiated by binding of the viral envelope glycoprotein to a specific receptor complex

on the cell surface (adsorption). The membranes of virus and cell fuse, and the virus core is released into the cytoplasm. During partially degradation of the virus core, the viral RNA is reversely transcribed into a double stranded proviral DNA which enters the nucleus and becomes integrated into the host genome. Transcription of the proviral DNA leads to expression of virus proteins, and only the packaging signal (Ψ) containing viral RNA becomes encapsidated to form a new virus particle by budding from the cell surface. The pCL vector system was developed by Naviaux and co-workers (Naviaux *et al.*, 1996). The principle of the production of recombinant, replication-incompetent retrovirus is shown in Fig. 80.

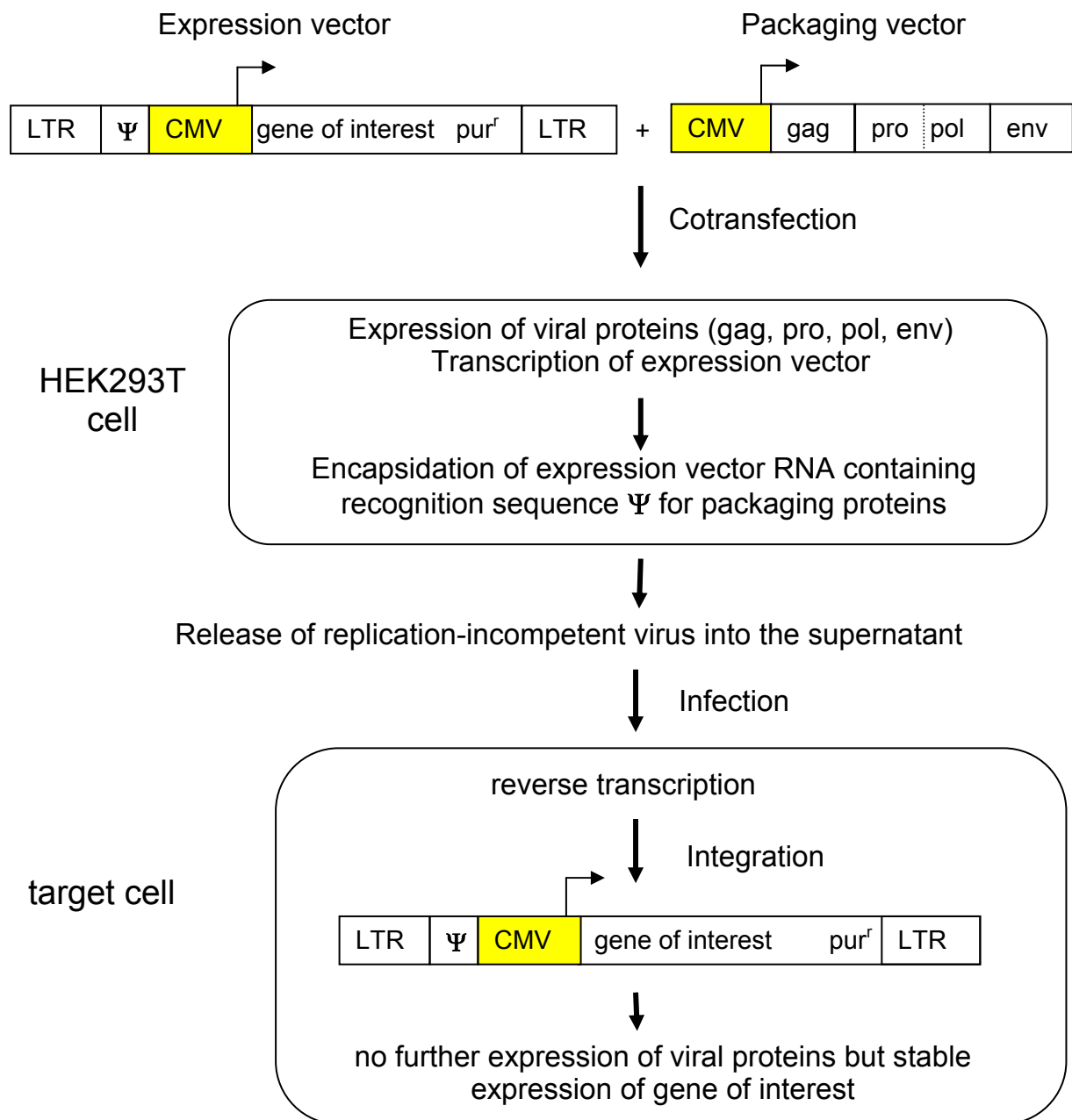


Fig. 80: Principle of retroviral transduction using the pCL vector system. Transient transfection of HEK293T cells with packaging and expression vector leads to production of replication-incompetent virus, which are used for infection of the target cells. Further explanations in the text. CMV: cytomegalovirus promoter, pur^r : puromycin resistance gene.

The packaging vector (e.g. pCL-Eco) and the expression vector (e.g. pQCXIP) containing the gene of interest are co-transfected into HEK293T cells. Viral proteins encoded by the *gag*, *pro*, *pol* and *env* genes are expressed and the expression vector is transcribed into mRNA. Only the vector RNA containing the psi (Ψ) sequence deriving from the expression vector becomes encapsidated. The released new viruses are replication-incompetent because they lack the genes *gag*, *pro*, *pol* and *env*. After infection of the target cells, the gene of interest becomes integrated into the genome and is stably expressed by the host cell.

5.2.2 Materials and Methods

5.2.2.1 Standard cloning techniques in molecular biology

Standard media, agar plates, reagents, enzyme and buffers were prepared and used as described in 3.1.2. Restriction enzyme digestion, ligation reaction, transformation, agarose gel electrophoresis and preparation of plasmid DNA were performed as described in 3.1.2.

5.2.2.2 Subcloning of the pcDNA3-hY₄ vector

The hY₄ construct was subcloned from the pRc/CMV-Y4 vector (obtained from Dr. H. Herzog, Garvan Institute of Medical Research, Sydney, Australia) into the *Bam*HI and *Eco*RI sites of pcDEF3 vector by Moser (Moser, 1999). Sequence analysis revealed 6 conservative mutations compared to the published sequence U42387 (Yan *et al.*, 1996). The pcDNA3-hY₅ was prepared by Moser (Moser, 1999). The hY₅ construct is subcloned into the *Bam*HI site of pcDNA3.

The pcDEF3-hY₄ plasmid was digested with *Bam*HI and *Eco*RI using buffer B (Roche Diagnostics, Mannheim, Germany). The DNA fragments were separated via gel electrophoresis revealing two expected bands at 6100 bp and 1134 bp (Fig. 81B). The pcDNA3-hY₅ vector was digested with *Bam*HI and *Eco*RI (buffer B, Roche Diagnostics) leading to the formation of DNA fragments with 5412 bp (linearized empty vector), 1400 bp (hY₅ construct) and 23 bp (fragment of the MCS, not detectable) as shown in Fig. 81C. The hY₄ construct (1134 bp) and the linearized pcDNA3 vector (5412 bp) were excised from the gel and purified using the QIAEX II purification kit.

Ligation reactions were performed using 2 µl of linearized pcDNA3 vector and increasing amounts (0.5 – 6 µl) of isolated hY₄ construct in a 20 µl ligation reaction. Plasmid DNA of ampicillin resistant transformants was isolated by MiniPrep and digested with *Bam*HI and *Eco*RI using buffer B. Agarose gel electrophoresis revealed the two expected bands at 5412 bp and 1134 bp (very weak, distinct band with 800 ng of digested vector in Fig. 81E,G). The linearized vector was detected after *Bam*HI digestion at 6546 bp (Fig. 81D,F).

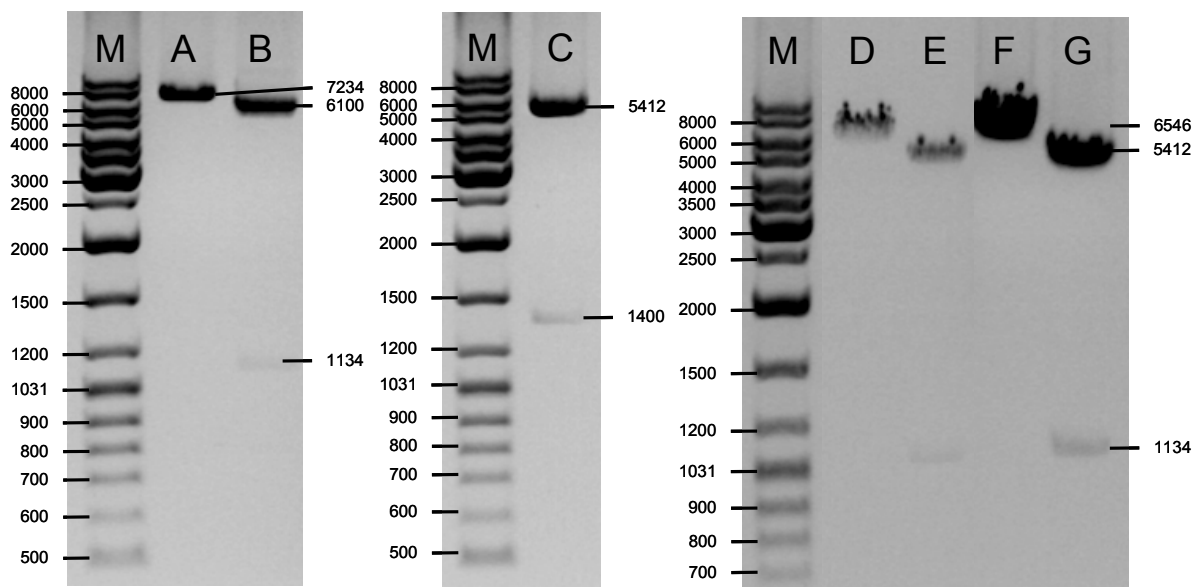


Fig. 81: **A:** *pcDEF3-hY₄* linearized with *EcoRI*. **B:** *pcDEF3-hY₄* digested with *BamHI* and *EcoRI*. **C:** *pcDNA3-hY₅* digested with *BamHI* and *EcoRI*. **D:** 200 ng *pcDNA3-hY₄* digested with *BamHI*. **E:** 200 ng *pcDNA3-hY₄* digested with *BamHI* and *EcoRI*. **F:** 800 ng *pcDNA3hY₄* digested with *BamHI*. **G:** 800 ng *pcDNA3-hY₄* digested with *BamHI* and *EcoRI*. **M:** *peqGOLD* DNA ladder mix (*Peqlab*).

5.2.2.3 Site-directed mutagenesis of *pcDNA3-hY₄*

Restriction endonuclease *DpnI* (10 U/μl), recombinant *Pfu* DNA polymerase (2.5 U/μl) and the corresponding 10x PCR buffer containing 200 mM tris-HCl (pH 8.8), 100 mM (NH₄)₂SO₄, 100 mM KCl, 1 % Triton-X-100, 1 mg/ml BSA and 20 mM MgSO₄ were purchased from MBI Fermentas (St. Leon-Rot, Germany). The mutagenic primer pair was synthesized by MWG (Ebersberg, Germany). The mutated base (guanine instead of thymine) is printed in bold type, the codon encoding for the mutated amino acid (alanine instead of serine) is underlined:

Sense: 5'- GCCAGCCGCTGACCGGCCGTCTACACCATCATGG -3' (33 b)

Antisense: 5'- CCATGATGGTGTAGACGGCGGTCAGCGGCTGGC -3' (33 b)

The site-directed mutagenesis (SDM) was performed by analogy with the QuikChange™ Site-Directed Mutagenesis Kit (Stratagene, La Jolla, CA, USA). This method allows the rapid introduction of point mutations into sequences of interest using a pair of complementary mutagenesis primers to amplify the entire plasmid in a single PCR. Treatment of the DNA with restriction enzyme *DpnI*, which will cut only fully or hemimethylated 5'-G^{m6}ATC-3' sequences in duplex DNA, leads to the

selective digestion of the PCR template DNA (Braman *et al.*, 1996; Weiner *et al.*, 1994). The in vitro synthesized unmethylated nicked vector DNA, including the introduced base change, is resistant to *DpnI* digestion and used for transformation of *E. coli* competent cells. After transformation, the nicks in the mutated plasmid are repaired by the bacteria.

The PCR reactions were prepared in a final volume of 49 μ l containing 5 μ l 10x PCR buffer, 10-50 ng template dsDNA, 15 pmol of each mutated primer, 5 μ l 2 mM dNTP mix and millipore water. The PCR tube was placed into the thermocycler, heated to 95 °C and 1 μ l of *Pfu* DNA polymerase was added. Cycling parameters were:

- 1) denaturation: 95 °C, 30 s
- 2) annealing: 55 °C, 1 min
- 3) extension: 68 °C, 13 min
- 4) final extension: 68 °C, 15 min
- 5) hold: 4 °C

Steps 1) – 3) were repeated 16 times. For the digestion of the nonmutated parental DNA template 1 μ l of *DpnI* was added. The reaction mixture was mixed and incubated for 1.5 h at 37 °C. The digested DNA was directly used for transformation in competent *E. coli* XL1-Blue. Transformed cells were plated on selective amp-plates and resistant colonies were used for plasmid preparation with the Qiagen Plasmid Purification Kit (Qiagen, Hilden, Germany). Restriction enzyme digestion with *Bam*HI and *Eco*RI revealed the expected bands at 1134 bp and 5412 bp (not shown) and sequencing of the construct (Entelechon, Regensburg, Germany) confirmed the mutation in position 294 (counted from the start codon). The mutated vector was designated as pcDNA3-S99A-hY₄.

5.2.2.4 Transfection of CHO-K1 cells

CHO-K1 cells were seeded in 500 μ l of Ham's F12 plus 10 % FCS on 24-well plates, grown to 60 – 70 % confluence and transfected under optimized conditions described in section 3.1.3.1 using 300 ng of plasmid DNA per well and a DNA - FuGENE transfection reagent ratio of 1:6.

Transient expression was analyzed two days posttransfection. Selection of resistant cells was carried out in selective medium containing 400 μ g/ml G418. Single resistant cell clones were isolated as described in 3.1.2.12.

5.2.2.5 Flow cytometric screening of transfected cells

Transient transfected cells or selected resistant cell clones were prepared for flow cytometric measurements as described in 3.2.2.3.

5.2.2.6 Subcloning of the pQCXIP-hY₄ and the QCXIP-S99A-hY₄ vector

The retroviral expression vector pQCXIP was a gift of Dr. Wulf Schneider, Department of Microbiology, University of Regensburg. Compared to the commercially available vector pQCXIP (BD Biosciences Clontech, Heidelberg, Germany) this vector contains a *Hpa*I site instead of the *Pac*I site and an additional *Xho*I site downstream the *Eco*RI site in the MCS.

The vectors pcDNA3-hY₄ and pcDNA3-S99A-hY₄ were digested with *Bam*HI and *Xho*I using buffer B (Roche Diagnostics) and the DNA fragments were separated via gel electrophoresis as shown in Fig. 82. The DNA fragments hY₄ and S99A-hY₄ (1167 bp) were isolated from the gel using the QIAEX II purification kit. The pQCXIP vector was digested with the same restriction enzymes and the linearized vector was separated from the MCS fragment and purified by analogy to the Y₄ fragments. Ligation reactions were carried out as described in 5.2.2.2.

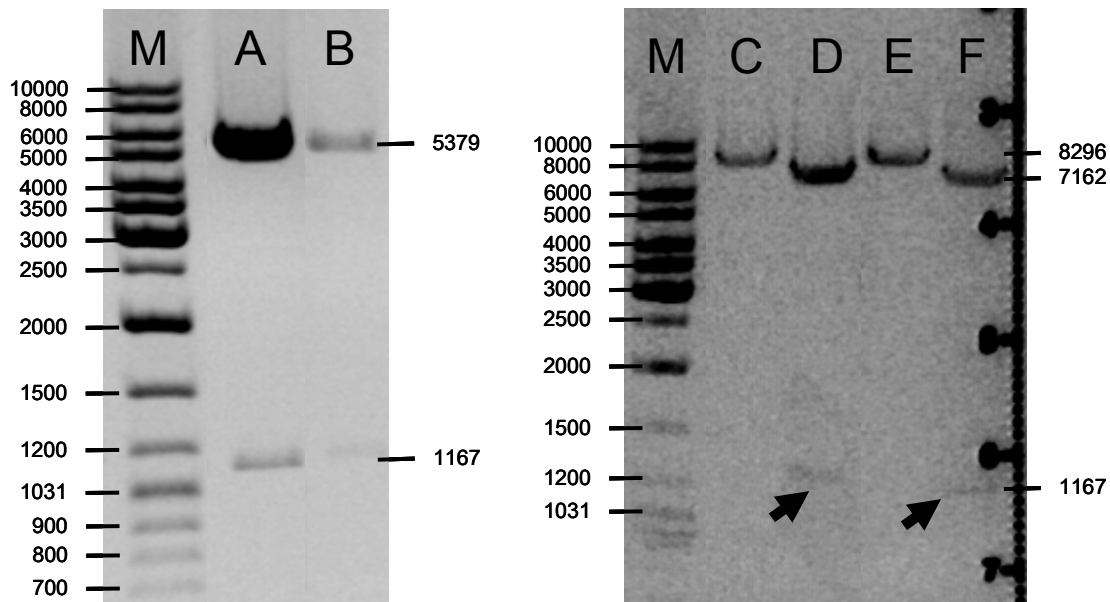


Fig. 82: Subcloning of the hY₄- and the S99A-hY₄-construct into the pQCXIP vector. *Bam*HI and *Xho*I digestion of pcDNA3-S99A-hY₄ (lane A) and pcDNA3- hY₄ (lane B). The hY₄ and the S99A-hY₄ fragments (1167 bp) were excised from the gel and used for ligation reactions. Restriction analysis of the ligated vectors pQCXIP-S99A-hY₄ (lane C, D) and pQCXIP-hY₄ (lane E, F). Linearization with *Bam*HI (C, E) and double digestion with *Bam*HI and *Xho*I (D, F). The black arrows indicate the weak bands of the released Y₄ inserts (1167 bp).

The ligation reaction was transformed into competent *E. coli*, resistant colonies were selected and plasmid DNA was prepared by MiniPrep. The correct insertion of the Y₄ constructs into the pQCXIP vector was confirmed by restriction enzyme digestion with *Bam*HI and *Xho*I. Linearization of the full-length vectors (Fig. 82C, E) revealed the expected bands with 8296 bp. Double digestion with *Bam*HI and *Xho*I (Fig. 82D, F) released the Y₄ inserts (1167 bp, very weak bands indicated by the black arrows) and the empty pQCXIP vectors (7162 bp). Sequencing (Entelechon) of the constructs further confirmed the correct composition of the retroviral expression vectors.

5.2.2.7 Transduction of P388-D1 cells

HEK293T cells and the pCL-Eco retrovirus packaging vector (Imgenex, San Diego, CA, USA) were obtained from Dr. Wulf Schneider, Department of Microbiology, University of Regensburg. The vector contains an ampicillin resistant gene for selection in *E. coli*. Retroviruses obtained by cotransfection with pCL-Eco vector and retroviral expression vector will infect mouse and rat cells, but not human cells. Therefore, retroviral production and transduction work can be performed in a Biosafety Level 1 (BL1) facility. HEK293T cells were maintained in DMEM plus 10 % FCS and passaged by 1:10 splitting twice a week. P388-D1 cells were maintained in RPMI plus 5 % FCS and diluted 1:20 every week.

2x HEPES-buffered saline solution (HeBS) contained 50 mM HEPES (Sigma), 280 mM NaCl (Merck) and 1.5 mM Na₂HPO₄ (Merck) in millipore water (pH 7.05).

CaCl₂-solution contained 2.5 M CaCl₂ in millipore water. Both solutions were sterile filtered and stored as aliquots at -20 °C. Sterile polybrene (hexadimethrine bromide) stock solution (8 mg/ml) and the pQCXIP-eYFP control vector were obtained from Dr. Schneider.

Two days prior the transfection $1.5 \cdot 10^6$ HEK293T cells were seeded in 10 ml DMEM plus 10 % FCS on a 10 cm tissue culture dish (Falcon) and cells were grown to 60 - 70 % confluence. One hour before the transfection the medium was replaced by fresh one in order to achieve optimal pH conditions at the time of transfection. 10 µg of retroviral expression vector (pQCXIP-hY₄, pQCXIP-S99A-hY₄ or pQCXIP-eYFP) and 10 µg of pCL-Eco in 450 µl millipore water were added to 50 µl of CaCl₂-solution. While vortexing, this solution was added dropwise to 500 µl of 2x HeBS in order to co-precipitate Ca₃(PO₄)₂ and plasmid DNA. Subsequently, the suspension was added dropwise to the HEK293T cells. 5 h after the transfection the medium was sucked off and 10 ml of fresh medium was added. One day before the infection 10^5

P388-D1 cells were seeded in 4 ml RPMI plus 5 % FCS on a 6-well plate. Two days after the transfection of the HEK293T cells, eYFP expression (> 70 %) of the control cells was determined with fluorescence microscopy. The virus-containing supernatant was sucked off and 10 µl of polybrene solution was added to 10 ml of supernatant. The virus suspension was filter sterilized (Pall® Acrodisc 25 mm Syringe Filter w/0.45 µm with HAT Tuffryn® membrane, Pall, New York, USA) and directly used for infection or stored on ice until the second infection. For the infection, P388-D1 cells were centrifuged at 300 g for 4 min and resuspended in a mixture of 2 ml of virus suspension and 2 ml of fresh medium. Cells were incubated for 6 h and infected again. Fresh medium was added to the cells 24 h after the first infection. Selection of transduced cells was carried out with selective medium containing 3 µg/ml puromycin (Sigma, München, Germany).

5.2.2.8 Cell sorting

P388-D1 cells transduced with the pQCXIP-S99A-hY₄ receptor were centrifuged at 300 g for 5 min and resuspended at $2 \cdot 10^6$ cells/ml in sterile binding buffer (see 3.2.2.3). 10 nM of **10** were added and the cells were incubated for 1 h at room temperature under slight shaking. The whole fluid system of the flow cytometer was disinfected by flushing with 70 % ethanol for 30 min and subsequently washed with sterile PBS for additional 30 min. The collection tubes were prepared by incubation with sterile PBS containing 4 % BSA overnight. The solution was discarded and the collection tubes were filled with 5 ml RPMI plus 20 % FCS and then installed into the sorting unit of the flow cytometer. The small subpopulation with high cell-bound fluorescence were gated (FL-4 > 400) and sorted using the single cell sorting mode. 30 – 40 ml of diluted sorted cells were centrifuged for 10 min at 300 g and resuspended in 500 µl RPMI plus 20 % FCS on a 24-well plate. The sorted cells were further expanded and maintained in RPMI plus 5 % FCS supplemented with 3 µg/ml puromycin.

5.2.2.9 Isolation of cell clones

Transduced and sorted P388 cells were seeded in selective medium at very low density on a 15 cm tissue culture dish. Although P388 cells are suspension cells, they grow slightly adherent and form loose cell aggregates after cell division. These

cell aggregates were picked with a sterile pipette, expanded and tested for specific binding of **10** as described in 3.2.2.3.

5.2.2.10 Flow cytometric binding assay

Transfected CHO cells were prepared for flow cytometric measurements as described in section 3.2.2.3. Transduced P388 cells were centrifuged at 300 g for 5 min at room temperature and resuspended at 10⁶ cells/ml in binding buffer (see 3.2.2.3).

485 µl of the cell suspension were incubated with 10 µl of fluorescent ligand and 5 µl of test compound. Unspecific binding was determined in presence of 1 µM hPP or GW1229. The cells were incubated for 90-120 min at room temperature under slight shaking to prevent cell aggregation and were subsequently analyzed without further processing. Instrument settings were the same as described in 3.2.2.3 for transfected CHO cells and FSC: E-1, SSC: 300 V, FL-4: 800 V for transduced P388 cells.

5.2.3 Results and discussion

5.2.3.1 Transfection of CHO-K1 cells

The CHO-K1 cells were transiently transfected with the pcDNA3-hY₄ and the pcDNA3-S99A-hY₄ vector. Two days after the transfection, the cells were tested for specific binding of 5 nM cy5-[K⁴]-hPP. As shown in Fig. 83, the bound fluorescence of the gated cells was not displaced by an excess (1 µM) of unlabelled hPP.

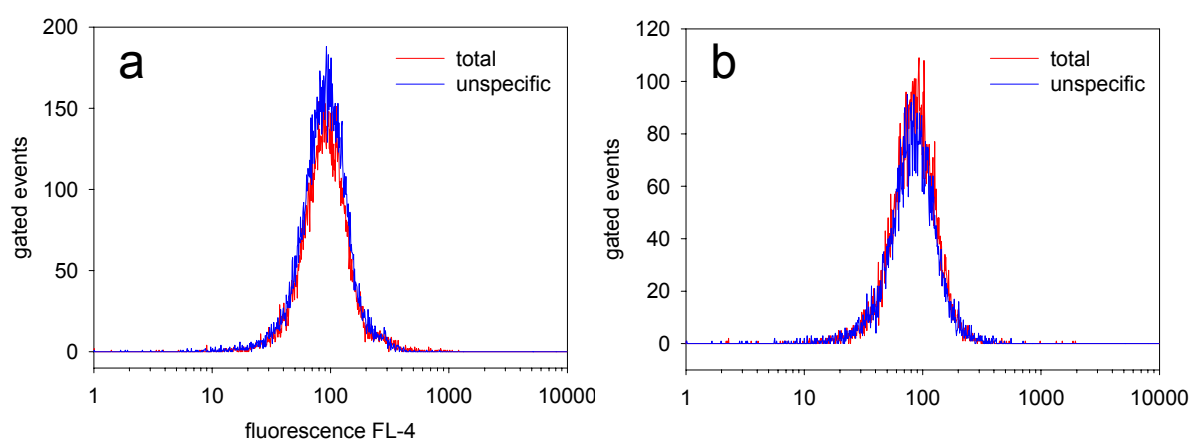


Fig. 83: Measurement of total (red) and unspecific (blue) binding of 5 nM cy5-[K⁴]-hPP. **a:** CHO-K1 cells transiently transfected with the pcDNA3-hY₄ vector. **b:** CHO-K1 cells transiently transfected with the pcDNA-S99A-hY₄ vector. Unspecific binding was determined in presence of 1 µM hPP.

Nevertheless, the transfected cells were selected by maintaining them in selective medium containing 400 $\mu\text{g/ml}$ G418 for 3 weeks and several single cell clones were isolated.

None of the cell clones stably transfected with the pcDNA-hY₄ vector showed distinct specific binding of **10** (data not shown). Some of the isolated cell clones stably transfected with the pcDNA3-S99A-hY₄ showed a considerable binding of **10** which could be displaced to some extent by hPP. But as shown exemplarily for clone CHO-pcDNA3-S99A-hY₄-K1A in Fig. 84, the fraction of unspecific binding was higher compared to the specific binding with each concentration tested.

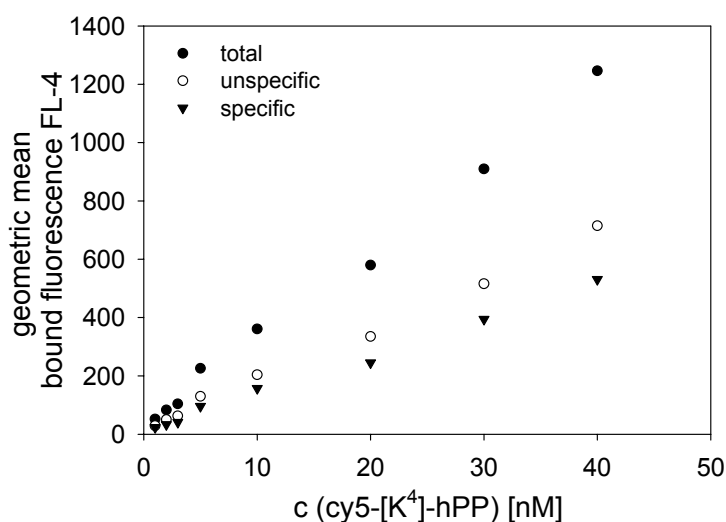


Fig. 84: CHO-pcDNA3-S99A-hY₄-K1A clone binding increasing concentrations of **10**. Unspecific binding was determined in the presence of 1 μM hPP.

This could be explained either by low affinity of **10** to the human Y₄ receptor or by low functional receptor expression of the selected cell clones. To allow for the latter explanation, the retroviral expression system was used.

5.2.3.2 Retroviral transduction of P388-D1 cells

P388-D1 cells were transduced with the pQCXIP-hY₄ and the pQCXIP-S99A-hY₄ vector. Binding of **10** to the transduced cells was measured by flow cytometry. Only the P388-D1 cells transduced with the pQCXIP-S99A-hY₄ vector consisted of a small cell population (1 % of the transduced cells) which bound the fluorescent ligand specifically.

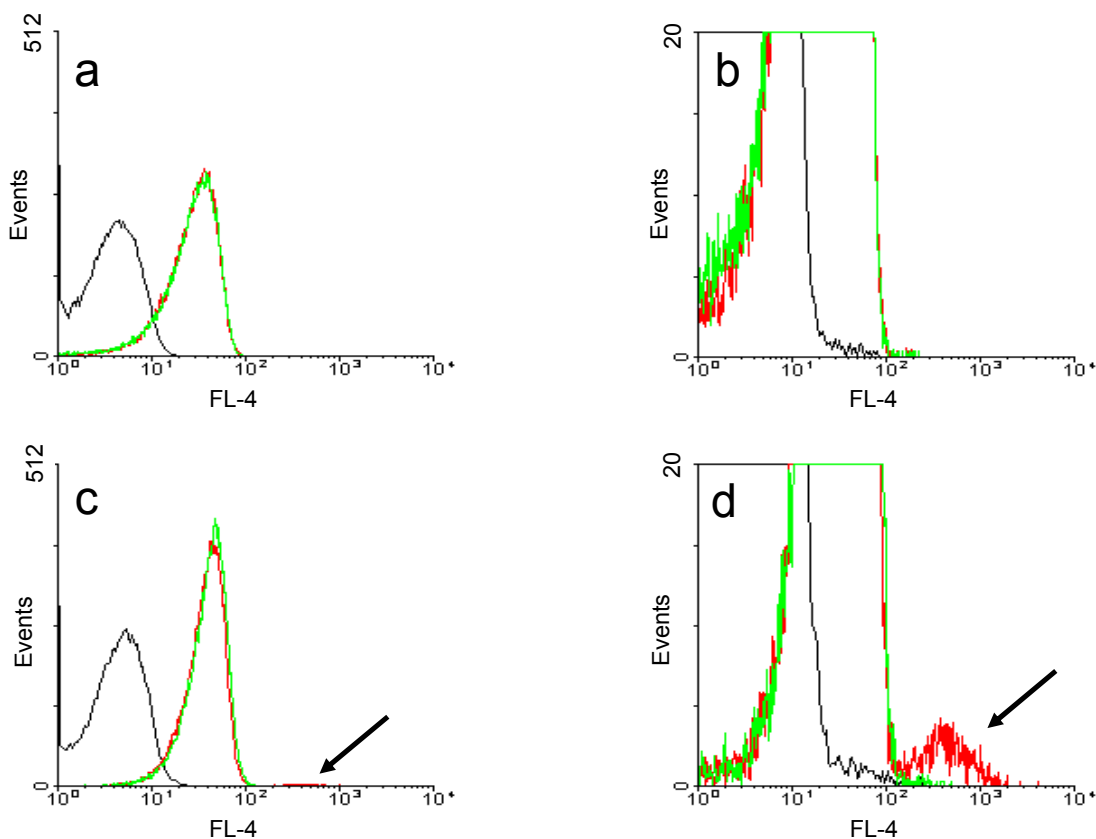


Fig. 85: Binding of 5 nM of **10** to P388-D1 cells transduced with the pQCXIP-S99A-hY₄ vector. About 99 % of the transduced cells (c,d) show no distinct specific binding of **10** as it is the case with wild-type cells (a,b). Low scaling range presentation reveals a small population of the transduced cells (indicated by arrow) binding **10** which was displaced by hPP (d). Autofluorescence (black), total (red) and unspecific (green) binding determined in presence of 1 μ M hPP.

Cells with specifically bound fluorescence were sorted using the sorting unit of the flow cytometer. As shown in Fig. 86, due to the cell sorting procedure the fraction of the cell population specifically binding the fluorescence labeled ligand could be increased up to > 70 % of the gated cells. But after some cell passages, the fraction decreased again because of faster growing puromycin-resistant cells with low receptor expression.

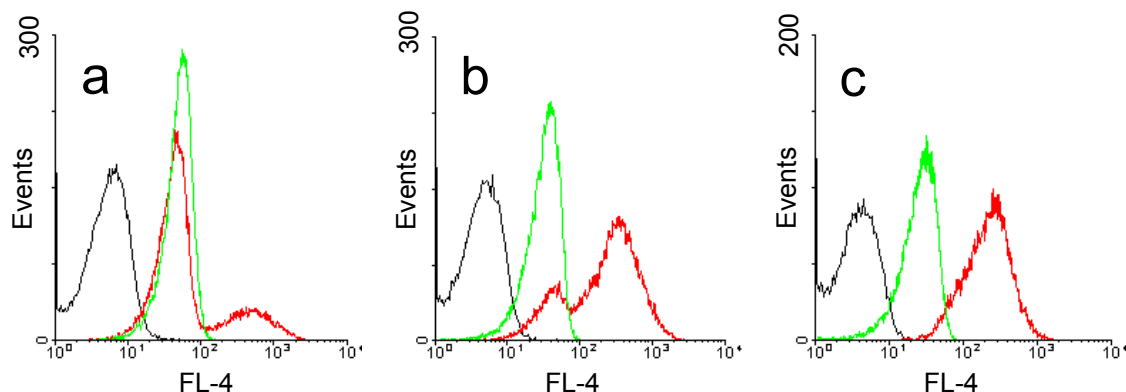


Fig. 86: Fluorescence activated cell sorting of P388-D1 cells transduced with the pQCIPX-S99A-hY₄ vector. The fraction of cells which specifically bound the fluorescent ligand **10** (5 nM) could be increased to 20 % after one sorting (panel a) and to > 70 % after two sorting procedures (panel b). A uniform cell population with highly specific binding of **10** was isolated after picking of cell aggregates (panel c). Autofluorescence (black), unspecific (green, determined in presence of 1 μM hPP) and specific (red) binding of **10**.

A cell clone (P388-S99A-hY₄-K23) stably expressing the S99A-hY₄ receptor was isolated after picking of cell aggregates (Fig. 86c). This cell clone was used for flow cytometric binding experiments. The dissociation constant $K_d = 36.6 \pm 3.8$ nM of **10** was determined in a saturation binding assay. This affinity is much lower compared to the K_i value determined with rat Y₄ expressing CHO cells (see 5.1.3.1).

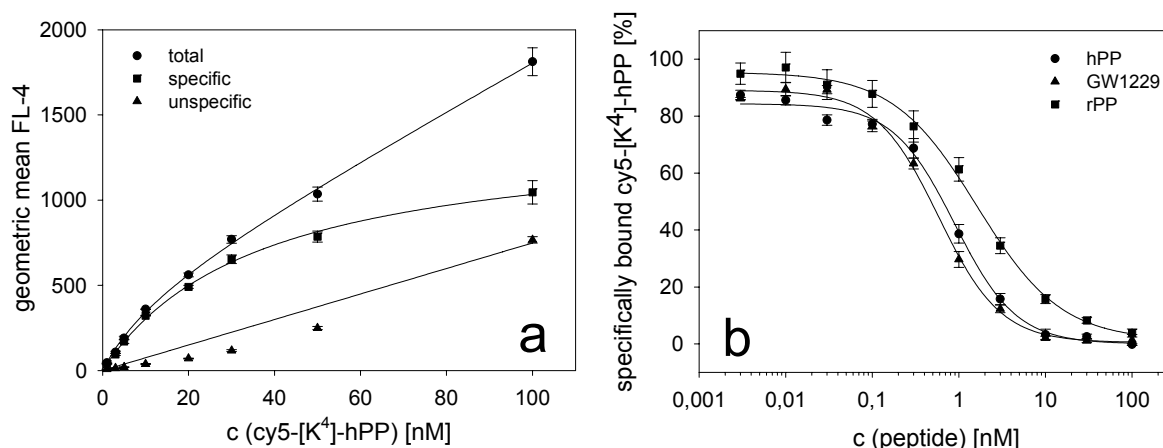


Fig. 87: Flow cytometric binding assay with P388-S99A-hY₄-K23 cells. **a:** Saturation analysis with cy5-[K⁴]-hPP ($K_d = 36.6 \pm 3.8$ nM). **b:** Competition binding of hPP ($IC_{50} = 893 \pm 74$ pM), GW1229 ($IC_{50} = 581 \pm 40$ pM) and rPP ($IC_{50} = 1.623 \pm 0.278$ nM) with 40 nM cy5-[K⁴]-hPP. Unspecific binding was determined in presence of 1 μM hPP (mean values \pm SEM, $n=3$).

40 nM of **10** were used for competition binding assays. hPP and GW1229 bound with high affinity (calculated K_i values are K_i (hPP) = 427 ± 42 pM and K_i (GW1229) = 277 ± 24 pM) to the S99A-hY₄ receptor. The K_i value for rPP was 776 ± 139 pM. The K_i

values published in the literature are determined in radioligand binding assays using the radioligands [¹²⁵I]-hPP (Parker *et al.*, 2002a; Voisin *et al.*, 2000), [¹²⁵I]-PYY (Bard *et al.*, 1995; Dautzenberg *et al.*, 2005; Lundell *et al.*, 1995) and [¹²⁵I]-GW1229 (Dumont and Quirion, 2000; Schober *et al.*, 2000). The published affinity data vary considerably; for hPP binding to the hY₄ receptor, K_i values range from 13.8 pM (Lundell *et al.*, 1995) to 0.7 nM (Voisin *et al.*, 2000). The pharmacological binding profile determined with the flow cytometric assay is in agreement with the literature (hPP ≥ GW1229 > rPP).

Unfortunately, the HEK293T cells used for the production of retroviruses were contaminated with mycoplasma and, consequently, the transduced P388-S99A-hY₄-K23 cells were also infected by the bacteria. As mycoplasma can interfere with cellular biological assays and influence the signal transduction (Drexler and Uphoff, 2002) decontamination was required. After treatment of the cells with Plasmocin™ (Invivogen, San Diego, USA) according to the manufacturer's instructions the affinity of the fluorescence labeled [K⁴]-hPP was determined in a saturation assay. The determined K_d values were 8.75 ± 1.52 nM for cy5-[K⁴]-hPP and 10.22 ± 0.84 nM for S0586-[K⁴]-hPP.

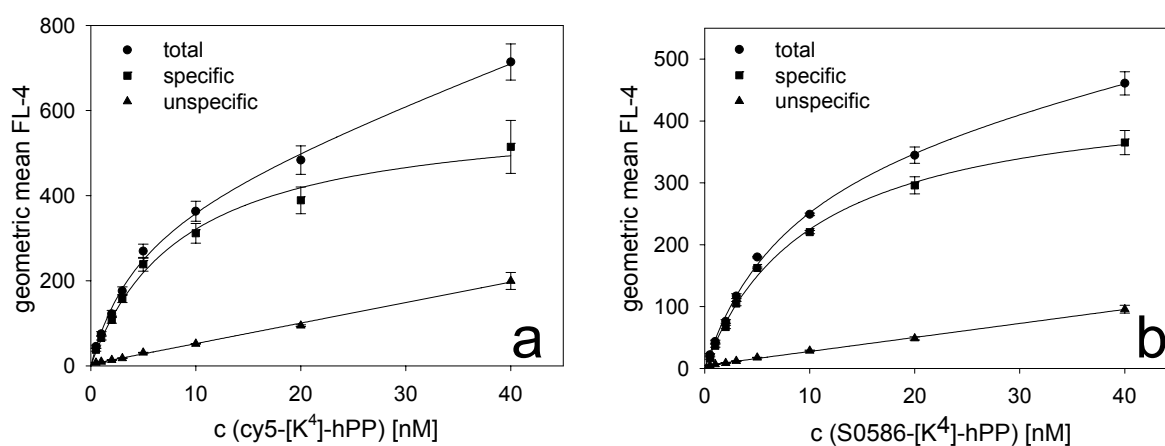


Fig. 88: Saturation analysis of Plasmocin™-treated P388-S99A-hY₄-K23 cells. **a:** Binding of cy5-[K⁴]-hPP. **b:** Binding of S0586-[K⁴]-hPP. Unspecific binding was determined in presence of 1 μM hPP (mean values ± SEM, n=3).

5.3 Development of functional assays for the hY₄ receptor

5.3.1 Introduction

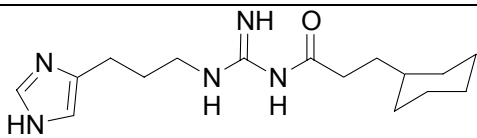
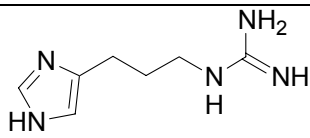
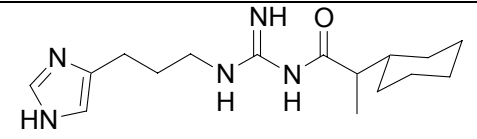
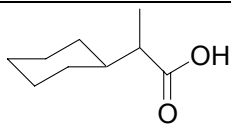
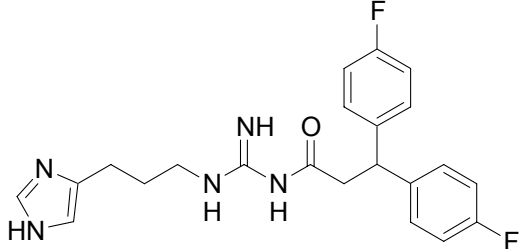
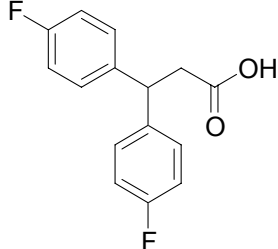
For the determination of functional data of NPY Y₄ receptor ligands, functional assays are required. As the Y₄ receptor is coupled to the G_i pathway, stimulation of the receptor leads to an inhibition of adenylyl cyclase resulting in a decreased formation of cAMP. Because the cAMP formation of unstimulated cells is usually very low, the potency of Y₄ receptor agonists is commonly determined by the measurement of inhibition of forskolin-stimulated cAMP formation. During the assay, the cAMP is quantitated using a radioimmunoassay kit. cAMP assays have been described for the hY₄ receptor expressed by HEK293, LMTK⁻ and CHO cells. Functional assays based on the inhibition of adenylyl cyclase are also described for the rat and the guinea pig Y₄ receptor. A different assay measures the short circuit current of human colonic adenocarcinoma cell lines pretreated with vasoactive intestinal polypeptide. A bioassay described for the Y₄ receptor determines the contractile responses of segments of the rat colon (Pheng *et al.*, 1999) in order to quantify the potency of Y₄ receptor agonists. Although the increase of intracellular free [Ca²⁺] was described for LMTK⁻ cells stably expressing the hY₄ receptor (Bard *et al.*, 1995), no complete concentration response curves or EC₅₀ values were determined. Recently, a calcium mobilization assay in the FLIPR format was described for the hY₄ receptor using HEK293 cells co-expressing the hY₄ receptor with the chimeric G proteins G_{q05}, G_{q15} or G_{q19} (Dautzenberg *et al.*, 2005). Comparing radioligand binding data with functional assays, Dautzenberg *et al.* found a high congruence only with binding and cAMP assays, but a rightward shift of the dose-response curves in GTP_γS binding and FLIPR assays. Another method measures the agonist-induced β-arrestin 2 interaction with the neuropeptide Y receptor (Berglund *et al.*, 2003c). A bioluminescence resonance energy transfer (BRET) occurs when the activated receptor tagged with Renilla luciferase comes to close vicinity to β-arrestin 2, fused to a GFP variant.

5.3.2 Materials and Methods

5.3.2.1 Y₄ receptor ligands

The peptides hPP, rPP, pNPY and BW1911U90 (Parker *et al.*, 1998) were synthesized by Dr. Chiara Cabrele, University of Regensburg, Germany. [³¹L,³⁴P]-pNPY, [⁴K]-hPP and [hPP¹⁹⁻²³,³⁴P]-pNPY were synthesized by Prof. Beck-Sickinger, University of Leipzig, Germany. The compounds PG 55B and PG 15 were synthesized by Dr. Prasanta Gohrai, the compounds AK 49, AK 59 and AK 1 were prepared by Anja Kraus and the compound MF 1 (Fig. 106) was synthesized by Matthias Freund (all from University of Regensburg, Germany).

Table 8: Compounds tested at the Y₄ receptor.

 <p style="text-align: center;">AK 49</p>	 <p style="text-align: center;">imidazolylpropylguanidine</p>
 <p style="text-align: center;">AK 59</p>	 <p style="text-align: center;">AK 1</p>
 <p style="text-align: center;">PG 55B</p>	 <p style="text-align: center;">PG15</p>

5.3.2.2 Introduction of a stop-codon and subcloning of the pcDNA3-hY₄ receptor

The hY₄-eYFP-QC_{kor} vector was obtained by Dr. Karin Mörl, University of Leipzig, Germany. The hY₄ sequence is identical with the sequence published by Bard *et al.*, 1995 except one silent mutation in position 66 (guanine instead of adenine). An optimized Kozak consensus sequence was introduced to increase protein translation. The eYFP gene is fused to the receptor DNA without linking amino acids; the

termination signal of the hY₄ and the ATG codon of the eYFP gene are deleted. Prior to subcloning of the hY₄ receptor DNA into the pcDNA3 vector, a new termination signal followed by a new *Xho*I restriction enzyme site at the 3' end were introduced via PCR. The following primers were used (termination signal in bold, *Xho*I site underlined):

Sense: 5'- GGC GTG TAC GGT GGG AGG TC -3'

Antisense: 5'- GGC CTC GAG TTA AAT GGG ATT GGA CCT GCC -3'

The PCR was performed in analogy to the PCR described in 5.2.2.3 using the following cycling parameters:

- 1) denaturation: 95 °C, 30 s
- 2) annealing: 60 °C, 1 min
- 3) extension: 72 °C, 2.5 min
- 4) final extension: 72 °C, 5 min
- 5) hold: 4 °C

Steps 1) – 3) were repeated 20 times. The PCR products (Fig. 89A) were purified with the PCR purification kit (Qiagen) and digested with *Bam*HI and *Xho*I using buffer B (Roche Diagnostics). The pcDNA3-hY₅ was also digested with *Bam*HI and *Xho*I. The hY₄ construct and the linearized vector pcDNA3 were isolated by agarose gel electrophoresis and purified using the QIAEX II purification kit.

Ligation reactions were performed using 2 µl of linearized pcDNA3 vector and increasing amounts (0.5 – 6 µl) of isolated hY₄ construct in a 20 µl ligation reaction. Plasmid DNA of ampicillin resistant transformants was isolated by MiniPrep and digested with *Bam*HI and *Xho*I using buffer B (Roche Diagnostics). Agarose gel electrophoresis revealed the two expected bands at 5382 bp and 1144 bp (Fig. 89B). The linearized vector was detected after *Bam*HI digestion at 6526 bp.

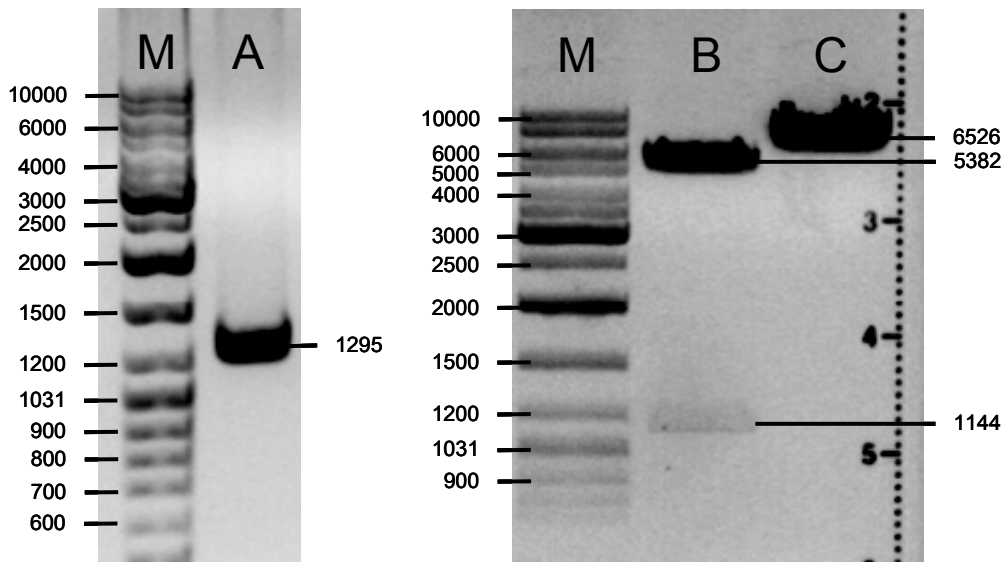


Fig. 89: Subcloning of the pcDNA3-hY₄ vector. **A:** PCR product after introduction of a stop codon and a XhoI restriction site at the 3' end of hY₄. **B:** Restriction analysis of pcDNA3-hY₄ (BamHI and XhoI digestion). **C:** BamHI linearized pcDNA3-hY₄ vector.

5.3.2.3 Transfection of CHO-K1 cells with the pcDNA3-hY₄ vector

CHO-K1 cells were seeded in 500 µl Ham's F12 plus 10 % FCS on a 24-well plate. On the day of transfection, the optical confluence reached 60 – 70 %. The transfection was carried out using the FuGENE™ (Roche Diagnostics) transfection reagent according to the manufacturer's instructions. 300 ng of vector DNA and 1.8 µl of transfection reagent were applied per well. Resistant cells were selected two days after the transfection by maintaining the cells in selective medium containing 400 µg/ml G418. Single cell clones were picked with a sterile pipette as described in section 3.1.2.12 and tested in a flow cytometric binding assay.

5.3.2.4 Screening of transfected cell clones for binding of cy5-[K⁴]-hPP

Cell clones were expanded in selective medium and prepared for the flow cytometric binding assay as described in section 3.2.2.3.

5.3.2.5 Transfection of CHO-hY₄-K13b cells with pcDNA3.1/hygro-qi5

The pcDNA3.1/hygro-qi5 vector was linearized with *Eam*11051 prior to the transfection procedure (see 4.1.2.3). The transfection was carried out as described in 5.3.2.3 using 300 ng of linearized vector and 1.8 µl FuGENE™ per well. The selective medium contained 400 µg/ml G418 and 400 µg/ml hygromycin. Single resistant cell clones were isolated (see section 3.1.2.12) and tested in a flow cytometric calcium assay.

5.3.2.6 Screening of transfected cell clones for calcium response upon stimulation with hPP

Cell clones were expanded in selective medium and prepared for the flow cytometric calcium assay as described in section 4.1.2.4. The signal was elicited with 20 nM hPP.

5.3.2.7 Transfection of CHO-hY₄-K13b-qi5-K8 cells with pcDNA3.1/zeo-mtAEQ

The pcDNA3.1/zeo-mtAEQ vector was linearized with *Eam*11051 prior to the transfection. The transfection was carried out as described in 5.3.2.3. Resistant cells were selected with Ham's F12 plus 10 % FCS containing 400 µg/ml G418, 400 µg/ml hygromycin and 250 µg/ml zeocin.

5.3.2.8 Screening of transfected CHO-hY₄-K13b-qi5-K8 cell clones for aequorin luminescence signal upon stimulation with hPP

After two weeks of selection in selective medium, 96 cell clones were picked with a sterile pipette and grown to 50 – 80 % confluence on a white, flat bottomed 96-well plate with transparent bottom. For the reconstitution of active aequorin, the medium was removed and 25 µl 2 µM coelenterazine h in DMEM (without phenol red) supplemented with 1 % FCS was added per well. The cells were incubated for 2 h at room temperature. The 96-well plate was loaded into the Tecan Genios Pro plate reader and 175 µl of loading buffer (see 4.1.2.4) containing hPP with a final concentration of 50 nM were injected per well. Luminescence was recorded in 200 ms integrations for 40 s. After the luminescence assay 20 µl DAPI (0.2 mg/ml) was added to each well and the cells were incubated for 15 min at room temperature. The whole medium was removed and the cells were washed with 200 µl PBS before adding 200 µl fresh PBS. The 96-well plate was loaded again into the plate reader and fluorescence was measured using the following instrument settings: $\lambda_{\text{ex}} = 340$ nm, $\lambda_{\text{em}} = 485$ nm, gain: 70, number of flashes: 3, integration time: 40 µs, mirror selection: bottom, multiple reads per well: 2x2, time between move and flash: 100 ms. Luminescence signal was plotted against time for each clone and the area under the curve was calculated using the SigmaPlot™ software. Total luminescence was divided by the fluorescence signal of the DAPI staining.

5.3.2.9 Aequorin assay

5.3.2.9.1 Agonist assay

Transfected CHO cells were prepared for the aequorin assay as described in 4.2.2.2.3. Unless otherwise stated, the cells were postincubated for 3 h at 5×10^5 cells/ml in loading buffer. 10-fold concentrated peptide dilutions were prepared in loading buffer and 20 μ l were provided per well. A blank sample containing solvent and a 100 %-sample containing 0.1 % triton-X-100 (final assay concentration) were included per row. 180 μ l of the stirred cell suspension were injected to each well and luminescence was recorded over 40 s as a series of 200 ms integrations. Total luminescence was calculated with SigmaPlot™ software (see 4.2.2.2.3). The blank value was subtracted from each value and the percentage of maximal luminescence was calculated using the triton-X-100 (100% value) sample.

5.3.2.9.2 Antagonist assay

For the determination of antagonist activity, the cells were postincubated for 2 h. 2 μ l of 100-fold concentrated dilutions of the compounds were added to 175 μ l of cell suspension per well and incubated for 1 h. A 100 % sample containing 2 μ l of solvent was included per row. 23 μ l of a 1.739 μ M rPP solution were injected per well and luminescence was recorded as described before. The percentage of the maximal luminescence signal was calculated using the 100 % sample.

Screening of compounds was performed at 10 μ M (final assay concentration).

5.3.2.9.3 Measurement with 2 injectors

CHO cells were prepared as described in 5.3.2.9.1. After 3 h postincubation, 162 μ l of cell suspension were injected to 18 μ l of peptide solution and luminescence was recorded for 43 s (peak 1) before injection of 20 μ l of 1 % triton-X-100 solution. Luminescence was recorded for further 22 s (peak 2) and the area under the two peaks was calculated with SigmaPlot™ software. Fractional luminescence was calculated by dividing the area of the agonist peak by the sum of the areas of peaks 1 and 2.

5.3.2.10 Flow cytometric binding assay

The flow cytometric binding assay was performed as described in section 3.2.2.3. Instrument settings were FSC: E-1, SSC: 280 V, FL-4: 800 V (700 V for CHO-hY₄-K13b-qi5-K8-mtAEQ-E11-K11 cells), flow rate: high.

5.3.2.11 Spectrofluorimetric calcium assay

The spectrofluorimetric fura-2 calcium assay was performed as described in section 4.1.2.5. The maximum signal (100 %) was elicited with 1 μ M rPP.

5.3.2.12 Luminescence detection with CCD camera

The luminescence measurements were performed by analogy with the procedure described in section 4.3.2.2 using the CHO-hY₄-K13b-qi5-K8-mtAEQ-E11 cells and dilutions of hPP to elicit the signal.

5.3.2.13 Confocal microscopy

CHO-hY₄-K13b-qi5-K8-mtAEQ-E11-K11 cells were seeded in 200 μ l Ham's F12 plus 10 % FCS on a Lab-Tek[®] II, 8 chamber coverglass system (Nalge Nunc) two days before the experiment and were grown to 50 – 70 % confluence. 500 nM Syto13 (Invitrogen) were added and the cells were incubated for 45 min. According to the manufacturer's specifications, the dye shows cytoplasmic or mitochondrial staining as well as nuclear staining in eukaryotic cells. After the incubation with the dye, the cells were washed with Ham's F12 and 200 μ l of binding buffer (see 3.2.2.3) containing 10 nM cy5-[K⁴]-hPP alone (total binding) or in combination with 1 μ M GW1229 (unspecific binding) were added. Confocal scanning microscopy was performed after 20 min using the same instrumentation described in section 3.2.2.4. The laser power was set to 51 % for the red diode laser (λ = 633 nm) and 3 % for the argon laser (λ = 488 nm). Scanning mode was multi track.

For the measurement of the increase of intracellular calcium concentration, the cells were loaded with fluo-4-AM and installed into the laser scanning microscope using the same instrumentation as described in section 4.3.2.1. The power of the argon laser (λ = 488 nm) was set to 5 % and the 505 nm longpass filter was used. A scanning region was defined for two neighboring cells and a time series was adjusted with a scan speed which allows the scanning of one frame in 1.6 s. The measurement was started and 30 μ l of hPP solution (1 μ M in loading buffer) were added to the cell chamber containing 300 μ l of Leibowitz L15 medium.

5.3.3 Results and discussion

5.3.3.1 Establishment of a stable cell clone co-expressing the hY₄ receptor, the chimeric G protein qi5 and mitochondrial targeted apoaequorin

CHO-K1 cells were transfected with the pcDNA3-hY₄ vector. Isolated cell clones resistant to 400 µg/ml G418 were tested for binding of cy5-[K⁴]-hPP. The cell clone CHO-hY₄-K13b was found to bind the fluorescent ligand in a concentration dependent manner (Fig. 90).

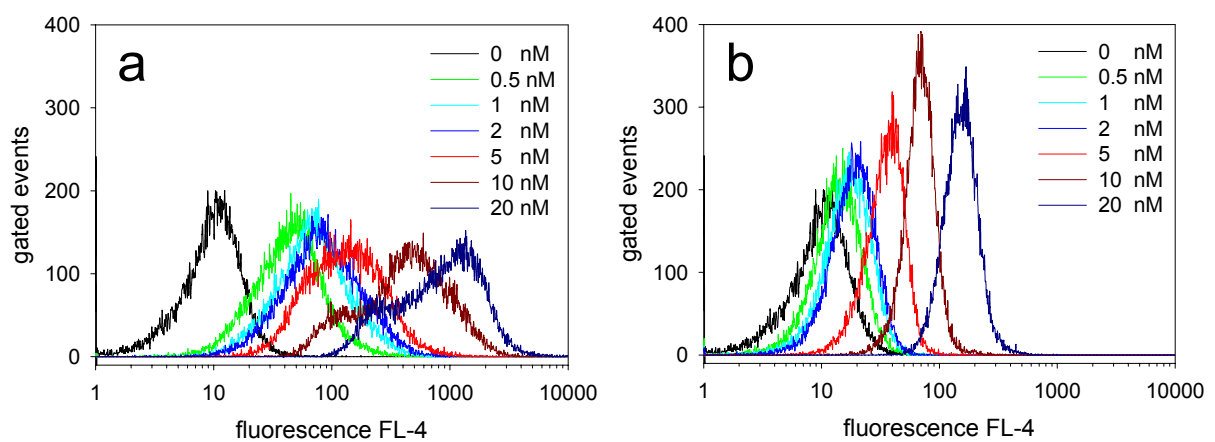


Fig. 90: Binding of **10** to CHO-hY₄-K13b cells. **a:** Total binding. **b:** Unspecific binding in presence of 1 µM hPP.

The bound ligand was displaced by 1 µM hPP as shown in Fig. 90b. However, the cells did not equally express the receptor, which became obvious after incubation with 10 and 20 nM of **10** (Fig. 90a). The CHO-hY₄-K13b cells consisted of at least two subpopulations binding the fluorescent ligand to different extents.

Nevertheless, the cells were further transfected with the pcDNA3.1/hygro-qi5 vector. Selected cell clones were tested for an increase in intracellular calcium upon stimulation with hPP. Injection of 20 nM of hPP led to a weak but distinct increase in fluorescence of fluo-4 loaded CHO-hY₄-K13b-qi5-K8 cells (Fig. 91).

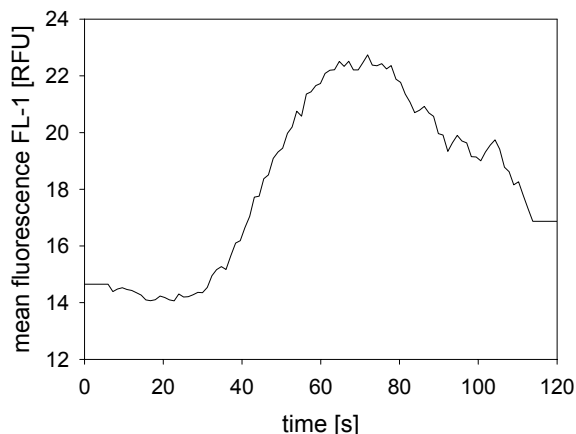


Fig. 91: Calcium response of CHO-hY₄-K13b-qi5-K8 cells after stimulation with 20 nM hPP. Raw data were smoothed with WinMDI and SigmaPlot software.

The cells were further transfected with the pcDNA3.1/zeo-mtAEQ vector. After selection with G418, hygromycin and zeocin, cell clones were isolated and screened for a luminescence signal following receptor activation with 50 nM hPP. The total luminescence light emitted was divided by the intensity of DAPI fluorescence representing the different cell numbers. The result is shown in Fig. 92.

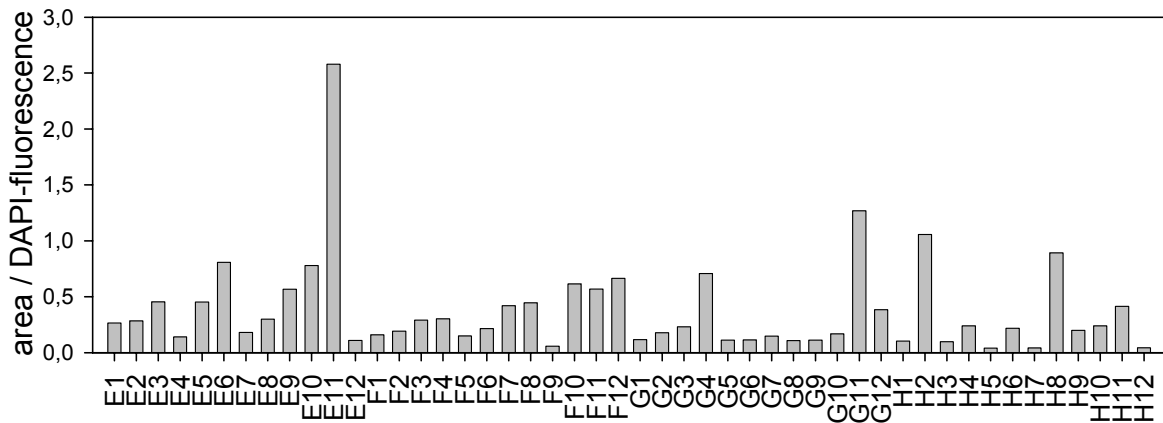


Fig. 92: Screening of CHO-hY₄-K13b-qi5-K8-mtAEQ cell clones.

The cell clone E11 showed the strongest luminescence signal in relation to the cell number. CHO-hY₄-K13b-qi5-K8-mtAEQ-E11 cells were further analyzed for their response to peptide agonists in the aequorin assay. As shown in Fig. 93, the courses of the luminescence signals were different from the luminescence signals measured with the CHO-hY₂-K9-qi5-K9-mtAEQ-A7 cells (see Fig. 56a). Injection of the cells to the full agonist hPP led to an initial increase of luminescence which was followed by a delayed rise of luminescence (Fig. 93a, red).

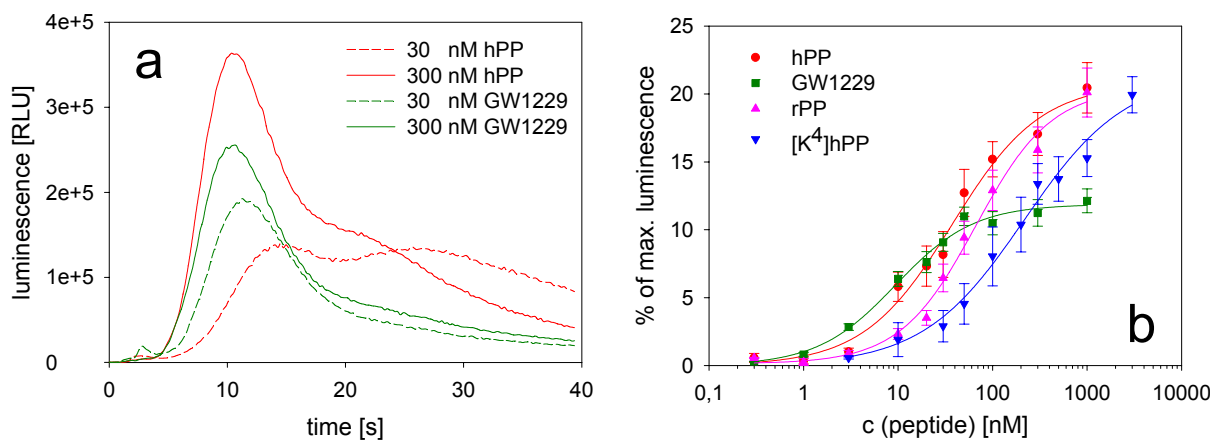


Fig. 93: Aequorin assay with CHO-hY₄-K13b-qi5-K8-mtAEQ-E11 cells. **a:** Luminescence signal of hPP (red) and GW1229 (green). **b:** Dose-response curves of peptide agonists (mean values \pm SEM, $n=3$).

This effect was less pronounced with the partial agonist GW1229 (Fig. 93a, green). Nevertheless, concentration-response curves for various peptide agonists were constructed with the expected pharmacological rank order concerning the full agonists hPP, rPP and [K⁴]-hPP. The partial agonist GW1229 reached 57 % of the maximal signal elicited by full agonists. The EC₅₀ was with 9.4 nM about 4-fold lower compared to hPP (37.3 nM).

Because the course of the aequorin assay indicated the existence of at least two cell populations with different kinetic responses upon agonist stimulation, the hY₄ receptors were labeled by binding to **10** and the receptor distribution was analyzed by flow cytometry.

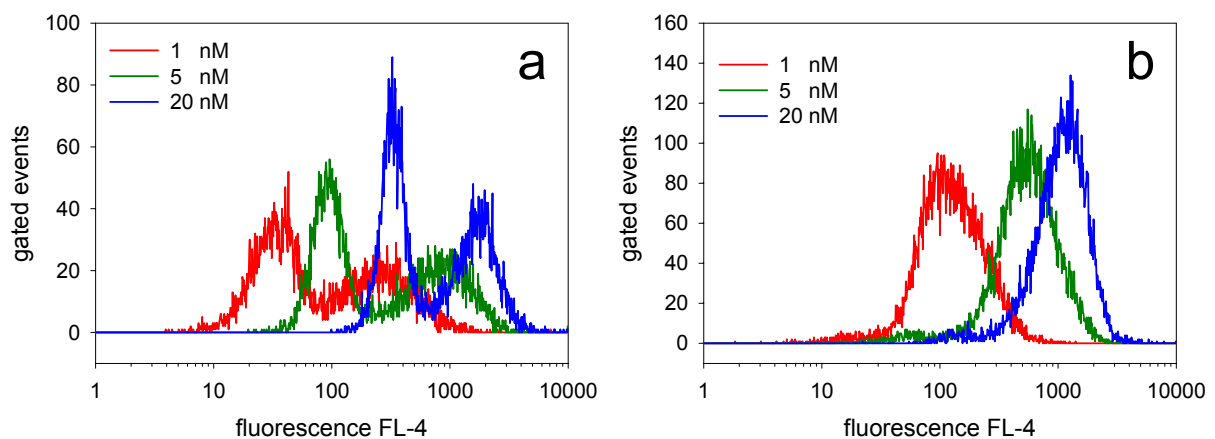


Fig. 94: Binding of cy5-[K⁴]-hPP to CHO-hY₄-K13b-qi5-K8-mtAEQ-E11 (panel a) and CHO-hY₄-K13b-qi5-K8-mtAEQ-E11-K11 (panel b) cells.

In fact, as shown in Fig. 94a, the CHO-hY₄-K13b-qi5-K8-mtAEQ-E11 cells bound the fluorescent ligand inhomogeneously indicated by the two maxima in the histogram presentation (Fig. 94a). Both maxima were shifted to the right with increasing concentrations of **10**, indicating the existence of two cell populations with different receptor expression. Therefore, new subclones were isolated and tested for their binding of **10**. The cell clone CHO-hY₄-K13b-qi5-K8-mtAEQ-E11-K11 exhibited high and homogeneous binding of the fluorescent ligand (Fig. 94b). The labeled ligands cy5-[K⁴]-hPP and S0586-[K⁴]-hPP could be displaced by 1 μM hPP and K_d values were determined after saturation analysis.

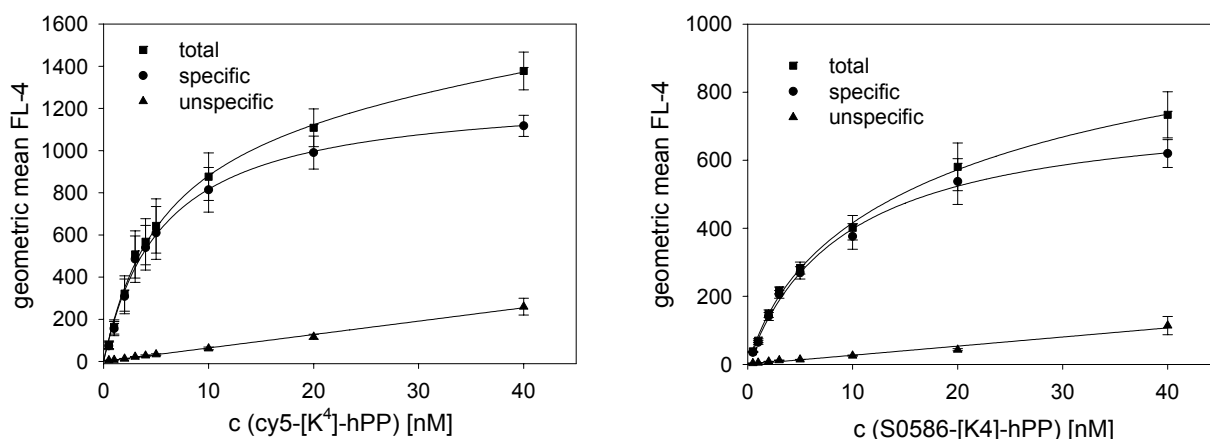


Fig. 95: Saturation assay with CHO- hY_4 -K13b-qi5-K8-mtAEQ-E11-K11 cells and cy5-[K⁴]-hPP (left panel; mean values \pm SEM, $n=3$) and S0586-[K⁴]-hPP (right panel; mean values \pm SEM, $n=2$).

The determined K_d values of 5.62 ± 1.08 nM for **10** and 9.24 ± 1.34 nM for **11** are in good agreement with the K_d values determined with the transduced P388 cells (see section 5.2.3.2). The ligand **10** (10 nM) was used in flow cytometric competition assays and K_i values of peptide ligands were determined. According to the literature, hPP ($K_i = 239 \pm 36$ pM) and GW1229 ($K_i = 217 \pm 44$ pM) showed the highest affinity to the hY_4 receptor. Rat PP bound with slightly lower affinity but still in the picomolar range ($K_i = 443 \pm 85$ pM). The peptides [L³¹,P³⁴]-pNPY ($K_i = 7.08 \pm 1.49$ nM), BW1911U90 ($K_i = 10.77 \pm 1.84$ nM) and [hPP¹⁹⁻²³,P³⁴]-pNPY ($K_i = 20.07 \pm 3.03$ nM) bound in the nanomolar range and pNPY showed only low affinity with a K_i value of 365 ± 79 nM.

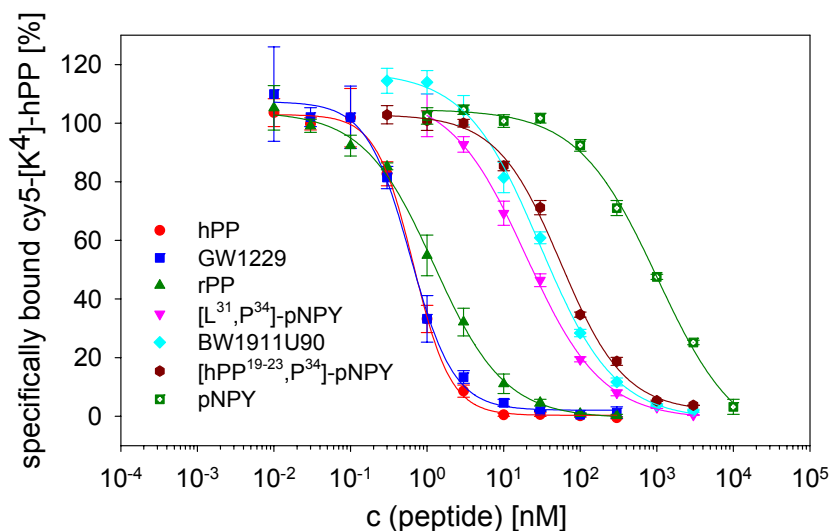


Fig. 96: Flow cytometric binding assay with CHO- hY_4 -K13b-qi5-K8-mtAEQ-E11-K11 cells. Displacement of 10 nM cy5-[K⁴]-hPP by various peptide ligands (mean values \pm SEM, $n=3-4$).

The same isolated cell clone CHO-hY₄-K13b-qi5-K8-mtAEQ-E11-K11 was used in an aequorin assay. In order to prevent adsorption of the peptides to the well-plate material, 1 % BSA and 0.1 mg/ml bacitracin were added to the peptide solutions.

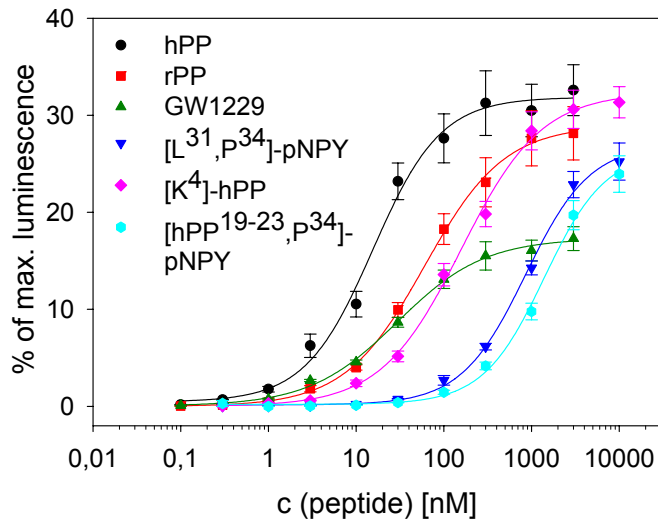


Fig. 97: Aequorin assay with CHO-hY₄-K13b-qi5-K8-mtAEQ-E11-K11 cells. EC₅₀ values are 15.5 ± 3.1 nM (hPP), 60.4 ± 12.7 nM (rPP), 29.4 ± 5.3 nM (GW1229), 857.1 ± 104.5 nM ([L³¹,P³⁴]-pNPY), 157.6 ± 22.2 nM ([K⁴]-hPP) and 1395.7 ± 204.5 nM ([hPP¹⁹⁻²³,P³⁴]-pNPY) (mean values ± SEM, n=3).

5.3.3.2 Aequorin assay with two injectors

After the upgrading of the Tecan Genios Pro™ plate reader with a second injector an additional injection of a triton-X-100 solution was included into the assay design by analogy with the assay described for the hY₂ receptor (see 4.2.3.5). The course of the measurement is shown in Fig. 98. The aequorin signal was elicited with increasing concentrations of agonist (hPP) at time point 'a'. The peak followed by the injection of triton-X-100 (time point 'b') decreased with increasing concentrations of hPP as more active aequorin was discharged by the previous aequorin signal.

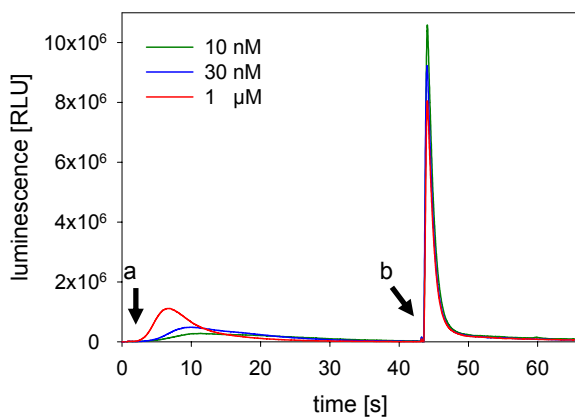


Fig. 98: Aequorin assay with CHO-hY₄-K13b-qi5-K8-mtAEQ-E11-K11 cells using 2 injectors. The cell suspension is injected to the agonist (hPP) solution at time point 'a' and the aequorin signal is recorded for 43 s. Injection of 0.1 % triton-X-100 at time point 'b' leads to cell lysis and causes consumption of residual active aequorin.

The influence of the postincubation step was analyzed in the next experiment. The cells were loaded with coelenterazine h for 2 h and postincubated for various times before injection to the full agonist hPP or to the partial agonist GW1229.

As shown in Fig. 100, the signals varied broadly when the postincubation step was

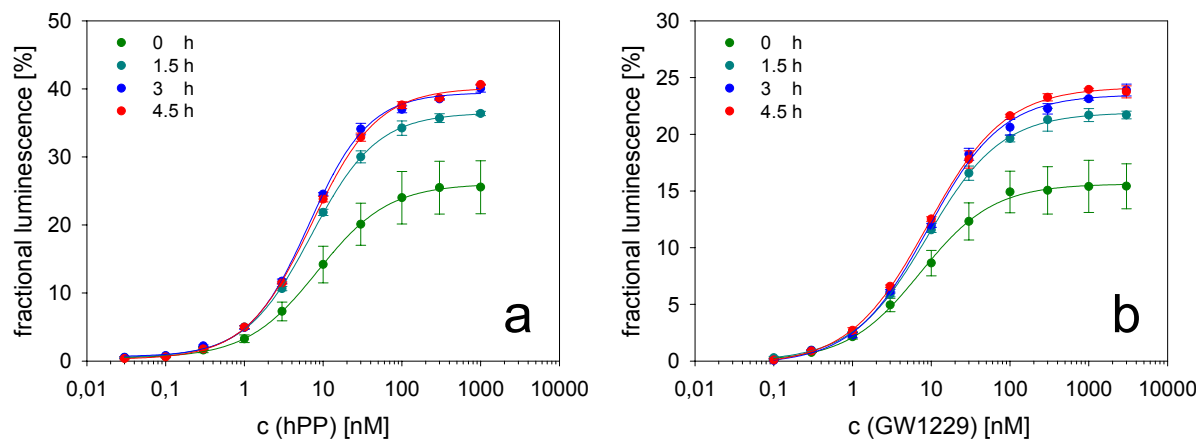


Fig. 100: Dose-response curves of hPP (a) and GW1229 (b) after various postincubation times. CHO-hY₄-K13b-qi5-K8-mtAEQ-E11-K11 cells were incubated with 2 μ M coelenterazine h for 2 h at room temperature, diluted to 5×10^5 cells/ml in loading buffer and postincubated for various periods before injection to the ligands (mean values \pm SEM, n=3).

omitted. The fractional luminescence elicited by the agonists increased during the measurement tempering the concentration-response curves. Although the EC₅₀ values were constant during the whole experiment (EC₅₀ (hPP) = 6.6 – 8.5 nM and EC₅₀ (GW1229) = 7.3 – 9.0 nM), the maxima of the concentration-response curves increased within the first 3 h after the loading procedure for hPP and GW1229. In agreement with the aequorin assay using CHO-hY₂-K9-qi5-K9-mtAEQ-A7 cells (see section 4.2.3.5), reproducible concentration-response curves were obtained after 3 h of postincubation allowing a discrimination between full and partial agonists.

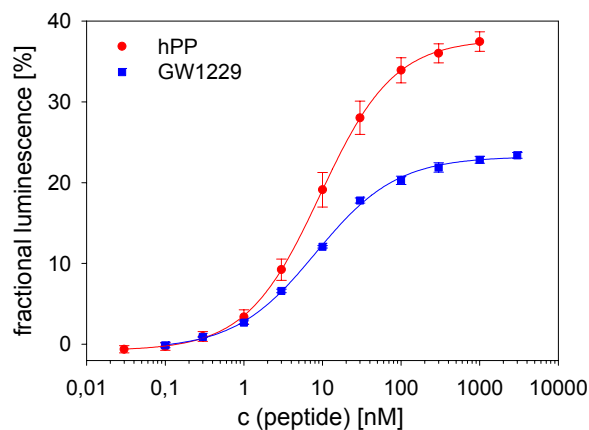


Fig. 99: Concentration-response curves of hPP and GW1229. Cells were postincubated for 3-6 h (mean values \pm SEM, n=9-13 in 3 independent experiments).

The determined EC₅₀ values (EC₅₀ (hPP) = 9.33 ± 1.29 nM and EC₅₀ (GW1229) = 8.19 ± 0.56 nM) were slightly lower compared to the ones obtained from the aequorin

assay performed with one injector and the triton-X-100 sample as external standard. The maximal signal elicited with GW1229 is 62 % of the maximal signal induced by the full agonist hPP.

5.3.3.3 Spectrofluorimetric fura-2 calcium assay

The CHO-hY₄-K13b-qj5-K8-mtAEQ-E11-K11 cells were also used in a fura-2 calcium assay (Fig. 101). The determined EC₅₀ value of hPP (3.67 ± 1.76 nM) was in the same range compared to the EC₅₀ value determined in the aequorin assay (Fig. 99). Rat PP (EC₅₀ = 14.75 ± 2.77 nM) was four times less active compared to hPP. This was also observed in the aequorin assay performed with one injector (Fig. 97).

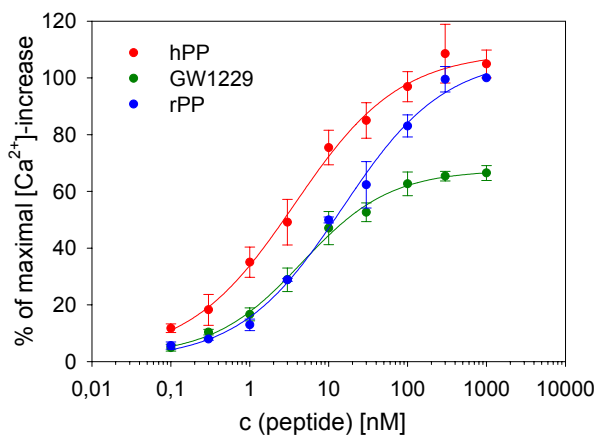


Fig. 101: Spectrofluorimetric fura-2 calcium assay with CHO-hY₄-K13b-qj5-K8-mtAEQ-E11-K11 cells. The maximum signal was determined with 1 μM rPP (mean values ± SEM, n= 3-4).

The maximum effect elicited by GW1229 was 68 % of the maximum effect released by the full agonists hPP and rPP which was also observed in the aequorin assay (62 %). The EC₅₀ value (4.55 ± 1.30 nM) was in the same range compared to one determined in the aequorin assay (8.19 ± 0.56 nM). The value is also in good agreement with the literature reporting EC₅₀ values of 7.16 nM (Schober *et al.*, 1998) and 2.51 nM (Parker *et al.*, 1998). In contrast, these reports refer to GW1229 as a full agonist determined in cAMP assays using CHO cells expressing the hY₄ receptor. On the other hand, a partial agonism of GW1229 was proposed based on the measurement of the reduction of VIP-induced short circuit current in Col-24 cells (Cox *et al.*, 2001) and for the rhY₄ receptor by measurement of the receptor-β-arrestin interactions (Berglund *et al.*, 2003c). In the latter study, the peptide could also provoke only 70 % of the response elicited with hPP. However, the same group reported on full agonism of GW1229 in HEK293 cells expressing GFP- and RLUC-tagged rhY₄ receptors (Berglund *et al.*, 2003b). Further functional assays in the

absence of the chimeric G-protein should be done to elucidate whether the observed partial agonism of GW1229 is an artefact due to the co-transfection of receptor and chimeric G-protein.

The fluorescent ligands cy5-[K⁴]-hPP and S0586-[K⁴]-hPP were also tested in the fura-2 assay (only at 3 concentrations in order to save labeled peptides) and the EC₅₀ values were calculated using the logit transformation (see 4.2.2.2.4). The labeled ligands were less active with pEC₅₀ (**10**) = 6.87 ± 0.73 and pEC₅₀ (**11**) = 7.12 ± 0.51. The decrease in potency after labeling with cy5 has also been observed for NPY at the Y₁ receptor expressed in HEL cells (Schneider, 2005).

5.3.3.4 Low throughput screening

Because there are no nonpeptidic antagonists for the hY₄ receptor known so far, a small library of known available drugs (~80) was screened for inhibition of the aequorin signal elicited with 200 nM rPP. Compounds which inhibited the luminescence signal by more than 50 % at a concentration of 10 μM were further analyzed and additionally tested in a flow cytometric binding assay with P388-S99A-hY₄-K23 cells. The antipsychotic drug chlorprothixene, the antidiabetic agent glibenclamide and the H₁-antihistamine terfenadine were able to inhibit the luminescence signal at concentrations in the micromolar range (see Fig. 102a). But in the flow cytometric binding assay, the compounds were not able to displace **10** up to a concentration of 100 μM (Fig. 102b) indicating that they do not bind to the same binding site as the labeled ligand. Therefore, it is more likely that these compounds act via other receptor signaling mechanisms present in the cells. Glibenclamide is known to block K⁺-channels and therefore induces the opening of voltage-gated Ca²⁺-channels in the B-cells of the pancreas. An increase in intracellular calcium in the transfected CHO cells would discharge a fraction of active aequorin and therefore reduce the luminescence signal elicited by the agonist rPP simulating an antagonism in the functional assay.

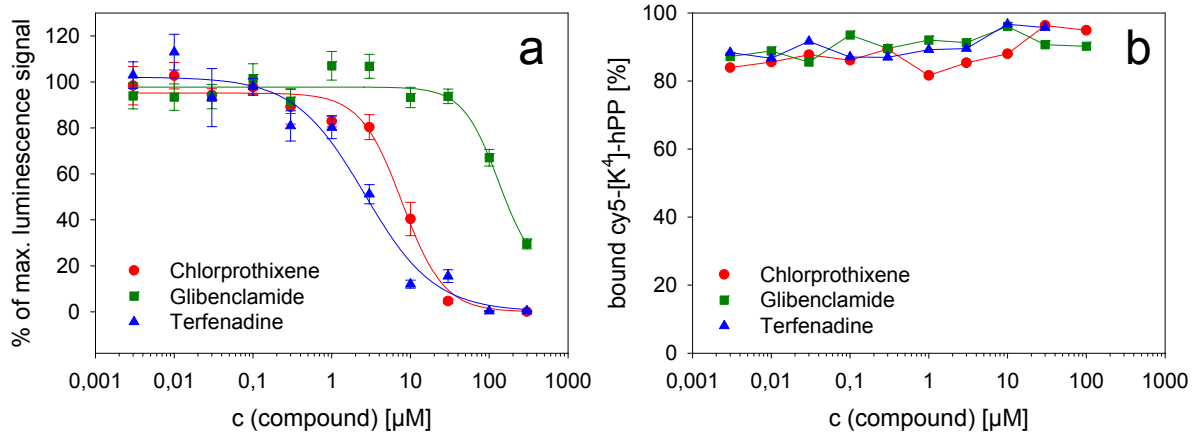


Fig. 102: Selected compounds tested in the aequorin assay inhibiting the luminescence signal elicited with 200 nM rPP using CHO-hY₄-K13b-q15-K8-mtAEQ-E11 cells (panel a; mean values \pm SEM, n=3) and in the flow cytometric binding assay competing with 20 nM cy5-[K⁺]-hPP using P388-S99A-hY₄ cells (panel b; mean values \pm SEM, n=1).

Guanidine-type histamine H₂ receptor agonists were the first nonpeptidic NPY Y₁ receptor antagonists described in the literature (Michel and Motulsky, 1990). Stimulated by the early discoveries in the Y₁ antagonist field, several recently synthesized novel H₂ agonists were tested for activity at Y₄ receptors in the aequorin assay. Preincubation with the compounds PG 55B, AK 49 and AK 59 reduced the luminescence signal elicited by 200 nM rPP (Fig. 103a). The IC₅₀ values were 10.5 \pm 1.1 μ M (PG 55B), 60.7 \pm 7.3 μ M (AK 49) and 83.9 \pm 4.2 μ M (AK 59). But in contrast to the compounds chlorprothixene, glibenclamide and terfenadine, the H₂ agonists were also able to displace the fluorescent ligand **10** from its binding sites at P388-S99A-hY₄-K23 cells (Fig. 103b) even though with high K_i values of 28.0 \pm 5.6 μ M (PG

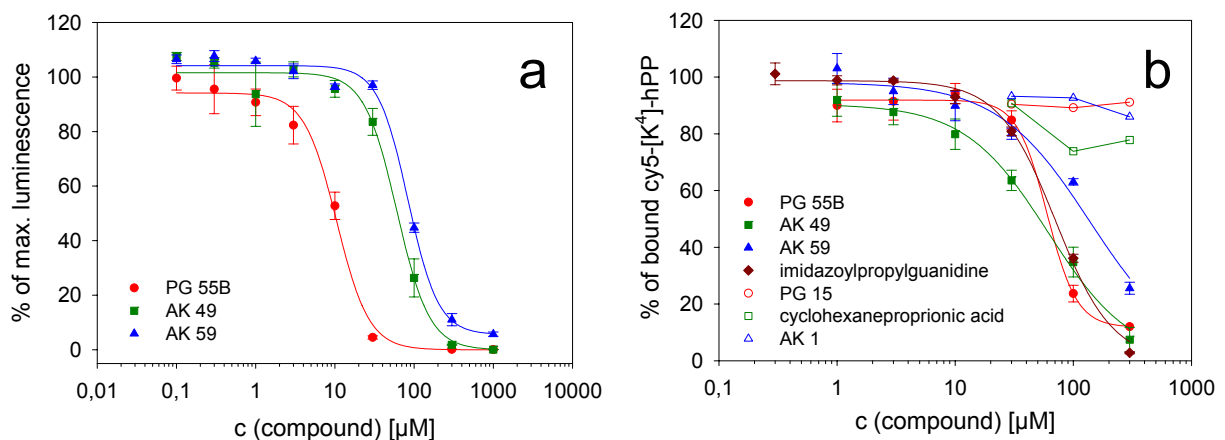


Fig. 103: Selected compounds tested in the aequorin assay inhibiting the luminescence signal elicited with 200 nM rPP using CHO-hY₄-K13b-q15-K8-mtAEQ-E11 cells (panel a; mean values \pm SEM, n=3) and in the flow cytometric binding assay competing with 10 nM cy5-[K⁺]-hPP using P388-S99A-hY₄ cells (panel b; mean values \pm SEM, n=1-3).

55B), $28.5 \pm 10.2 \mu\text{M}$ (AK 49) and $64.4 \pm 54.4 \mu\text{M}$ (AK 59). Concentrations above $300 \mu\text{M}$ could not be tested because there were too few gated cells indicating a toxic effect on the P388 cells. The separate building blocks of the compounds were also tested in the flow cytometric binding assay and, surprisingly, even the common parent compound of the guanidine-type H_2 agonists, imidazolylpropylguanidine, displaced the fluorescent ligand **10** from its binding sites with a calculated K_i value of $33.0 \pm 4.1 \mu\text{M}$. By contrast, the free acids representing the variable parts of the compounds, PG 15, cyclohexaneproprionic acid and AK 1, did not compete with **10** for binding at the hY_4 receptor (Fig. 103b).

The binding of the compounds was further confirmed in a flow cytometric assay using CHO- hY_4 -K13b-qi5-K8-mtAEQ-E11-K11 cells and 3 nM of **10** (Fig. 104). The compounds were tested up to a concentration of $300 \mu\text{M}$ but no complete binding curves could be measured because the CHO cells could not be gated after incubation with higher concentrations of compounds. No reliable IC_{50} values could be determined for PG 55B and AK 59 but the calculated K_i values for AK 49 ($68.2 \pm 27.0 \mu\text{M}$) and the imidazolylpropylguanidine ($71.7 \pm 12.5 \mu\text{M}$) were in the same range as determined with P388-S99A- hY_4 -K23 cells.

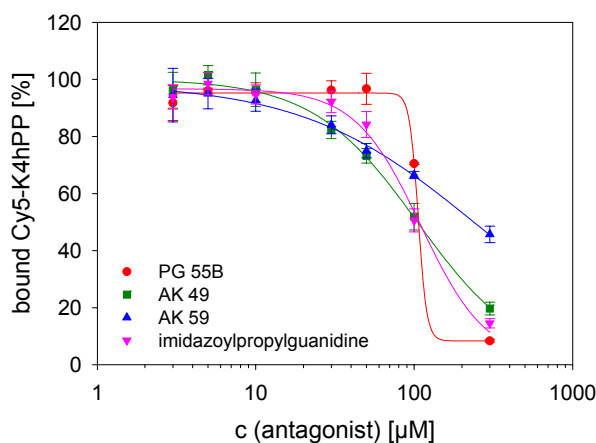


Fig. 104: Flow cytometric binding assay with CHO- hY_4 -K13b-qi5-K8-mtAEQ-E11-K11 cells. Competition of selected compounds with 3 nM $\text{cy5-[K}^4\text{]-hPP}$ (mean values \pm SEM, $n=3$).

Because of the preincubation of the cells in the presence of the test compounds prior to the aequorin assay, a potential luminescence signal elicited immediately after addition of the compounds would not be detected whereas active aequorin would be consumed. This would result in a decreased luminescence signal when the agonist is added pretending an antagonistic effect of the compound.

Therefore, the compounds AK 49, PG 55B and MF 1 (a Y_1 receptor antagonist) were tested in the spectrofluorimetric fura-2 calcium assay.

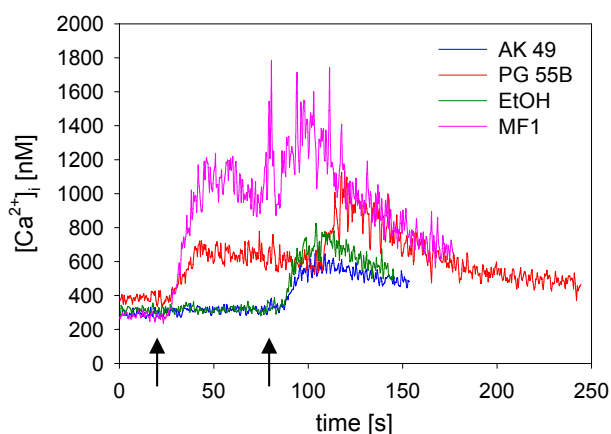


Fig. 105: Calcium responses of CHO-hY₄-K13b-qi5-K8-mtAEQ-E11-K11 cells after addition of 50 µM compound (first arrow) and subsequently 100 nM rPP (second arrow; in case of PG 55B, the addition of rPP was delayed).

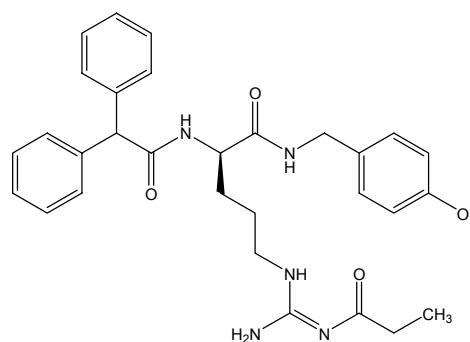


Fig. 106: Y₁ receptor antagonist MF 1.

As shown in Fig. 105, the addition of the solvent ethanol did not induce an increase in intracellular calcium concentration. Subsequent addition of 100 nM rPP elicited the calcium signal. Also the addition of 50 µM AK 49 did not release a calcium response, but the calcium signal subsequently released by rPP was reduced compared to the control experiment, indicating an antagonistic effect of AK 49. Addition of 50 µM PG 55B or MF 1 elicited a strong calcium signal. After the increase in intracellular calcium concentration, the cells were still excitable with the Y₄ receptor agonist rPP indicating that the hY₄ receptors were not desensitized after the first rise in intracellular calcium concentration. This behavior suggests that the increase in intracellular calcium concentration caused by PG 55B and MF1 is not mediated by the hY₄ receptor, but is a result of other signaling pathways, e.g. direct G-protein activation.

To confirm this observation, the compounds PG 55B, AK 49 and MF1 were tested for their agonistic potency in the aequorin assay. As shown in Fig. 107a, 30 µM of MF 1 elicited a luminescence signal whereas the compound PG 55B was not able to induce a luminescence signal up to the highest concentration tested (100 µM). This is in contrast to the results of the fura-2 assay (see Fig. 105) where the addition of 50 µM of PG 55B led to an increase in intracellular calcium concentration. The compound AK 49 was found to be inactive in the aequorin agonist assay up to a concentration of 100 µM. Addition of the cells to 300 µM of AK 49 induced a weak

luminescence signal, which was not inhibited by preincubation of the cells with 20 μM of the H_2 antagonist ranitidine, indicating that this signal was not mediated by the H_2 receptor.

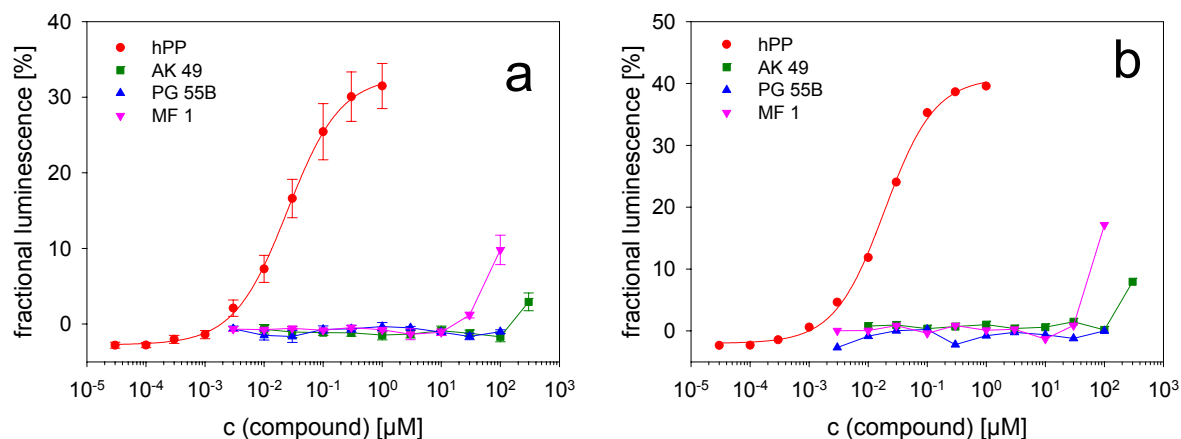


Fig. 107: Aequorin agonist assay with CHO-hY₄-K13b-qi5-K8-mtAEQ-E11-K11 cells. The cells were directly injected to the compound solutions (panel a; mean values \pm SEM, $n=3$) or prior preincubated with 20 μM of the H_2 antagonist ranitidine (panel b; $n=1$).

Taken together, the compound AK 49 did not induce an increase in intracellular calcium concentration up to a concentration of 50 μM in the fura-2 assay and did not elicit a luminescence signal in the aequorin assay up to a concentration of 100 μM . Instead, it reduced the calcium signal elicited with 100 nM rPP in the fura-2 assay and suppressed the luminescence signal elicited with 200 nM rPP in the aequorin assay with an IC_{50} value of 60.7 μM . cy5-[K⁴]-hPP was displaced at the hY₄ receptor by AK 49 in flow cytometric binding assays using hY₄-expressing CHO- and P388 cells with calculated K_i values of 68.2 μM resp. 28.5 μM . Therefore, AK 49 could be a starting point for the search for new nonpeptidic Y₄ antagonists.

5.3.3.5 Luminescence detection with the CCD camera

The luminescence signals could also be detected with a CCD camera as shown in Fig. 108. The emitted luminescence light (recorded for 60 s) increased depending on the concentration of hPP.

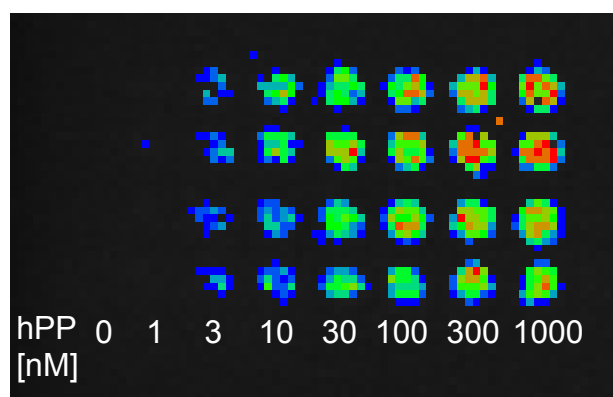


Fig. 108: Overlay picture of false color presentation of light intensities generated by CHO-hY₄-K13b-qi5-K8-mtAEQ-E11 cells detected with a CCD camera. Luminescence signals were released by the addition of the cells to increasing concentrations of hPP.

The calculation of an EC₅₀ value failed because of missing data points (below 1 nM hPP) necessary for a complete concentration-response curve. Unfortunately, the CCD camera was not available for further measurements. Nevertheless, the obtained data indicate that the concentration-dependent increase of luminescence can be detected with a CCD camera, making the assay suitable for high-throughput applications performed with an instrumentation using a CCD camera.

5.3.3.6 Confocal microscopy

Specific binding of **10** to CHO-hY₄-K13b-qi5-K8-mtAEQ-E11-K11 cells was verified with confocal microscopy. For counterstaining of cytoplasm, mitochondria and nucleus, the dye Syto13 was used to ensure that the scanning plane was within the

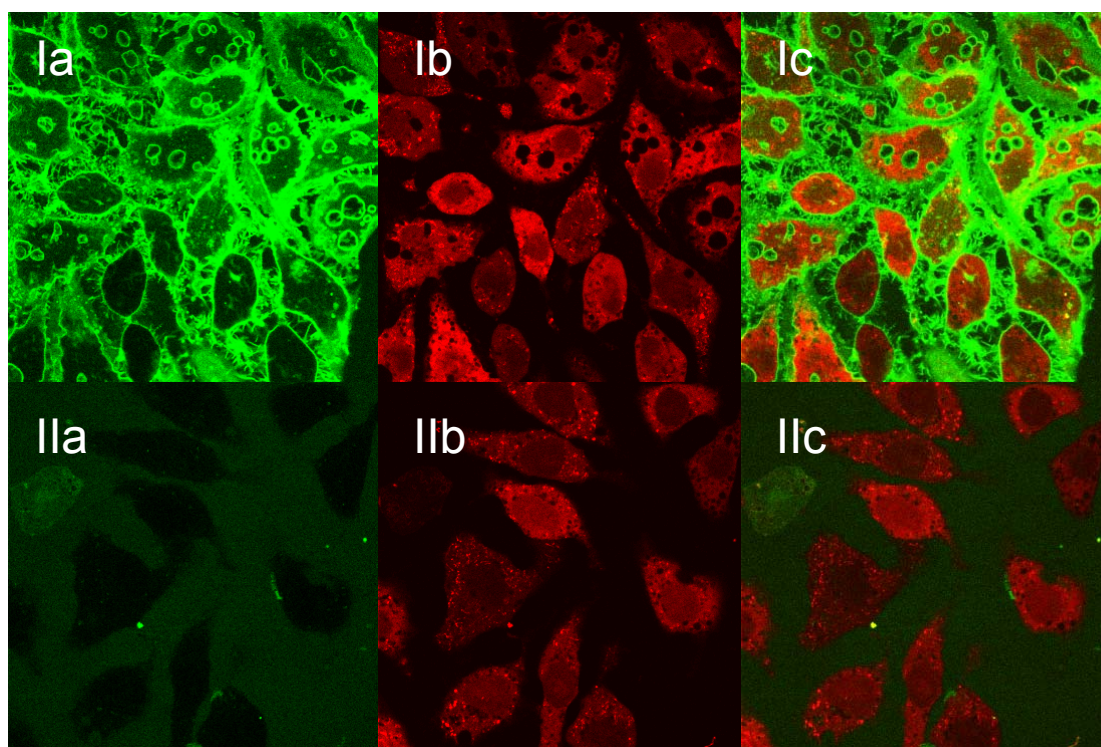


Fig. 109: Total and unspecific binding of 10 nM cy5-[K⁴]-hPP to CHO-hY₄-K13b-qi5-K8-mtAEQ-E11-K11 cells measured by confocal microscopy. Total binding (**Ia-c**) was determined in absence, unspecific binding (**IIa-c**) was determined in presence of 1 μM GW1229. Fluorescence of cy5-[K⁴]-hPP is shown in green (**a**); staining of Syto 13 is shown in red (**b**). Merged images are shown in panels **c**.

cells. Because this dye is membrane permeable, fixation and permeabilization of the cells is not necessary. The cells were incubated with 10 nM of **10** and for the determination of unspecific binding in presence of additional 1 μ M GW1229. As shown in Fig. 109 I, the fluorescence-labeled ligand binds to the cell membrane of the cells. This binding was abolished in presence of the unlabeled ligand GW1229 (Fig. 109 II). The formation of vesicles during the incubation could be due to agonist-induced internalization (Parker *et al.*, 2001b) or to toxic effect of the Syto13 dye.

The increase in intracellular calcium concentration could be visualized with confocal microscopy. CHO-hY₄-K13b-qi5-K8-mtAEQ-E11-K11 cells were loaded with fluo-4 and the calcium signal was elicited with 91 nM hPP. As shown in Fig. 110, the fluorescence increased after the addition of the agonist, reached its maximum after 22 -25 s and subsequently decreased again. This time course is characteristic for a transient calcium response, although the rise in intracellular calcium is delayed compared to the kinetics measured with the spectrofluorimetric fura-2, the flow cytometric fluo-4 or the aequorin assay. This was also observed for the CHO-hY₂-K9-qi5-K9-mtAEQ-A7 cells (see section 4.3.3.1). The reasons for the differences in the observed kinetics have already been discussed in 4.3.3.1.

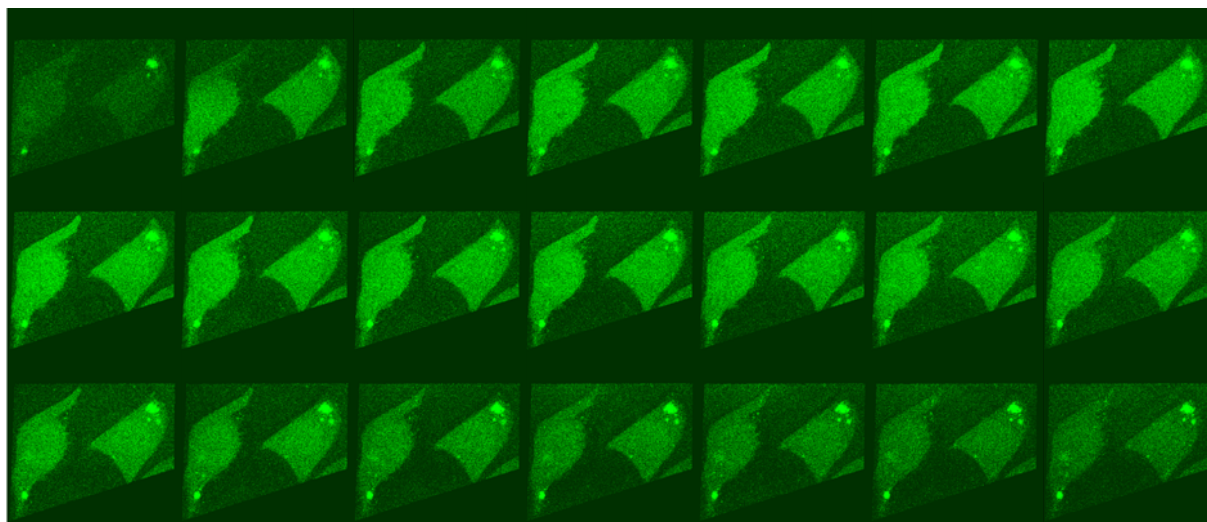


Fig. 110: Time series of CHO-hY₄-K13b-qi5-K8-mtAEQ-E11-K11 cells loaded with fluo-4 in response to 91 nM hPP measured with confocal microscopy. Displayed images were recorded every 3.2 s (scanning time per image was 1.6 s).

5.3.3.7 Transfection of CHO-rY₄ cells with the qi5 construct

By analogy with the approach for the hY₂ and hY₄ receptor, CHO cells stably expressing the rat Y₄ receptor were transfected with the cDNA encoding the chimeric

G-protein G_{q15} in order to redirect the signal transduction pathway towards the activation of PLC. The vector pcDNA3.1/hygro-qi5 was linearized with *Eam*11051 prior to the transfection using the FuGENE™ transfection reagent, and selection was carried out with Ham's F12 plus 10 % FCS containing 400 µg/ml G418 and 400 µg/ml hygromycin. Resistant cells were maintained for 4 weeks in selective medium, before single cell clones were picked and analyzed for calcium responses upon agonist stimulation with hPP in the flow cytometric fluo-4 assay. The cell clone CHO-rY₄-qi5-K2 showed a distinct, concentration-dependent calcium response as shown in Fig. 111.

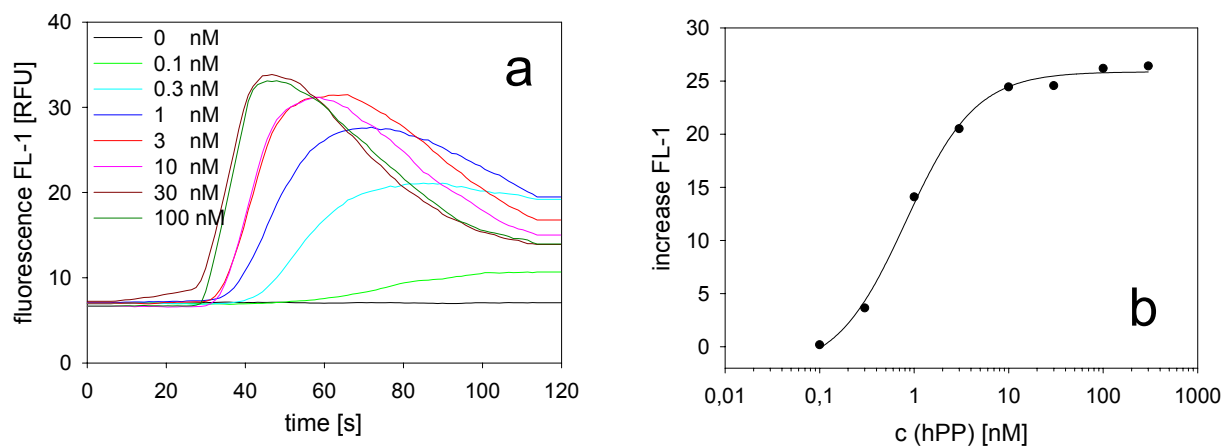


Fig. 111: CHO-rY₄-qi5-K2 cells in response to increasing concentrations of hPP. The cells were loaded with fluo-4 and the increase in fluorescence was detected in channel FL-1 of the flow cytometer (panel a) and used for the construction of a concentration-response curve (panel b, $EC_{50} = 0.82$ nM; $n = 1$).

These data suggest that the principle of co-transfection of receptor and chimeric G-protein gene is also transferable to the rat Y₄ receptor. Functional assays using fluo-4 or fura-2 might be established in analogy to the assays presented for the hY₂ and hY₄ receptor. Further transfection with the gene encoding for the mitochondrial targeted aequorin could enable an aequorin assay performed with the 96-well plate reader.

5.4 Conclusions

The fluorescent ligand cy5-[K⁴]-hPP bound with high affinity to the rat and human Y₄ receptor. Therefore, it could be used for flow cytometric binding assays with cells stably expressing the respective receptor. The determined binding constants (summarized in Table 9) were in good agreement with the literature. The principle of stable co-transfection of the receptor and the *qi5* gene is also applicable to the hY₄ (and rY₄) receptor. EC₅₀ values obtained from fluorimetric calcium assays were comparable with pharmacological constants determined in an aequorin assay after stable transfection with the *mtAEQ* gene.

Table 9: Binding and functional data of selected peptides.

Y ₄ receptor ligand	CHO-rY ₄ (flow cytometry)	P388-S99A-hY ₄ -K23 (flow cytometry)	CHO-hY ₄ ^a (flow cytometry)	CHO-hY ₄ ^a (fura-2 assay)	CHO-hY ₄ ^a (aequorin assay)
cy5-[K ⁴]-hPP	1.44 ± 0.29 nM ^b	8.75 ± 1.52 nM ^b	5.62 ± 1.08 nM ^b	6.87 ± 0.73 nM ^f	ND
S0586-[K ⁴]-hPP	ND	10.22 ± 0.84 nM ^b	9.24 ± 1.34 nM ^b	7.12 ± 0.51 nM ^f	ND
hPP	33.8 ± 8.6 pM ^c	427 ± 42 pM ^d	239 ± 36 pM ^e	3.67 ± 1.76 nM ^g	15.5 ± 3.1 nM ^g 9.33 ± 1.29 nM ^{g,h}
rPP	18.0 ± 3.3 pM ^c	776 ± 139 pM ^d	443 ± 85 pM ^e	14.75 ± 2.77 nM ^g	60.4 ± 12.7 nM ^g
GW1229	1.23 ± 0.20 nM ^c	277 ± 24 pM ^d	217 ± 44 pM ^e	4.55 ± 1.30 nM ^g	29.4 ± 5.3 nM ^g 8.19 ± 0.56 nM ^{g,h}

^aCHO- hY₄- K13b-qi5-K8-mtAEQ-E11-K11 cells; ^bK_d value, determined with saturation analysis; ^cK_i value, determined in presence of 2 nM cy5-[K⁴]-hPP; ^dK_i value, determined in presence of 40 nM cy5-[K⁴]-hPP; ^eK_i value, determined in presence of 10 nM cy5-[K⁴]-hPP; ^fpEC₅₀ value, determined using the logit-transformation; ^gEC₅₀ value; ^hdetermined with subsequent recording of residual active aequorin; ND: not determined

The binding of the fluorescent ligand and the calcium signal elicited with Y₄ agonists can be visualized with confocal microscopy. The luminescence signals were detectable with a CCD camera, indicating that the assay is suited for the application in appropriate HTS instruments. The observed partial agonism of GW1229 is in contrast to the predominant results in the literature and further investigations should be done to confirm or to disprove the described agonistic nature of the peptide.

Chapter 6

Summary

Summary

The development of simple, fast and robust binding and functional assays is an important step in the course of drug research. As large compound libraries are available by combinatorial chemistry and the number of new possible targets is increasing due to the sequencing of the human genome, appropriate techniques are required not only for HTS but especially for in-depth pharmacological characterization of receptor-ligand interactions.

This thesis was aimed at the development of new binding and functional assays for the hY_2 , hY_4 and rY_4 receptor. CHO cells were stably transfected with the hY_2 receptor gene and used in a flow cytometric binding assay. Binding of unlabeled receptor ligands in competition with cy5-labeled pNPY was determined at equilibrium. Binding of the fluorescent ligand could be visualized by confocal microscopy. A radioligand binding assay was established and the determined binding constants were in good agreement with the ones obtained from the flow cytometric binding assay and with data from literature, respectively. The existence of a large fraction of spare receptors described in the literature was confirmed. It turned out that the Y_2 receptor antagonist BIIE0246 tends to adsorb to the different (synthetic) materials of microplates, cups and other utensils used in the assay, hampering the pharmacological characterization of this specific class of compounds.

As the cells, stably transfected with the hY_2 receptor gene, showed only a moderate calcium signal upon receptor activation, the cells were further stably transfected with the gene encoding the chimeric G-protein G_{qi5} , allowing the redirection of the signal transduction pathway towards the $PLC\beta$, resulting in a large increase in intracellular calcium concentration. Binding properties of the transfected cells were not altered and the calcium signal was quantitated in a flow cytometric and a spectrofluorimetric calcium assay. Functional data of agonists as well as antagonists were determined.

Additional stable transfection of the cells with the gene encoding for apoaequorin targeted to the mitochondrion converted the calcium signal into a luminescence signal. Assay parameters were optimized and an aequorin assay was established in the 96-well format of a luminescence plate reader. Functional data of selected peptides and nonpeptidic compounds were determined and compared with the fluorescence-based calcium assays. The compound BIIE0246 behaved as a competitive and an insurmountable antagonist depending on the incubation period prior to agonist addition, which is in agreement with recently published results.

The calcium responses could be visualized by means of confocal microscopy and a CCD camera.

New fluorescent ligands for the Y_4 receptor were synthesized by coupling the fluorescent dyes cy5 and S0586 to the peptide [K⁴]-hPP. A flow cytometric binding assay was established for the rat Y_4 receptor using stably transfected CHO cells.

As the stable transfection of CHO cells with the hY_4 gene failed, a retroviral approach was used to transduce the hY_4 gene into P388-D1 cells. After enrichment of receptor expressing cells by sorting with the flow cytometer a cell clone with high receptor expression was isolated. Competition binding of known peptide ligands in the presence of the fluorescent ligands was measured by flow cytometry.

Furthermore, CHO cells were co-transfected with the hY_4 (containing a Kozak sequence for enhanced protein translation), $G_{q/15}$ and $mtAEQ$ gene. Stable cell clones were isolated and flow cytometric binding as well as fluorescence- and luminescence-based functional assays were established. It turned out that the peptide GW1229 behaved as a partial agonist in the spectofluorimetric as well as in the aequorin assay. The calcium signal could be detected by confocal microscopy and by a CCD camera, indicating that the aequorin assay is applicable to HTS-instruments equipped with a CCD camera.

The screening of a small compound library revealed a small molecule with micromolar antagonistic activity at the hY_4 receptor, which may be a starting point for the search for new Y_4 receptor antagonists.

The main advantage of the established aequorin assay is the automation of the injection and recording process. Thereby, it is possible to perform more than 400 single calcium assays per day compared to about 40 assays performed with the spectrofluorimetric or flow cytometric calcium assay. After addition of the cofactor washing steps are not required, which is in contrast to the case when fluorescence dyes are used. Dye leakage is not an issue of the aequorin assay. The injection speed, which turned out to be an important parameter, is constant, and because the assay volume is very small (200 μ l) costs are low and only small amounts of test compounds are required. The fact that the aequorin assay measures an event more distal in the GPCR signal transduction pathway seems not to affect the determined functional data. The major drawback of the assay is the need for transfection of the cells and the long postincubation periods, required to obtain constant luminescence

signals. Nevertheless, the aequorin assay is a powerful method for the determination of functional data amenable to high throughput screening.

Taken together, the established flow cytometric binding assays using fluorescence labeled ligands and stably transfected cells are an innovative alternative to radioligand binding assays. The principle of stable co-expression of receptor, chimeric G-protein and mitochondrially targeted aequorin gene for the development of functional fluorescence- and luminescence-based assays has proven to be an efficient approach. This methodology is transferable to other GPCRs, and will facilitate the search for new GPCR ligands as well as their functional characterization.

References

- Aakerlund, L., Gether, U., Fuhlendorff, J., Schwartz, T.W., and Thastrup, O. (1990) Y1 receptors for neuropeptide Y are coupled to mobilization of intracellular calcium and inhibition of adenylate cyclase. *FEBS Lett* **260**: 73-78.
- Abbott, C.R., Small, C.J., Kennedy, A.R., Neary, N.M., Sajedi, A., Ghatei, M.A., and Bloom, S.R. (2005) Blockade of the neuropeptide Y Y2 receptor with the specific antagonist BIIE0246 attenuates the effect of endogenous and exogenous peptide YY(3-36) on food intake. *Brain Res* **1043**: 139-144.
- Adham, N., Ellerbrock, B., Hartig, P., Weinshank, R., and Branchek, T. (1993) Receptor reserve masks partial agonist activity of drugs in a cloned rat 5-hydroxytryptamine1B receptor expression system. *Mol Pharmacol* **43**: 427-433.
- Adler, C., Meller, E., and Goldstein, M. (1987) Receptor reserve at the alpha-2 adrenergic receptor in the rat cerebral cortex. *J Pharmacol Exp Ther* **240**: 508-515.
- Allen, J., Novotny, J., Martin, J., and Heinrich, G. (1987) Molecular structure of mammalian neuropeptide Y: analysis by molecular cloning and computer-aided comparison with crystal structure of avian homologue. *Proc Natl Acad Sci U S A* **84**: 2532-2536.
- Amatruda, T.T., 3rd, Steele, D.A., Slepak, V.Z., and Simon, M.I. (1991) G alpha 16, a G protein alpha subunit specifically expressed in hematopoietic cells. *Proc Natl Acad Sci U S A* **88**: 5587-5591.
- Andrews, P.C., Hawke, D., Shively, J.E., and Dixon, J.E. (1985) A nonamidated peptide homologous to porcine peptide YY and neuropeptide YY. *Endocrinology* **116**: 2677-2681.
- Ariens, E.J. (1954) Affinity and intrinsic activity in the theory of competitive inhibition. I. Problems and theory. *Arch Int Pharmacodyn Ther* **99**: 32-49.
- Asakawa, A., Inui, A., Ueno, N., Fujimiya, M., Fujino, M.A., and Kasuga, M. (1999) Mouse pancreatic polypeptide modulates food intake, while not influencing anxiety in mice. *Peptides* **20**: 1445-1448.
- Asakawa, A., Inui, A., Yuzuriha, H., Ueno, N., Katsuura, G., Fujimiya, M., Fujino, M.A., Nijima, A., Meguid, M.M., and Kasuga, M. (2003) Characterization of the effects of pancreatic polypeptide in the regulation of energy balance. *Gastroenterology* **124**: 1325-1336.
- Bader, R., Bettio, A., Beck-Sickinger, A.G., and Zerbe, O. (2001) Structure and dynamics of micelle-bound neuropeptide Y: comparison with unligated NPY and implications for receptor selection. *J Mol Biol* **305**: 307-329.
- Bajaj, A., Celic, A., Ding, F.X., Naider, F., Becker, J.M., and Dumont, M.E. (2004) A fluorescent alpha-factor analogue exhibits multiple steps on binding to its G protein coupled receptor in yeast. *Biochemistry* **43**: 13564-13578.
- Balasubramaniam, A., Andrews, P.C., Renugopalakrishnan, V., and Rigel, D.F. (1989) Glycine-extended anglerfish peptide YG (aPY) a neuropeptide Y (NPY) homologue may be a precursor of a biologically active peptide. *Peptides* **10**: 581-585.
- Balasubramaniam, A., and Sheriff, S. (1990) Neuropeptide Y (18-36) is a competitive antagonist of neuropeptide Y in rat cardiac ventricular membranes. *J Biol Chem* **265**: 14724-14727.
- Balasubramaniam, A., Sheriff, S., Rigel, D.F., and Fischer, J.E. (1990) Characterization of neuropeptide Y binding sites in rat cardiac ventricular membranes. *Peptides* **11**: 545-550.
- Balasubramaniam, A., Sheriff, S., Johnson, M.E., Prabhakaran, M., Huang, Y., Fischer, J.E., and Chance, W.T. (1994) [D-TRP32]neuropeptide Y: a competitive antagonist of NPY in rat hypothalamus. *J Med Chem* **37**: 811-815.
- Balasubramaniam, A., Ujhelyi, M., Borchers, M., Huang, Y., Zhai, W., Zhou, Y., Johnson, M., Sheriff, S., and Fischer, J.E. (1996) Antagonistic properties of centrally truncated analogs of [D-Trp(32)]NPY. *J Med Chem* **39**: 1142-1147.
- Balasubramaniam, A., Dhawan, V.C., Mullins, D.E., Chance, W.T., Sheriff, S., Guzzi, M., Prabhakaran, M., and Parker, E.M. (2001) Highly selective and potent neuropeptide Y (NPY) Y1 receptor antagonists based on [Pro(30), Tyr(32), Leu(34)]NPY(28-36)-NH2 (BW1911U90). *J Med Chem* **44**: 1479-1482.
- Baldock, P.A., Sainsbury, A., Couzens, M., Enriquez, R.F., Thomas, G.P., Gardiner, E.M., and Herzog, H. (2002) Hypothalamic Y2 receptors regulate bone formation. *J Clin Invest* **109**: 915-921.
- Banks, W.A., Kastin, A.J., and Jaspan, J.B. (1995) Regional variation in transport of pancreatic polypeptide across the blood-brain barrier of mice. *Pharmacol Biochem Behav* **51**: 139-147.
- Bard, J.A., Walker, M.W., Branchek, T.A., and Weinshank, R.L. (1995) Cloning and functional expression of a human Y4 subtype receptor for pancreatic polypeptide, neuropeptide Y, and peptide YY. *J Biol Chem* **270**: 26762-26765.
- Batterham, R.L., Cowley, M.A., Small, C.J., Herzog, H., Cohen, M.A., Dakin, C.L., Wren, A.M., Brynes, A.E., Low, M.J., Ghatei, M.A., Cone, R.D., and Bloom, S.R. (2002) Gut hormone PYY(3-36) physiologically inhibits food intake. *Nature* **418**: 650-654.

- Batterham, R.L., Le Roux, C.W., Cohen, M.A., Park, A.J., Ellis, S.M., Patterson, M., Frost, G.S., Ghatei, M.A., and Bloom, S.R. (2003) Pancreatic Polypeptide Reduces Appetite and Food Intake in Humans. *J Clin Endocrinol Metab* **88**: 3989-3992.
- Baubet, V., Le Mouellic, H., Campbell, A.K., Lucas-Meunier, E., Fossier, P., and Brulet, P. (2000) Chimeric green fluorescent protein-aequorin as bioluminescent Ca²⁺ reporters at the single-cell level. *Proc Natl Acad Sci U S A* **97**: 7260-7265.
- Beck-Sickinger, A.G., Grouzmann, E., Hoffmann, E., Gaida, W., van Meir, E.G., Waeber, B., and Jung, G. (1992) A novel cyclic analog of neuropeptide Y specific for the Y2 receptor. *Eur J Biochem* **206**: 957-964.
- Berglund, M.M., Lundell, I., Eriksson, H., Soll, R., Beck-Sickinger, A.G., and Larhammar, D. (2001) Studies of the human, rat, and guinea pig Y4 receptors using neuropeptide Y analogues and two distinct radioligands. *Peptides* **22**: 351-356.
- Berglund, M.M., Fredriksson, R., Salaneck, E., and Larhammar, D. (2002) Reciprocal mutations of neuropeptide Y receptor Y2 in human and chicken identify amino acids important for antagonist binding. *FEBS Lett* **518**: 5-9.
- Berglund, M.M., Hipskind, P.A., and Gehlert, D.R. (2003a) Recent Developments in Our Understanding of the Physiological Role of PP-Fold Peptide Receptor Subtypes. *Exp Biol Med* **228**: 217-244.
- Berglund, M.M., Schober, D.A., Esterman, M.A., and Gehlert, D.R. (2003b) Neuropeptide Y Y4 receptor homodimers dissociate upon agonist stimulation. *J Pharmacol Exp Ther* **307**: 1120-1126.
- Berglund, M.M., Schober, D.A., Statnick, M.A., McDonald, P.H., and Gehlert, D.R. (2003c) The use of bioluminescence resonance energy transfer 2 to study neuropeptide Y receptor agonist-induced beta-arrestin 2 interaction. *J Pharmacol Exp Ther* **306**: 147-156.
- Bernhardt, G., Reile, H., Birnbock, H., Spruss, T., and Schonemberger, H. (1992) Standardized kinetic microassay to quantify differential chemosensitivity on the basis of proliferative activity. *J Cancer Res Clin Oncol* **118**: 35-43.
- Bettio, A., Dinger, M.C., and Beck-Sickinger, A.G. (2002) The neuropeptide Y monomer in solution is not folded in the pancreatic-polypeptide fold. *Protein Sci* **11**: 1834-1844.
- Bhattacharya, S., Paul, C., and Mobbs, C. (1994) Detection of rat prepropancreatic polypeptide mRNA in rat brain using RT-PCR. *Society for Neurosciences Abstracts* **20**: 361.365.
- Birnboim, H.C., and Doly, J. (1979) A rapid alkaline extraction procedure for screening recombinant plasmid DNA. *Nucleic Acids Res* **7**: 1513-1523.
- Bischoff, A., Puttmann, K., Kotting, A., Moser, C., Buschauer, A., and Michel, M.C. (2001) Limited signal transduction repertoire of human Y(5) neuropeptide Y receptors expressed in HEC-1B cells. *Peptides* **22**: 387-394.
- Bleakman, D., Colmers, W.F., Fournier, A., and Miller, R.J. (1991) Neuropeptide Y inhibits Ca²⁺ influx into cultured dorsal root ganglion neurones of the rat via a Y2 receptor. *Br J Pharmacol* **103**: 1781-1789.
- Blinks, J.R. (1978) Applications of calcium-sensitive photoproteins in experimental biology. *Photochem Photobiol* **27**: 423-432.
- Blum, C.A., Zheng, X., and De Lombaert, S. (2004) Design, synthesis, and biological evaluation of substituted 2-cyclohexyl-4-phenyl-1H-imidazoles: potent and selective neuropeptide Y Y5-receptor antagonists. *J Med Chem* **47**: 2318-2325.
- Blundell, T., Pitts, J., Tickle, I., Wood, S., and Wu, C.-W. (1981) X-ray analysis (1.4-Å resolution) of avian pancreatic polypeptide: Small globular protein hormone. *Proc Natl Acad Sci U S A* **78**: 4175-4179.
- Bockaert, J., and Pin, J.P. (1999) Molecular tinkering of G protein-coupled receptors: an evolutionary success. *EMBO J* **18**: 1723-1729.
- Boggiano, M.M., Chandler, P.C., Oswald, K.D., Rodgers, R.J., Blundell, J.E., Ishii, Y., Beattie, A.H., Holch, P., Allison, D.B., Schindler, M., Arndt, K., Rudolf, K., Mark, M., Schoelch, C., Joost, H.G., Klaus, S., Thone-Reineke, C., Benoit, S.C., Seeley, R.J., Beck-Sickinger, A.G., Koglin, N., Raun, K., Madsen, K., Wulff, B.S., Stidsen, C.E., Birringer, M., Kreuzer, O.J., Deng, X.Y., Whitcomb, D.C., Halem, H., Taylor, J., Dong, J., Datta, R., Culler, M., Ortmann, S., Castaneda, T.R., and Tschop, M. (2005) PYY3-36 as an anti-obesity drug target. *Obesity Reviews* **6**: 307-322.
- Bonaventure, P., Nepomuceno, D., Mazur, C., Lord, B., Rudolph, D.A., Jablonowski, J.A., Carruthers, N.I., and Lovenberg, T.W. (2004) Characterization of N-(1-Acetyl-2,3-dihydro-1H-indol-6-yl)-3-(3-cyano-phenyl)-N-[1-(2-cyclopentyl-ethyl)-piperidin-4yl]acrylamide (JNJ-5207787), a Small Molecule Antagonist of the Neuropeptide Y Y2 Receptor. *J Pharmacol Exp Ther* **308**: 1130-1137.
- Borowsky, B., Walker, M.W., Bard, J., Weinshank, R.L., Laz, T.M., Vaysse, P., Branchek, T.A., and Gerald, C. (1998) Molecular biology and pharmacology of multiple NPY Y5 receptor species homologs. *Regul Pept* **75-76**: 45-53.

- Bouritius, H., Oprins, J.C., Bindels, R.J., Hartog, A., and Groot, J.A. (1998) Neuropeptide Y inhibits ion secretion in intestinal epithelium by reducing chloride and potassium conductance. *Pflugers Arch* **435**: 219-226.
- Boyer, M.J., and Hedley, D.W. (1994) Measurement of intracellular pH. *Methods Cell Biol* **41**: 135-148.
- Braman, J., Papworth, C., and Greener, A. (1996) Site-directed mutagenesis using double-stranded plasmid DNA templates. *Methods Mol Biol* **57**: 31-44.
- Brennauer, A., Dove, S., and Buschauer, A. (2004) Structure-activity relationships of nonpeptide neuropeptide Y receptor antagonists. In *Handbook of experimental pharmacology*. Vol. 162. Michel, M.C. (ed): Springer-Verlag, pp. 505-546.
- Brini, M., Marsault, R., Bastianutto, C., Alvarez, J., Pozzan, T., and Rizzuto, R. (1995) Transfected aequorin in the measurement of cytosolic Ca²⁺ concentration ([Ca²⁺]_c). A critical evaluation. *J Biol Chem* **270**: 9896-9903.
- Brini, M., Pinton, P., Pozzan, T., and Rizzuto, R. (1999) Targeted recombinant aequorins: tools for monitoring [Ca²⁺] in the various compartments of a living cell. *Microsc Res Tech* **46**: 380-389.
- Broqua, P., Wettstein, J.G., Rocher, M.N., Gauthier-Martin, B., Riviere, P.J., Junien, J.L., and Dahl, S.G. (1996) Antinociceptive effects of neuropeptide Y and related peptides in mice. *Brain Res* **724**: 25-32.
- Burkhoff, A., Linemeyer, D.L., and Salon, J.A. (1998) Distribution of a novel hypothalamic neuropeptide Y receptor gene and its absence in rat. *Brain Res Mol Brain Res* **53**: 311-316.
- Button, D., and Brownstein, M. (1993) Aequorin-expressing mammalian cell lines used to report Ca²⁺ mobilization. *Cell Calcium* **14**: 663-671.
- Cabrele, C., and Beck-Sickinger, A.G. (2000) Molecular characterization of the ligand-receptor interaction of the neuropeptide Y family. *J Pept Sci* **6**: 97-122.
- Cabrele, C., Langer, M., Bader, R., Wieland, H.A., Doods, H.N., Zerbe, O., and Beck-Sickinger, A.G. (2000) The first selective agonist for the neuropeptide YY₅ receptor increases food intake in rats. *J Biol Chem* **275**: 36043-36048.
- Cabrele, C., Wieland, H.A., Langer, M., Stidsen, C.E., and Beck-Sickinger, A.G. (2001) Y-receptor affinity modulation by the design of pancreatic polypeptide/neuropeptide Y chimera led to Y(5)-receptor ligands with picomolar affinity. *Peptides* **22**: 365-378.
- Cabrera-Vera, T.M., Vanhauwe, J., Thomas, T.O., Medkova, M., Preininger, A., Mazzoni, M.R., and Hamm, H.E. (2003) Insights into G protein structure, function, and regulation. *Endocr Rev* **24**: 765-781.
- Campbell, R.E., Smith, M.S., Allen, S.E., Grayson, B.E., French-Mullen, J.M., and Grove, K.L. (2003) Orexin neurons express a functional pancreatic polypeptide Y₄ receptor. *J Neurosci* **23**: 1487-1497.
- Capurro, D., and Huidobro-Toro, J.P. (1999) The involvement of neuropeptide Y Y₁ receptors in the blood pressure baroreflex: studies with BIBP 3226 and BIBO 3304. *Eur J Pharmacol* **376**: 251-255.
- Cerda-Reverter, J.M., Martinez Rodriguez, G., Zanuy, S., Carrillo, M., and Larhammar, D. (1998) Cloning of neuropeptide Y, peptide YY, and peptide Y from sea bass (*Dicentrarchus labrax*), a marine teleost. *Ann N Y Acad Sci* **839**: 493-495.
- Cerda-Reverter, J.M., and Larhammar, D. (2000) Neuropeptide Y family of peptides: structure, anatomical expression, function, and molecular evolution. *Biochem Cell Biol* **78**: 371-392.
- Chalfie, M., Tu, Y., Euskirchen, G., Ward, W.W., and Prasher, D.C. (1994) Green fluorescent protein as a marker for gene expression. *Science* **263**: 802-805.
- Chen, C., and Okayama, H. (1987) High-efficiency transformation of mammalian cells by plasmid DNA. *Mol Cell Biol* **7**: 2745-2752.
- Cheng, Y., and Prusoff, W.H. (1973) Relationship between the inhibition constant (K₁) and the concentration of inhibitor which causes 50 per cent inhibition (I₅₀) of an enzymatic reaction. *Biochem Pharmacol* **22**: 3099-3108.
- Civelli, O., Nothacker, H.P., Saito, Y., Wang, Z., Lin, S.H., and Reinscheid, R.K. (2001) Novel neurotransmitters as natural ligands of orphan G-protein-coupled receptors. *Trends Neurosci* **24**: 230-237.
- Clark, A.J. (1933) *The mode of action of drugs on cells*. London: Edward Arnold.
- Clark, A.J. (1937) General Pharmacology. In *Heffner's Handbuch der Experimentellen Pharmakologie. Ergänzungswerk, Band 4*: Springer-Verlag, Berlin Heidelberg New York.
- Clark, J.T., Kalra, P.S., Crowley, W.R., and Kalra, S.P. (1984) Neuropeptide Y and human pancreatic polypeptide stimulate feeding behavior in rats. *Endocrinology* **115**: 427-429.
- Cobbold, P.H. (1980) Cytoplasmic free calcium and amoeboid movement. *Nature* **285**: 441-446.
- Conklin, B., Herzmark, P., Ishida, S., Voyno-Yasenetskaya, T., Sun, Y., Farfel, Z., and Bourne, H. (1996) Carboxyl-terminal mutations of Gq alpha and Gs alpha that alter the fidelity of receptor activation. *Mol Pharmacol* **50**: 885-890.
- Conklin, B.R., Farfel, Z., Lustig, K.D., Julius, D., and Bourne, H.R. (1993) Substitution of three amino acids switches receptor specificity of Gq alpha to that of Gi alpha. *Nature* **363**: 274-276.

- Conlon, J.M., and O'Harte, F. (1992) The primary structure of a PYY-related peptide from chicken intestine suggests an anomalous site of cleavage of the signal peptide in preproPYY. *FEBS Lett* **313**: 225-228.
- Conlon, J.M. (2002) The origin and evolution of peptide YY (PYY) and pancreatic polypeptide (PP). *Peptides* **23**: 269-278.
- Connor, M., Yeo, A., and Henderson, G. (1997) Neuropeptide Y Y2 receptor and somatostatin sst2 receptor coupling to mobilization of intracellular calcium in SH-SY5Y human neuroblastoma cells. *Br J Pharmacol* **120**: 455-463.
- Coward, P., Chan, S.D.H., Wada, H.G., Humphries, G.M., and Conklin, B.R. (1999) Chimeric G Proteins Allow a High-Throughput Signaling Assay of Gi-Coupled Receptors. *Anal Biochem* **270**: 242-248.
- Cowen, M.S., Chen, F., and Lawrence, A.J. (2004) Neuropeptides: implications for alcoholism. *J Neurochem* **89**: 273-285.
- Cowley, D.J., Hoflack, J.M., Pelton, J.T., and Saudek, V. (1992) Structure of neuropeptide Y dimer in solution. *Eur J Biochem* **205**: 1099-1106.
- Cox, H.M. (1998) Peptidergic regulation of intestinal ion transport. A major role for neuropeptide Y and the pancreatic polypeptides. *Digestion* **59**: 395-399.
- Cox, H.M., Tough, I.R., Zandvliet, D.W., and Holliday, N.D. (2001) Constitutive neuropeptide Y Y(4) receptor expression in human colonic adenocarcinoma cell lines. *Br J Pharmacol* **132**: 345-353.
- Criscione, L., Yamaguchi, Y., and Mah, R. (1997) Receptor Antagonists, Receptor Antagonists, Switzerland
- Criscione, L., Rigollier, P., Batzl-Hartmann, C., Rueger, H., Stricker-Krongrad, A., Wyss, P., Brunner, L., Whitebread, S., Yamaguchi, Y., Gerald, C., Heurich, R.O., Walker, M.W., Chiesi, M., Schilling, W., Hofbauer, K.G., and Levens, N. (1998) Food intake in free-feeding and energy-deprived lean rats is mediated by the neuropeptide Y5 receptor. *J Clin Invest* **102**: 2136-2145.
- Cuatrecasas, P. (1974) Membrane receptors. *Annu Rev Biochem* **43**: 169-214.
- Daniels, A.J., Matthews, J.E., Humberto Viveros, O., and Lazarowski, E.R. (1992) Characterization of the neuropeptide Y-induced intracellular calcium release in human erythroleukemic cells. *Mol Pharmacol* **41**: 767-771.
- Daniels, A.J., Matthews, J.E., Slepatis, R.J., Jansen, M., Viveros, O.H., Tadepalli, A., Harrington, W., Heyer, D., Landavazo, A., Leban, J.J., and et al. (1995) High-affinity neuropeptide Y receptor antagonists. *Proc Natl Acad Sci U S A* **92**: 9067-9071.
- Darbon, H., Bernassau, J.M., Deleuze, C., Chenu, J., Roussel, A., and Cambillau, C. (1992) Solution conformation of human neuropeptide Y by ¹H nuclear magnetic resonance and restrained molecular dynamics. *Eur J Biochem* **209**: 765-771.
- Darzynkiewicz, Z., Juan, G., Li, X., Gorczyca, W., Murakami, T., and Traganos, F. (1997) Cytometry in cell necrobiology: analysis of apoptosis and accidental cell death (necrosis). *Cytometry* **27**: 1-20.
- Dascal, N. (2001) Ion-channel regulation by G proteins. *Trends Endocrinol Metab* **12**: 391-398.
- Dautzenberg, F.M. (2005) Stimulation of neuropeptide Y-mediated calcium responses in human SMS-KAN neuroblastoma cells endogenously expressing Y2 receptors by co-expression of chimeric G proteins. *Biochem Pharmacol* **69**: 1493-1499.
- Dautzenberg, F.M., Higelin, J., Pflieger, P., Neidhart, W., and Guba, W. (2005) Establishment of robust functional assays for the characterization of neuropeptide Y (NPY) receptors: identification of 3-(5-benzoyl-thiazol-2-ylamino)-benzonitrile as selective NPY type 5 receptor antagonist. *Neuropharmacology* **48**: 1043-1055.
- Dautzenberg, F.M., and Neysari, S. (2005) Irreversible binding kinetics of neuropeptide Y ligands to Y2 but not to Y1 and Y5 receptors. *Pharmacology* **75**: 21-29.
- De Giorgi, F., Brini, M., Bastianutto, C., Marsault, R., Montero, M., Pizzo, P., Rossi, R., and Rizzuto, R. (1996) Targeting aequorin and green fluorescent protein to intracellular organelles. *Gene* **173**: 113-117.
- De Lean, A., Stadel, J.M., and Lefkowitz, R.J. (1980) A ternary complex model explains the agonist-specific binding properties of the adenylate cyclase-coupled beta-adrenergic receptor. *J Biol Chem* **255**: 7108-7117.
- Della Zuana, O., Sadlo, M., Germain, M., Feletou, M., Chamorro, S., Tisserand, F., de Montrion, C., Boivin, J.F., Duhault, J., Boutin, J.A., and Levens, N. (2001) Reduced food intake in response to CGP 71683A may be due to mechanisms other than NPY Y5 receptor blockade. *Int J Obes Relat Metab Disord* **25**: 84-94.
- Di Fabio, R., Giovannini, R., Bertani, B., Borriello, M., Bozzoli, A., Donati, D., Falchi, A., Ghirlanda, D., Leslie, C.P., and Pecunioso, A. (2006) Synthesis and SAR of substituted tetrahydrocarbazole derivatives as new NPY-1 antagonists. *Bioorg Med Chem Lett* **16**: 1749-1752.

- Dinger, M.C., Bader, J.E., Kobor, A.D., Kretzschmar, A.K., and Beck-Sickinger, A.G. (2003) Homodimerization of neuropeptide y receptors investigated by fluorescence resonance energy transfer in living cells. *J Biol Chem* **278**: 10562-10571.
- Doods, H., Gaida, W., Wieland, H.A., Dollinger, H., Schnorrenberg, G., Esser, F., Engel, W., Eberlein, W., and Rudolf, K. (1999) BIIE0246: A selective and high affinity neuropeptide Y Y2 receptor antagonist. *Eur J Pharmacol* **384**: R3-R5.
- Dressler, L.G., and Seamer, L.C. (1994) Controls, standards, and histogram interpretation in DNA flow cytometry. *Methods Cell Biol* **41**: 241-262.
- Drexler, H., and Uphoff, C. (2002) Mycoplasma contamination of cell cultures: Incidence, sources, effects, detection, elimination, prevention. *Cytotechnology* **39**: 75-90.
- Dryden, S., Pickavance, L., Frankish, H.M., and Williams, G. (1995) Increased neuropeptide Y secretion in the hypothalamic paraventricular nucleus of obese (fa/fa) Zucker rats. *Brain Res* **690**: 185-188.
- Duchen, M.R. (2000) Mitochondria and calcium: from cell signalling to cell death. *J Physiol* **529 Pt 1**: 57-68.
- Duhault, J., Boulanger, M., Chamorro, S., Boutin, J.A., Della Zuana, O., Douillet, E., Fauchere, J.L., Feletou, M., Germain, M., Husson, B., Vega, A.M., Renard, P., and Tisserand, F. (2000) Food intake regulation in rodents: Y5 or Y1 NPY receptors or both? *Can J Physiol Pharmacol* **78**: 173-185.
- Dumont, Y., Cadieux, A., Doods, H., Pheng, L.H., Abounader, R., Hamel, E., Jacques, D., Regoli, D., and Quirion, R. (2000) BIIE0246, a potent and highly selective non-peptide neuropeptide Y Y2 receptor antagonist. *Br J Pharmacol* **129**: 1075-1088.
- Dumont, Y., and Quirion, R. (2000) [(125)I]-GR231118: a high affinity radioligand to investigate neuropeptide Y Y(1) and Y(4) receptors. *Br J Pharmacol* **129**: 37-46.
- Dumont, Y., Thakur, M., Beck-Sickinger, A., Fournier, A., and Quirion, R. (2003) Development and characterization of a highly selective neuropeptide Y Y5 receptor agonist radioligand: [125I][hPP1-17, Ala31, Aib32]NPY. *Br J Pharmacol* **139**: 1360-1368.
- Dumont, Y., Thakur, M., Beck-Sickinger, A., Fournier, A., and Quirion, R. (2004) Characterization of a new neuropeptide Y Y5 agonist radioligand: [(125)I][cPP(1-7), NPY(19-23), Ala(31), Aib(32), Gln(34)]hPP. *Neuropeptides* **38**: 163-174.
- Dupriez, V.J., Maes, K., Le Poul, E., Burgeon, E., and Detheux, M. (2002) Aequorin-based functional assays for G-protein-coupled receptors, ion channels, and tyrosine kinase receptors. *Receptors Channels* **8**: 319-330.
- Durkin, M.M., Walker, M.W., Smith, K.E., Gustafson, E.L., Gerald, C., and Branchek, T.A. (2000) Expression of a novel neuropeptide Y receptor subtype involved in food intake: an in situ hybridization study of Y5 mRNA distribution in rat brain. *Exp Neurol* **165**: 90-100.
- Edwards, B.S., Oprea, T., Prossnitz, E.R., and Sklar, L.A. (2004) Flow cytometry for high-throughput, high-content screening. *Curr Opin Chem Biol* **8**: 392-398.
- Ekblad, E., and Sundler, F. (2002) Distribution of pancreatic polypeptide and peptide YY. *Peptides* **23**: 251-261.
- Ekman, R., Wahlestedt, C., Bottcher, G., Sundler, F., Hakanson, R., and Panula, P. (1986) Peptide YY-like immunoreactivity in the central nervous system of the rat. *Regul Pept* **16**: 157-168.
- El Bahh, B., Cao, J.Q., Beck-Sickinger, A.G., and Colmers, W.F. (2002) Blockade of neuropeptide Y2 receptors and suppression of NPY's anti-epileptic actions in the rat hippocampal slice by BIIE0246. *Br J Pharmacol* **136**: 502-509.
- Ellis, C. (2004) THE STATE OF GPCR RESEARCH IN 2004. *Nat Rev Drug Discov* **3**: 577-626.
- El-Salhy, M., Wilander, E., Juntti-Berggren, L., and Grimelius, L. (1983) The distribution and ontogeny of polypeptide YY (PYY)- and pancreatic polypeptide (PP)-immunoreactive cells in the gastrointestinal tract of rat. *Histochemistry* **78**: 53-60.
- Erickson, J.C., Clegg, K.E., and Palmiter, R.D. (1996) Sensitivity to leptin and susceptibility to seizures of mice lacking neuropeptide Y. *Nature* **381**: 415-421.
- Ericsson, A., Hemsén, A., Lundberg, J.M., and Persson, H. (1991) Detection of neuropeptide Y-like immunoreactivity and messenger RNA in rat platelets: the effects of vinblastine, reserpine, and dexamethasone on NPY expression in blood cells. *Exp Cell Res* **192**: 604-611.
- Eriksson, H., Berglund, M.M., Holmberg, S.K., Kahl, U., Gehlert, D.R., and Larhammar, D. (1998) The cloned guinea pig pancreatic polypeptide receptor Y4 resembles more the human Y4 than does the rat Y4. *Regul Pept* **75-76**: 29-37.
- Eto, B., Boisset, M., Anini, Y., Voisin, T., and Desjeux, J.F. (1997) Comparison of the antisecretory effect of endogenous forms of peptide YY on fed and fasted rat jejunum. *Peptides* **18**: 1249-1255.
- Eva, C., Keinänen, K., Monyer, H., Seeburg, P., and Sprengel, R. (1990) Molecular cloning of a novel G protein-coupled receptor that may belong to the neuropeptide receptor family. *FEBS Lett* **271**: 81-84.

- Fabry, M., Langer, M., Rothen-Rutishauser, B., Wunderli-Allenspach, H., Hocker, H., and Beck-Sickingler, A.G. (2000) Monitoring of the internalization of neuropeptide Y on neuroblastoma cell line SK-N-MC. *Eur J Biochem* **267**: 5631-5637.
- Fang, Y., Lahiri, J., and Picard, L. (2003) G protein-coupled receptor microarrays for drug discovery. *Drug Discovery Today* **8**: 755-761.
- Feletou, M., Nicolas, J.P., Rodriguez, M., Beauverger, P., Galizzi, J.P., Boutin, J.A., and Duhault, J. (1999) NPY receptor subtype in the rabbit isolated ileum. *Br J Pharmacol* **127**: 795-801.
- Ferguson, S.S.G., Zhang, J., Barakt, L.S., and Caron, M.G. (1998) Molecular mechanisms of G protein-coupled receptor desensitization and resensitization. *Life Sci* **62**: 1561-1565.
- Ferrer, M., Kolodin, G.D., Zuck, P., Peltier, R., Berry, K., Mandala, S.M., Rosen, H., Ota, H., Ozaki, S., Inglese, J., and Strulovici, B. (2003) A fully automated [³⁵S]GTPγS scintillation proximity assay for the high-throughput screening of Gi-linked G protein-coupled receptors. *Assay Drug Dev Technol* **1**: 261-273.
- Fetissov, S.O., Kopp, J., and Hokfelt, T. (2004) Distribution of NPY receptors in the hypothalamus. *Neuropeptides* **38**: 175-188.
- Figler, R.A., Graber, S.G., Lindorfer, M.A., Yasuda, H., Linden, J., and Garrison, J.C. (1996) Reconstitution of recombinant bovine A1 adenosine receptors in Sf9 cell membranes with recombinant G proteins of defined composition. *Mol Pharmacol* **50**: 1587-1595.
- Fogh, J., Fogh, J.M., and Orfeo, T. (1977a) One hundred and twenty-seven cultured human tumor cell lines producing tumors in nude mice. *J Natl Cancer Inst* **59**: 221-226.
- Fogh, J., Wright, W.C., and Loveless, J.D. (1977b) Absence of HeLa cell contamination in 169 cell lines derived from human tumors. *J Natl Cancer Inst* **58**: 209-214.
- Franco-Cereceda, A., and Liska, J. (1998) Neuropeptide Y Y1 receptors in vascular pharmacology. *Eur J Pharmacol* **349**: 1-14.
- Fredriksson, R., Larson, E.T., Yan, Y.L., Postlethwait, J.H., and Larhammar, D. (2004) Novel neuropeptide Y Y2-like receptor subtype in zebrafish and frogs supports early vertebrate chromosome duplications. *J Mol Evol* **58**: 106-114.
- Fredriksson, R., Sjodin, P., Larson, E.T., Conlon, J.M., and Larhammar, D. (2006) Cloning and characterization of a zebrafish Y2 receptor. *Regul Pept* **133**: 32-40.
- Fuhlendorff, J., Gether, U., Aakerlund, L., Langeland-Johansen, N., Thogersen, H., Melberg, S.G., Olsen, U.B., Thastrup, O., and Schwartz, T.W. (1990) [Leu31, Pro34]neuropeptide Y: a specific Y1 receptor agonist. *Proc Natl Acad Sci U S A* **87**: 182-186.
- Fujimiya, M., Itoh, E., Kihara, N., Yamamoto, I., Fujimura, M., and Inui, A. (2000) Neuropeptide Y induces fasted pattern of duodenal motility via Y(2) receptors in conscious fed rats. *Am J Physiol Gastrointest Liver Physiol* **278**: G32-38.
- Gehlert, D., Beavers, L., Johnson, D., Gackenhimer, S., Schober, D., and Gadski, R. (1996a) Expression cloning of a human brain neuropeptide Y Y2 receptor. *Mol Pharmacol* **49**: 224-228.
- Gehlert, D. (1998) Multiple receptors for the pancreatic polypeptide (PP-fold) family: physiological implications. *Proc Soc Exp Biol Med* **218**: 7-22.
- Gehlert, D.R., Schober, D.A., Beavers, L., Gadski, R., Hoffman, J.A., Smiley, D.L., Chance, R.E., Lundell, I., and Larhammar, D. (1996b) Characterization of the peptide binding requirements for the cloned human pancreatic polypeptide-preferring receptor. *Mol Pharmacol* **50**: 112-118.
- Gehlert, D.R., Schober, D.A., Gackenhimer, S.L., Beavers, L., Gadski, R., Lundell, I., and Larhammar, D. (1997) [125I]Leu31, Pro34-PYY is a high affinity radioligand for rat PP1/Y4 and Y1 receptors: evidence for heterogeneity in pancreatic polypeptide receptors. *Peptides* **18**: 397-401.
- Gerald, C., Walker, M.W., Vaysse, P.J.-J., He, C., Branchek, T.A., and Weinshank, R.L. (1995) Expression Cloning and Pharmacological Characterization of a Human Hippocampal Neuropeptide Y/Peptide YY Y2 Receptor Subtype. *J Biol Chem* **270**: 26758-26761.
- Gerald, C., Walker, M.W., Criscione, L., Gustafson, E.L., Batzl-Hartmann, C., Smith, K.E., Vaysse, P., Durkin, M.M., Laz, T.M., Linemeyer, D.L., Schaffhauser, A.O., Whitebread, S., Hofbauer, K.G., Taber, R.I., Branchek, T.A., and Weinshank, R.L. (1996) A receptor subtype involved in neuropeptide-Y-induced food intake. *Nature* **382**: 168-171.
- Gessele, K. (1998) Zelluläre Testsysteme zur pharmakologischen Charakterisierung neuer Neuropeptid Y-Rezeptorantagonisten. In *Doctoral thesis, University of Regensburg*.
- Gibas, Z., Becher, R., Kawinski, E., Horoszewicz, J., and Sandberg, A.A. (1984) A high-resolution study of chromosome changes in a human prostatic carcinoma cell line (LNCaP). *Cancer Genet Cytogenet* **11**: 399-404.
- Gicquiaux, H., Lecat, S., Gaire, M., Dieterlen, A., Mely, Y., Takeda, K., Bucher, B., and Galzi, J.L. (2002) Rapid internalization and recycling of the human neuropeptide Y Y(1) receptor. *J Biol Chem* **277**: 6645-6655.

- Gilbert, W.R., Frank, B.H., Gavin, J.R., 3rd, and Gingerich, R.L. (1988) Characterization of specific pancreatic polypeptide receptors on basolateral membranes of the canine small intestine. *Proc Natl Acad Sci U S A* **85**: 4745-4749.
- Gilkey, J.C., Jaffe, L.F., Ridgway, E.B., and Reynolds, G.T. (1978) A free calcium wave traverses the activating egg of the medaka, *Oryzias latipes*. *J Cell Biol* **76**: 448-466.
- Goldman, L.A., Cutrone, E.C., Kottenko, S.V., Krause, C.D., and Langer, J.A. (1996) Modifications of vectors pEF-BOS, pcDNA1 and pcDNA3 result in improved convenience and expression. *BioTechniques* **21**: 1013-1015.
- Golombek, D.A., Biello, S.M., Rendon, R.A., and Harrington, M.E. (1996) Neuropeptide Y phase shifts the circadian clock in vitro via a Y2 receptor. *Neuroreport* **7**: 1315-1319.
- Goumain, M., Voisin, T., Lorinet, A.M., and Laburthe, M. (1998) Identification and distribution of mRNA encoding the Y1, Y2, Y4, and Y5 receptors for peptides of the PP-fold family in the rat intestine and colon. *Biochem Biophys Res Commun* **247**: 52-56.
- Goumain, M., Voisin, T., Lorinet, A.-M., Ducroc, R., Tsocas, A., Roze, C., Rouet-Benzineb, P., Herzog, H., Balasubramaniam, A., and Laburthe, M. (2001) The Peptide YY-Preferring Receptor Mediating Inhibition of Small Intestinal Secretion Is a Peripheral Y2 Receptor: Pharmacological Evidence and Molecular Cloning. *Mol Pharmacol* **60**: 124-134.
- Grady, E.F., Garland, A.M., Gamp, P.D., Lovett, M., Payan, D.G., and Bunnett, N.W. (1995) Delineation of the endocytic pathway of substance P and its seven-transmembrane domain NK1 receptor. *Mol Biol Cell* **6**: 509-524.
- Graichen, F. (2002) Neuropeptid Y Y1-Rezeptorantagonisten der Argininamid-Reihe: Entwicklung von Synthesemethoden an polymeren Trägern und Strategien zu Herstellung von Radioliganden. In *Doctoral Thesis, University of Regensburg*.
- Greene, L.A., and Tischler, A.S. (1976) Establishment of a noradrenergic clonal line of rat adrenal pheochromocytoma cells which respond to nerve growth factor. *Proc Natl Acad Sci U S A* **73**: 2424-2428.
- Gregor, P., Feng, Y., DeCarr, L.B., Cornfield, L.J., and McCaleb, M.L. (1996a) Molecular characterization of a second mouse pancreatic polypeptide receptor and its inactivated human homologue. *J Biol Chem* **271**: 27776-27781.
- Gregor, P., Millham, M.L., Feng, Y., DeCarr, L.B., McCaleb, M.L., and Cornfield, L.J. (1996b) Cloning and characterization of a novel receptor to pancreatic polypeptide, a member of the neuropeptide Y receptor family. *FEBS Lett* **381**: 58-62.
- Grisshammer, R. (1998) Expression of G protein-coupled receptors in *Escherichia coli*. In *Identification and Expression of G Protein-Coupled Receptors*. Lynch, K.R. (ed): Wiley-Liss, pp. 133-150.
- Grouzmann, E., Buclin, T., Martire, M., Cannizzaro, C., Dorner, B., Razaname, A., and Mutter, M. (1997) Characterization of a Selective Antagonist of Neuropeptide Y at the Y2 Receptor. Synthesis and pharmacological evaluation of a Y2 antagonist. *J Biol Chem* **272**: 7699-7706.
- Grouzmann, E., Meyer, C., Burki, E., and Brunner, H. (2001) Neuropeptide Y Y2 receptor signalling mechanisms in the human glioblastoma cell line LN319. *Peptides* **22**: 379-386.
- Grynkiewicz, G., Poenie, M., and Tsien, R. (1985) A new generation of Ca²⁺ indicators with greatly improved fluorescence properties. *J Biol Chem* **260**: 3440-3450.
- Guo, H., Castro, P.A., Palmiter, R.D., and Baraban, S.C. (2002) Y5 receptors mediate neuropeptide Y actions at excitatory synapses in area CA3 of the mouse hippocampus. *J Neurophysiol* **87**: 558-566.
- Gurney, A.M. (1990) Measurement and control of intracellular calcium. In *Receptor-Effector Coupling*. Hulme, E.C. (ed): Oxford University Press, pp. 117-154.
- Gurrath, M. (2001) Peptide-binding G protein-coupled receptors: new opportunities for drug design. *Curr Med Chem* **8**: 1605-1648.
- Haigler, H., Maxfield, F., Willingham, M., and Pastan, I. (1980) Dansylcadaverine inhibits internalization of 125I-epidermal growth factor in BALB 3T3 cells. *J Biol Chem* **255**: 1239-1241.
- Hamm, H.E. (1998) The Many Faces of G Protein Signaling. *J Biol Chem* **273**: 669-672.
- Hansel, D.E., Eipper, B.A., and Ronnett, G.V. (2001) Neuropeptide Y functions as a neuroproliferative factor. *Nature* **410**: 940-944.
- Hatse, S., Princen, K., Liekens, S., Vermeire, K., De Clercq, E., and Schols, D. (2004) Fluorescent CXCL12AF647 as a novel probe for nonradioactive CXCL12/CXCR4 cellular interaction studies. *Cytometry A* **61**: 178-188.
- Hazelwood, R.L. (1993) The pancreatic polypeptide (PP-fold) family: gastrointestinal, vascular, and feeding behavioral implications. *Proc Soc Exp Biol Med* **202**: 44-63.
- Hermans, E. (2003) Biochemical and pharmacological control of the multiplicity of coupling at G-protein-coupled receptors. *Pharmacol Ther* **99**: 25-44.

- Herzog, H., Hort, Y.J., Ball, H.J., Hayes, G., Shine, J., and Selbie, L.A. (1992) Cloned human neuropeptide Y receptor couples to two different second messenger systems. *Proc Natl Acad Sci U S A* **89**: 5794-5798.
- Herzog, H., Baumgartner, M., Vivero, C., Selbie, L.A., Auer, B., and Shine, J. (1993a) Genomic organization, localization, and allelic differences in the gene for the human neuropeptide Y Y1 receptor. *J Biol Chem* **268**: 6703-6707.
- Herzog, H., Hort, Y.J., Shine, J., and Selbie, L.A. (1993b) Molecular cloning, characterization, and localization of the human homolog to the reported bovine NPY Y3 receptor: lack of NPY binding and activation. *DNA Cell Biol* **12**: 465-471.
- Herzog, H., Darby, K., Ball, H., Hort, Y., Beck-Sickinger, A., and Shine, J. (1997) Overlapping gene structure of the human neuropeptide Y receptor subtypes Y1 and Y5 suggests coordinate transcriptional regulation. *Genomics* **41**: 315-319.
- Hipskind, P.A., Lobb, K.L., Nixon, J.A., Britton, T.C., Bruns, R.F., Catlow, J., Dieckman-McGinty, D.K., Gackenheimer, S.L., Gitter, B.D., Iyengar, S., Schober, D.A., Simmons, R.M., Swanson, S., Zarrinmayeh, H., Zimmerman, D.M., and Gehlert, D.R. (1997) Potent and selective 1,2,3-trisubstituted indole NPY Y-1 antagonists. *J Med Chem* **40**: 3712-3714.
- Holliday, N.D., Michel, M.C., and Cox, H.M. (2004) NPY receptor subtypes and their signal transduction. In *Handbook of experimental pharmacology*. Vol. 162. Michel, M.C. (ed): Springer-Verlag, pp. 45-73.
- Hu, Y., Bloomquist, B.T., Cornfield, L.J., DeCarr, L.B., Flores-Riveros, J.R., Friedman, L., Jiang, P., Lewis-Higgins, L., Sadlowski, Y., Schaefer, J., Velazquez, N., and McCaleb, M.L. (1996) Identification of a novel hypothalamic neuropeptide Y receptor associated with feeding behavior. *J Biol Chem* **271**: 26315-26319.
- Huhman, K.L., Gillespie, C.F., Marvel, C.L., and Albers, H.E. (1996) Neuropeptide Y phase shifts circadian rhythms in vivo via a Y2 receptor. *Neuroreport* **7**: 1249-1252.
- Hulsey, M.G., Pless, C.M., White, B.D., and Martin, R.J. (1995) ICV administration of anti-NPY antisense oligonucleotide: effects on feeding behavior, body weight, peptide content and peptide release. *Regul Pept* **59**: 207-214.
- Hwa, J.J., Witten, M.B., Williams, P., Ghibaudi, L., Gao, J., Salisbury, B.G., Mullins, D., Hamud, F., Strader, C.D., and Parker, E.M. (1999) Activation of the NPY Y5 receptor regulates both feeding and energy expenditure. *Am J Physiol* **277**: R1428-1434.
- Inouye, S., Noguchi, M., Sakaki, Y., Takagi, Y., Miyata, T., Iwanaga, S., Miyata, T., and Tsuji, F.I. (1985) Cloning and Sequence Analysis of cDNA for the Luminescent Protein Aequorin. *PNAS* **82**: 3154-3158.
- Inui, A., Mizuno, N., Ooya, M., Suenaga, K., Morioka, H., Ogawa, T., Ishida, M., and Baba, S. (1985) Cross-reactivities of neuropeptide Y and peptide YY with pancreatic polypeptide antisera: evidence for the existence of pancreatic polypeptide in the brain. *Brain Res* **330**: 386-389.
- Inui, A., Okita, M., Nakajima, M., Inoue, T., Sakatani, N., Oya, M., Morioka, H., Okimura, Y., Chihara, K., and Baba, S. (1991) Neuropeptide regulation of feeding in dogs. *Am J Physiol* **261**: R588-594.
- Inui, A., Okita, M., Miura, M., Hirose, Y., Mizuno, N., Baba, S., and Kasuga, M. (1993) Plasma and cerebroventricular fluid levels of pancreatic polypeptide in the dog: effects of feeding, insulin-induced hypoglycemia, and physical exercise. *Endocrinology* **132**: 1235-1239.
- Irvine, R. (2001) Inositol phosphates: Does IP4 run a protection racket? *Curr Biol* **11**: R172-R174.
- Ishiguchi, T., Amano, T., Matsubayashi, H., Tada, H., Fujita, M., and Takahashi, T. (2001) Centrally administered neuropeptide Y delays gastric emptying via Y2 receptors in rats. *Am J Physiol Regul Integr Comp Physiol* **281**: R1522-1530.
- Itani, H., Ito, H., Sakata, Y., Hatakeyama, Y., Oohashi, H., and Satoh, Y. (2002) Novel potent antagonists of human neuropeptide Y Y5 receptors. Part 2: substituted benzo[a]cycloheptene derivatives. *Bioorg Med Chem Lett* **12**: 757-761.
- Jablonowski, J.A., Chai, W., Li, X., Rudolph, D.A., Murray, W.V., Youngman, M.A., Dax, S.L., Nepomuceno, D., Bonaventure, P., Lovenberg, T.W., and Carruthers, N.I. (2004) Novel non-peptidic neuropeptide Y Y2 receptor antagonists. *Bioorg Med Chem Lett* **14**: 1239-1242.
- Jackson, W.C., Bennett, T.A., Edwards, B.S., Prossnitz, E., Lopez, G.P., and Sklar, L.A. (2002a) Performance of in-line microfluidic mixers in laminar flow for high-throughput flow cytometry. *BioTechniques* **33**: 220-226.
- Jackson, W.C., Kuckuck, F., Edwards, B.S., Mammoli, A., Gallegos, C.M., Lopez, G.P., Buranda, T., and Sklar, L.A. (2002b) Mixing small volumes for continuous high-throughput flow cytometry: performance of a mixing Y and peristaltic sample delivery. *Cytometry* **47**: 183-191.
- Jazin, E.E., Yoo, H., Blomqvist, A.G., Yee, F., Weng, G., Walker, M.W., Salon, J., Larhammar, D., and Wahlestedt, C. (1993) A proposed bovine neuropeptide Y (NPY) receptor cDNA clone, or its human homologue, confers neither NPY binding sites nor NPY responsiveness on transfected cells. *Regul Pept* **47**: 247-258.

- Jones, K., Hibbert, F., and Keenan, M. (1999) Glowing jellyfish, luminescence and a molecule called coelenterazine. *Trends Biotechnol* **17**: 477-481.
- Jorgensen, J.C., Fuhlendorff, J., and Schwartz, T.W. (1990) Structure-function studies on neuropeptide Y and pancreatic polypeptide--evidence for two PP-fold receptors in vas deferens. *Eur J Pharmacol* **186**: 105-114.
- Juanenea, L., Galiano, S., Erviti, O., Moreno, A., Perez, S., Aldana, I., and Monge, A. (2004) Synthesis and evaluation of new hydrazide derivatives as neuropeptide Y Y5 receptor antagonists for the treatment of obesity. *Bioorg Med Chem* **12**: 4717-4723.
- June, C.H., and Rabinovitch, P.S. (1994) Intracellular ionized calcium. *Methods Cell Biol* **41**: 149-174.
- Kaga, T., Fujimiya, M., and Inui, A. (2001) Emerging functions of neuropeptide Y Y(2) receptors in the brain. *Peptides* **22**: 501-506.
- Kaighn, M.E., Narayan, K.S., Ohnuki, Y., Lechner, J.F., and Jones, L.W. (1979) Establishment and characterization of a human prostatic carcinoma cell line (PC-3). *Invest Urol* **17**: 16-23.
- Kalra, S.P., Xu, B., Dube, M.G., Moldawer, L.L., Martin, D., and Kalra, P.S. (1998) Leptin and ciliary neurotropic factor (CNTF) inhibit fasting-induced suppression of luteinizing hormone release in rats: role of neuropeptide Y. *Neurosci Lett* **240**: 45-49.
- Kalra, S.P., and Kalra, P.S. (2004) NPY and cohorts in regulating appetite, obesity and metabolic syndrome: beneficial effects of gene therapy. *Neuropeptides* **38**: 201-211.
- Kanatani, A., Ishihara, A., Iwaasa, H., Nakamura, K., Okamoto, O., Hidaka, M., Ito, J., Fukuroda, T., MacNeil, D.J., Van der Ploeg, L.H., Ishii, Y., Okabe, T., Fukami, T., and Ihara, M. (2000a) L-152,804: orally active and selective neuropeptide Y Y5 receptor antagonist. *Biochem Biophys Res Commun* **272**: 169-173.
- Kanatani, A., Mashiko, S., Murai, N., Sugimoto, N., Ito, J., Fukuroda, T., Fukami, T., Morin, N., MacNeil, D.J., Van der Ploeg, L.H., Saga, Y., Nishimura, S., and Ihara, M. (2000b) Role of the Y1 receptor in the regulation of neuropeptide Y-mediated feeding: comparison of wild-type, Y1 receptor-deficient, and Y5 receptor-deficient mice. *Endocrinology* **141**: 1011-1016.
- Kanatani, A., Hata, M., Mashiko, S., Ishihara, A., Okamoto, O., Haga, Y., Ohe, T., Kanno, T., Murai, N., Ishii, Y., Fukuroda, T., Fukami, T., and Ihara, M. (2001) A typical Y1 receptor regulates feeding behaviors: effects of a potent and selective Y1 antagonist, J-115814. *Mol Pharmacol* **59**: 501-505.
- Kao, J.P., Harootunian, A.T., and Tsien, R.Y. (1989) Photochemically generated cytosolic calcium pulses and their detection by fluo-3. *J Biol Chem* **264**: 8179-8184.
- Kaplan, J., Ward, D.M., and Wiley, H.S. (1985) Phenylarsine oxide-induced increase in alveolar macrophage surface receptors: evidence for fusion of internal receptor pools with the cell surface. *J Cell Biol* **101**: 121-129.
- Kask, A., Vasar, E., Heidmets, L.T., Allikmets, L., and Wikberg, J.E. (2001) Neuropeptide Y Y(5) receptor antagonist CGP71683A: the effects on food intake and anxiety-related behavior in the rat. *Eur J Pharmacol* **414**: 215-224.
- Katsuura, G., Asakawa, A., and Inui, A. (2002) Roles of pancreatic polypeptide in regulation of food intake. *Peptides* **23**: 323-329.
- Katz, A., Wu, D., and Simon, M.I. (1992) Subunits beta gamma of heterotrimeric G protein activate beta 2 isoform of phospholipase C. *Nature* **360**: 686-689.
- Kawabata, A., and Kuroda, R. (2000) Protease-activated receptor (PAR), a novel family of G protein-coupled seven trans-membrane domain receptors: activation mechanisms and physiological roles. *Jpn J Pharmacol* **82**: 171-174.
- Kawanishi, Y., Takenaka, H., and Hanasaki, K. (2001) Preparation of sulfonamides and sulfonamides as NPY Y5 antagonists, Patent, WO 0137826, Japan
- Keire, D.A., Kobayashi, M., Solomon, T.E., and Reeve, J.R., Jr. (2000) Solution structure of monomeric peptide YY supports the functional significance of the PP-fold. *Biochemistry* **39**: 9935-9942.
- Keith, I.M., and Ekman, R. (1990) PYY-like material and its spatial relationship with NPY, CGRP and 5-HT in the lung of the Syrian golden hamster. *Cell Tissue Res* **262**: 543-550.
- Kenakin, T., Morgan, P., Lutz, M., and Weiss, J. (2000) The evolution of drug-receptor models: The cubic ternary complex model for G protein-coupled receptors. In *Handbook of Experimental Pharmacology*. Vol. 148. Kenakin, T. and Angus, J.A. (eds): Springer-Verlag, Berlin Heidelberg New York, pp. 147-165.
- Kenakin, T. (2004) G-protein coupled receptors as allosteric machines. *Receptors Channels* **10**: 51-60.
- Kenakin, T.P. (1989) Challenges for receptor theory as a tool for drug and drug receptor classification. *Trends Pharmacol Sci* **10**: 18-22.
- Khiat, A., Labelle, M., and Boulanger, Y. (1998) Three-dimensional structure of the Y1 receptor agonist [Leu31, Pro34]NPY as determined by NMR and molecular modeling. *J Pept Res* **51**: 317-322.

- Kimmel, J.R., Pollock, H.G., and Hazelwood, R.L. (1968) Isolation and characterization of chicken insulin. *Endocrinology* **83**: 1323-1330.
- Kimmel, J.R., Hayden, L.J., and Pollock, H.G. (1975) Isolation and characterization of a new pancreatic polypeptide hormone. *J Biol Chem* **250**: 9369-9376.
- King, P.J., Williams, G., Doods, H., and Widdowson, P.S. (2000) Effect of a selective neuropeptide Y Y2 receptor antagonist, BIIE0246 on neuropeptide Y release. *Eur J Pharmacol* **396**: R1-R3.
- Knight, P.J., and Grigliatti, T.A. (2004) Chimeric G proteins extend the range of insect cell-based functional assays for human G protein-coupled receptors. *J Recept Signal Transduct Res* **24**: 241-256.
- Knight, P.J.K., Pfeifer, T.A., and Grigliatti, T.A. (2003) A functional assay for G-protein-coupled receptors using stably transformed insect tissue culture cell lines. *Anal Biochem* **320**: 88-103.
- Kobilka, B.K. (1995) Amino and carboxyl terminal modifications to facilitate the production and purification of a G protein-coupled receptor. *Anal Biochem* **231**: 269-271.
- Koglin, N., Zorn, C., Beumer, R., Cabrele, C., Bubert, C., Sewald, N., Reiser, O., and Beck-Sickingher, A.G. (2003) Analogues of neuropeptide Y containing beta-aminocyclopropane carboxylic acids are the shortest linear peptides that are selective for the Y1 receptor. *Angew Chem Int Ed Engl* **42**: 202-205.
- Kopp, J., Xu, Z.Q., Zhang, X., Pedrazzini, T., Herzog, H., Kresse, A., Wong, H., Walsh, J.H., and Hokfelt, T. (2002) Expression of the neuropeptide Y Y1 receptor in the CNS of rat and of wild-type and Y1 receptor knock-out mice. Focus on immunohistochemical localization. *Neuroscience* **111**: 443-532.
- Kostenis, E. (2001) Is Galpha16 the optimal tool for fishing ligands of orphan G-protein-coupled receptors? *Trends Pharmacol Sci* **22**: 560-564.
- Kozak, M. (2002) Pushing the limits of the scanning mechanism for initiation of translation. *Gene* **299**: 1-34.
- Kraiczi, H., Karlsson, G., and Ekman, R. (1997) Analytical extraction of regulatory peptides from rat lung tissue. *Peptides* **18**: 1597-1601.
- Krause, J., Eva, C., Seeburg, P.H., and Sprengel, R. (1992) Neuropeptide Y1 subtype pharmacology of a recombinantly expressed neuropeptide receptor. *Mol Pharmacol* **41**: 817-821.
- Kristiansen, K. (2004) Molecular mechanisms of ligand binding, signaling, and regulation within the superfamily of G-protein-coupled receptors: molecular modeling and mutagenesis approaches to receptor structure and function. *Pharmacol Ther* **103**: 21-80.
- Larhammar, D., Blomqvist, A.G., Yee, F., Jazin, E., Yoo, H., and Wahlested, C. (1992) Cloning and functional expression of a human neuropeptide Y/peptide YY receptor of the Y1 type. *J Biol Chem* **267**: 10935-10938.
- Larhammar, D. (1996) Evolution of neuropeptide Y, peptide YY and pancreatic polypeptide. *Regul Pept* **62**: 1-11.
- Larhammar, D., Wraith, A., Berglund, M.M., Holmberg, S.K., and Lundell, I. (2001) Origins of the many NPY-family receptors in mammals. *Peptides* **22**: 295-307.
- Larhammar, D., Fredriksson, R., Larson, E.T., and Salaneck, E. (2004) Phylogeny of NPY-family peptides and their receptors. In *Handbook of experimental pharmacology*. Vol. 162. Michel, M.C. (ed): Springer-Verlag, pp. 75-100.
- Larhammar, D., and Salaneck, E. (2004) Molecular evolution of NPY receptor subtypes. *Neuropeptides* **38**: 141-151.
- Larsen, P.J., Sheikh, S.P., Jakobsen, C.R., Schwartz, T.W., and Mikkelsen, J.D. (1993) Regional distribution of putative NPY Y1 receptors and neurons expressing Y1 mRNA in forebrain areas of the rat central nervous system. *Eur J Neurosci* **5**: 1622-1637.
- Larsson, T.A., Larson, E.T., Fredriksson, R., Conlon, J.M., and Larhammar, D. (2005) Characterization of NPY receptor subtypes Y2 and Y7 in rainbow trout *Oncorhynchus mykiss*. *Peptides*.
- Le Poul, E., Hisada, S., Mizuguchi, Y., Dupriez, V.J., Burgeon, E., and Detheux, M. (2002) Adaptation of aequorin functional assay to high throughput screening. *J Biomol Screen* **7**: 57-65.
- Lee, A., and Durieux, M.E. (1998) The use of *Xenopus laevis* oocytes for the study of G protein-coupled receptors. In *Identification and Expression of G Protein-Coupled Receptors*. Lynch, K.R. (ed): Wiley-Liss, pp. 73-96.
- Lee, C.C., and Miller, R.J. (1998) Is there really an NPY Y3 receptor? *Regul Pept* **75-76**: 71-78.
- Leff, P. (1995) The two-state model of receptor activation. *Trends Pharmacol Sci* **16**: 89-97.
- Leibovitz, A., Stinson, J.C., McCombs, W.B., 3rd, McCoy, C.E., Mazur, K.C., and Mabry, N.D. (1976) Classification of human colorectal adenocarcinoma cell lines. *Cancer Res* **36**: 4562-4569.
- Levens, N.R., Feletou, M., Galizzi, J.-P., Fauchere, J.-L., and Della-Zuana, O. (2004) NPY effects on food intake and metabolism. In *Handbook of experimental pharmacology*. Vol. 162. Michel, M.C. (ed): Springer-Verlag, pp. 283-325.

- Li, A.-J., and Ritter, S. (2005) Functional expression of neuropeptide Y receptors in human neuroblastoma cells. *Regul Pept* **129**: 119-124.
- Lieber, M., Mazzetta, J., Nelson-Rees, W., Kaplan, M., and Todaro, G. (1975) Establishment of a continuous tumor-cell line (panc-1) from a human carcinoma of the exocrine pancreas. *Int J Cancer* **15**: 741-747.
- Lin, S., Boey, D., and Herzog, H. (2004) NPY and Y receptors: lessons from transgenic and knockout models. *Neuropeptides* **38**: 189-200.
- Lin, T.-M., and Chance, R. (1974) Gastrointestinal actions of a new bovine pancreatic peptide (BPP). In *Endocrinology of the Gut*. Brooks, C.a. (ed): Charles B. Slack, Inc.
- Lipp, P., Bootman, M.D., and Collins, T. (2001) Photometry, video imaging, confocal and multi-photon microscopy approaches in calcium signalling studies. In *Calcium Signalling*. Tepikin, A.V. (ed): Oxford University Press, pp. 17-44.
- Lopez-Valpuesta, F.J., Nyce, J.W., Griffin-Biggs, T.A., Ice, J.C., and Myers, R.D. (1996) Antisense to NPY-Y1 demonstrates that Y1 receptors in the hypothalamus underlie NPY hypothermia and feeding in rats. *Proc Biol Sci* **263**: 881-886.
- Lundberg, J.M., Tatemoto, K., Terenius, L., Hellstrom, P.M., Mutt, V., Hokfelt, T., and Hamberger, B. (1982) Localization of peptide YY (PYY) in gastrointestinal endocrine cells and effects on intestinal blood flow and motility. *Proc Natl Acad Sci U S A* **79**: 4471-4475.
- Lundell, I., Blomqvist, A.G., Berglund, M.M., Schober, D.A., Johnson, D., Statnick, M.A., Gadski, R.A., Gehlert, D.R., and Larhammar, D. (1995) Cloning of a human receptor of the NPY receptor family with high affinity for pancreatic polypeptide and peptide YY. *J Biol Chem* **270**: 29123-29128.
- Lundell, I., Statnick, M.A., Johnson, D., Schober, D.A., Starback, P., Gehlert, D.R., and Larhammar, D. (1996) The cloned rat pancreatic polypeptide receptor exhibits profound differences to the orthologous receptor. *Proc Natl Acad Sci U S A* **93**: 5111-5115.
- Lundell, I., Eriksson, H., Marklund, U., and Larhammar, D. (2001) Cloning and characterization of the guinea pig neuropeptide Y receptor Y5. *Peptides* **22**: 357-363.
- Lundell, I., Boswell, T., and Larhammar, D. (2002) Chicken neuropeptide Y-family receptor Y4: a receptor with equal affinity for pancreatic polypeptide, neuropeptide Y and peptide YY. *J Mol Endocrinol* **28**: 225-235.
- Lynch, J.W., Lemos, V.S., Bucher, B., Stoclet, J.C., and Takeda, K. (1994) A pertussis toxin-insensitive calcium influx mediated by neuropeptide Y2 receptors in a human neuroblastoma cell line. *J Biol Chem* **269**: 8226-8233.
- M. E. Granados, E.S., A. Saavedra-Molina, (1997) Use of pluronic acid F-127 with Fluo-3/AM probe to determine intracellular calcium changes elicited in bean protoplasts. *Phytochemical Analysis* **8**: 204-208.
- Magalhaes, P., Pinton, P., Filippin, L., and Pozzan, T. (2001) Targeting of bioluminescent probes and calcium measurements in different subcellular compartments. In *Calcium Signalling (2nd Edition)*: Oxford University Press, Oxford, UK, pp. 59-75.
- Malendowicz, L.K., Markowska, A., and Zabel, M. (1996) Neuropeptide Y-related peptides and hypothalamo-pituitary-adrenal axis function. *Histol Histopathol* **11**: 485-494.
- Malis, D.D., Grouzmann, E., Morel, D.R., Mutter, M., and Lacroix, J.S. (1999) Influence of TASP-V, a novel neuropeptide Y (NPY) Y2 agonist, on nasal and bronchial responses evoked by histamine in anaesthetized pigs and in humans. *Br J Pharmacol* **126**: 989-996.
- Malmstrom, R.E. (2001) Vascular pharmacology of BIIIE0246, the first selective non-peptide neuropeptide Y Y(2) receptor antagonist, in vivo. *Br J Pharmacol* **133**: 1073-1080.
- Malmstrom, R.E., Balmer, K.C., Weilitz, J., Nordlander, M., and Sjolander, M. (2001) Pharmacology of H 394/84, a dihydropyridine neuropeptide Y Y(1) receptor antagonist, in vivo. *Eur J Pharmacol* **418**: 95-104.
- Marklund, U., Bystrom, M., Gedda, K., Larefalk, A., Juneblad, K., Nystrom, S., and Ekstrand, A.J. (2002) Intron-mediated expression of the human neuropeptide Y Y1 receptor. *Mol Cell Endocrinol* **188**: 85-97.
- Marsh, D.J., Hollopeter, G., Kafer, K.E., and Palmiter, R.D. (1998) Role of the Y5 neuropeptide Y receptor in feeding and obesity. *Nat Med* **4**: 718-721.
- Marullo, S., Delavier-Klutchko, C., Eshdat, Y., Strosberg, A.D., and Emorine, L. (1988) Human beta 2-adrenergic receptors expressed in Escherichia coli membranes retain their pharmacological properties. *Proc Natl Acad Sci U S A* **85**: 7551-7555.
- Mashiko, S., Ishihara, A., Iwaasa, H., Sano, H., Oda, Z., Ito, J., Yumoto, M., Okawa, M., Suzuki, J., Fukuroda, T., Jitsuoka, M., Morin, N.R., MacNeil, D.J., Van der Ploeg, L.H., Ihara, M., Fukami, T., and Kanatani, A. (2003) Characterization of neuropeptide Y (NPY) Y5 receptor-mediated obesity in mice: chronic intracerebroventricular infusion of D-Trp(34)NPY. *Endocrinology* **144**: 1793-1801.

- Matsumoto, M., Nomura, T., Momose, K., Ikeda, Y., Kondou, Y., Akiho, H., Togami, J., Kimura, Y., Okada, M., and Yamaguchi, T. (1996) Inactivation of a novel neuropeptide Y/peptide YY receptor gene in primate species. *J Biol Chem* **271**: 27217-27220.
- Mayer, M. (2002) Entwicklung fluorimetrischer Methoden zur Bestimmung der Affinität und Aktivität von Liganden G-Protein-gekoppelter Rezeptoren an intakten Zellen. In *Doctoral Thesis, University of Regensburg*.
- Michel, M. (1994) Rapid desensitization of adrenaline- and neuropeptide Y-stimulated Ca²⁺ mobilization in HEL-cells. *Br J Pharmacol* **112**: 499-504.
- Michel, M.C., and Motulsky, H.J. (1990) HE 90481: A competitive nonpetidergic antagonist at neuropeptide Y receptors. *Ann N Y Acad Sci* **611**: 392-394.
- Michel, M.C. (1998) Concomitant regulation of Ca²⁺ mobilization and Gi3 expression in human erythroleukemia cells. *Eur J Pharmacol* **348**: 135-141.
- Michel, M.C., Beck-Sickingler, A., Cox, H., Doods, H.N., Herzog, H., Larhammar, D., Quirion, R., Schwartz, T., and Westfall, T. (1998) XVI. International Union of Pharmacology recommendations for the nomenclature of neuropeptide Y, peptide YY, and pancreatic polypeptide receptors. *Pharmacol Rev* **50**: 143-150.
- Miller, A.D. (1993) Use of Retroviral Vectors for Gene Transfer and Expression. In *Recombinant DNA, Part H*. Vol. 217. Wu, R. (ed): Academic Press, pp. 581-599.
- Miller, L.K. (1988) Baculoviruses as gene expression vectors. *Annu Rev Microbiol* **42**: 177-199.
- Milligan, G., Marshall, F., and Rees, S. (1996) G16 as a universal G protein adapter: implications for agonist screening strategies. *Trends Pharmacol Sci* **17**: 235-237.
- Milligan, G., and Rees, S. (1999) Chimaeric G alpha proteins: their potential use in drug discovery. *Trends Pharmacol Sci* **20**: 118-124.
- Miyawaki, A., Griesbeck, O., Heim, R., and Tsien, R.Y. (1999) Dynamic and quantitative Ca²⁺ measurements using improved cameleons. *Proc Natl Acad Sci U S A* **96**: 2135-2140.
- Miyawaki, A., Mizuno, H., Llopis, J., R.Y., T., and Jalink, K. (2001) Cameleons as cytosolic and intraorganellar calcium probes. In *Calcium signalling*. Tepikin, A. (ed): Oxford University Press, pp. 3-16.
- Miyazaki, K., and Funakoshi, A. (1988) Distribution of pancreatic polypeptide-like immunoreactivity in rat tissues. *Regul Pept* **21**: 37-43.
- Monks, S.A., Karagianis, G., Howlett, G.J., and Norton, R.S. (1996) Solution structure of human neuropeptide Y. *J Biomol NMR* **8**: 379-390.
- Moran, T.H. (2003) Pancreatic polypeptide: more than just another gut hormone? *Gastroenterology* **124**: 1542-1544.
- Moreno, A., Perez, S., Galiano, S., Juanenea, L., Erviti, O., Frigola, C., Aldana, I., and Monge, A. (2004) Synthesis and evaluation of new arylsulfonamidomethylcyclohexyl derivatives as human neuropeptide Y Y5 receptor antagonists for the treatment of obesity. *Eur J Med Chem* **39**: 49-58.
- Morris, M.J. (2004) Neuropeptide Y and cardiovascular function. In *Handbook of experimental pharmacology*. Vol. 162. Michel, M.C. (ed): Springer-Verlag, pp. 327-359.
- Morton, K.D., McCloskey, M.J., and Potter, E.K. (1999) Cardiorespiratory responses to intracerebroventricular injection of neuropeptide Y in anaesthetised dogs. *Regul Pept* **81**: 81-88.
- Moser, C. (1999) Pharmakologische Untersuchungen zur Neuropeptid Y Y1-, Y2-, und Y5-Rezeptorselektivität peptidischer und nichtpeptidischer Liganden: Klonierung und funktionelle Expression des humanen Y5-Rezeptors in HEC-1-B-Zellen. In *Doctoral Thesis, University of Regensburg*.
- Moser, C., Bernhardt, G., Michel, J., Schwarz, H., and Buschauer, A. (2000) Cloning and functional expression of the hNPY Y5 receptor in human endometrial cancer (HEC-1B) cells. *Can J Physiol Pharmacol* **78**: 134-142.
- Motulsky, H.J., and Michel, M.C. (1988) Neuropeptide Y mobilizes Ca²⁺ and inhibits adenylate cyclase in human erythroleukemia cells. *Am J Physiol* **255**: E880-885.
- Mullins, D., Kirby, D., Hwa, J., Guzzi, M., Rivier, J., and Parker, E. (2001) Identification of potent and selective neuropeptide Y Y(1) receptor agonists with orexigenic activity in vivo. *Mol Pharmacol* **60**: 534-540.
- Mullins, D.E., Guzzi, M., Xia, L., and Parker, E.M. (2000) Pharmacological characterization of the cloned neuropeptide Y y(6) receptor. *Eur J Pharmacol* **395**: 87-93.
- Murakami, Y., Hara, H., Okada, T., Hashizume, H., Kii, M., Ishihara, Y., Ishikawa, M., Shimamura, M., Mihara, S., Kato, G., Hanasaki, K., Hagishita, S., and Fujimoto, M. (1999) 1,3-Disubstituted benzazepines as novel, potent, selective neuropeptide Y Y1 receptor antagonists. *J Med Chem* **42**: 2621-2632.
- Myers, A.K., Farhat, M.Y., Vaz, C.A., Keiser, H.R., and Zukowska-Grojec, Z. (1988) Release of immunoreactive-neuropeptide by rat platelets. *Biochem Biophys Res Commun* **155**: 118-122.

- Nakajima, M., Inui, A., Asakawa, A., Momose, K., Ueno, N., Teranishi, A., Baba, S., and Kasuga, M. (1998) Neuropeptide Y produces anxiety via Y2-type receptors. *Peptides* **19**: 359-363.
- Nakamura, M., Sakanaka, C., Aoki, Y., Ogasawara, H., Tsuji, T., Kodama, H., Matsumoto, T., Shimizu, T., and Noma, M. (1995) Identification of two isoforms of mouse neuropeptide Y-Y1 receptor generated by alternative splicing. Isolation, genomic structure, and functional expression of the receptors. *J Biol Chem* **270**: 30102-30110.
- Naveilhan, P., Canals, J.M., Arenas, E., and Ernfors, P. (2001) Distinct roles of the Y1 and Y2 receptors on neuropeptide Y-induced sensitization to sedation. *J Neurochem* **78**: 1201-1207.
- Naviaux, R.K., Costanzi, E., Haas, M., and Verma, I.M. (1996) The pCL vector system: rapid production of helper-free, high-titer, recombinant retroviruses. *J Virol* **70**: 5701-5705.
- Neve, K.A., and Neve, R.L. (1998) Stable expression of G protein-coupled receptors in mammalian cells. In *Identification and Expression of G Protein-Coupled Receptors*. Lynch, K.R. (ed): Wiley-Liss.
- Nolan, J.P., Posner, R.G., Martin, J.C., Habberset, R., and Sklar, L.A. (1995) A rapid mix flow cytometer with subsecond kinetic resolution. *Cytometry* **21**: 223-229.
- Nolan, J.P., and Sklar, L.A. (1998) The emergence of flow cytometry for sensitive, real-time measurements of molecular interactions. *Nat Biotechnol* **16**: 633-638.
- Nomura, M., Inouye, S., Ohmiya, Y., and Tsuji, F.I. (1991) A C-terminal proline is required for bioluminescence of the Ca²⁺-binding photoprotein, aequorin. *FEBS Lett* **295**: 63-66.
- Nordmann, A., Blommers, M.J., Fretz, H., Arvinte, T., and Drake, A.F. (1999) Aspects of the molecular structure and dynamics of neuropeptide Y. *Eur J Biochem* **261**: 216-226.
- Offermanns, S., and Simon, M.I. (1995) G alpha 15 and G alpha 16 couple a wide variety of receptors to phospholipase C. *J Biol Chem* **270**: 15175-15180.
- Offermanns, S. (2003) G-proteins as transducers in transmembrane signalling. *Prog Biophys Mol Biol* **83**: 101-130.
- Palczewski, K., Kumasaka, T., Hori, T., Behnke, C.A., Motoshima, H., Fox, B.A., Le Trong, I., Teller, D.C., Okada, T., Stenkamp, R.E., Yamamoto, M., and Miyano, M. (2000) Crystal structure of rhodopsin: A G protein-coupled receptor. *Science* **289**: 739-745.
- Parker, E.M., Babij, C.K., Balasubramaniam, A., Burrier, R.E., Guzzi, M., Hamud, F., Mukhopadhyay, G., Rudinski, M.S., Tao, Z., Tice, M., Xia, L., Mullins, D.E., and Salisbury, B.G. (1998) GR231118 (1229U91) and other analogues of the C-terminus of neuropeptide Y are potent neuropeptide Y Y1 receptor antagonists and neuropeptide Y Y4 receptor agonists. *Eur J Pharmacol* **349**: 97-105.
- Parker, E.M., Balasubramaniam, A., Guzzi, M., Mullins, D.E., Salisbury, B.G., Sheriff, S., Witten, M.B., and Hwa, J.J. (2000) [D-Trp(34)] neuropeptide Y is a potent and selective neuropeptide Y Y(5) receptor agonist with dramatic effects on food intake. *Peptides* **21**: 393-399.
- Parker, M.S., Berglund, M.M., Lundell, I., and Parker, S.L. (2001a) Blockade of pancreatic polypeptide-sensitive neuropeptide Y (NPY) receptors by agonist peptides is prevented by modulators of sodium transport. Implications for receptor signaling and regulation. *Peptides* **22**: 887-898.
- Parker, M.S., Lundell, I., and Parker, S.L. (2002a) Pancreatic polypeptide receptors: affinity, sodium sensitivity and stability of agonist binding. *Peptides* **23**: 291-303.
- Parker, M.S., Sah, R., Sheriff, S., Balasubramaniam, A., and Parker, S.L. (2005) Internalization of cloned pancreatic polypeptide receptors is accelerated by all types of Y4 agonists. *Regul Pept* **132**: 91-101.
- Parker, R.M., and Herzog, H. (1998) Comparison of Y-receptor subtype expression in the rat hippocampus. *Regul Pept* **75-76**: 109-115.
- Parker, R.M., and Herzog, H. (1999) Regional distribution of Y-receptor subtype mRNAs in rat brain. *Eur J Neurosci* **11**: 1431-1448.
- Parker, S.L., Kane, J.K., Parker, M.S., Berglund, M.M., Lundell, I.A., and Li, M.D. (2001b) Cloned neuropeptide Y (NPY) Y1 and pancreatic polypeptide Y4 receptors expressed in Chinese hamster ovary cells show considerable agonist-driven internalization, in contrast to the NPY Y2 receptor. *Eur J Biochem* **268**: 877-886.
- Parker, S.L., Parker, M.S., Kane, J.K., and Berglund, M.M. (2002b) A pool of Y2 neuropeptide Y receptors activated by modifiers of membrane sulfhydryl or cholesterol balance. *Eur J Biochem* **269**: 2315-2322.
- Pedrazzini, T., Pralong, F., and Grouzmann, E. (2003) Neuropeptide Y: the universal soldier. *Cell Mol Life Sci* **60**: 350-377.
- Perney, T., and Miller, R. (1989) Two different G-proteins mediate neuropeptide Y and bradykinin-stimulated phospholipid breakdown in cultured rat sensory neurons. *J Biol Chem* **264**: 7317-7327.
- Petr, M.J., and Wurster, R.D. (1997) Determination of in situ dissociation constant for Fura-2 and quantitation of background fluorescence in astrocyte cell line U373-MG. *Cell Calcium* **21**: 233-240.

- Pheng, L.H., Fournier, A., Dumont, Y., Quirion, R., and Regoli, D. (1997) The dog saphenous vein: a sensitive and selective preparation for the Y2 receptor of neuropeptide Y. *Eur J Pharmacol* **327**: 163-167.
- Pheng, L.H., Perron, A., Quirion, R., Cadieux, A., Fauchere, J.L., Dumont, Y., and Regoli, D. (1999) Neuropeptide Y-induced contraction is mediated by neuropeptide Y Y2 and Y4 receptors in the rat colon. *Eur J Pharmacol* **374**: 85-91.
- Pieribone, V.A., Brodin, L., Friberg, K., Dahlstrand, J., Soderberg, C., Larhammar, D., and Hokfelt, T. (1992) Differential expression of mRNAs for neuropeptide Y-related peptides in rat nervous tissues: possible evolutionary conservation. *J Neurosci* **12**: 3361-3371.
- Pinton, P., Brini, M., Bastianutto, C., Tuft, R.A., Pozzan, T., and Rizzuto, R. (1998) New light on mitochondrial calcium. *Biofactors* **8**: 243-253.
- Polidori, C., Ciccocioppo, R., Regoli, D., and Massi, M. (2000) Neuropeptide Y receptor(s) mediating feeding in the rat: characterization with antagonists. *Peptides* **21**: 29-35.
- Potter, E.K., Fuhlendorff, J., and Schwartz, T.W. (1991) [Pro34]neuropeptide Y selectively identifies postjunctional-mediated actions of neuropeptide Y in vivo in rats and dogs. *Eur J Pharmacol* **193**: 15-19.
- Pozzan, T., Rizzuto, R., Volpe, P., and Meldolesi, J. (1994) Molecular and cellular physiology of intracellular calcium stores. *Physiol Rev* **74**: 595-636.
- Pozzan, T., Magalhaes, P., and Rizzuto, R. (2000) The comeback of mitochondria to calcium signalling. *Cell Calcium* **28**: 279-283.
- Pozzan, T., and Rizzuto, R. (2000) The renaissance of mitochondrial calcium transport. *Eur J Biochem* **267**: 5269-5273.
- Prasher, D., McCann, R.O., and Cormier, M.J. (1985) Cloning and expression of the cDNA coding for aequorin, a bioluminescent calcium-binding protein. *Biochem Biophys Res Commun* **126**: 1259-1268.
- Premont, R.T., Matsuoka, I., Mattei, M.G., Pouille, Y., Defer, N., and Hanoune, J. (1996) Identification and characterization of a widely expressed form of adenylyl cyclase. *J Biol Chem* **271**: 13900-13907.
- Prieto, D., Buus, C.L., Mulvany, M.J., and Nilsson, H. (2000) Neuropeptide Y regulates intracellular calcium through different signalling pathways linked to a Y(1)-receptor in rat mesenteric small arteries. *Br J Pharmacol* **129**: 1689-1699.
- Quinn, L.A., Moore, G.E., Morgan, R.T., and Woods, L.K. (1979) Cell lines from human colon carcinoma with unusual cell products, double minutes, and homogeneously staining regions. *Cancer Res* **39**: 4914-4924.
- Raposo, P.D., Broqua, P., Hayward, A., Akinsanya, K., Galyean, R., Schteingart, C., Junien, J., and Aubert, M.L. (2000) Stimulation of the gonadotropic axis by the neuropeptide Y receptor Y1 antagonist/Y4 agonist 1229U91 in the male rat. *Neuroendocrinology* **71**: 2-7.
- Raposo, P.D., Pierroz, D.D., Broqua, P., White, R.B., Pedrazzini, T., and Aubert, M.L. (2001) Chronic administration of neuropeptide Y into the lateral ventricle of C57BL/6J male mice produces an obesity syndrome including hyperphagia, hyperleptinemia, insulin resistance, and hypogonadism. *Mol Cell Endocrinol* **185**: 195-204.
- Raposo, P.D., Aubert, M.L., Tommaselli, G.A., Herzog, H., and Pedrazzini, T. (2004a) NPY receptor Y1 and Y4 subtypes are not involved in the stimulation of LH secretion by ICV injection of 1229U91 as seen in NPY1R^{-/-} and NPY4R^{-/-}. In *7th International NPY Conference, Coimbra, February 3-7*, pp. 119 (abstract book).
- Raposo, P.D., Pedrazzini, T., White, R.B., Palmiter, R.D., and Aubert, M.L. (2004b) Chronic neuropeptide Y infusion into the lateral ventricle induces sustained feeding and obesity in mice lacking either Npy1r or Npy5r expression. *Endocrinology* **145**: 304-310.
- Redrobe, J.P., Dumont, Y., Fournier, A., and Quirion, R. (2002a) The neuropeptide Y (NPY) Y1 receptor subtype mediates NPY-induced antidepressant-like activity in the mouse forced swimming test. *Neuropsychopharmacology* **26**: 615-624.
- Redrobe, J.P., Dumont, Y., and Quirion, R. (2002b) Neuropeptide Y (NPY) and depression: from animal studies to the human condition. *Life Sci* **71**: 2921-2937.
- Redrobe, J.P., Carvajal, C., Kask, A., Dumont, Y., and Quirion, R. (2004) Neuropeptide Y and its receptor subtypes in the central nervous system: Emphasis on their role in animal models of psychiatric disorders. In *Handbook of experimental pharmacology*. Vol. 162. Michel, M.C. (ed): Springer-Verlag, pp. 101-136.
- Ridgway, E.B., and Ashley, C.C. (1967) Calcium transients in single muscle fibers. *Biochem Biophys Res Commun* **29**: 229-234.
- Ridgway, E.B., Gilkey, J.C., and Jaffe, L.F. (1977) Free calcium increases explosively in activating medaka eggs. *Proc Natl Acad Sci U S A* **74**: 623-627.

- Rimland, J.M., Seward, E.P., Humbert, Y., Ratti, E., Trist, D.G., and North, R.A. (1996) Coexpression with potassium channel subunits used to clone the Y2 receptor for neuropeptide Y. *Mol Pharmacol* **49**: 387-390.
- Rist, B., Zerbe, O., Ingenhoven, N., Scapozza, L., Peers, C., Vaughan, P.F.T., McDonald, R.L., Wieland, H.A., and Beck-Sickinger, A.G. (1996) Modified, cyclic dodecapeptide analog of neuropeptide Y is the smallest full agonist at the human Y2 receptor. *FEBS Lett* **394**: 169-173.
- Rizzuto, R., Simpson, A.W., Brini, M., and Pozzan, T. (1992) Rapid changes of mitochondrial Ca²⁺ revealed by specifically targeted recombinant aequorin. *Nature* **358**: 325-327.
- Rizzuto, R., Brini, M., and Pozzan, T. (1993) Intracellular targeting of the photoprotein aequorin: a new approach for measuring, in living cells, Ca²⁺ concentrations in defined cellular compartments. *Cytotechnology* **11 Suppl 1**: S44-46.
- Rizzuto, R., Pinton, P., Carrington, W., Fay, F.S., Fogarty, K.E., Lifshitz, L.M., Tuft, R.A., and Pozzan, T. (1998) Close contacts with the endoplasmic reticulum as determinants of mitochondrial Ca²⁺ responses. *Science* **280**: 1763-1766.
- Rizzuto, R., Bernardi, P., and Pozzan, T. (2000) Mitochondria as all-round players of the calcium game. *J Physiol (Lond)* **529**: 37-47.
- Robert, V., Pinton, P., Tosello, V., Rizzuto, R., and Pozzan, T. (2000) Recombinant aequorin as tool for monitoring calcium concentration in subcellular compartments. *Methods Enzymol* **327**: 440-456.
- Robinson, J.P., Carter, W.O., and Narayanan, P.K. (1994) Oxidative product formation analysis by flow cytometry. *Methods Cell Biol* **41**: 437-447.
- Ropp, J.D., Donahue, C.J., Wolfgang-Kimball, D., Hooley, J.J., Chin, J.Y., Hoffman, R.A., Cuthbertson, R.A., and Bauer, K.D. (1995) Aequorea green fluorescent protein analysis by flow cytometry. *Cytometry* **21**: 309-317.
- Rose, P.M., Fernandes, P., Lynch, J.S., Frazier, S.T., Fisher, S.M., Kodukula, K., Kienzle, B., and Seethala, R. (1995) Cloning and functional expression of a cDNA encoding a human type 2 neuropeptide Y receptor. *J Biol Chem* **270**: 22661-22664.
- Rose, P.M., Lynch, J.S., Frazier, S.T., Fisher, S.M., Chung, W., Battaglino, P., Fathi, Z., Leibel, R., and Fernandes, P. (1997) Molecular genetic analysis of a human neuropeptide Y receptor. The human homolog of the murine "Y5" receptor may be a pseudogene. *J Biol Chem* **272**: 3622-3627.
- Rudolf, K., Eberlein, W., Engel, W., Wieland, H.A., Willim, K.D., Entzeroth, M., Wiene, W., Beck-Sickinger, A.G., and Doods, H.N. (1994) The first highly potent and selective non-peptide neuropeptide Y Y1 receptor antagonist: BIBP3226. *Eur J Pharmacol* **271**: R11-13.
- Sahu, A., Kalra, P.S., and Kalra, S.P. (1988) Food deprivation and ingestion induce reciprocal changes in neuropeptide Y concentrations in the paraventricular nucleus. *Peptides* **9**: 83-86.
- Sala-Newby, G.B., Badminton, M.N., Evans, W.H., George, C.H., Jones, H.E., Kendall, J.M., Ribeiro, A.R., and Campbell, A.K. (2000) Targeted bioluminescent indicators in living cells. *Methods Enzymol* **305**: 479-498.
- Samama, P., Cotecchia, S., Costa, T., and Lefkowitz, R.J. (1993) A mutation-induced activated state of the beta 2-adrenergic receptor. Extending the ternary complex model. *J Biol Chem* **268**: 4625-4636.
- Scampavia, L.D., Blankenstein, G., Ruzicka, J., and Christian, G.D. (1995) A coaxial jet mixer for rapid kinetic analysis in flow injection and flow injection cytometry. *Anal Chem* **67**: 2743-2749.
- Schaffhauser, A.O., Stricker-Krongrad, A., Brunner, L., Cumin, F., Gerald, C., Whitebread, S., Criscione, L., and Hofbauer, K.G. (1997) Inhibition of food intake by neuropeptide Y Y5 receptor antisense oligodeoxynucleotides. *Diabetes* **46**: 1792-1798.
- Schertler, G.F., Villa, C., and Henderson, R. (1993) Projection structure of rhodopsin. *Nature* **362**: 770-772.
- Schneider, E. (2005) Development of Fluorescence-Based Methods for the Determination of Ligand Affinity, Selectivity and Activity at G-Protein Coupled Receptors. In *Doctoral thesis, University of Regensburg*.
- Schober, D.A., Van Abbema, A.M., Smiley, D.L., Bruns, R.F., and Gehlert, D.R. (1998) The neuropeptide Y Y1 antagonist, 1229U91, a potent agonist for the human pancreatic polypeptide-preferring (NPY Y4) receptor. *Peptides* **19**: 537-542.
- Schober, D.A., Gackenhaimer, S.L., Heiman, M.L., and Gehlert, D.R. (2000) Pharmacological characterization of (125)I-1229U91 binding to Y1 and Y4 neuropeptide Y/Peptide YY receptors. *J Pharmacol Exp Ther* **293**: 275-280.
- Schroeder, J.P., Olive, F., Koenig, H., and Hodge, C.W. (2003) Intra-amygdala infusion of the NPY Y1 receptor antagonist BIBP 3226 attenuates operant ethanol self-administration. *Alcohol Clin Exp Res* **27**: 1884-1891.
- Schwartz, T.W., Rehfeld, J.F., Stadil, F., Larson, L.I., Chance, R.E., and Moon, N. (1976) Pancreatic-polypeptide response to food in duodenal-ulcer patients before and after vagotomy. *Lancet* **1**: 1102-1105.

- Schwartz, T.W. (1983) Pancreatic polypeptide: a hormone under vagal control. *Gastroenterology* **85**: 1411-1425.
- Schwartz, T.W., Sheikh, S.P., and O'Hare, M.M. (1987) Receptors on pheochromocytoma cells for two members of the PP-fold family--NPY and PP. *FEBS Lett* **225**: 209-214.
- Selbie, L.A., Darby, K., Schmitz-Peiffer, C., Browne, C.L., Herzog, H., Shine, J., and Biden, T.J. (1995) Synergistic interaction of Y1-neuropeptide Y and alpha 1b-adrenergic receptors in the regulation of phospholipase C, protein kinase C, and arachidonic acid production. *J Biol Chem* **270**: 11789-11796.
- Serradeil-Le Gal, C., Valette, G., Rouby, P.E., Pellet, A., Oury-Donat, F., Brossard, G., Lespy, L., Marty, E., Neliat, G., de Cointet, P., and et al. (1995) SR 120819A, an orally-active and selective neuropeptide Y Y1 receptor antagonist. *FEBS Lett* **362**: 192-196.
- Serradeil-Le Gal, C., Lafontan, M., Raufaste, D., Marchand, J., Pouzet, B., Casellas, P., Pascal, M., Maffrand, J.P., and Le Fur, G. (2000) Characterization of NPY receptors controlling lipolysis and leptin secretion in human adipocytes. *FEBS Lett* **475**: 150-156.
- Shapiro, H.M. (1994) Cell membrane potential analysis. *Methods Cell Biol* **41**: 121-133.
- Shigeri, Y., and Fujimoto, M. (1994) Y2 receptors for neuropeptide Y are coupled to three intracellular signal transduction pathways in a human neuroblastoma cell line. *J Biol Chem* **269**: 8842-8848.
- Shimomura, O., Johnson, F.H., and Saiga, Y. (1962) Extraction, purification and properties of aequorin, a bioluminescent protein from the luminous hydromedusan, *Aequorea*. *J Cell Comp Physiol* **59**: 223-239.
- Shimomura, O., and Johnson, F.H. (1975) Regeneration of the photoprotein aequorin. *Nature* **256**: 236-238.
- Shimomura, O., and Johnson, F.H. (1978) Peroxidized coelenterazine, the active group in the photoprotein aequorin. *Proc Natl Acad Sci U S A* **75**: 2611-2615.
- Silva, A.P., Cavadas, C., and Grouzmann, E. (2002) Neuropeptide Y and its receptors as potential therapeutic drug targets. *Clin Chim Acta* **326**: 3-25.
- Simon, S., Chambers, J., Butcher, E., and Sklar, L. (1992) Neutrophil aggregation is beta 2-integrin- and L-selectin-dependent in blood and isolated cells. *J Immunol* **149**: 2765-2771.
- Smith-White, M.A., Hardy, T.A., Brock, J.A., and Potter, E.K. (2001) Effects of a selective neuropeptide Y Y2 receptor antagonist, BIIIE0246, on Y2 receptors at peripheral neuroeffector junctions. *Br J Pharmacol* **132**: 861-868.
- Smith-White, M.A., Herzog, H., and Potter, E.K. (2002) Role of neuropeptide Y Y2 receptors in modulation of cardiac parasympathetic neurotransmission. *Regul Pept* **103**: 105-111.
- Soll, R.M., Dinger, M.C., Lundell, I., Larhammer, D., and Beck-Sickingler, A.G. (2001) Novel analogues of neuropeptide Y with a preference for the Y1-receptor. *Eur J Biochem* **268**: 2828-2837.
- Stables, J., Green, A., Marshall, F., Fraser, N., Knight, E., Sautel, M., Milligan, G., Lee, M., and Rees, S. (1997) A bioluminescent assay for agonist activity at potentially any G-protein-coupled receptor. *Anal Biochem* **252**: 115-126.
- Stables, J., Mattheakis, L.C., Chang, R., and Rees, S. (2000) Recombinant aequorin as reporter of changes in intracellular calcium in mammalian cells. *Methods Enzymol* **327**: 456-471.
- Stanley, B.G., Magdalin, W., Seirafi, A., Nguyen, M.M., and Leibowitz, S.F. (1992) Evidence for neuropeptide Y mediation of eating produced by food deprivation and for a variant of the Y1 receptor mediating this peptide's effect. *Peptides* **13**: 581-587.
- Starback, P., Lundell, I., Fredriksson, R., Berglund, M.M., Yan, Y.L., Wraith, A., Soderberg, C., Postlethwait, J.H., and Larhammar, D. (1999) Neuropeptide Y receptor subtype with unique properties cloned in the zebrafish: the zYa receptor. *Brain Res Mol Brain Res* **70**: 242-252.
- Statnick, M.A., Schober, D.A., Gackenheimer, S., Johnson, D., Beavers, L., Mayne, N.G., Burnett, J.P., Gadski, R., and Gehlert, D.R. (1998) Characterization of the neuropeptide Y5 receptor in the human hypothalamus: a lack of correlation between Y5 mRNA levels and binding sites. *Brain Res* **810**: 16-26.
- Stein, R.A., Wilkinson, J.C., Guyer, C.A., and Staros, J.V. (2001) An analytical approach to the measurement of equilibrium binding constants: application to EGF binding to EGF receptors in intact cells measured by flow cytometry. *Biochemistry* **40**: 6142-6154.
- Stephenson, R.P. (1956) A modification of receptor theory. *Br J Pharmacol Chemother* **11**: 379-393.
- Sternweis, P.C., Northup, J.K., Smigel, M.D., and Gilman, A.G. (1981) The regulatory component of adenylate cyclase. Purification and properties. *J Biol Chem* **256**: 11517-11526.
- Stone, K.R., Mickey, D.D., Wunderli, H., Mickey, G.H., and Paulson, D.F. (1978) Isolation of a human prostate carcinoma cell line (DU 145). *Int J Cancer* **21**: 274-281.
- Sullivan, S.J., and Schonbrunn, A. (1986) The processing of receptor-bound [125I-Tyr11]somatostatin by RINm5F insulinoma cells. *J Biol Chem* **261**: 3571-3577.

- Sundler, F., Böttcher, G., Ekblad, E., and Hakanson, R. (1993) PP, PYY, and NPY. Occurrence and distribution in the periphery. In *Handbook of experimental pharmacology*. Colmers, W.F. and Wahlestedt, C. (eds). Totowa, New Jersey: Humana Press, pp. 157-196.
- Szabadkai, G., Simoni, A.M., and Rizzuto, R. (2003) Mitochondrial Ca²⁺ Uptake Requires Sustained Ca²⁺ Release from the Endoplasmic Reticulum. *J Biol Chem* **278**: 15153-15161.
- Takebayashi, Y., Koga, H., Togami, J., Inui, A., Kurihara, H., Koshiya, K., Furuya, T., Tanaka, A., and Murase, K. (2000) Design of the Y1-receptor-selective cyclic peptide based on the C-terminal sequence of neuropeptide Y. *J Pept Res* **56**: 409-415.
- Tanabe, S., Kreutz, B., Suzuki, N., and Kozasa, T. (2004) Regulation of RGS-RhoGEFs by Galph12 and Galph13 proteins. *Methods Enzymol* **390**: 285-294.
- Tanaka, Y., Nakazawa, T., Ishiro, H., Saito, M., Uneyama, H., Iwata, S., Ishii, K., and Nakayama, K. (1995) Ca²⁺ handling mechanisms underlying neuropeptide Y-induced contraction in canine basilar artery. *Eur J Pharmacol* **289**: 59-66.
- Tang, W.J., and Gilman, A.G. (1991) Type-specific regulation of adenylyl cyclase by G protein beta gamma subunits. *Science* **254**: 1500-1503.
- Tatemoto, K. (1982a) Neuropeptide Y: complete amino acid sequence of the brain peptide. *Proc Natl Acad Sci U S A* **79**: 5485-5489.
- Tatemoto, K. (1982b) Isolation and characterization of peptide YY (PYY), a candidate gut hormone that inhibits pancreatic exocrine secretion. *Proc Natl Acad Sci U S A* **79**: 2514-2518.
- Tatemoto, K., Carlquist, M., and Mutt, V. (1982) Neuropeptide Y—a novel brain peptide with structural similarities to peptide YY and pancreatic polypeptide. *Nature* **296**: 659-660.
- Tepikin, A. (2001) *Calcium signalling*: Oxford Univ. Press.
- Thiele, T.E., and Heilig, M. (2004) Behavioral effects of neuropeptide Y. In *Handbook of experimental pharmacology*. Vol. 162. Michel, M.C. (ed): Springer-Verlag, pp. 251-282.
- Thiele, T.E., Sparta, D.R., Hayes, D.M., and Fee, J.R. (2004) A role for neuropeptide Y in neurobiological responses to ethanol and drugs of abuse. *Neuropeptides* **38**: 235-243.
- Tiff, C.J., Proia, R.L., and Camerini-Otero, R.D. (1992) The folding and cell surface expression of CD4 requires glycosylation. *J Biol Chem* **267**: 3268-3273.
- Torfs, H., Detheux, M., Oonk, H.B., Akerman, K.E., Poels, J., Loy, T.V., Loof, A.D., Vassart, G., Parmentier, M., and Broeck, J.V. (2002) Analysis of C-terminally substituted tachykinin-like peptide agonists by means of aequorin-based luminescent assays for human and insect neurokinin receptors. *Biochem Pharmacol* **63**: 1675-1682.
- Trinh, T., van Dumont, Y., and Quirion, R. (1996) High levels of specific neuropeptide Y/pancreatic polypeptide receptors in the rat hypothalamus and brainstem. *Eur J Pharmacol* **318**: R1-3.
- Tschop, M., Castaneda, T.R., Joost, H.G., Thone-Reineke, C., Ortman, S., Klaus, S., Hagan, M.M., Chandler, P.C., Oswald, K.D., Benoit, S.C., Seeley, R.J., Kinzig, K.P., Moran, T.H., Beck-sickinger, A.G., Koglin, N., Rodgers, R.J., Blundell, J.E., Ishii, Y., Beattie, A.H., Holch, P., Allison, D.B., Raun, K., Madsen, K., Wulff, B.S., Stidsen, C.E., Birringer, M., Kreuzer, O.J., Schindler, M., Arndt, K., Rudolf, K., Mark, M., Deng, X.Y., Whitcomb, D.C., Halem, H., Taylor, J., Dong, J., Datta, R., Culler, M., Craney, S., Flora, D., Smiley, D., and Heiman, M.L. (2004) Physiology: does gut hormone PYY3-36 decrease food intake in rodents? *Nature* **430**: 1 p following 165; discussion 162 p following 165.
- Tsutsumi, Y. (1984) Immunohistochemical studies on glucagon, glicentin and pancreatic polypeptide in human stomach: normal and pathological conditions. *Histochem J* **16**: 869-883.
- Turnbull, A.V., Ellershaw, L., Masters, D.J., Birtles, S., Boyer, S., Carroll, D., Clarkson, P., Loxham, S.J., McAulay, P., Teague, J.L., Foote, K.M., Pease, J.E., and Block, M.H. (2002) Selective antagonism of the NPY Y5 receptor does not have a major effect on feeding in rats. *Diabetes* **51**: 2441-2449.
- Uegaki, K., Murase, S., Nemoto, N., Kobayashi, Y., Yoshikawa, S., and Yumoto, N. (1997) Effects of covalent dimerization on the structure and function of the carboxy-terminal fragment of neuropeptide Y. *Biochem Biophys Res Commun* **241**: 737-743.
- Unger, V.M., Hargrave, P.A., Baldwin, J.M., and Schertler, G.F. (1997) Arrangement of rhodopsin transmembrane alpha-helices. *Nature* **389**: 203-206.
- Ungrin, M.D., Singh, L.M., Stocco, R., Sas, D.E., and Abramovitz, M. (1999) An automated aequorin luminescence-based functional calcium assay for G-protein-coupled receptors. *Anal Biochem* **272**: 34-42.
- Vaillant, C., and Taylor, I.L. (1981) Demonstration of carboxyl-terminal PP-like peptides in endocrine cells and nerves. *Peptides* **2 Suppl 2**: 31-35.
- Van Riper, D.A., and Bevan, J.A. (1991) Evidence that neuropeptide Y and norepinephrine mediate electrical field-stimulated vasoconstriction of rabbit middle cerebral artery. *Circ Res* **68**: 568-577.

- Voisin, T., Goumain, M., Lorinet, A.M., Maoret, J.J., and Laburthe, M. (2000) Functional and molecular properties of the human recombinant Y4 receptor: resistance to agonist-promoted desensitization. *J Pharmacol Exp Ther* **292**: 638-646.
- von Horsten, S., Hoffmann, T., Alfalah, M., Wrann, C.D., Karl, T., Pabst, R., and Bedoui, S. (2004) PP, PYY and NPY: Synthesis, Storage, Release and Degradation. In *Handbook of experimental pharmacology*. Vol. 162. Michel, M.C. (ed): Springer-Verlag, pp. 23-44.
- Wahlestedt, C., Yanaihara, N., and Hakanson, R. (1986) Evidence for different pre-and post-junctional receptors for neuropeptide Y and related peptides. *Regul Pept* **13**: 307-318.
- Wahlestedt, C., Pich, E.M., Koob, G.F., Yee, F., and Heilig, M. (1993) Modulation of anxiety and neuropeptide Y-Y1 receptors by antisense oligodeoxynucleotides. *Science* **259**: 528-531.
- Walker, M.W., Smith, K.E., Bard, J., Vaysse, P.J., Gerald, C., Daouti, S., Weinshank, R.L., and Branchek, T.A. (1997) A structure-activity analysis of the cloned rat and human Y4 receptors for pancreatic polypeptide. *Peptides* **18**: 609-612.
- Wedegaertner, P., Chu, D., Wilson, P., Levis, M., and Bourne, H. (1993) Palmitoylation is required for signaling functions and membrane attachment of Gq alpha and Gs alpha. *J Biol Chem* **268**: 25001-25008.
- Weinberg, D.H., Sirinathsingji, D.J., Tan, C.P., Shiao, L.L., Morin, N., Rigby, M.R., Heavens, R.H., Rapoport, D.R., Bayne, M.L., Cascieri, M.A., Strader, C.D., Linemeyer, D.L., and MacNeil, D.J. (1996) Cloning and expression of a novel neuropeptide Y receptor. *J Biol Chem* **271**: 16435-16438.
- Weiner, M.P., Costa, G.L., Schoettlin, W., Cline, J., Mathur, E., and Bauer, J.C. (1994) Site-directed mutagenesis of double-stranded DNA by the polymerase chain reaction. *Gene* **151**: 119-123.
- Weiser, T., Wieland, H.A., and Doods, H.N. (2000) Effects of the neuropeptide Y Y(2) receptor antagonist BIIE0246 on presynaptic inhibition by neuropeptide Y in rat hippocampal slices. *Eur J Pharmacol* **404**: 133-136.
- Weiss, H.M., Haase, W., Michel, H., and Reilander, H. (1995) Expression of functional mouse 5-HT5A serotonin receptor in the methylotrophic yeast *Pichia pastoris*: pharmacological characterization and localization. *FEBS Lett* **377**: 451-456.
- Weiss, J.M., Morgan, P.H., Lutz, M.W., and Kenakin, T.P. (1996a) The Cubic Ternary Complex Receptor-Occupancy Model I. Model Description. *J Theor Biol* **178**: 151-167.
- Weiss, J.M., Morgan, P.H., Lutz, M.W., and Kenakin, T.P. (1996b) The Cubic Ternary Complex Receptor-Occupancy Model II. Understanding Apparent Affinity. *J Theor Biol* **178**: 169-182.
- Weiss, J.M., Morgan, P.H., Lutz, M.W., and Kenakin, T.P. (1996c) The Cubic Ternary Complex Receptor-Occupancy Model III. Resurrecting Efficacy. *J Theor Biol* **181**: 381-397.
- Wettstein, J.G., Earley, B., and Junien, J.L. (1995) Central nervous system pharmacology of neuropeptide Y. *Pharmacol Ther* **65**: 397-414.
- Wharton, J., Gordon, L., Byrne, J., Herzog, H., Selbie, L.A., Moore, K., Sullivan, M.H., Elder, M.G., Moscoso, G., Taylor, K.M., and et al. (1993) Expression of the human neuropeptide tyrosine Y1 receptor. *Proc Natl Acad Sci U S A* **90**: 687-691.
- Whitcomb, D.C., Taylor, I.L., and Vigna, S.R. (1990) Characterization of saturable binding sites for circulating pancreatic polypeptide in rat brain. *Am J Physiol* **259**: G687-691.
- Whitcomb, D.C., Vigna, S.R., McVey, D.C., and Taylor, I.L. (1992) Localization and characterization of pancreatic polypeptide receptors in rat adrenal glands. *Am J Physiol* **262**: G532-536.
- Whitcomb, D.C., Puccio, A.M., Leifer, J.M., Finley, G., Ehrlich, G.D., and Sved, A.F. (1994) Pancreatic polypeptide (PP) and peptide YY (PYY) mRNA in the brainstem of rats detected by reverse-transcriptase PCR (RT-PCR). *Society for Neurosciences Abstracts* **20**: 1373.
- Whitcomb, D.C., Puccio, A.M., Vigna, S.R., Taylor, I.L., and Hoffman, G.E. (1997) Distribution of pancreatic polypeptide receptors in the rat brain. *Brain Res* **760**: 137-149.
- Wieland, H.A., Engel, W., Eberlein, W., Rudolf, K., and Doods, H.N. (1998) Subtype selectivity of the novel nonpeptide neuropeptide Y Y1 receptor antagonist BIBO 3304 and its effect on feeding in rodents. *Br J Pharmacol* **125**: 549-555.
- Wiest, R., Jurzik, L., Moleda, L., Froh, M., Schnabl, B., Horsten, S.v., Scholmerich, J., and Straub, R.H. (2006) Enhanced Y1-receptor-mediated vasoconstrictive action of neuropeptide Y (NPY) in superior mesenteric arteries in portal hypertension. *J Hepatol* **44**: 512-519.
- Wiley, J.W., Gross, R.A., and MacDonald, R.L. (1993) Agonists for neuropeptide Y receptor subtypes NPY-1 and NPY-2 have opposite actions on rat nodose neuron calcium currents. *J Neurophysiol* **70**: 324-330.
- Wilkie, T.M., Scherle, P.A., Strathmann, M.P., Slepak, V.Z., and Simon, M.I. (1991) Characterization of G-protein alpha subunits in the Gq class: expression in murine tissues and in stromal and hematopoietic cell lines. *Proc Natl Acad Sci U S A* **88**: 10049-10053.
- Wise, A., Jupe, S.C., and Rees, S. (2004) The identification of ligands at orphan G-protein coupled receptors. *Annu Rev Pharmacol Toxicol* **44**: 43-66.

- Woldbye, D.P., and Kokaia, M. (2004) Neuropeptide Y and seizures: effects of exogenously applied ligands. *Neuropeptides* **38**: 253-260.
- Yan, H., Yang, J., Marasco, J., Yamaguchi, K., Brenner, S., Collins, F., and Karbon, W. (1996) Cloning and functional expression of cDNAs encoding human and rat pancreatic polypeptide receptors. *Proc Natl Acad Sci U S A* **93**: 4661-4665.
- Yannielli, P.C., and Harrington, M.E. (2001) Neuropeptide Y in the mammalian circadian system: effects on light-induced circadian responses. *Peptides* **22**: 547-556.
- Yannielli, P.C., Brewer, J.M., and Harrington, M.E. (2004) Blockade of the NPY Y5 receptor potentiates circadian responses to light: complementary in vivo and in vitro studies. *Eur J Neurosci* **19**: 891-897.
- Zhang, X., Shi, T., Holmberg, K., Landry, M., Huang, W., Xiao, H., Ju, G., and Hokfelt, T. (1997) Expression and regulation of the neuropeptide Y Y2 receptor in sensory and autonomic ganglia. *Proc Natl Acad Sci U S A* **94**: 729-734.
- Zhang, Y., Lundberg, T., and Yu, L. (2000) Involvement of neuropeptide Y and Y1 receptor in antinociception in nucleus raphe magnus of rats. *Regul Pept* **95**: 109-113.
- Zhu, X., and Birnbaumer, L. (1996) G protein subunits and the stimulation of phospholipase C by Gs- and Gi-coupled receptors: Lack of receptor selectivity of Galpha(16) and evidence for a synergic interaction between Gbeta gamma and the alpha subunit of a receptor activated G protein. *Proc Natl Acad Sci U S A* **93**: 2827-2831.
- Zukowska-Grojec, Z., Karwatowska-Prokopczuk, E., Rose, W., Rone, J., Movafagh, S., Ji, H., Yeh, Y., Chen, W.T., Kleinman, H.K., Grouzmann, E., and Grant, D.S. (1998) Neuropeptide Y: a novel angiogenic factor from the sympathetic nerves and endothelium. *Circ Res* **83**: 187-195.